

Electrochemical Filtration Technology for the Removal and Degradation
of Ibuprofen and Bisphenol A from Aqueous Solutions

Ahmed Refaat Bakr

A Thesis
In the Department
of
Building, Civil and Environmental Engineering

Presented in Partial Fulfillment of the Requirements
For the Degree of
Doctor of Philosophy (Environmental Engineering) at
Concordia University
Montreal, Quebec, Canada

January 2017

CONCORDIA UNIVERSITY
SCHOOL OF GRADUATE STUDIES

This is to certify that the thesis prepared

By: Ahmed R. Bakr

Entitled: Electrochemical Filtration Technology for the Removal and Degradation of
Ibuprofen and Bisphenol A from Aqueous solutions

and submitted in partial fulfillment of the requirements for the degree of

Doctor of Philosophy (Environmental Engineering)

complies with the regulations of the University and meets the accepted standards with respect to originality and quality.

Signed by the final examining committee:

| | | |
|--------------------------|-------|---------------------|
| Dr. Mohammed Zaheeruddin | _____ | Chair |
| Dr. Subhasis Ghoshal | _____ | External Examiner |
| Dr. M. Zahangir Kabir | _____ | External to program |
| Dr. Fariborz Haghghat | _____ | Examiner |
| Dr. Catherine Mulligan | _____ | Examiner |
| Dr. Md. Saifur Rahaman | _____ | Thesis Supervisor |

Approved by _____

Chair of Department or Graduate Program Director

January 2017

Dean of Faculty

ABSTRACT

Electrochemical filtration technology for the removal and degradation of ibuprofen and bisphenol A from aqueous solutions

Ahmed R. Bakr, PhD

Concordia University, 2017

Electrochemical filtration is a promising technology that aims for the efficient removal of persistent contaminants that cannot be effectively eliminated through conventional treatment methods. Multiwalled carbon nanotubes (MWNTs) and carbon substrates can be employed as filtration media to which a DC potential can be applied for further electrochemical treatment.

Ibuprofen and Bisphenol A, two emerging contaminants of concern, have been reported to exist in natural waters, influent, secondary treated effluent of wastewater, and in primary and secondary wastewater sludge. In this study, dead-end electrochemical filtration was investigated as a removal method for these contaminants. This technique has shown promise in the elimination of both of these compounds and the reduction of their overall toxicity.

Carboxylated multiwalled carbon nanotubes (MWNTs-COOH) were used with the aim of increasing the filtration efficiency for the removal of carboxylated ibuprofen under different pH and electrolytic conditions. It was found that the presence of oxy-functional groups can increase the functional surface area of MWNTs and increase the filtration capacity in low voltage applications. In high voltage applications, it was found that electrochemical filtration is controlled by bulk electroactive species. Boron doped multiwalled carbon nanotubes (BMWNTs) were also studied, with the goal of improving electrical conductivity during bisphenol A electrochemical filtration experiments. It was found that despite previous reports describing the higher oxidative power of doped carbon nanotubes, with the highest reported for BMWNTs, pristine MWNTs and BMWNTs showed similar outcomes in eliminating bisphenol A.

The removal of ibuprofen and bisphenol A was also investigated by using crossflow electrochemical filtration. The crossflow configuration shows great potential in eliminating these two contaminants in both individual component and mixed solutions from pure and fouling electrolytes. This outcome can mainly be attributed to the crossflow mechanism and can be assigned to the horizontal shear flow, which likely leads to a consistent surface coverage. The long residence time within the membrane

likely leads to a significant reduction in toxicity under applied voltage. Our results suggest that the electrochemical filtration technology has a potential for use as a polishing step for removal of emerging contaminants from different water sources.

DEDICATION

I dedicate this work to my parents who stood by my side the whole time with both spiritual and financial support, and who always lifted my spirits during the toughest of times.

To my friends who always encouraged me to go all the way, stay strong and patient, and never let me feel lonely.

Moreover, to my research mates, who were always by my side with enlightenment and knowledge.

ACKNOWLEDGEMENTS

I extend all of my sincere gratitude, and I would like to acknowledge the contributions of my supervisor, Dr. Saifur Rahaman. For his wise guidance throughout my research and the Ph.D. program, his financial support, and for giving me the opportunity to be a member of his research team and to work on such an interesting project in the first place, I wholeheartedly thank him.

I express my sincere appreciation to my committee members, Dr. Catherine Mulligan, Dr. Fariborz Haghighat, and Dr. M. Zahangir Kabir for their time, their dedication, and their constructive criticism, providing me with the valuable advice needed to complete this project.

My gratitude and genuine thanks go out to my group members, former and current; Farah Rahaman Omi, and Alexandra Meikleham for their guidance and help during my first days in the lab, Gregory Brennan for his significant, and continued technical input into this work, Wen Ma for her sincere help on technical matters, Natalia Toriello, Charlotte Clement, Luca Malaguti, and Myriam Cyr, for their participation, and to all my other teammates, thank you all so much.

Finally, I express my deep thanks to those who made this work possible financially, Concordia University for support through the Graduate Student Support Program (GSSP) and the Natural Science and Engineering Research Council of Canada (NSERC).

Table of Contents

| | |
|---|-------------|
| List of Figures | xi |
| List of Abbreviations | xvii |
| Chapter 1: Introduction | 1 |
| Chapter 2: Literature Review and Thesis Motivation and Objectives | 10 |
| 2.1. Emerging Contaminants | 10 |
| 2.2. Advanced Oxidation Processes | 10 |
| 2.2.1. Ozonation | 11 |
| 2.2.2. UV photolysis..... | 14 |
| 2.2.3. UV photocatalytic oxidation | 16 |
| 2.2.4. Electrooxidation | 18 |
| 2.3. Thesis Objectives and Description of the Implemented Process | 22 |
| Chapter 3: Electrochemical Efficacy of a Carboxylated Multiwalled Carbon Nanotube Filter for the Removal of Ibuprofen from Aqueous Solutions under Acidic Conditions 25 | |
| Abstract | 25 |
| Keywords | 25 |
| 3.1. Introduction | 26 |
| 3.2. Materials and Methods | 28 |
| 3.2.1. Materials..... | 28 |
| 3.2.2. MWNTs and MWNTs-COOH Characterization..... | 29 |
| 3.2.3. Cyclic Voltammetry | 29 |
| 3.2.4. Electrochemical MWNTs and MWNTs-COOH Filter Preparation..... | 30 |
| 3.2.5. Electrolyte Solutions | 30 |
| 3.2.6. Filtration and Electrochemical Filtration | 31 |

| | |
|---|-----------|
| 3.2.7. Quantification of Ibuprofen Removal and Sample Analysis..... | 31 |
| 3.3. Results and Discussion..... | 32 |
| 3.3.1. MWNTs and MWNTs-COOH Stability and Surface Morphology..... | 32 |
| 3.3.2. MWNTs and MWNTs-COOH Electrochemical Performance Characterization | 35 |
| 3.3.3. Efficiency of MWNTs and MWNTs-COOH for Ibuprofen Removal at High Concentration (Single Passage)..... | 40 |
| 3.3.4. Efficiency of MWNTs and MWNTs-COOH for Ibuprofen Removal at Low Concentration (Breakthrough Experiments) | 45 |
| 3.3.5. Insight into Ibuprofen Degradation and its By-products..... | 49 |
| 3.3.5.1. Effect of the Flow Rate on MWNTs-COOH Filter Electrochemical Performance | 52 |
| 3.3.5.2. Possible degradation pathways for ibuprofen during electrochemical filtration 55 | |
| 3.4. Conclusions | 57 |
| Acknowledgements | 57 |
| Chapter 4: Perceiving Different Factors of Influence during Dead-end Electrochemical Filtration of Bisphenol A using Multiwalled Carbon Nanotubes: Resistance to Surface Passivation, Reactive Oxygen Species and Residence Time | 58 |
| Abstract | 58 |
| Keywords | 59 |
| 4.1. Introduction | 59 |
| 4.2. Materials and Methods | 61 |
| 4.2.1. Materials..... | 61 |
| 4.2.2. Electrochemical MWNTs and BMWNTs Filter Preparation | 62 |
| 4.2.3. Electrolyte Solutions and pH Conditions | 63 |
| 4.2.4. Filtration and Electrochemical Filtration Processes | 63 |

| | |
|---|-----------|
| 4.2.5. Stability and morphology characterization of the MWNTs and BMWNTs Filters | 64 |
| 4.2.6. Cyclic Voltammetry | 64 |
| 4.2.7. Quantification of Bisphenol A Removal | 65 |
| 4.3. Results and Discussion | 65 |
| 4.3.1. MWNTs and BMWNTs Stability and Surface Morphology | 65 |
| 4.3.2. The Salting Out Effect on Bisphenol A Removal during the Electrochemical Filtration Process | 68 |
| 4.3.3. MWNTs and BMWNTs Electrochemical Performance Characterization through Cyclic Voltammetry | 70 |
| 4.3.4. Electrochemical Filtration Performance in the Presence and Absence of NaCl and in Different pH Conditions | 74 |
| 4.3.5. Liquid Chromatography Mass Spectrometry for Monitoring Bisphenol A Degradation and Factors Affecting Degradation Pathways | 78 |
| 4.3.5.1. Effect of Applied Voltage | 78 |
| 4.3.5.2. Major Degradation Pathways of Bisphenol A | 82 |
| 4.3.5.3. The Effect of Flow Rate and the MWNTs Loading (Residence Time) | 84 |
| 4.3.6. The Effect of the Initial Concentration of Bisphenol A on Electrochemical Oxidation Reaction Kinetics during the Electrochemical Filtration Process | 85 |
| 4.4. Conclusion | 87 |
| Acknowledgements | 88 |
| Chapter 5: Crossflow Electrochemical Filtration for Eliminating Ibuprofen and Bisphenol A from Electrolytic Solutions in Pure and Fouling Conditions | 89 |
| Abstract | 89 |
| Keywords | 89 |
| 5.1. Introduction | 90 |
| 5.2. Materials and Methods | 93 |

| | |
|---|------------|
| 5.2.1. Materials | 93 |
| 5.2.2. Electrolyte solution..... | 94 |
| 5.2.3. Crossflow electrochemical filtration setup..... | 94 |
| 5.2.4. Buckypaper surface characterization and purity | 95 |
| 5.2.5. Analysis and quantification | 95 |
| 5.3. Results and discussion..... | 96 |
| 5.3.1. Buckypaper surface characterization, purity and stability | 96 |
| 5.3.2. Crossflow filtration and electrochemical filtration performance over time | 97 |
| 5.3.3. Crossflow filtration and electrochemical filtration flux | 101 |
| 5.3.4. Qualification of Ibuprofen and bisphenol A (1:1) mixture removal, and by-products characterization by liquid chromatography mass spectrometry | 104 |
| 5.4. Conclusion..... | 108 |
| Acknowledgements | 109 |
| Chapter 6: Contribution, Conclusion and Future Recommendations..... | 110 |
| 6.1. Contribution..... | 110 |
| 6.2. Conclusion..... | 112 |
| 6.3. Future Recommendations..... | 115 |
| References | 117 |
| Appendices..... | 133 |
| Appendix A | 133 |
| Appendix B | 152 |
| Appendix C | 189 |
| Appendix D | 202 |

List of Figures

| | |
|--|----|
| <i>Figure 1-1.</i> Drinking water treatment stages. Figure modified from [9]..... | 4 |
| <i>Figure 1-2.</i> Wastewater treatment stages , figure from [11]..... | 6 |
| <i>Figure 1-3.</i> Different pathways of exposure to ECs, figure from [13]..... | 8 |
| | 12 |
| <i>Figure 2-1.</i> Reaction of gaseous phase ozone with C=C forming unstable ozonide followed by the formation of oxide by-products | 12 |
| <i>Figure 2-2.</i> Wastewater ozonation treatment system, figure from [30] | 13 |
| <i>Figure 2-3.</i> Ozone generation reaction catalyzed by UV-ray or high voltage application, figure from [31]..... | 13 |
| <i>Figure 2-4.</i> UV photolysis bench scale reaction system, figure from [34]..... | 15 |
| <i>Figure 2-5.</i> UV photocatalytic oxidation (UV/O ₃) unit, figure from [44]..... | 17 |
| <i>Figure 2-6.</i> Electrochemical oxidation (batch electrolysis) unit and reaction system for wastewater treatment, figure modified from [69]..... | 20 |
| <i>Figure 3-1.</i> SEM images, EDS and TGA analysis for MWNTs and MWNTs-COOH where (A) is SEM for MWNTs filter at a surface loading of 0.84 mg/cm ² , (B) EDS analysis for MWNTs filter at a surface loading of 0.84 mg/cm ² , (C) SEM for MWNTs-COOH filter at a surface loading of 0.84 mg/cm ² , (D) EDS analysis for MWNTs-COOH filter at a surface loading of 0.84 mg/cm ² , (E) TGA analysis for pure MWNTs and (F) is TGA analysis for pure MWNTs-COOH. | 33 |
| <i>Figure 3-2.</i> EDS analysis after subjecting of MWNTs and MWNTs-COOH to 270 mL of 1 mg/L ibuprofen for 135 minutes where (A) MWNTs are under conditions of ibuprofen in 10 mM NaCl, pH 6 and under 0 V of applied potential, (B) MWNTs are under conditions of ibuprofen in 10 mM NaCl, pH 6 and under 2 V of applied potential, (C) MWNTs are under conditions of ibuprofen in 10 mM NaCl, pH 6 and under 3 V of applied potential, (D) MWNTs-COOH are under conditions of ibuprofen in 10 mM HCl, pH 2 and under 0 V of applied potential, (E) MWNTs-COOH are under conditions of ibuprofen in 10 mM HCl, pH 2 and under 2 V of applied potential and (F) MWNTs-COOH are under conditions of ibuprofen in 10 mM HCl, pH 2 and under 3 V of applied potential. Surface loading for both MWNTs types was 0.84 mg/cm ² . Experiments were performed at 23 °C. | 34 |

Figure 3-3. (A) Cyclic voltammogram for ibuprofen in 10 mM NaCl (pH 6), electrofiltered by MWNTs, (B) Cyclic voltammogram for ibuprofen in 10 mM HCl (pH 2), electrofiltered by MWNTs-COOH, (C) Linear correlation for current vs. ibuprofen concentration (current values reported corresponding to 1.13 V vs. Ag/AgCl) for the cyclic voltammogram recorded on MWNTs and (D) Linear correlation for current vs. ibuprofen concentration (current values reported corresponding to 1.13 V vs. Ag/AgCl) for the cyclic voltammogram recorded on MWNTs-COOH. Ibuprofen concentrations were 1, 10 and 20 mg/L, scan rate was 50 mV/sec, potential range was -1 to +1.5 V vs. Ag/AgCl, MWNTs and MWNTs-COOH loading was 0.84 mg/cm², flow rate was 2 mL/min, and temperature was 23°C. 36

Figure 3-4. (A) Steady state current densities for MWNTs and MWNTs-COOH at surface loadings of 0.32 and 0.84 mg/cm², (B) Anode potential vs. Ag/AgCl for electrochemical filtration of 20 mg/L ibuprofen by 0.32 mg/cm² MWNTs and MWNTs-COOH in 10mM NaCl and 10 mM HCl (C) is MWNTs and MWNTs-COOH energy consumption (EC) in kWh/kg and (D) is mineralization current efficiency (MCE) in %, for electrochemical filtration of 20 mg/L ibuprofen by 0.32 mg/cm² MWNTs and MWNTs-COOH in 10mM NaCl and 10 mM HCl. At 23°C, flow rate of 2 mL/min and applied voltages 1, 2 and 3 volts. 39

Figure 3-5. Percent removal of Ibuprofen by MWNTs and MWNTs-COOH using (A) 10 mM NaCl as the background solution at pH 6 and (B) 10 mM HCl as the background solution at pH 2, with no voltage application, at temperature 23 °C. Percent removal of ibuprofen by MWNTs and MWNTs-COOH filters using (C) 10 mM NaCl as the background solution (pH 6) and (D) 10 mM HCl as the background solution (pH 2), with an applied DC potential of 1 V, at temperature 23 °C. (E) Percent removal of ibuprofen by MWNTs using 10 mM NaCl as the background solution at pH 6, at DC voltages of 2 and 3 V and at 23 and 40°C. (F) Percent removal of ibuprofen by MWNTs-COOH using 10 mM HCl as the background solution at pH 2, at DC voltages of 2 and 3 V and at 23 and 40°C. The concentration of ibuprofen was 20 mg/L, MWNTs and MWNTs-COOH surface loading was 0.32 mg/cm² and flow rate was 2 mL/min. 43

Figure 3-6. Breakthrough trends and flux values for MWNTs and MWNTs-COOH filters over time at 0, 1, 2 and 3 V of applied DC voltage, where (A) is breakthrough plots in pure 10 mM NaCl (pH 6) for MWNTs and 10 mM HCl (pH 2) for MWNTs-COOH, (B) is breakthrough plots in synthetic secondary effluent of the same composition and pH (7.3) for both filter types, (C) are MWNTs flux values corresponding to 0, 1, 2 and 3 V of applied potential for ibuprofen in pure 10

mM NaCl (pH 6) and (D) are MWNTs-COOH flux values corresponding to 0, 1, 2 and 3 V of applied potential for ibuprofen in pure 10 mM HCl (pH 2). The ibuprofen concentration was 1 mg/L (4.8 μ M). MWNTs and MWNTs-COOH surface loading was 0.84 mg/cm², and temperature was 23°C. 47

Figure 3-7. Electrostatic filtration flux in μ g/m²-hr of MWNTs and MWNTs-COOH for 20 mg/L ibuprofen in 10 mM NaCl (pH 6) and 10 mM HCl (pH 2), respectively. MWNTs loadings were 0.32 mg/cm², applied voltage was 1 V and temperature was 23°C (Corresponding to Figure 3-5 C and D)..... 48

Figure 3-8. (A) Chromatograms of ibuprofen in a 10 mM NaCl background solution at pH 6, where the upper trace is before treatment and the lower is after treatment with MWNTs at a 3 V DC potential. (B) Chromatograms of ibuprofen in a 10 mM HCl background solution at pH 2, where the upper trace is before treatment and the lower is after treatment with MWNTs-COOH at a 3 V DC potential. (C) Mass spectra at RT 2.3 min of ibuprofen in 10 mM HCl (pH2) before treatment. (D) Mass spectra at RT 4.1 min for ibuprofen in 10 mM HCl (pH2) before treatment. (E) Mass spectra at RT 2.3 min of ibuprofen in 10 mM HCl (pH2) after treatment with MWNTs-COOH at a 3 V DC potential. (F) Mass spectra at RT 4.1 min for ibuprofen in 10 mM HCl (pH2) after treatment with MWNTs-COOH at a 3 V DC potential. The ibuprofen concentration was 20 mg/L, MWNTs and MWNTs-COOH surface loading was 0.32 mg/cm², flow rate was 2 mL/min and temperature was 40°C. 51

Figure 3-9. (A) Chromatograms of ibuprofen in 10 mM HCl as the background solution at pH 2, where the upper (black) trace is before treatment, the middle (blue) trace is after treatment with MWNTs-COOH at a voltage of 2 DC with a flow rate of 0.2 mL/min, and the lower (red) trace is after treatment with MWNTs-COOH at a voltage of 2 DC with a flow rate of 1 mL/min. (B) Mass spectra for ibuprofen in 10 mM HCl (pH 2) at RT 6.8 min before treatment and (C) after treatment with MWNTs-COOH at a 2V DC potential. (D) Mass spectra for ibuprofen at RT 7.3 min in 10 mM HCl pH 2 after treatment with MWNTs-COOH at a 2V DC potential. (E) Mass spectra for ibuprofen at RT 7.7 min in 10 mM HCl pH 2 after treatment with MWNTs-COOH at a 2V DC potential. The ibuprofen concentration was 10 mg/L, MWNTs-COOH surface loading was 0.84 mg/cm², and the temperature was 23 °C..... 53

Figure 3-10. Possible degradation pathways for ibuprofen during electrochemical filtration, based on the LC-MS results. 56

Figure 4-1. SEM and EDX for MWNTs and BMWNTs where (A) is the SEM for the MWNT filter with a surface loading of 1.04 mg/cm², (B) is the EDX analysis for the MWNT filter at a surface loading of 1.04 mg/cm², (C) is the SEM for the BMWNT filter with a surface loading of 1.04 mg/cm², (D) is the EDX analysis for the BMWNT filter with a surface loading of 1.04 mg/cm², (E) is TGA weight percent vs. temperature for MWNTs, (F) is TGA weight percent vs. temperature for BMWNTs. Characterization for the MWNTs and BMWNTs was done before use in treatment. 67

Figure 4-2. (A) Breakthrough plots for filtration and electrochemical filtration of 1 mg/L BPA in 1, 2, 10, 50 and 100 mM NaCl (pH 5.7 – 6) by MWNTs at 0, 1 and 2 V of applied DC potential and (B) is instantaneous and steady-state current densities for electrochemical filtration of 1 mg/L BPA in 1, 2, 10, 50 and 100 mM NaCl by MWNTs at 1 and 2 V of applied DC potential. Flow rate was 2 mL/min., MWNTs surface loading was 1.04 mg/cm² and experiments were performed at room temperature. 69

Figure 4-3. Cyclic voltammetry for electrofiltration of 1, 50, and 100 mg/L BPA in 10 mM NaCl. Where (A) is the cyclic voltammogram for electrofiltration by MWNTs, (B) is the cyclic voltammogram for electrofiltration by BMWNTs, (C) is the linear correlation for current vs. BPA concentration on MWNTs (corresponding to (A), current peak at 0.75 V), (D) is the linear correlation for current vs. BPA concentration on BMWNTs (corresponding to (B), current peak at 0.75 V), and (E) is the anode potentials vs. Ag/AgCl corresponding to 1, 2 and 3 V of applied DC potential and. MWNTs and BMWNTs loading was 1.04 mg/cm². Experiments were performed at a flow rate of 2 mL/min and at room temperature. 72

Figure 4-4. Breakthrough plots for filtration and electrochemical filtration of 1 mg/L BPA in the presence and absence of 10 mM NaCl, at different pH values, and at 0 and 3 V of applied DC potential where (A) is electrochemical MWNTs filtration in the presence of 10 mM NaCl (pH 6), (B) is electrochemical MWNTs filtration in the absence of NaCl (pH 3), (C) is electrochemical MWNTs filtration in the absence of NaCl (pH 9), (D) is electrochemical BMWNTs filtration in the presence of 10 mM NaCl (pH 6), (E) is electrochemical BMWNTs filtration absence of NaCl (pH 3) and (D) is electrochemical BMWNTs filtration absence of NaCl (pH 9). Experiments were performed at room temperature with a flow rate of 2 mL/min and the MWNTs and BMWNTs loading was 1.04 mg/cm². 75

Figure 4-5. Removal flux for filtration and electrochemical filtration of 1 mg/L bisphenol A in the presence of 10 mM NaCl (pH 6), absence of NaCl (pH 3) and absence of NaCl (pH 9) using (A) MWNTs and (B) BMWNTs, corresponding to Figure 4-4..... 77

Figure 4-6. Energy consumption and mineralization current efficiency, where (A) is the energy consumption for pH variation in the presence of 10 mM NaCl (pH6) and absence of NaCl (pH 3 and 9) using MWNTs and BMWNTs at 3V of applied DC potential, (B) is the mineralization current efficiency for pH variation in the presence of 10 mM NaCl (pH6) and absence of NaCl (pH 3 and 9) using MWNTs and BMWNTs at 3V of applied DC potential. The loading for MWNTs and BMWNTs was 1.04 mg/cm², the BPA concentration was 1 mg/L and the flow rate was 2 mL/min and at room temperature. 77

Figure 4-7. Mass spectra of 10 mg/L BPA in 10 mM NaCl (pH6) before treatment (red trace) and after electrochemical MWNT filtration treatment (black traces) at 2 and 3 V of applied DC potential after 5, 46 and 106 minutes of electrochemical filtration time. Experiments were performed at room temperature with a 2 mL/min flow rate and an MWNTs loading of 1.04 mg/cm². 79

Figure 4-8. LC-MS of 10 mg/L BPA in 10 mM NaCl (pH6) before treatment (red trace) and after electrochemical MWNT filtration treatment at 2 and 3 V of applied DC potential at 5, 46 and 106 minutes of electrochemical filtration time (black traces) showing the formation of a by-product at RT 7.8 min (243 m/z), where (A) is the liquid chromatograms for 7.8 min and (B) is the mass spectra at 243 m/z (corresponding to 7.8 min). Experiments were performed at room temperature with a flow rate of 2 mL/min and the MWNTs loading was 1.04 mg/cm²..... 81

Figure 4-9. Degradation reaction pathways for BPA during the electrochemical filtration process at 2 and 3 V in the presence (pH 6) and absence (pH 3 and 9) of 10 mM NaCl. Experiments were performed at room temperature with a flow rate of 2 mL/min. and an MWNT loading of 1.04 mg/cm². 83

Figure 4-10. Mass spectra for 10 mg/L BPA in 10 mM NaCl before treatment (red trace) and after electrochemical MWNTs filtration treatment at 3 V of applied DC potential after 20, 184, and 424 minutes of electrochemical filtration time (black traces). Experiments were performed at room temperature with a flow rate of 0.5 mL/min and an MWNTs loading of 2.08 mg/cm². 85

Figure 4-11. Electrochemical removal rates vs. initial concentration for the electrochemical MWNT filtration of 4.4 to 439.6 μM BPA in 10 mM NaCl (pH 6) at 1, 2 and 3 V of DC potential.

Experiments were performed at room temperature using a flow rate of 2 mL/min and an MWNT loading of 1.04 mg/cm²..... 86

Figure 5-1. SEM images, EDS and TGA analysis for MWNT blend buckypaper where (A) is SEM for buckypaper membrane at a surface loading of 102.5 mg/cm², (B) EDS analysis for buckypaper membrane filter at a surface loading of 102.5 mg/cm², (C) is TGA analysis for MWNTs blend buckypaper..... 97

Figure 5-2. (A) Breakthrough plots for the removal of 1 mg/L Ibuprofen from 10 mM NaCl and (B) for the removal of 1 mg/L bisphenol A from 10 mM NaCl, under 0, 1, 2 and 3 V of applied DC potential, applied pressure is 20 psi (137.9 kPa), permeate flow rate is 1 mL/min and experiments performed at room temperature..... 99

Figure 5-3. (A) Breakthrough plots for the removal of 1 mg/L Ibuprofen and bisphenol A (1:1) mixture from 10 mM NaCl and (B) from synthetic secondary wastewater (TOC 34 mg/L, pH 7.4), under 0, 1, 2 and 3 V of applied DC potential, applied pressure is 20 psi (137.9 kPa), permeate flow rate is 1 mL/min and at room temperature. 101

Figure 5-4. (A) Electrochemical filtration flux for the removal of 1 mg/L Ibuprofen from 10 mM NaCl and (B) for the removal of 1 mg/L bisphenol a from 10 mM NaCl, under 0, 1, 2 and 3 V of applied DC potential, applied pressure is 20 psi (137.9 kPa), permeate flow rate is 1 mL/min and at room temperature..... 103

Figure 5-5. (A) Electrochemical filtration flux for the removal of 1 mg/L Ibuprofen and bisphenol A (1:1) mixture from 10 mM NaCl and (B) from synthetic secondary wastewater (TOC 34 mg/L, pH 7.4), under 0, 1, 2 and 3 V of applied DC potential, applied pressure is 20 psi (137.9 kPa), permeate flow rate is 1 mL/min and at room temperature..... 103

Figure 5-6. LCMS for the treatment of 20 mg/L Ibuprofen and bisphenol A (1:1) mixture from 10 mM NaCl, where (A) are the overlaid LC chromatograms for mixture before treatment (Blue trace) and after treatment (Black traces) and (B) is MS spectra for mixture before treatment (Blue trace) and after treatment (Black traces). Applied voltages were 2 and 3 V of applied DC potential, applied pressure is 20 psi (137.9 kPa), permeate flow rate is 1 mL/min and at room temperature. 106

Figure 5-7. Possible degradation pathway for ibuprofen and bisphenol A during crossflow electrochemical filtration 107

List of Abbreviations

| | |
|-------------------|---|
| CNTs | Carbon Nanotubes |
| MWNTs | Multiwalled Carbon Nanotubes |
| MWNTs-COOH | Carboxylated Multiwalled Carbon Nanotubes |
| BWMNTs | Boron Doped Multiwalled Carbon Nanotubes |
| BPA | Bisphenol A |
| ECs | Emerging Contaminants |
| CECs | Chemicals of Emerging Concern |
| NSAID | Non-Steroidal Anti-Inflammatory Drug |
| OCD | Over the Counter Drug |
| EDCs | Endocrine Disrupting Chemicals |
| AOPs | Advanced Oxidation Processes |
| ROS | Reactive Oxygen species |
| BDD | Boron Doped Diamond |
| DC | Direct Current |
| EC | Energy Consumption |
| MCE | Mineralization Current efficiency |

Chapter 1: Introduction

Increased drought conditions and water scarcity have made water and wastewater treatment a factor of critical global importance from environmental, economic and security points of view. There are millions of people worldwide who lack access to clean and safe water, an issue that requires urgent and critical attention. Over 780 million people worldwide do not have access to purified, safe drinking water and about 4 billion do not have access to sanitized water. Moreover, approximately 2.2 million people, mostly children under the age of 5, die of diarrheal related infections each year, most likely due to water transmitted infectious diseases [1-3].

A major industrial sector that is directly affected by water scarcity is agriculture, as food production is often a water intensive process. A lack of clean water can lead to food insufficiency and sanitation/human health implications. Also, agriculture plays a critical role in the support and development of rural economic growth, as rural inhabitants of many countries depend on agriculture as a primary source of income. Thus, water scarcity is directly related to food security, human health, and poverty eradication, and stands as a major obstacle to the progress of rural inhabitants in overcoming long-standing poverty and food concerns [3]. The other main sectors that can suffer from water scarcity are industrial food and beverage production, and the energy sector.

Water scarcity is an urgent problem that affects many countries, including many in northern and eastern Africa, as well as Mexico, Pakistan, South Africa, and large parts of China and India. In these countries, among others, agriculture represents a major demand on the water supply. Consequently, agriculture is often reported as the first sector to suffer from a shortage of clean water, which results in a reduced ability to maintain adequate per-capita food production, a major concern considering the large populations of these nations. Therefore, there needs to be a concerted, dedicated effort to solve issues surrounding equity of access to water and water allocation [3].

Over the past few decades, water conservation efforts focused on the development of large-scale physical infrastructures, such as dams and water reservoirs, to preserve excess river flow and rainwater; an effort that has been shown to be insufficient to cope with the growing

demands on water caused by increasing populations. As noted by the United Nations, water “is distributed unevenly and too much of it is wasted, polluted and unsustainably managed” (UN 2012b) [4]. It is now widely known that numerous other human activities greatly contribute to this global water crisis, namely: improper water use, pollution, insufficient or poorly maintained infrastructure, and inadequate management systems. Mitigating these issues requires intense efforts toward better and wide-scale water conservation.

Supply of clean water has become an increasingly important yet complicated issue, due to the growing global population and increased industrial contamination, along with growing concerns about climate change. It is expected that in the next few decades, global population will increase by almost 50 percent, leading to greater requirements in agricultural and industrial sectors, and thus creating further demand on the already limited supply of clean water [2, 3]. Therefore, both new sources of fresh water are needed while existing water resources need greater protections, to fulfill the fast growing demand for clean water.

The demands on water resources make urgent and innovative advances in water and wastewater treatment technologies a high priority. Historically, the traditional approach of supplying clean water was through the control of certain parameters including turbidity, iron and manganese content, taste, odor, color, and coliforms. Today, regulations mandate that a wider scale and larger number of parameters need to be held to acceptable standards for human consumption. These regulations emerged as a result of rapidly expanding anthropogenic activities that led to increased water contamination, and thus, the need to provide acceptable quality water for human use became more sophisticated and costly [5].

Presently, the most widely and conventionally employed method of water and wastewater treatment is a treatment train made up of unit treatment processes, individual treatment steps. Drinking water and wastewater treatment plants are comprised of unit processes that are essentially the same. In drinking water and sewage treatment plants, individual units are applied in an operational succession, where each step is a different operation undertaken with the aim to improve the quality of water [6, 7].

Generally, unit processes can be classified into three stages; the physical stage, chemical stage, and biological stage. The physical stage can also be referred to as solid-liquid separation

techniques, and this is the step where particulate or coarse matter is physically separated from water. Settling is one such technique where particulate matter settles out by gravity.

Filtration is another physical process that plays a dominant role in most unit treatment processes. In this technique, a specific material can be used to filter suspended solids from water. Filtration can be classified into two categories; conventional filtration and non-conventional filtration. Conventional filtration uses a layered bed of fine sand, gravel, filter fabrics, and charcoal, which can effectively remove mud particles, large particulate, and large suspended solid matter. Non-conventional filtration uses specifically designed membranes to remove or eliminate contaminants that cannot be removed through conventional filtration. This can be referred to as membrane filtration (micro and ultrafiltration processes)[6, 7].

The chemical stage includes any processes in which chemicals are added to treat the water. These chemicals may interact with soluble particulate or colloidal matter through physical interactions, leading to their physical separation from water (i.e. coagulation and flocculation). In another pathway of chemical processes, chemicals may react with contaminants in complex reaction pathways that are mostly referred to as chemical oxidation processes, all, however, leading to the destruction of the soluble contaminants and the reduction of their toxic effects [7, 8]. Physio-chemical processes or the physical separation of colloidal particles from water is traditionally referred to as “primary treatment” and in many parts of the world is applied as a stand-alone step (e.g. Montreal wastewater treatment facility), or as a follow-up step to the physical separation stage.

The common steps in drinking water treatment are shown in Figure 1-1. Here settling or pre-sedimentation refers to the step of collecting water from rivers, wells, or lakes and allowing larger particles or grit to settle by gravity. This is followed by coagulation and mixing (chemical treatment) to separate colloidal particles from water by physical interaction with coagulants. Sedimentation then follows, in which the reacting colloidal particles are then allowed to settle by gravity and the water becomes clearer. Conventional filtration then takes place as a further purification, or cleaning, step removing further particulate matter, and finally, disinfection is a chemical step that takes place by adding chemicals or sparging gas (e.g. chlorine), to kill microorganisms in water.

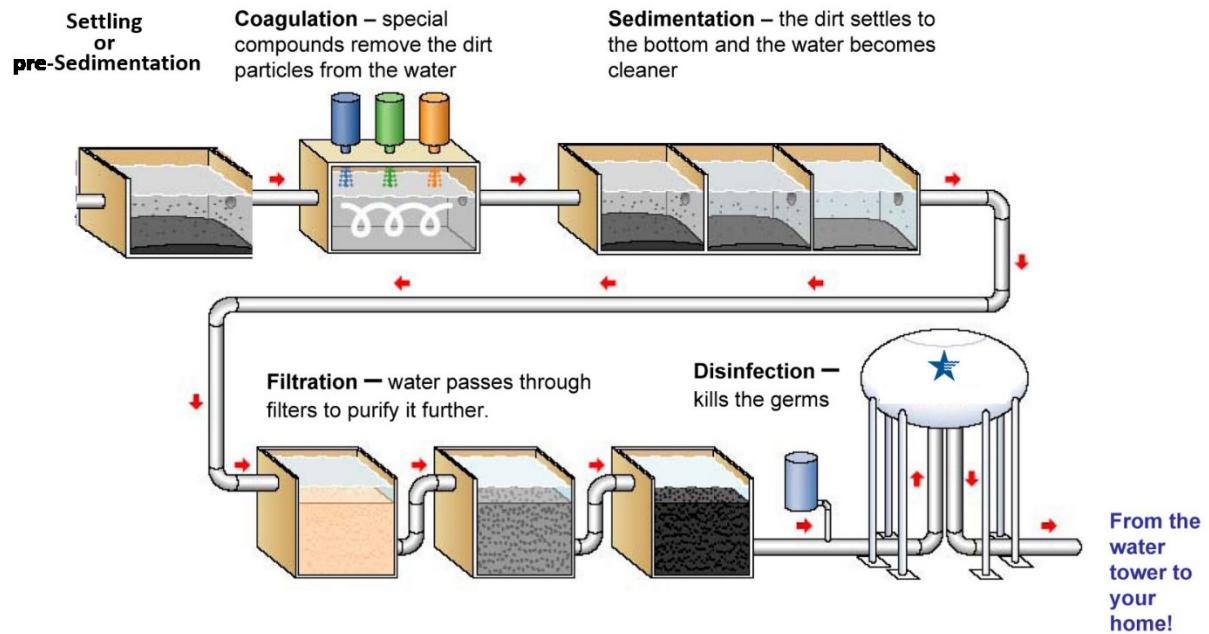


Figure 1-1. Drinking water treatment stages. Figure modified from [9]

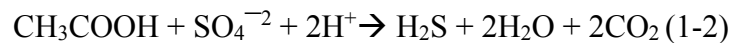
The biological process is a step that is only employed in wastewater treatment, due to the large organic loads frequently found in sewage, often requiring this additional step after primary treatment. Appropriately, biological treatment has traditionally been referred to as a secondary treatment. Biological wastewater treatment takes place entirely through biological mechanisms, in which microorganisms (i.e. bacteria), convert organic matter into inert mineralized products or biomass. This is followed by a subsequent separation or removal of the biomass through sedimentation or clarifying [6, 10]. In biological treatment, there are different assimilation reactions (biochemical reactions) that take place within the microorganismal cellular structure. These reactions are responsible for the generation of energy for the survival of the cell. The main reactions in biological processes are aerobic, anaerobic, and anoxic reactions (bacterial reactions conditions). Because aerobic microorganisms can produce more energy through their reactions, aerobic organisms can reproduce faster, and therefore can produce larger amounts of sludge by-products than anaerobic microorganisms can. Major examples of the main energy producing reactions by

microorganisms of differing conditions are represented by the following chemical equations (1-1), (1-2) and (1-3) [10];

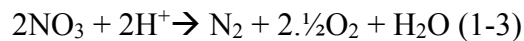
Aerobic conditions (Glucose oxidation):



Anaerobic conditions (Sulfate reduction):



Anoxic conditions (Nitrate reduction or denitrification):



There are three major steps in wastewater treatment, mainly employed for the treatment of domestic or sewage water: primary, secondary, and tertiary treatment. Pre-treatment is a minor step that precedes primary treatment which screens and removes step coarse material and grit through settling or specially designed filters. The pre-treatment step is sometimes considered part of the primary treatment. Following pre-treatment, similar to the process of drinking water treatment, chemical treatment takes place through the introduction of coagulants, after which the coagulated matter is allowed to settle in a primary clarifier.

Secondary treatment, in which microorganisms break down and degrade the remaining organic content, follows primary treatment, and “sludge” is created as a primary product of this process. In the activated sludge process, part of this sludge material is recirculated into an aeration tank to be used as a substrate for aerobic microorganisms. Again, similar to drinking water treatment, a disinfection process then follows, in which microorganisms that might flow with water from secondary treatment are eliminated through chlorination, UV irradiation, or ozonation.

The final step in wastewater treatment is tertiary treatment, in which nutrients such as phosphorous and nitrogen are removed. These nutrients loading can cause an increase in microbial activity, increasing the demand for oxygen that can lead to eutrophication of water bodies. Figure 1-2 shows the different steps of wastewater treatment [6].

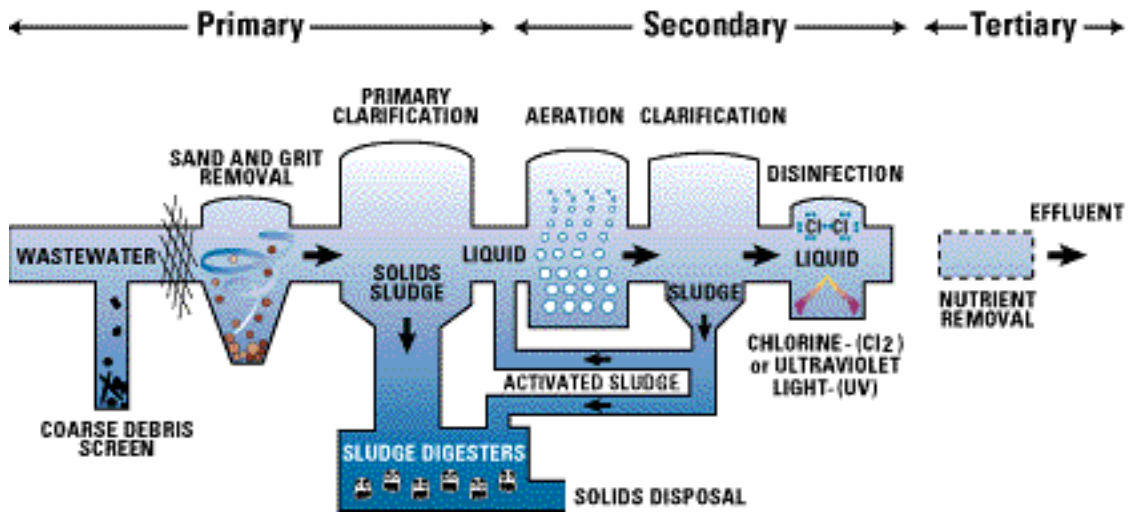


Figure 1-2. Wastewater treatment stages , figure from [11]

Conventional water and wastewater treatment steps are successful in greatly improving water quality through the removal of coarse matter and grit, and by largely reducing major parameters as suspended solids, chemical oxygen demand (COD), biological oxygen demand (BOD), and nutrients (phosphorous and nitrogen). However, these processes have not been able to remove other persistent contaminants and refractory organic contents emerging primarily from different industrial processes explicitly. These contaminants have been reported to exist in water sources including natural water, wastewater, and secondary treated wastewater in a wide yet significant range of concentrations. Such contaminants are reported to be of great concern due to adverse effects on human health and are widely known as emerging contaminants (ECs).

ECs not only refer to chemical compounds but also include emerging microbial contaminants such as bacterial pathogens, viruses, protozoa, and antibiotic-resistant bacteria. The source of emerging microbial contaminants is known to be fecal contamination. Fecal contamination often ends up ineffectively eliminated in sewage water treatment plants and thus is discharged to surface water in some parts of the world, or contaminates soil and agricultural water in most others [12, 13].

Due to the novel nature and rudimentary capacity of analytical and detection technologies over the past few decades, and due to the extremely numerous number of chemicals and pathogens that have been entering the environment, there is a great concern that toxic contaminants have been present in the ecosystem for a significantly extended period, and therefore, humans and animals have been long exposed to these chemicals [13-16]. For example, one of the major techniques of analysis and detection widely in use is mass spectrometry. This technique was traditionally employed in the past to screen and target known contaminants, however, at low resolutions (e.g. triple quadrupole detectors). Triple quadrupole detectors are mass filters allowing only previously selected molecules to be detected. This approach may have resulted in a countless number of chemicals and transition by-products going undetected [17]. Today, pulsed ionization technology could be executed through time of flight detectors (TOFs) with numerous advances at satisfactory rates. Such approach could allow the accurate detection of bulk molecules with high resolution and could provide high practical mass ranges compared to classic quadrupole and magnetic mass analyzers. Therefore, to be properly able to track and estimate the actual scale of the ECs problem, continuous advances in analytical and detection technologies are of critical importance.

Persistent chemicals of emerging concern (CECs) come primarily from a variety of industries and are expected to be found in industrial wastewater and industrial discharge. Some common categories of CECs are pharmaceuticals (over-the-counter and prescription drugs), personal care products, plasticizers, flame retardants, and pesticides. These are considered major categories due to their massive production and consumption volumes. Other categories of concern are surfactants, synthetic hormones, and chemicals of commercial uses. This can include sucralose, an artificial sweetener ingested in food and drugs which is only partially absorbed in the digestive tract and is now widely detected in sewage wastewater and classified as a persistent chemical. Also of a persistent nature, antimony, used as a catalyst in the production of plastic bottles, is leached from plastic bottles made of polyethylene terephthalate (PET). Siloxanes are persistent compounds largely used in consumer products such as cosmetics, deodorants, soaps, hair conditioners, hair dyes, car waxes, baby pacifiers, cleaners, furniture polishes, and water-repellent windshield coatings. Synthetic musks, used as fragrance additives in perfumes, lotions, sunscreens, deodorants, and laundry detergents, are currently known to exist widely throughout the environment and can accumulate and affect wildlife [13,

16]. Nevertheless, these are only a few of the numerous chemicals of a persistent nature that can be detected in water and wastewater.

One of the main pathways to ECs exposure is the discharge of municipal wastewater effluent and treated sludge, mainly because treated sewage water and treated sludge can be applied to agricultural lands. Treated sewage sludge (biosolids) is often used as fertilizer or soil conditioner, thus leading to the release of ECs through leaching which can contaminate surface and ground water. The other main sources of exposure to ECs are industrial wastewater effluents, untreated wastewater from industrial facilities, effluents from poultry and feed animal farms, facilities in which antibiotics are used for veterinary practices, and agricultural runoff that can contain pesticides, and Figure 1-3 shows the different pathways of exposure to ECs [13].

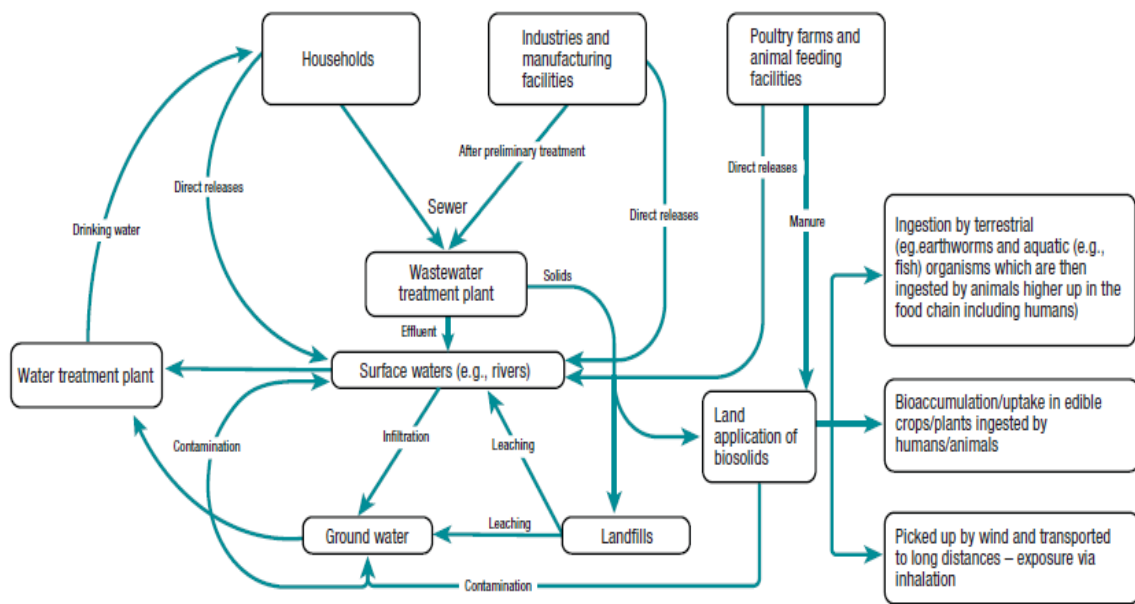


Figure 1-3. Different pathways of exposure to ECs, figure from [13]

Therefore, it has become a matter of necessity to develop innovative methods to eliminate these harmful contaminants from different water sources before the water can enter general use or treated wastewater can be discharged to water bodies [12-16, 18, 19].

The inability of conventional water and wastewater treatment processes to remove CECs lays mainly in the lack of effective chemical pathways, which incorporate powerful reactive species capable of interacting with and decomposing these recalcitrant chemicals. Therefore, current and future efforts must focus on developing effective methods that are capable of incorporating chemical reaction pathways and enhancing these reactions by energy incentive means. Together with integrating other physical processes e.g. micro and ultra-filtration, this is a subject of crucial importance to overcome the problem of existence of ECs in nature.

Chapter 2: Literature Review and Thesis Motivation and Objectives

2.1. Emerging Contaminants

Emerging contaminants (ECs) are chemicals and pathogens of particular concern in recent years due to their emergence in the environment by anthropogenic activities, mainly industrial and technological processes. Of the most concerning ECs to exist in nature, pharmaceuticals and endocrine disrupting chemicals (EDCs) are critical, due to their reported health impacts and resilience against conventional treatment steps. It has recently been reported that as many as 200 unique pharmaceuticals have been detected in river waters and secondary treated wastewaters around the world with concentrations ranging from 10 ng/L up to 6.5 mg/L (e.g. ciprofloxacin) [15]. This continuous human and animal exposure to these pharmaceuticals can have an impact on vital organs such as the kidneys or liver, along with other reported health effects. Also, the propagation of antibiotic-resistant bacteria as a result of continuous exposure of bacterial cells to antibiotics is of mounting concern [15].

EDCs are chemicals used in the manufacture of household products and reportedly show toxic effects upon prolonged exposure. The production quantities of some EDCs (e.g. Bisphenol A), are significant. It has been reported that over six billion pounds of bisphenol A are produced daily worldwide [20]. Bisphenol A is frequently used as a starting chemical in many industries including the production of adhesives, plastics, powder paints, thermal paper and paper coatings, and epoxy resins among many others. The reported concentrations of bisphenol A in wastewater are 0.07 to 150 µg/L, moreover bisphenol A was reported to exist in primary and secondary treated wastewater sludge in concentrations of 0.013 to 0.24 µg/g [20-22].

2.2. Advanced Oxidation Processes

Due to the existence of harmful and resilient chemicals in water sources, the research community has dedicated time and effort to provide effective, innovative methodologies for the removal and elimination of these chemicals from water. Advanced oxidation processes (AOPs) have been widely explored in the fields of water and wastewater treatment due to the capacity of these methods to leverage powerful oxidative pathways, leading to efficient degradation and removal of recalcitrant contaminants. Different AOPs that have been explored and shown some

successful outcomes include ozonation, UV photolysis, UV photocatalytic oxidation (UV/O₃ or UV/H₂O₂), and electrooxidation. In the following subsections, a brief overview of each method is provided.

2.2.1. Ozonation

Ozonation is the process of sparging wastewater with a controlled amount of reactive ozone gas, which decomposes into reactive hydroxyl radicals (OH[•]) with oxidative power. Ozone can attack and interact with organic molecules in two separate phases, the gas phase, in which ozone gas (O₃) molecules can react with C=C bonds via a cycloaddition, forming unstable adducts. The formed ozone adducts then tend to decompose, forming oxides. Another pathway for ozone interaction is the aqueous phase, where ozone decomposes in water forming hydroxyl radicals that can interact with organic molecules in different pathways including oxygen addition, hydrogen abstraction, and electron transfer, leading to oxidation and subsequently the degradation of the organic molecules [23-25].

Controlling water pH can control the norm of ozone and its interaction with water contaminants. At acidic pH, it is expected that ozone will be more stable in the gaseous phase ozone (O₃), while in alkaline pH it is anticipated that ozone (O₃) will be more unstable and will decompose into OH[•] radicals and other oxidants, according to equations (2-1) and (2-2) [24];

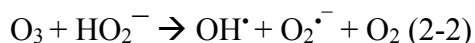


Figure 2-1 shows the mechanism of interaction of gaseous phase ozone with unsaturated hydrocarbons. The reaction of ozone starts with attacking the cis C=C bonds in the organic molecule, leading to the formation of unstable ozonide, which decomposes forming oxide products[23].

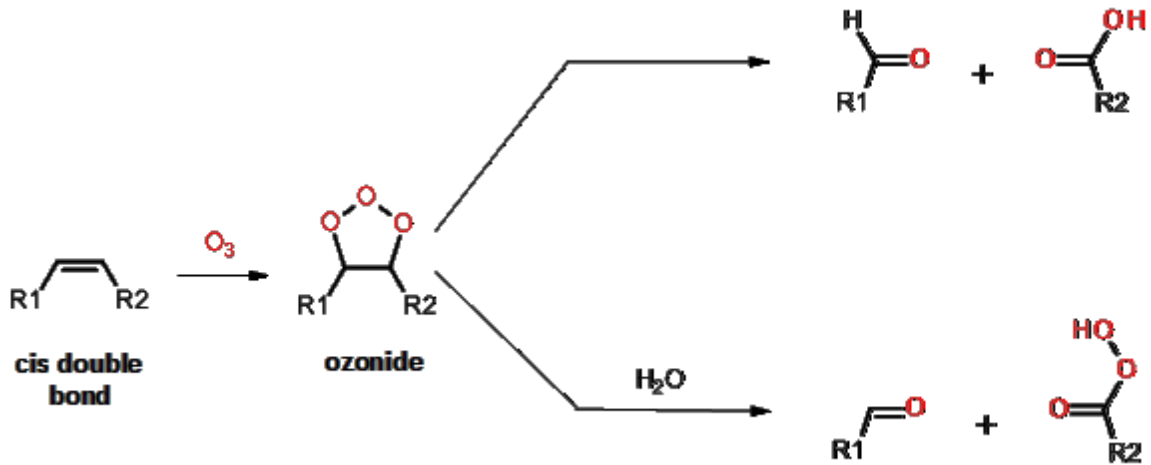


Figure 2-1. Reaction of gaseous phase ozone with C=C forming unstable ozonide followed by the formation of oxide by-products

The ozonation system is not restricted to, but in most cases consists of a sedimentation tank connected to a treatment tank, to which an inlet from an ozone generator is connected. The function of the ozone generator is to create ozone (O₃) from the UV splitting of diatomic oxygen (O₂), and coupling of the formed reactive monoatomic oxygen (O) with diatomic oxygen in a separate chamber to form ozone (Figure 2-3 shows ozone formation reactions in ozone generator). The formed ozone is then sparged into the treatment tank containing the contaminated water where it is allowed to react with the contaminants. Ozonation can disinfect water and oxidize organic and inorganic contaminants. Treated water effluent is collected from the treatment tank (Figure 2-2) and stored in a treated water storage tank. The successive tanks are connected by tubing, and the water flows by application of pressure.

Disinfection takes place mainly through the interaction of microorganisms with gaseous phase ozone, while the oxidation process occurs through the interaction of the organic and inorganic content with powerful hydroxyl radicals [24, 26-28]. Augmentation of hydroxyl radicals during ozonation can be assisted through the addition of adequate amounts of hydrogen peroxide to the system, which can interact with ozone leading to the further formation of hydroxyl radicals [29].

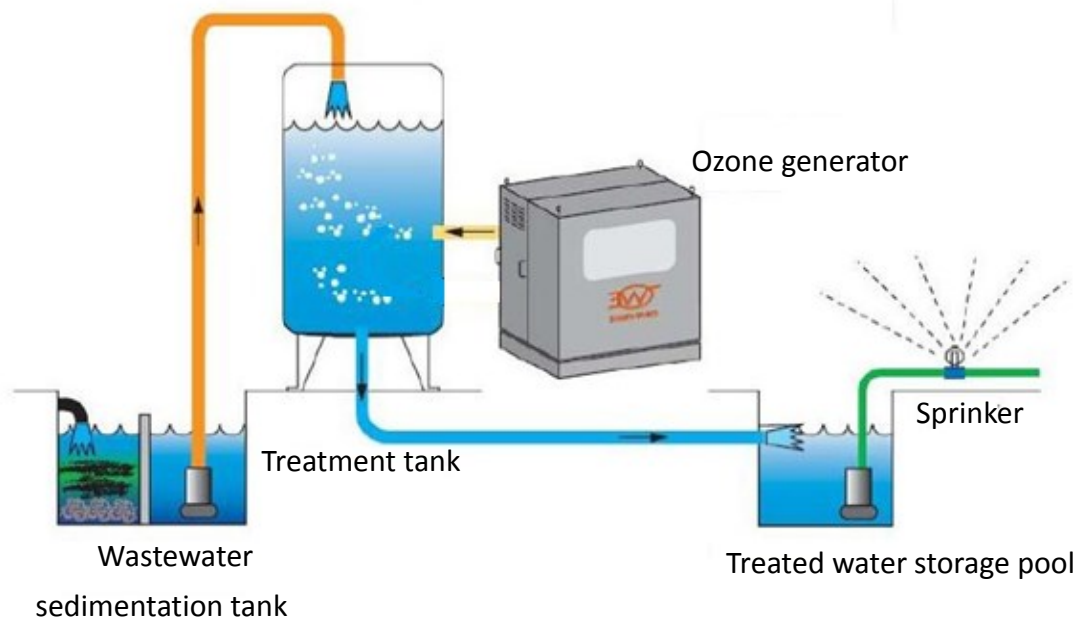


Figure 2-2. Wastewater ozonation treatment system, figure from [30]

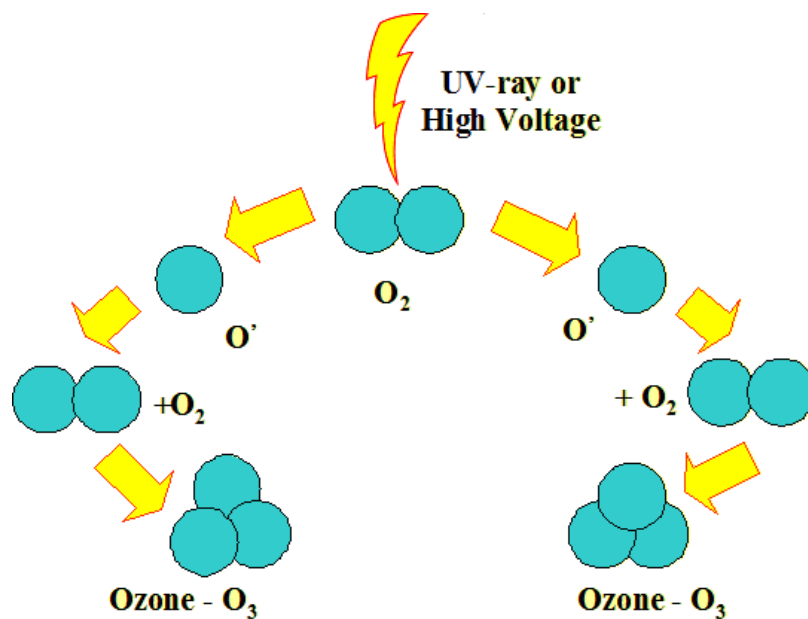


Figure 2-3. Ozone generation reaction catalyzed by UV-ray or high voltage application, figure from [31]

Lin et al. [29] studied the ozonation and hydrogen peroxide assisted ozonation (O_3 and O_3/H_2O_2) treatment of two groups of antibiotics, sulfonamides and macrolides, which are reported to exist in treated wastewater and receiving water bodies. They observed that removal kinetics were faster for sulfonamide as compared to macrolides, due to the aromaticity and presence of more C=C in sulfonamides. The removal kinetics for the molecules containing the unsaturated C=C, (e.g. sulfamethoxazole, sulfadimethoxine and sulfamethazine) took place faster and more efficiently at low pH, due to the predominance of the gaseous phase ozone that can efficiently attack C=C bonds.

The removal of erythromycin, with its fully saturated structure, was more efficient at a higher pH or with the addition of H_2O_2 , due to a higher production of unselective hydroxyl radicals in these conditions [29]. Hollender et al. [32] studied the elimination of pharmaceuticals, among numerous micropollutants, via ozonation followed by sand filtration. They found that compounds containing aromatic rings, amine functions, and double bonds, such as sulfamethoxazole, diclofenac, and carbamazepine were more readily removed by ozonation and with faster kinetics than among other observed micropollutants. They also observed that the production of harmful by-products, like N-nitrosodimethylamine, was very low and in the acceptable range of potable water standards [32].

In most cases, this process has shown positive outcomes with a high removal efficiency, however, on the other hand, it requires a lot of mechanical parts including tubing, pumps, valves, and electrical connections in addition to the multi-tank system and maintenance. Moreover, the process consumes a high amount of energy, due to the general operational energy requirement. In some cases, this process requires long operation times to achieve complete removal of target contaminants, especially at low influent concentrations.

2.2.2. UV photolysis

Ultra-violet photodegradation or UV photolysis is the process of subjecting an organic substrate to a specific wavelength of non-visible light radiation (254 nm), resulting in the excitation of the electrons of the organic molecules to the outermost energy level, making them more reactive with surrounding water species, such as dissolved oxygen. Subjecting the organic molecules to the 254 nm light, which is the optimum UV wavelength of light absorbance by natural organic matter

(NOM), can also lead to homolysis of the organic molecules forming reactive organic radicals that can interact with molecular oxygen. Indirect photolysis is another pathway that can take place during UV photolysis and is commonly detected with dissolved organic matter (DOM), in which DOM can be excited to a triplet state ($^3\text{DOM}^*$) that has high reactivity and can interact with other organics and degrade or deform them. In this pathway the DOM are called photosensitizers, and they can also excite diatomic oxygen, through energy transfer, into more reactive singlet molecular oxygen ($^1\text{O}_2$) [33].

The UV photolysis setup consists of a reactor tank with a thermostat and thermometer for water temperature adjustment and monitoring. This reactor tank is subjected directly to a UV lamp (Figure 2-4).

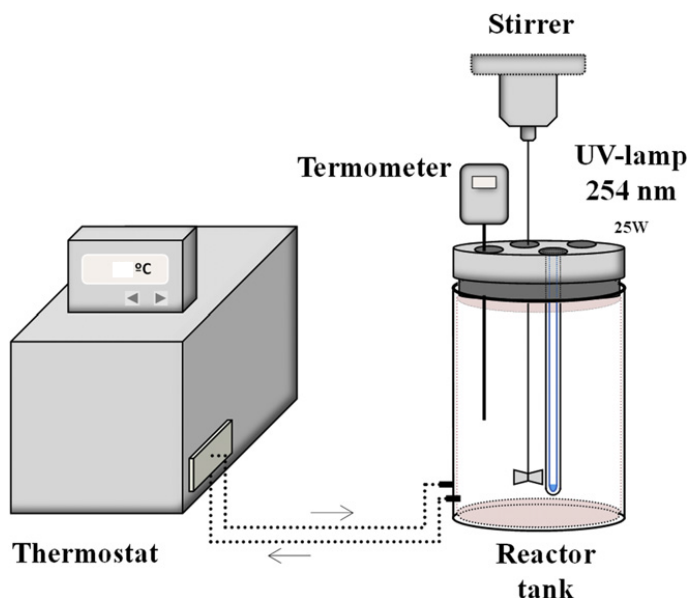


Figure 2-4. UV photolysis bench scale reaction system, figure from [34]

According to previous studies, UV photolysis is one of the least successful treatment methods for considerable removal of organic contaminants. The limited outcomes of this process are due to the lack of a powerful oxidizing species, as this process mainly depends on setting the organic molecules into a reactive state with the hope to interact with less reactive oxidizing agents (i.e. molecular oxygen) [34-41]. De la Cruz et al. [42] studied the removal of 22 micropollutants, including pharmaceuticals of emerging concern, using a pilot-scale UV photolysis unit equipped

with reservoirs of ferric chloride and hydrogen peroxide, for the application of UV/H₂O₂ and photo-Fenton process. They concluded that an overall removal percentage of only 26% could be achieved by UV photolysis for all studied compounds and that the removal percentage was collectively 33% for the five targeted compounds: carbamazepine, diclofenac, sulfa-methoxazole, benzotriazole, and mecoprop. Only two of the studied micropollutants (diclofenac and ketoprofen) could be removed to less than 10%, while no other individual pollutant achieved more than 48% removal [42].

Kim et al. [43] studied the removal of 41 pharmaceuticals, including 12 antibiotics, using UV and UV/H₂O₂, finding that significant removal by UV photolysis alone could be observed for very few pharmaceuticals such as ketoprofen, diclofenac, and antipyrine, and only with the introduction of significantly high dose of UV light. However, H₂O₂ assisted photolysis could achieve greater than 90% removal for 39 of the 41 pharmaceuticals at lower UV dosages [43].

2.2.3. UV photocatalytic oxidation

In the UV photocatalytic oxidation process, an enhancement in the production of powerful oxidizing agents (i.e. hydroxyl radicals) from the decomposition of oxidants (e.g. ozone and hydrogen peroxide) takes place by the photolysis of the introduced oxidants in the reaction system. Therefore, this process is aimed at advancing and improving the oxidative performance of other procedures (e.g. ozonation, hydrogen peroxide oxidation, and UV photolysis). In UV photocatalytic oxidation, a UV lamp of a specific wavelength is placed within the reaction system in which the oxidant has been introduced. The introduced oxidant is subjected to the UV light, which excites the compound, leading to its ready decomposition into other oxidizing agents as hydroxyl radicals, which have a superior oxidative power. The formed hydroxyl radicals then interact with and degrade the organic contaminants.

This process has proven successful in removing various refractory organic contaminants with extraordinary removal efficiency. However, this process requires complex installations including ozone generators, electrical connections, tubing, valves, pumps, and ozone scrubbers. Figure 2-5 shows a diagram demonstrating a UV photocatalytic degradation setup. The use of hydrogen peroxide may require, in cases, the incorporation of Fenton's chemistry into the process, which is the catalyzed production of hydroxyl radicals from hydrogen peroxide by the use of

metallic elements like iron or copper ions, in order to further improve the process outcomes [34, 42, 44, 45], combining the Fenton chemistry with UV photocatalytic oxidation is known as photo-Fenton process. The addition of a subsequent multi-reaction tank system for the achievement of higher removal capacity of emerging contaminants from wastewater can be an additional shortcoming to the economic efficiency of the process [43].

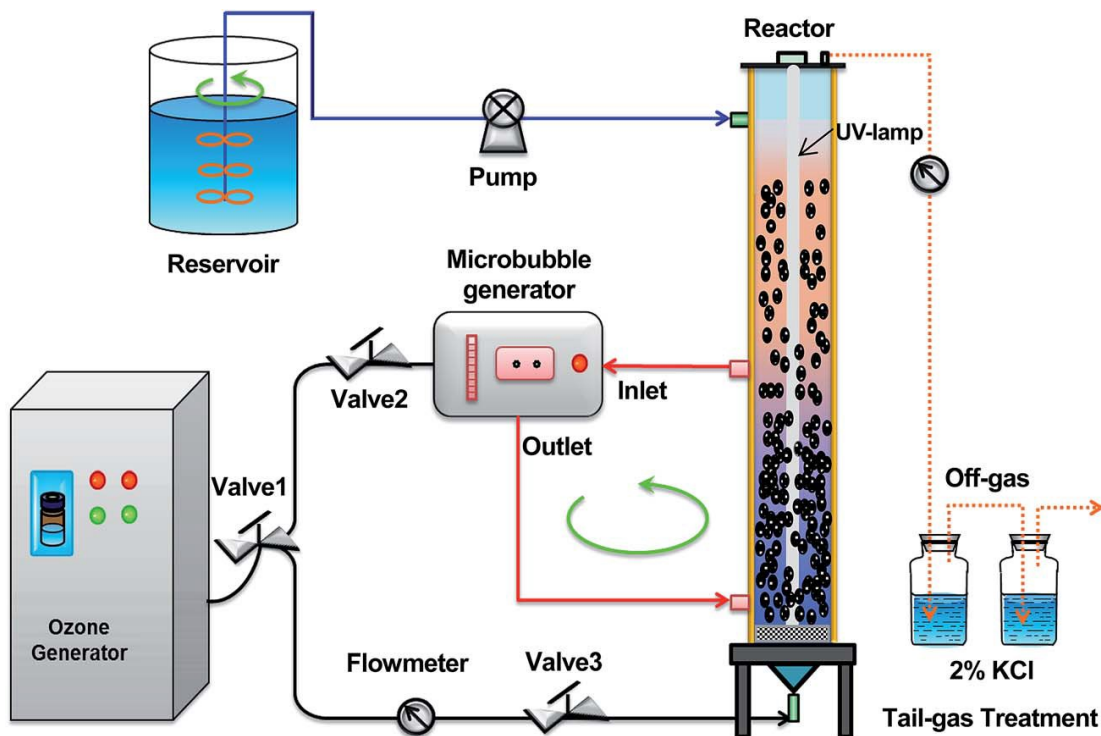


Figure 2-5. UV photocatalytic oxidation (UV/O₃) unit, figure from [44]

Rosenfeldt et al. [37] studied the removal of three EDCs: bisphenol A, ethinyl estradiol, and estradiol, using UV photolysis and UV/H₂O₂. They observed that during UV/H₂O₂, degradation efficiency was greatly enhanced due to the production of hydroxyl radicals with irradiation below 300 nm as compared to UV photolysis that had a lower degradation efficiency and only at UV ranges of 220-230 or 270-290 nm. The second-order rate constants for the UV/H₂O₂ were developed through a competition kinetics model to determine hydroxyl radical concentration as a final result, and the rate constants showed fast kinetics for the decomposition of the 3 EDCs [37].

It was reported that the combination of UV during ozonation is not always successful. Esplugas et al. [46] investigated the efficacy of the different AOPs: O₃, O₃/H₂O₂, UV, UV/O₃, UV/H₂O₂, O₃/UV/H₂O₂, and Fe²⁺/H₂O₂, for the removal of phenol. They concluded that none of the ozone-assisted processes (O₃/H₂O₂, UV/O₃, and O₃/UV/H₂O₂) could lead to any improvements as compared to sole ozonation, with the best outcome at high pH. It was concluded that the inclusion of hydrogen peroxide and UV had a slight adverse effect on the ozonation results. This result indicated that the assisted ozonation processes might have an inhibitory effect on the hydroxyl radicals produced from ozone, rather than an enhancing effect, or negatively affect the stability of gaseous phase ozone. For the UV/H₂O₂, it was observed that the degradation rate was five times faster than that of UV photolysis, and the Fe²⁺/H₂O₂ had the highest degradation rate among all processes, due to the incorporation of Fenton's chemistry [46].

2.2.4. Electrooxidation

Electrooxidation, or electrochemical degradation, is a technology in wastewater treatment that relies on the application of voltage or current to degrade aqueous organic contaminants. The degradation pathways in electrooxidation are numerous, and not all pathways are clearly known, though, there exists a vast body of research discussing this process in wastewater treatment. The major known electrochemical pathways are direct and indirect oxidation. Electrochemical oxidation takes place when two conductive materials (electrodes) are placed within the reaction medium and are connected to an external power supply for voltaic (potentiostatic mode) or current (galvanostatic mode) application.

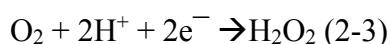
Direct oxidation takes place when organic molecules are adsorbed on the positively charged electrode (anode) and are oxidized via direct electron transfer from the adsorbed molecules into the anode, without the involvement of oxidative intermediates. Indirect oxidation takes place when organic molecules react with oxidative intermediates through a chemical reaction and are oxidized by the intermediates through alternate reaction pathways, like oxygen addition, electron transfer, or hydrogen abstraction [47-56].

One of the key factors affecting the electrochemical performance of the electrooxidation process is the electrode material, which has a major influence on the production of electroactive species and the limitation of parasitic or unwanted reactions. Heterogeneous water oxidation and

oxygen evolution is an extreme unwanted (parasitic) reaction, causing the consumption of electrode surface active sites, loss of reactive oxygen, and increased surface hydrophilicity. Therefore, this parasitic reaction limits hydrophobic adsorption, thus restricting the direct oxidation, and increasing energy consumption. Electrode materials can be classified into active electrode materials (e.g. platinum (Pt) and stainless-steel), and inactive electrode materials (e.g. boron doped-diamond (BDD), tin dioxide (SnO₂) and lead dioxide (PbO₂)). Inactive electrodes are preferred for use in the electrooxidation of organic contaminants due to their high overpotential for water oxidation and oxygen evolution. Thus, they can provide a wider potential window for oxidation of organics. Moreover, inactive electrodes provide a better catalytic surface for the production of powerful oxidants like hydroxyl radicals [55-62].

One of the major drawbacks of the electrooxidation process for wastewater treatment is the high cost of manufacture for inactive electrodes, plus the need for multi-electrode systems to achieve maximum removal efficiency. Also, the process may require extended operation hours to achieve complete removal of trace organic contaminants.

A widely employed advancement to electrooxidation is the electro-Fenton advanced oxidation, in which Fenton's chemistry is initiated during the electrooxidation process aiming to enrich the system with hydroxyl radicals [63-67]. In the electro-Fenton process, hydrogen peroxide decomposes into hydroxyl radicals under the catalytic effect of dissolved iron species in the media. An advantage of the electro-Fenton method over conventional Fenton oxidation is that the in-situ generation of hydrogen peroxide can take place within the reaction media from the reduction of dissolved oxygen, according to equation (2-3) [66, 68];



Electrooxidation is an advantageous process as compared to traditional chemical and biological oxidation processes, in that electrooxidation does not overly require the addition of chemicals that chemical oxidation processes do (e.g. permanganate oxidation and conventional Fenton oxidation). Electrooxidation can work with hazardous industrial chemicals, which can suppress biological processes by killing or inactivating bacteria. Furthermore, and unlike biological methods, electrooxidation does not have a specific temperature requirement and has faster kinetics. A further drawback of the electrooxidation process is the high-energy consumption,

which is mainly due to mass transfer limitations. Figure 2-6 shows a representation of a water treatment unit using an electrochemical oxidation process.

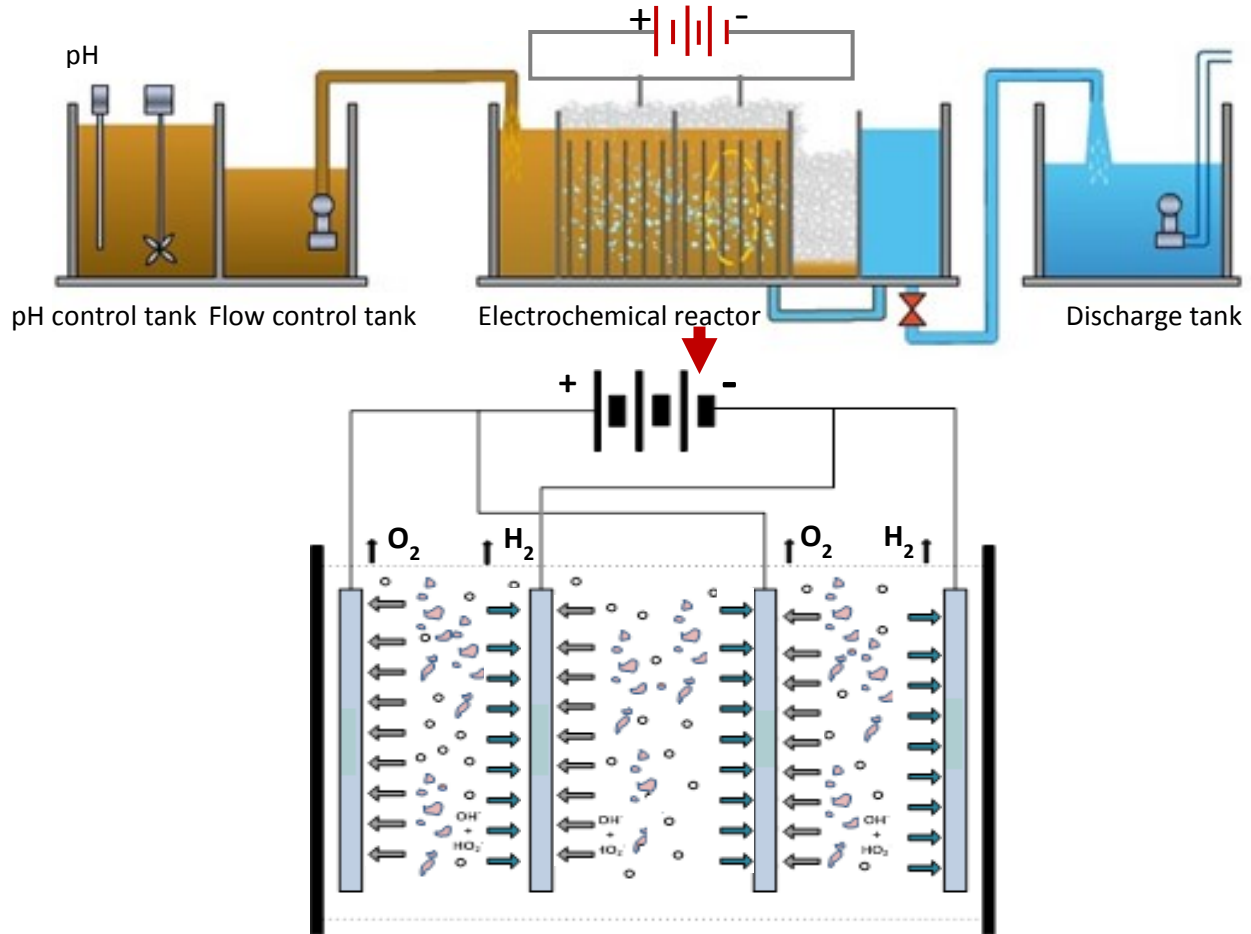


Figure 2-6. Electrochemical oxidation (batch electrolysis) unit and reaction system for wastewater treatment, figure modified from [69]

Ciríaco et al. [62] studied the electrodegradation of ibuprofen on Pt/Ti/PbO₂ and Si/BDD anodes. They concluded that anodic oxidation was very efficient in the degradation of ibuprofen using both materials, with slightly better removal efficiency and current efficiency with BDD at lower current densities. It was found that through increasing the current density by 10 mA/cm², a

significant deterioration in the current efficiency was observable with the BDD electrode. This indicated that water oxidation and oxygen evolution increased, leading to the loss of the reactive hydroxyl radicals formed at the BDD surface. However, in case of the Pt/Ti/PbO₂ electrode, increasing the current density by the same value did not alter the current efficiency to a great extent, indicating that oxidation is predominantly diffusion controlled on the Pt/Ti/PbO₂ electrode, and that oxidation of ibuprofen takes place predominantly at the electrode surface [62].

Cui et al. [59] studied the removal of bisphenol A using four different electrodes, Ti/BDD, Ti/Sb–SnO₂, Ti/RuO₂ and Pt, in a batch electrolysis system. They concluded that BDD and Ti/Sb–SnO₂ had the highest effectiveness in eliminating the contaminant and reducing its toxicity at a current density of 10 mA/cm², due to the electrodes' higher potential for oxygen evolution and a higher anodic potential for BPA oxidation. The capacity of the two inactive electrodes (BDD and Ti/Sb–SnO₂) in producing reactive hydroxyl radicals at their surfaces, allowed them to have a much higher oxidation power as compared to Ti/RuO₂ and Pt. However, when the current density was increased to 50 mA/cm², the instability of the Ti/Sb–SnO₂ electrode was indicated by a gradual increase in output voltage, which suggested the deactivation of the SnO₂ layer of the electrode and a general structural deterioration. Passivation of the Ti/Sb–SnO₂ electrode was also observed, all of which point to the superiority and durability of BDD and its ability to perform better in a broad range of current applications [59].

Murugananthan et al. [57] studied the anodic oxidation of bisphenol A using BDD as an anode in a galvanostatic mode of operation. They found that the rate of mineralization of bisphenol A is highly dependent on the applied current. Operation time to reach total mineralization of the contaminant was observed to decrease significantly with an increase in current density, which was attributed to the enhanced generation of hydroxyl radicals at increased currents and improved mass transfer kinetics. They also deduced that electrolytic species plays a major role in the indirect oxidation of the target contaminant (i.e. the formation of reactive peroxodisulphate (S₂O₈²⁻) from the oxidation of sulfate ions). From cyclic voltammetric studies, the authors observed a clear fouling effect of bisphenol A on the BDD electrode during electrochemical degradation, indicated by a drop in oxidation current peaks with subsequent sweep cycles. This fouling effect could be controlled and removed by increasing the hydrophilicity at the BDD electrode surface through raising applied current, which results in anodic polarization in the potential region for water

oxidation on BDD electrode (>2.3 V), and thus decreasing the surface propensity to polymeric fouling. Therefore, the solution to this problem would require a high potential application, which would lead to loss of considerable amounts of reactive hydroxyl radicals into oxygen, a substantial disadvantage. The complete mineralization of bisphenol A during different applied conditions indicated that the main oxidation pathway is through interaction with hydroxyl radicals. In this study, pH also played a significant role in the process. At pH 10, it was observed that mass transfer kinetics were enhanced due to the deprotonation and increased negative charge on bisphenol A, which made the molecule more readily attacked by the electrophilic hydroxyl radicals. As well, in this study, a comparison between BDD, platinum, and glassy carbon electrodes showed that BDD is the best in removing the target contaminant under different applied conditions [57].

Flox et al. [56] investigated the performance of the BDD anode in comparison to a PbO_2 anode in the removal of cresols during electrochemical degradation. The authors concluded that overall, BDD showed more degradation power for the target contaminant, attributed to its ability to generate more hydroxyl radicals at its surface, which becomes freer and unselective at the surface. Whereas PbO_2 generated more adsorbed hydroxyl radicals to its surface, which in general known to interact slower and more selectively with adsorbed organic molecules [56, 70, 71]. However, the degradation rate was found to be slightly faster on PbO_2 as compared to BDD, mainly attributed to a greater readiness or faster kinetics in the interaction of $\text{PbO}_2(\text{OH}^\bullet)$ with m-cresols and its formed by-products than $\text{BDD}(\text{OH}^\bullet)$ [56].

2.3. Thesis Objectives and Description of the Implemented Process

Electrochemical filtration technology has advantageous characteristics as compared to other AOPs referred to in the previous section. This process shows uniqueness in the combination of the advantages of the processes mentioned above, and at the same time avoiding most of their limitations. Electrochemical filtration processes require only simple installations and automation, can overcome solute transfer limitations, resulting in longer operational times, and can provide in-situ generated reactive electrolytic species with oxidative capabilities. Electrochemical filtration is a multi-aspect, yet simple process that combines adsorptive filtration and electrochemical degradation, offering excellent overall treatment capacity, yet significant efficiency.

In this thesis, two different modes of electrochemical filtration were studied with the aim of delivering a comprehensive overview of electrochemical filtration. The “dead-end” mode was investigated with the aim of investigating the flow-through mechanism for the removal of two contaminants of emerging concern, ibuprofen and bisphenol A in an electrochemical filtration process. The bench-scale dead-end setup used is a simple combination of two electrodes, one a metallic cathode and another comprised of multiwalled carbon nanotubes (MWNTs) as a carbon based filter anode. The two electrodes were constructed within a flow through filtration holder made of polypropylene and connected to an external power supply using wires and clips (Setup images can be found in Appendix D). The ability of dead-end electrochemical filtration for the removal of the two ECs of growing concern, ibuprofen and bisphenol A, has not been previously discussed. Moreover, dead-end electrochemical filtration’s ability to removing other various ECs found in different source waters has not been shown enough concern in the literature. Therefore, the main objectives of the dead-end electrochemical filtration study in this thesis were: to explore the capacity of the electrochemical filtration process in removal of these two contaminants, to understand different factors that contribute to process performance, the adjustment of the various critical parameters to reinforce the prospects of this process, and to increase the process potential and overcome its limitations.

Crossflow mode was also employed in an electrochemical filtration process. Crossflow electrochemical filtration setup consisted of a flat sheet holder with one inlet (Feed) and two outlets (Permeate and concentrate). MWNTs-blend buckypaper, which is a blend of MWNTs of different dimensions possessing resistance to shear flow, was employed as a dual membrane electrode (Setup images can be found in Appendix D). This crossflow setup was not previously used in an electrochemical filtration process for the aim of removing ECs of emerging concern. Rather, crossflow mode has been thoroughly experimented in micro and ultrafiltration processes for wastewater treatment in previous studies, with the purpose of providing a membrane antifouling capacity under the shear flow. Therefore, in this study, a primary objective was to test the shear flow mechanism in a crossflow electrochemical filtration process for the removal of ibuprofen and bisphenol A and to compare the findings to those from dead-end electrochemical filtration.

The investigation of carbon nanotubes (CNTs), their capacity, as well as limitations, as a filtration substrate, and electrochemical filtration was given more concern and deeper insight in

this study as compared to previous studies. MWNTs were employed as electrochemical membrane electrodes and filtration materials. The choice of MWNTs was due to the famously advantageous characteristics of a large specific surface area, excellent conductivity, and adsorptive affinity to organics.

Chapter 3: Electrochemical Efficacy of a Carboxylated Multiwalled Carbon Nanotube Filter for the Removal of Ibuprofen from Aqueous Solutions under Acidic Conditions

Abstract

In this chapter, insights into the efficiency of a functionalized multiwalled carbon nanotube filter for the removal of an anti-inflammatory drug, ibuprofen, through conventional filtration and electrochemical filtration processes, is provided. A comparison was made between carboxylated multiwalled carbon nanotubes (MWNTs-COOH) and pristine multiwalled carbon nanotubes (MWNTs) to emphasize the enhanced performance of MWNTs-COOH for the removal of ibuprofen using an electrochemical filtration process under acidic conditions. Ibuprofen-removal trials were evaluated based on absorbance values obtained using a UV/Vis spectrophotometer, and possible degradation products were identified using liquid chromatography-mass spectrometry (LC-MS). The results exhibited near complete removal of ibuprofen by MWNTs-COOH at lower applied potentials (2 V), lower flow rates, and under acidic conditions, which can be attributed to the generation of superoxide species and their active participation in the simultaneous degradation of ibuprofen, and its by-products, under these circumstances. At a higher applied potential (3 V), the possible involvement of both bulk indirect oxidation reactions, and direct electron transfer were hypothesized for the removal behavior over time (breakthrough). At 3 V under acidic conditions, a near 100% elimination of the target molecule was achieved which can be attributed to the enhanced generation of electroactive species toward bulk chemical reactions and possible contributions from direct electron transfer under these conditions. The degradation by-products of ibuprofen were effectively removed through the allowance of longer residence time during the filtration process. Moreover, the effect of temperature was studied, yet showed a non-significant effect on the overall removal process.

Keywords: Multiwalled carbon nanotubes, electrochemical filtration, electrooxidation, ibuprofen

3.1.Introduction

Carbon nanotubes (CNTs) have been shown to be uniquely successful in their ability to remove organic contaminants and pathogenic microorganisms through filtration and electrochemical filtration [72-76]. A comprehensive study of the aqueous dye oxidation reactive transport mechanism during electrochemical filtration was conducted by Liu et al. [74]. In this study, a six-fold enhancement of mass transfer was observed during electrochemical filtration as compared to that observed during batch electrolysis. This improvement was related to the convection mass transport of organic molecules to the electrode surface under hydrodynamic flow [74]. In another study, it was reported that multilayer CNTs supported on a polyvinylidene fluoride substrate, integrated to provide more stability and flexibility for the filter, can be efficiently employed for the mineralization of nitrobenzene by sequential reduction/oxidation processes, using CNTs as both the anode and cathode material [76]. Moreover, Rahaman et al. [72] reported on the efficiency of a CNT filter for the removal and inactivation of viruses through electrodisinfection.

The adsorptive ability of CNTs for the removal of various organic contaminants from aqueous solutions has also been previously investigated. Shao et al. [77] discussed the efficacy of MWNTs grafted with methyl methacrylate in the removal of 4,4'-dichlorinated biphenyl. They reported that such surface modifications could enhance the ability of MWNTs for the removal of the target molecule with an increased thermal stability due to strong adsorption of the model contaminant on the modified surface. The surface structure and the nature of CNTs related to the adsorption of organic molecules was also investigated by molecular dynamic (MD) simulations in a study investigating the adsorption of perfluorooctanesulfonate on single-walled carbon nanotubes (SWNTs). Factors such as the size of the CNTs and electrostatic interactions were observed to have significant influences on the affinity of adsorption. It was concluded that adsorption of perfluorooctanesulfonate on SWNTs was controlled by hydrophobic interactions[78]. Moreover, the useful application of CNTs as a substrate for the growth of boron-doped diamond (BDD), a widely used material for electrode fabrication in electrochemical wastewater treatment, was introduced, and a methodology to increase the double-layer capacitance, decrease impedance, and enhance the current collection of BDD was proposed[79].

The presence of pharmaceuticals in surface and ground water is an emerging concern due to their persistence and their harmful effects on human and aquatic ecology. Several pharmaceuticals (e.g., ibuprofen, naproxen, sulfamethoxazole, and iopromide) have been reported to escape primary treatment and exhibit a resistance to complete removal in subsequent biological treatments[80]. Antibiotics have been shown to be resistant to conventional biological methods of wastewater treatment; therefore, an efficient methodology for the removal of antibiotics requires the application of other advanced treatment processes.

Electrochemical degradation is a subject of ongoing interest for researchers working in the field of environmental science and engineering. The complete removal of the antibiotic sulfachloropyridazine by electrooxidation was investigated on both BDD and platinum anodes, and it was shown that complete elimination of the antibiotic could be achieved on both types of electrode materials under the conditions of Fenton chemistry with sufficient residence time [63]. Electrochemical degradation of nitrobenzene was also successfully achieved using fabricated titanium dioxide nanotubes/antimony-doped tin dioxide/lead dioxide electrodes with enhanced electrochemical stability, increased potential for oxygen evolution, and enriched formation of hydroxyl radicals for the electrooxidation of the carcinogenic molecule [54]. Motoc et al. [81] investigated the electrochemical degradation of ibuprofen (2-[4-(2-methylpropyl)phenyl]propanoic acid) on multiwalled carbon nanotube/epoxy (MWCNT) and silver-modified zeolite/multiwalled carbon nanotube-epoxy (AgZMWCNT) composites and found that AgZMWCNT provided better electrical conductivity, larger active surface areas, and better electrooxidative removal performance of ibuprofen than MWCNT. However, studies on the efficiency of CNTs for the removal of persistent organic molecules, such as ibuprofen by electrochemical filtration, are notably absent in the literature. Electrochemical filtration removes contaminants through adsorptive filtration, as well as electrochemical degradation of the target molecules through applied voltage. Moreover, this process overcomes solute transfer limitations faced by current batch electrochemical processes, in which the contaminants are degraded through direct electron transfer onto the electrode surface. Therefore, this method is advantageous over conventional batch electrolysis, in regards to time requirements and overall energy efficiency.

The current study aimed to investigate and provide suitable conditions for the removal of ibuprofen from aqueous solutions via an electrochemical filtration process with CNTs. This

removal of ibuprofen through electrochemical filtration has not previously been tested, even though electrochemical filtration has been shown to be an innovative technology with simple installation requirements and promising outcomes [73, 76].

The goals of this research were twofold. The first was to establish appropriate pH conditions and filter type and therefore accommodate suitable surface interactions between the ibuprofen molecules and the CNTs, such that filtration capacity is increased. Secondly, applied voltage was tested for the removal of the target molecule, observing the contributions of both direct electron transfer from ibuprofen molecules to CNTs under the applied positive potential, and bulk oxidation by the generation of electroactive species. To investigate the effect of residence time on effective ibuprofen removal, the residence time of ibuprofen molecules within the filter body was increased (low flow rate) at these applied potential (2 V) conditions to allow for optimal and complete removal of the target molecule. A comparison was also made between pristine MWNTs and MWNTs-COOH to gauge the difference in total removal of ibuprofen from aqueous solutions. Throughout the course of the study, MWNTs-COOH consistently exhibited better ibuprofen removal performance under acidic conditions; these conditions led to the almost complete elimination of ibuprofen at applied DC potentials of 2 and 3 volts.

3.2. Materials and Methods

3.2.1. Materials

Multiwalled carbon nanotube filters were prepared using both pristine MWNTs (99.8% purity) and carboxylated MWNTs (MWNTs-COOH) (> 95% purity and 1.8% COOH groups by weight), purchased from Cheap Tubes Inc., Cambridge port, VT, USA. Upon further investigation, the purity was found to be $\geq 98\%$ for both MWNTs types, as determined by TGA. Both types of MWNTs have an outer diameter (OD) of 10–20 nm, inner diameter (ID) of 3–5 nm, and a length of 10–30 μm (as specified by the manufacturer). As observed by SEM, the OD ranges from 10-35 nm. An electrical conductivity of >100 S/cm was reported by the manufacturer, and the specific surface area was determined to be 125.04 m^2/g for MWNTs and 133.03 m^2/g for MWNTs-COOH. Ibuprofen ($\text{C}_{13}\text{H}_{18}\text{O}_2$) with $\geq 98\%$ purity and a molecular weight of 206.29 g/mole was purchased from Sigma-Aldrich (Oakville, ON, Canada). Sodium chloride and hydrochloric acid were both $\geq 99\%$ trace purity, purchased from Sigma-Aldrich (Oakville, ON, Canada) and were used in the

preparation of the background solutions. Nitro blue tetrazolium chloride (assay 98%), taurine (assay $\geq 99\%$), and hydrogen peroxide were purchased from Sigma-Aldrich (Oakville, ON, Canada) and were used for superoxide and hypochlorous acid assays. MWNTs and MWNTs-COOH suspensions were prepared in $\geq 99\%$ purity dimethyl sulfoxide (DMSO), purchased from Fisher Scientific (Ottawa, ON, Canada). Magnesium sulfate, sodium bicarbonate, calcium chloride, potassium dihydrogen phosphate, ammonium chloride, and trisodium citrate were purchased from Fisher Scientific (Ottawa, ON, Canada) and were used for synthetic secondary wastewater effluent preparation. 5- μm polytetrafluoroethylene (PTFE) membranes were purchased from Millipore (Etobicoke, ON, Canada) and used as filter substrates.

3.2.2. MWNTs and MWNTs-COOH Characterization

Thermogravimetric analysis (TGA) was performed on both MWNTs types using TA instruments, Trios V3.3 (Waters LLC, New Castle, DE, USA), to investigate the actual purity and stability. The analysis was performed as described by Gao et al. [82], where MWNTs and MWNTs-COOH were subjected to step-wise temperature elevations of $10^\circ\text{C min}^{-1}$, from room temperature, up to 150°C and kept at 150°C for 30 minutes, then temperature was again elevated at the same rate of $10^\circ\text{C min}^{-1}$, up to 1000°C , where it was maintained for another 30 minutes. Specific surface area, pore volume, surface area, and volume distribution were characterized using Brunauer–Emmett–Teller (BET), Quantachrome Autosorb Automated Gas Sorption System, Autosorb 1 (Boynton Beach, Florida, USA). This analysis used nitrogen gas, with an outgas temperature of 100°C and time of 2.5 hours, bath temperature of 77.3°C , and analysis time of 1054.1 minutes. Surface morphology analyses were performed using Scanning electron microscopy (SEM) and Energy dispersive X-ray (EDS), FEI Inspect F-50 FE-SEM with EDAX Octane Super 60 mm² SDD and TEAM EDS Analysis System (Dawson Creek, Oregon, USA).

3.2.3. Cyclic Voltammetry

Cyclic voltammetry was performed using an 8 channel Multi-Potentiostats + Frequency Analyzer (MPFA) 1470/1255B, Solartron Instruments (Hampshire, United Kingdom). The experiments were performed using 0.84 mg/cm^2 MWNTs and MWNTs-COOH filters as working electrodes, perforated stainless steel as a counter electrode, and Ag/AgCl (1 M KCl) (Pine

Research Instrumentation, Durham, NC 27705, USA) as the reference electrode. The scan rate used was 50 mV/sec, and scan range was -1 to +1.5 V vs. Ag/AgCl for all experiments.

3.2.4. Electrochemical MWNTs and MWNTs-COOH Filter Preparation

Multiwalled carbon nanotube filters were prepared using the same protocol introduced by Rahaman et al. [72]. The preparation method included vacuum filtration of MWNTs and MWNTs-COOH suspensions in DMSO on 5- μm PTFE membranes (Millipore) as the substrate material. The amounts of MWNTs and MWNTs-COOH suspensions (0.5 mg/mL) used were 6 and 16 mL, resulting in surface loadings of 0.32 mg/cm² that provided a thickness range of 5.3 to 9 μm and 0.84 mg/cm² that provided a thickness range of 14.2 to 24 μm , as indicated by x-sectional view SEM imaging. The preparation process involved depositing the MWNTs or MWNTs-COOH onto the filter, rinsing once with ethanol (50 mL), rinsing once with a 50:50 ethanol and DI water (50 mL) solution, and finally rinsing six times (50 mL each) with DI water (a total 325 mL of DI water and 75 mL ethanol) to wash off all remaining organic solvent. The solution pH was adjusted to 2 during the MWNTs-COOH filter preparation process by using HCl to preserve -COOH groups in the protonated form and to mimic the experimental conditions. Freshly prepared MWNTs, and MWNTs-COOH filters were used for each experiment.

3.2.5. Electrolyte Solutions

Solutions of 10 mM NaCl and 10 mM HCl (pH 2) were used as background solutions for the electrochemical oxidation of ibuprofen on MWNTs and MWNTs-COOH, respectively. Electrolyte solutions were shown to enhance electrical conductivity during the electrochemical process as well as to provide electroactive chlorine species for indirect electrochemical oxidation reactions in the bulk solutions. Throughout the course of the experiments, the MWNTs-COOH as a filter material and 10 mM HCl (pH 2) as the background electrolyte were found to exhibit the highest output current (both instantaneous and steady-state), steady-state currents were at around 1-4 mA compared to MWNTs as the filter material and 10 mM NaCl at 1 mA, probably due to higher chlorine and hydrogen evolution. Conductivity calculations, based on the MWNTs and MWNTs-COOH total anode surface area and current outputs, were in the range of 4.1×10^{-7} - 6.3×10^{-7} S/cm² for a loading of 0.84 mg/cm² and 1.1×10^{-6} - 1.7×10^{-6} S/cm² for a loading of 0.32

mg/cm² (currents used for these calculations are instantaneous currents). The concentrations of the ibuprofen solutions were 1, 10 and 20 mg/L.

3.2.6. Filtration and Electrochemical Filtration

Both filtration without applying a DC potential and electrochemical filtration experiments with an applied DC potential were performed. The DC potential was supplied by an Agilent E364xA power supply (Agilent Technologies, Rockaway, NJ, USA). The filtration and electrochemical filtration setup used were the same as described in earlier studies [72-74, 83] for dead-end filtration, in which a carbon nanotube filter was employed as the anode material and a 0.1-mm-thick titanium ring used as an electrical connector. A rubber ring was used to separate the titanium ring from the cathode, which was a 0.05-mm-thick perforated stainless steel shim. The DC potentials applied during the electrochemical filtration experiments were 1, 2 and 3 volts, and the flow rates varied between 0.2, 1 and 2 mL/min, resulting in permeate flux values of 8.89×10^{-5} , 4.44×10^{-4} , and 8.89×10^{-4} L/m².h, respectively. The effect of temperature on the efficiency of the electrochemical filtration process was also investigated at two different temperatures, 23 and 40 °C. The cell temperature was controlled by placing the whole reaction medium (the cell and a collection beaker within a larger sealed beaker) in a water bath with an adjusted cell temperature of 40±2 °C. The cell temperature was measured using a thermometer.

3.2.7. Quantification of Ibuprofen Removal and Sample Analysis

The quantification of ibuprofen removal from aqueous solutions was performed using a PerkinElmer Lambda750UV/VIS spectrophotometer (Waltham, MA, USA). The influent and effluent ibuprofen concentrations in 2mL were calculated based on the absorbance values at 222 nm, and the removal percentages were determined from this data. The UV/VIS spectrophotometer detects as precisely as 0.0003 (AU) and the MDL (method detection limits) for ibuprofen is 0.027 mg/L. The MDL calculation was performed by taking the average standard deviation values and multiplying by a six-degree freedom factor of 3.143, as described by PerkinElmer. LC-MS analysis was performed using an Agilent 6210 ESI-TOF instrument (Agilent Technologies, Santa Clara, CA, USA) in positive ESI mode using MassHunter acquisition software (v B.02.00). The dual ESI source was operated with a capillary voltage of 4000 V and a nitrogen gas temperature of 350 °C with a flow rate of 12 L/min. The nebulizer pressure was maintained at 35 psi (241.3 kPa), and the

fragmenter and skimmer voltages were 100 and 60 V, respectively. The mass range was m/z 50–1000 with internal calibration using the reference masses m/z 121 and 922 in the Agilent reference-mass solution. All raw data was processed using MassHunter software after injecting 20 μL of influent and effluent samples. The injection gradient was as follows: initial conditions of 30% acetonitrile with a 1 min hold, up to 85% at 5 min, then 95% at 8 min and held for 1 min. The column was re-equilibrated at 30% acetonitrile for 4 min before the next injection. The mobile phases A and B were water and acetonitrile (both containing 0.1% formic acid), respectively, with a flow rate of 0.4 mL/min.

3.3. Results and Discussion

3.3.1. MWNTs and MWNTs-COOH Stability and Surface Morphology

SEM and EDS were performed on freshly prepared MWNTs and MWNTs-COOH filters as mentioned in the methods section. Fig.3-1 A and 3-1 C, show the SEM images of MWNTs and MWNTs-COOH, respectively. Carbon and oxygen content were examined by EDS (Figure 3-1 B and 3-1 D), for MWNTs and MWNTs-COOH, respectively. The results show a weight percent of 97.82% for carbon and 0.58% for oxygen in MWNTs, and comparatively, 94.24% and 1.81% for MWNTs-COOH. SEM and EDS were also performed on both filter types after subjecting the filters to solutions of 1 mg/L of ibuprofen at neutral (10 mM NaCl, pH 6) and acidic (10 mM HCl, pH 2) conditions as well as 0, 2, and 3 volts of applied potential at a flow rate of 2 mL/min and at room temperature. The EDS analysis did not show any signs of surface oxidation after treatment except an increase in the oxygen weight % from 1.81 to 7.57 for the MWNTs-COOH filter when subjected to the ibuprofen solution under 0 volts (Figure 3-2 D). Figure 3-1 E and 3-1 F represent the TGA results for as-received MWNTs and MWNTs-COOH, respectively. The TGA shows a purity of ≥ 98 % for both MWNTs types, indicated by a sharp drop in the weight percent between 600 and 650 $^{\circ}\text{C}$, the temperature at which all carbon content is degraded. Below this temperature, a slight, gradual drop in weight would be due to the release of hydrogen content as water vapor.

Total pore volume for MWNT is 0.002 cm^3 (0.241 cm^3/g x 0.008 g), the surface area is 10003.2 cm^2 (125.04 m^2/g x 0.008g) for a loading of 0.84 mg/cm^2 , 7×10^{-4} cm^3 , and 3751.2 cm^2 , respectively, for 0.32 mg/cm^2 for pristine MWNT. The total pore volume for MWNT-COOH is

0.0016 cm³ (0.198 cm³/g x 0.008g), and the surface area is 10642.4 cm² (133.03 m²/g x 0.008 g) for a loading of 0.84 mg/cm², 6 x 10⁻⁴ cm³, and 3990.9 cm², respectively, for 0.32 mg/cm², for MWNT-COOH and as measured by BET. The thickness is 14.2 – 24 μm, as indicated by SEM (for further details, please refer to appendix A).

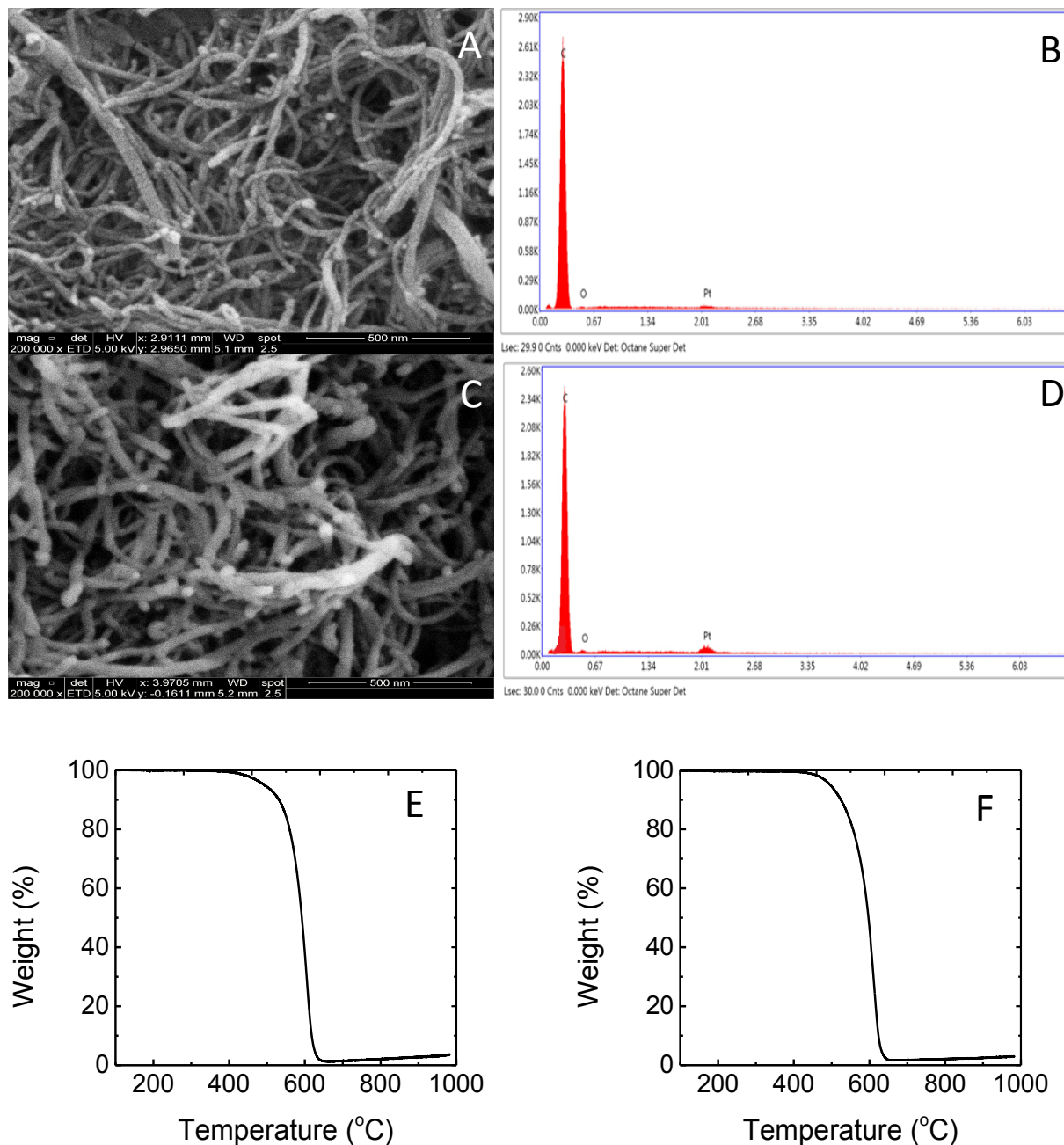


Figure 3-1. SEM images, EDS and TGA analysis for MWNTs and MWNTs-COOH where (A) is SEM for MWNTs filter at a surface loading of 0.84 mg/cm², (B) EDS analysis for MWNTs filter

at a surface loading of 0.84 mg/cm^2 , (C) SEM for MWNTs-COOH filter at a surface loading of 0.84 mg/cm^2 , (D) EDS analysis for MWNTs-COOH filter at a surface loading of 0.84 mg/cm^2 , (E) TGA analysis for pure MWNTs and (F) is TGA analysis for pure MWNTs-COOH.

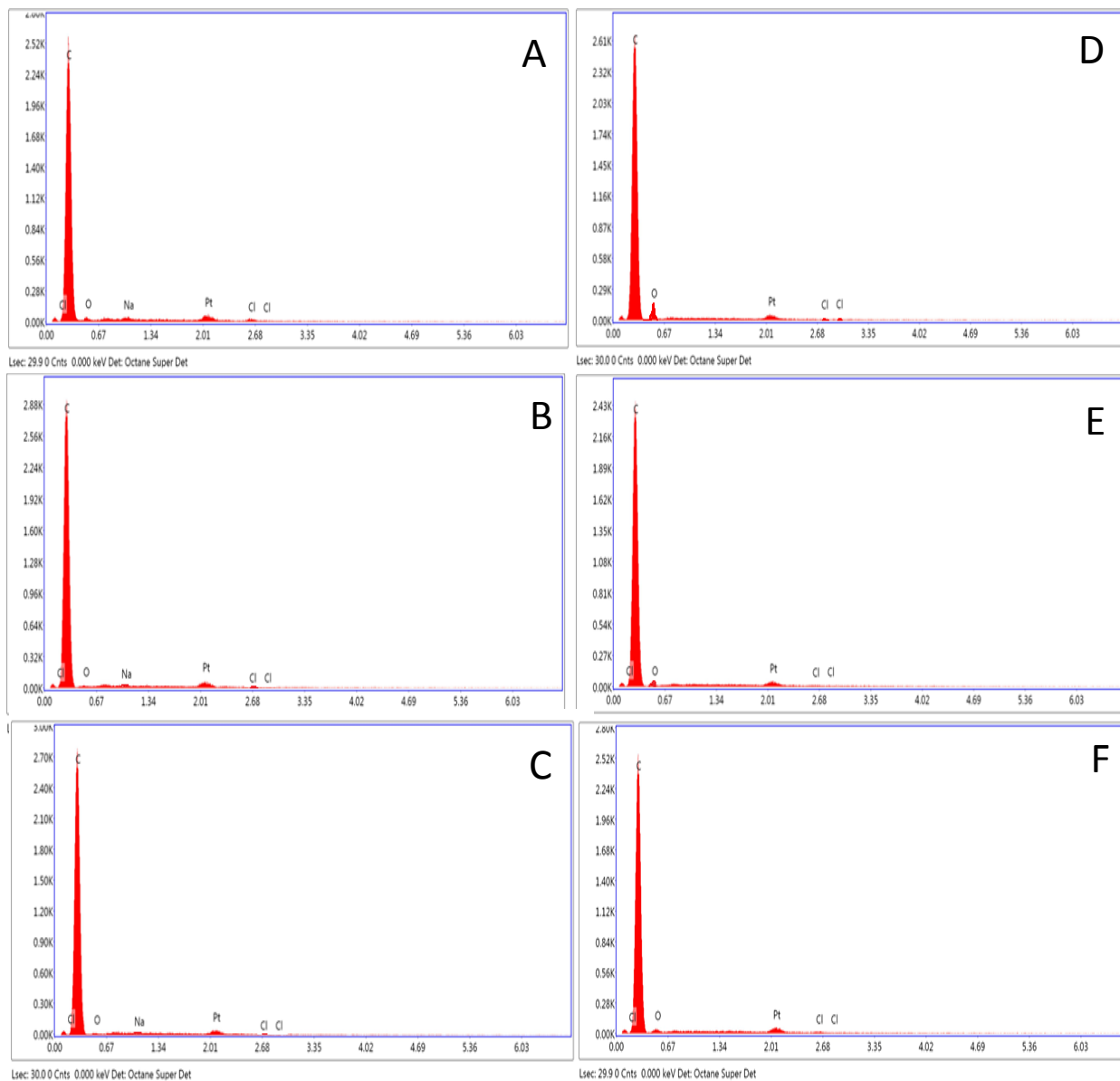


Figure 3-2. EDS analysis after subjecting of MWNTs and MWNTs-COOH to 270 mL of 1 mg/L ibuprofen for 135 minutes where (A) MWNTs are under conditions of ibuprofen in 10 mM NaCl, pH 6 and under 0 V of applied potential, (B) MWNTs are under conditions of ibuprofen in 10 mM NaCl, pH 6 and under 2 V of applied potential, (C) MWNTs are under conditions of ibuprofen in

10 mM NaCl, pH 6 and under 3 V of applied potential, (D) MWNTs-COOH are under conditions of ibuprofen in 10 mM HCl, pH 2 and under 0 V of applied potential, (E) MWNTs-COOH are under conditions of ibuprofen in 10 mM HCl, pH 2 and under 2 V of applied potential and (F) MWNTs-COOH are under conditions of ibuprofen in 10 mM HCl, pH 2 and under 3 V of applied potential. Surface loading for both MWNTs types was 0.84 mg/cm². Experiments were performed at 23 °C.

3.3.2. MWNTs and MWNTs-COOH Electrochemical Performance Characterization

Cyclic voltammetry was completed for both MWNTs and MWNTs-COOH anode filters under the selected conditions of a) ibuprofen in 10 mM NaCl electrofiltered by MWNTs and b) in 10 mM HCl electrofiltered by MWNTs-COOH. Figure 3-3 shows the cyclic voltammograms recorded at a scan rate of 50 mV/sec, a potential range of -1 to 1.5 V vs. Ag/AgCl, and the linear correlations between ibuprofen concentration and the current values at 1.13 V vs. Ag/AgCl. Ibuprofen concentrations varied from 1 to 20 mg/L (1, 10 and 20 mg/L) on one filter for each MWNTs type, each ibuprofen concentration passing through the filter was maintained for 1 minute before any step potential, and the cyclic voltammogram was overlaid.

From Figure 3-3 A and 3-3 B, a trend can be observed for a current increase with increasing ibuprofen concentrations from 1 to 20 mg/L on both MWNTs types, indicating that the current peaks corresponding to 1.13 V vs. Ag/AgCl are likely due to ibuprofen oxidation on the working MWNTs electrodes. Other researchers reported similar behavior at 1.2 to 1.3 V vs. Ag/AgCl [81, 84, 85]. No other features corresponding to oxidation could be observed from the voltammogram, except for the significant difference at and above 0.6 V vs. Ag/AgCl in both cases (Figure 3-3 A and 3-3 B). The increased current values above 0.6 V might be attributed only to the oxygen or chlorine evolution resulting from the water and background chloride oxidation at the MWNTs and MWNTs-COOH anode surfaces. The maximum current peak was observed to be broader on MWNTs-COOH (Figure 3-3 B) as compared to MWNTs (Figure 3-3 A). Nevertheless, the maximum current values were observed to be higher on MWNTs-COOH than on MWNTs, which could be attributed to strong chlorine evolution occurring on MWNTs-COOH at pH 2, leading to the broader peak at 1.2 to 1.3 V.

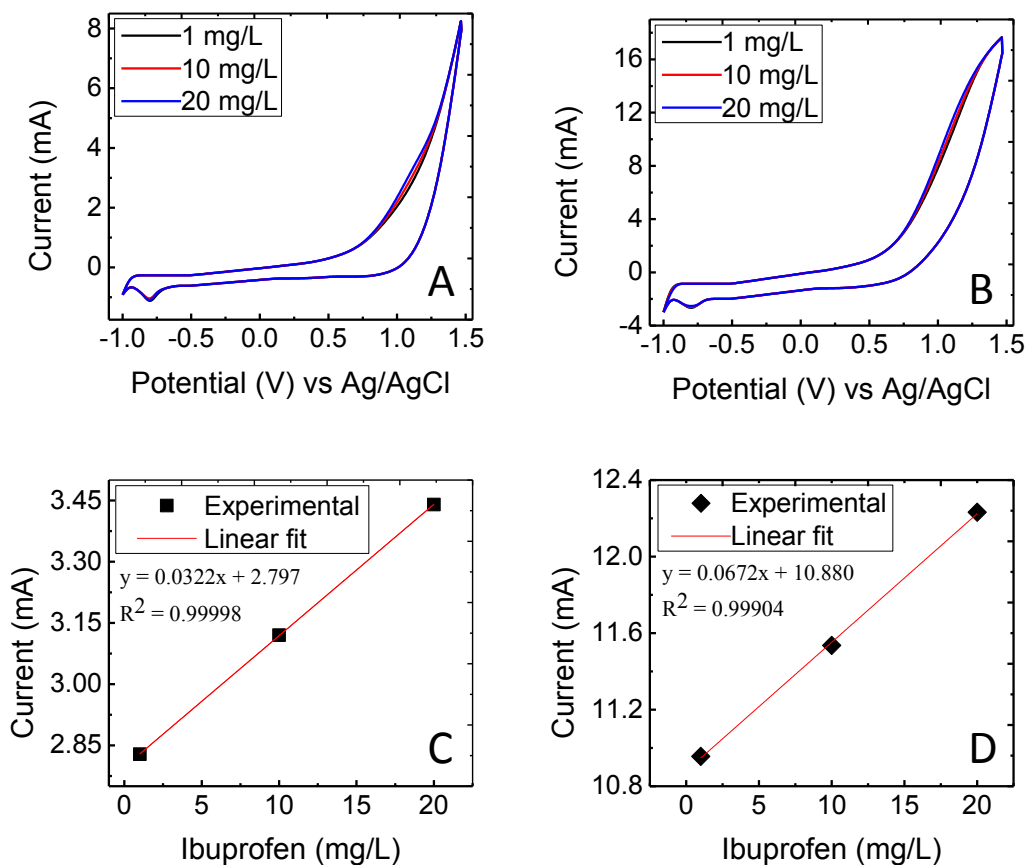


Figure 3-3. (A) Cyclic voltammogram for ibuprofen in 10 mM NaCl (pH 6), electrofiltered by MWNTs, (B) Cyclic voltammogram for ibuprofen in 10 mM HCl (pH 2), electrofiltered by MWNTs-COOH, (C) Linear correlation for current vs. ibuprofen concentration (current values reported corresponding to 1.13 V vs. Ag/AgCl) for the cyclic voltammogram recorded on MWNTs and (D) Linear correlation for current vs. ibuprofen concentration (current values reported corresponding to 1.13 V vs. Ag/AgCl) for the cyclic voltammogram recorded on MWNTs-COOH. Ibuprofen concentrations were 1, 10 and 20 mg/L, scan rate was 50 mV/sec, potential range was -1 to +1.5 V vs. Ag/AgCl, MWNTs and MWNTs-COOH loading was 0.84 mg/cm², flow rate was 2 mL/min, and temperature was 23°C.

The linear increase in current, along with ibuprofen concentration, suggests that diffusion cannot be neglected. Motoc et al. [81] reported that removal of ibuprofen on MWNTs, as indicated by cyclic voltammetry, was neglected through batch electrolysis [81]. In this current study, the flow significantly assists molecule delivery to the MWNTs electrode surface as indicated by the cyclic voltammetry (Figure 3-3 A and C). Therefore, the overall electrochemical filtration process

can be described as diffusion mass transfer to MWNTs anode filters surfaces assisted by the flow. For the case of MWNTs-COOH, the increased maximum current indicates that electrochemical activity is higher and the selectivity of chlorine evolution was probably favored over oxygen evolution in acidic pH, which could apparently be considered an advantage for the electrodegradation of emerging contaminants due to the spontaneous formation of reactive chlorine. However, this results in higher energy consumption, when the applied voltage is increased above 2 V, (Figure 3-4 C). The anode potentials corresponding to applied positive potentials of 1, 2, and 3 V were determined to be 0.33, 0.74, and 1.4 V for MWNTs in 10 mM NaCl (pH 6) and 0.39, 0.9, and 1.72 V for MWNTs-COOH in 10 mM HCl (pH 2).

A reduction peak was observed around -0.7 to -0.8 V, which can be attributed to superoxide radical formation, in agreement with previous reports [86]. Since it is not clearly possible to predict direct oxidation by electron transfer of ibuprofen at an applied potential of 2 V, other oxidation pathways may be taking place, mainly through bulk chemical reactions. To investigate the possible contribution of reactive oxygen species (ROS) and reactive chlorine, a superoxide assay was done for electrofiltration of NBT at 2 V of applied DC potential to observe if superoxide formation is taking place, as well a hypochlorous acid assay was done for electrofiltration of pure background 10 mM NaCl and 10 mM HCl at 3 V (Detailed information on the assays and their discussion can be found in Appendix A). Both assays showed positive results and it was found that both oxidants were produced during the electrofiltration process in the acidic and neutral conditions and on both MWNTs types, at 2 and 3 V of applied potential. The acidic conditions likely lead to a non-significantly less stable superoxide, as indicated by the assay, showing fast kinetics for the interaction of superoxide with target molecules, as well, a higher production of hypochlorous acid over the neutral conditions. From these results, it could be concluded that reactive oxygen is likely responsible for degradation of ibuprofen during electrofiltration at an applied voltage of 2 V on both filter types.

Figure 3-4 A shows the steady state current density corresponding to applied voltages of 1, 2 and 3 V during the treatment of 20 mg/L ibuprofen by MWNTs from 10 mM NaCl (pH 6) and MWNTs-COOH from 10 mM HCl (pH 2). The current density increased significantly with increasing applied voltage for the treatment by MWNTs-COOH in acidic condition, indicating an increased conductivity, most likely due to improved chlorine evolution and hydrogen evolution

reactions. Figure 3-4 C and D show the energy consumption (EC) in kWh/kg and mineralization current efficiency (MCE) in % for the same aforementioned conditions of Figure 3-4 A. From Figure 3-4 C and D it is evident that the treatment by MWNTs-COOH is more power efficient up to 2 V of applied potential while at 3 V, the energy consumption increases significantly and thus, the mineralization current efficiency drops, due to the increased chlorine and hydrogen evolution reactions on MWNTs-COOH in acidic conditions.

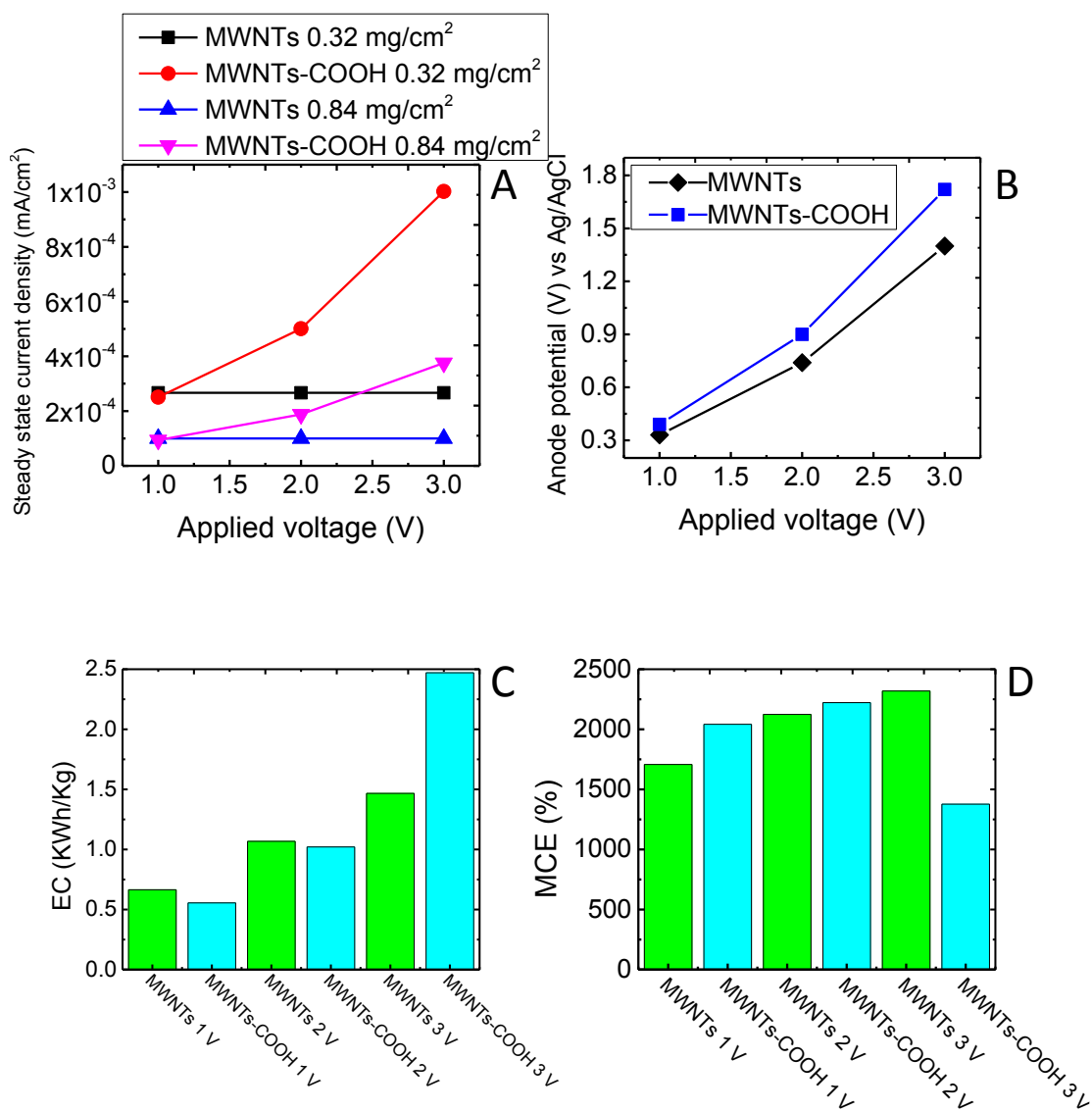


Figure 3-4. (A) Steady state current densities for MWNTs and MWNTs-COOH at surface loadings of 0.32 and 0.84 mg/cm², (B) Anode potential vs. Ag/AgCl for electrochemical filtration of 20 mg/L ibuprofen by 0.32 mg/cm² MWNTs and MWNTs-COOH in 10mM NaCl and 10 mM HCl (C) is MWNTs and MWNTs-COOH energy consumption (EC) in kWh/kg and (D) is mineralization current efficiency (MCE) in %, for electrochemical filtration of 20 mg/L ibuprofen by 0.32 mg/cm² MWNTs and MWNTs-COOH in 10mM NaCl and 10 mM HCl. At 23°C, flow rate of 2 mL/min and applied voltages 1, 2 and 3 volts.

3.3.3. Efficiency of MWNTs and MWNTs-COOH for Ibuprofen Removal at High Concentration (Single Passage)

The performance of both pristine and carboxylated MWNTs was examined for the filtration of ibuprofen from aqueous solutions at a high concentration and through a single effluent collection. The MWNTs filters were supplied with ibuprofen at a concentration of 20 mg/L at room temperature and under a flow rate of 2 mL/min, to allow evaluation of the filter for the removal of ibuprofen in high concentrations by a low surface loading of 0.32 mg/cm². The filtration experiments were performed at zero voltage to investigate the adsorption (retention) capacity of the MWNTs filters. The background solution was passed through the filter at 0 voltage for 5 minutes (10 ml of background solution at a flow rate of 2 mL/min) to saturate the filter in the background solutions. Then, a step potential was applied, and the background solution was allowed to pass for another minute to allow for the generation of electroactive species. The ibuprofen was then allowed to pass for one minute, and afterward, samples were collected. Figure 3-5 shows that the percent removal observed was 68.1-70.6% on the MWNTs-COOH filter using 10 mM HCl as a background solution. Ibuprofen contains a –COOH group at the terminus of the propionic acid chain. When filtration occurs with MWNTs-COOH at a low pH (pH = 2), and below the pKa of ibuprofen (pKa = 4.9)¹, ibuprofen molecules are efficiently trapped on the nanotubes, most likely due to hydrogen bond formation between the protonated –COOH groups of ibuprofen and those of the MWNTs-COOH, along with strong pi–pi and hydrophobic interactions. Previous studies showed that both carboxylated and hydroxylated MWNTs have higher adsorption capacities for organic molecules with oxygen-containing functional groups due to enhanced surface interactions between carbon nanotubes and the target molecules [87-89].

On the other hand, when applying the filtration process for ibuprofen dissolved in a 10 mM NaCl background solution at pH 6 with MWNTs and MWNTs-COOH filters, removal percentages were around 55.8 - 56.7 and 52.8 - 54.6%, respectively (Figure 3-5 A). We correlate the low removal of ibuprofen by MWNTs and MWNTs-COOH filters at neutral pH and using NaCl as the background solution to an increased hydration effect, induced by the salt electrolyte, leading to deficiency of hydrophobic interactions between ibuprofen molecules due to the hydration barrier

formed and the lack of effective hydrophilic interactions. However, studies have reported that the salting-out effect of sodium-containing electrolytes leads to enhanced sorption of organic molecules; yet, it is significant only at higher salt concentrations [90]. Therefore, by comparing the performance of MWNTs at neutral conditions to MWNTs-COOH at acidic conditions for the removal of ibuprofen by filtration, it is likely that the hydration effect is still significant at the ibuprofen carboxylate head-groups.

Tang et al. [91] studied the ionic binding of sodium and potassium ions to the –COOH groups of palmitic acid and the effect on the monolayer coherence at the water interface. They observed that palmitic acid molecules are typically protonated at pH 6. Nonetheless, the introduction of the positively charged monovalent cations introduces a high degree of deprotonation of the –COOH groups of palmitic acid. Ionic binding between the positively charged ions and the negatively charged carboxylate ions can then occur, leading to higher rates of hydration-shell formation and consequently larger intermolecular separations. Other researchers have also reported similar observations with the introduction of salts, their role in increasing hydration shells, and their effect on surface and hydrophobic interactions [92, 93].

Furthermore, another study showed that the adsorption of the antibiotic sulfamethoxazole on functionalized carbon nanotubes could be altered by the introduction of cations and anions. In this study, the effect of the large hydration diameters of calcium and cesium, which block the hydrophobic adsorption sites for sulfamethoxazole on the CNTs surface, was discussed [94]. In the case of ibuprofen filtration with MWNTs under acidic conditions, we attribute the percent removal of around 52.1-52.9% to the lack of polar interaction (–COOH) sites on the pristine MWNTs and therefore the deficiency of hydrophilic interactions (hydrogen bonds) (Figure 3-5 B).

Electrofiltration with MWNTs and MWNTs-COOH filters was examined for the removal of ibuprofen from aqueous solutions. At an applied DC potential of 1 V, the filters were provided with ibuprofen in NaCl and HCl solutions in the same manner as the filtration experiments. Removal percentages increased to around 59.8- 60% in the case of electrofiltration by MWNTs and around 59.5-60.4 % by MWNTs-COOH, with ibuprofen solutions at neutral pH values (Figure 3-5 C). Electrofiltration by MWNTs with ibuprofen solutions under acidic conditions also did not exceed 59.2 - 60.2 % removal, whereas the removal was increased to 73.7 -74.5 % in the case of electrofiltration with MWNTs-COOH with ibuprofen solutions under acidic conditions (Figure 3-

5 D). The improved removal percentages from the application of low DC voltage indicates enhanced adsorption by the electrostatic surface interaction between the MWNTs and MWNTs-COOH filters and ibuprofen molecules. Nevertheless, enhanced removal by MWNTs-COOH at pH 2 indicates that the amount of voltage applied at this point was not sufficient to reduce the bulk acidity (pH remained at 2-2.1 for effluents after 1 V of electrofiltration). Consequently, surface protonation was not lost and, therefore, hydrophilic interactions were maintained.

It was reported that CNTs can provide a high electrocatalytic activity for efficient electron transfer at low applied voltages [95]. Previous studies on the electrofiltration of organic contaminants at similar voltages showed that the removal of organic molecules from the anode surface was under the control of direct electron transfer and that the negative contribution of water oxidation and oxygen evolution could be avoided [74, 75]. Due to the low anode potentials (0.33 and 0.39 V vs. Ag/AgCl for MWNTs and MWNTs-COOH, respectively) corresponding to 1 V of applied DC potential as compared to the observed potential for ibuprofen oxidation (1.13 V vs. Ag/AgCl), the enhanced removal cannot be attributed to an initiated direct oxidation at 1 V of DC potential.

When the applied DC voltage was increased to 2 V, the removal was enhanced significantly for both filter types. In this set of experiments, only MWNTs at neutral conditions and MWNTs-COOH at acidic conditions were tested, as the selected comparison conditions for the rest of the study. The percent removal values were around 74.1 - 74.9% and 79 - 82.4% for MWNTs and MWNTs-COOH, respectively (Figure 3-5 E and F). Increased ibuprofen removal by increasing the applied potential to 2 V could be attributed to bulk oxidation by superoxide anion, especially knowing that at 2 V of applied DC potential, the anode potentials are still below the direct oxidation potential for ibuprofen (0.74 and 0.9 V for MWNTs and MWNTs-COOH; 1.13 V for ibuprofen), and therefore, as indicated by a superoxide assay (Figure A-5, Appendix A), superoxide is most likely participating in an indirect degradation reaction of ibuprofen during 2 V of applied potential.

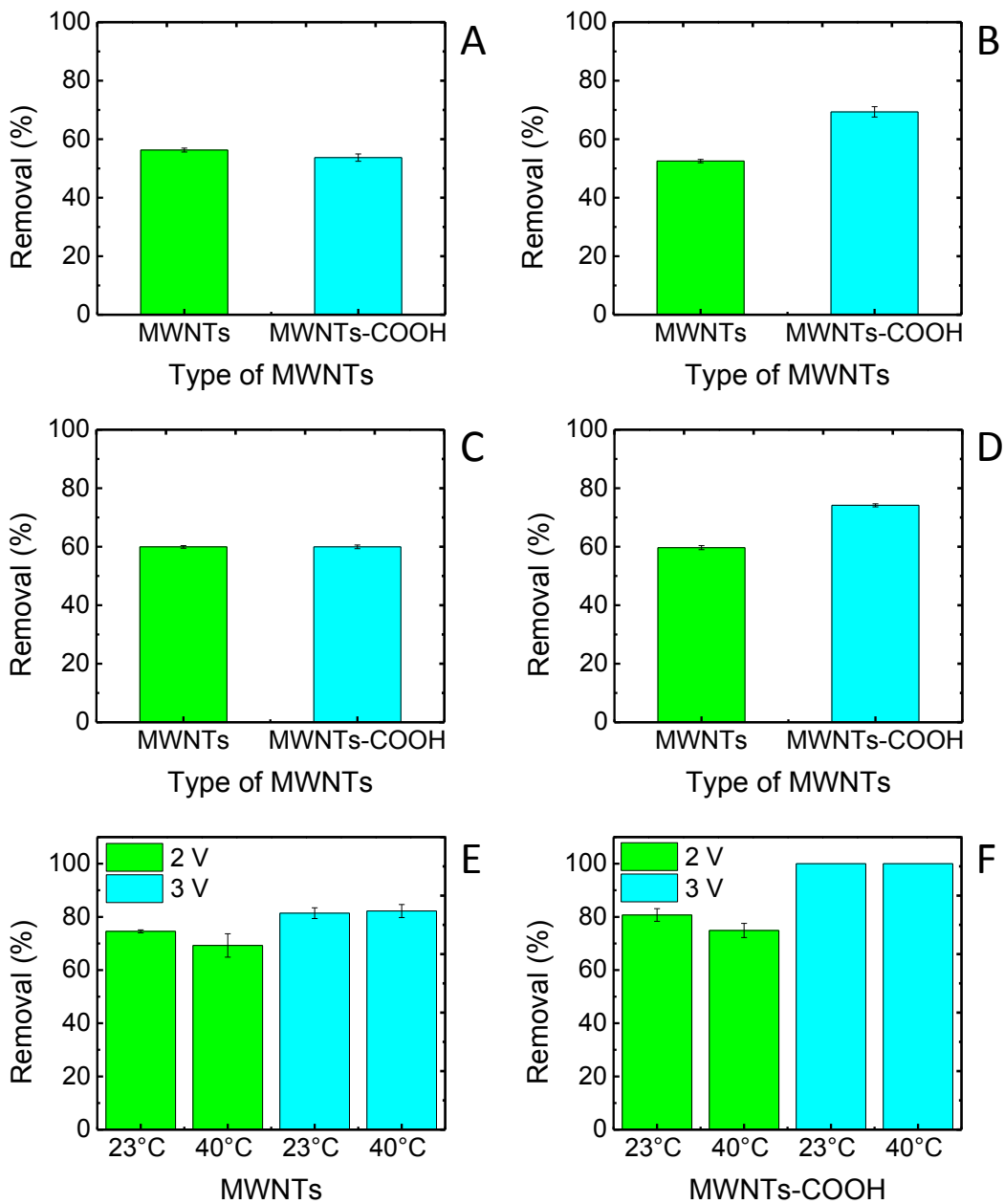


Figure 3-5. Percent removal of Ibuprofen by MWNTs and MWNTs-COOH using (A) 10 mM NaCl as the background solution at pH 6 and (B) 10 mM HCl as the background solution at pH 2, with no voltage application, at temperature 23 °C. Percent removal of ibuprofen by MWNTs and MWNTs-COOH filters using (C) 10 mM NaCl as the background solution (pH 6) and (D) 10 mM HCl as the background solution (pH 2), with an applied DC potential of 1 V, at temperature 23 °C. (E) Percent removal of ibuprofen by MWNTs using 10 mM NaCl as the background solution at pH 6, at DC voltages of 2 and 3 V and at 23 and 40°C. (F) Percent removal of ibuprofen by

MWNTs-COOH using 10 mM HCl as the background solution at pH 2, at DC voltages of 2 and 3 V and at 23 and 40°C. The concentration of ibuprofen was 20 mg/L, MWNTs and MWNTs-COOH surface loading was 0.32 mg/cm² and flow rate was 2 mL/min.

Liu et al. [74] studied the removal of methyl orange (MO) and methylene blue (MB) by MWNTs filters under similar conditions, and reported that the enhanced removal kinetics of MO and MB correspond to faster direct oxidation pathways initiated by increasing the applied voltage from 1 to 2 V. Rahaman et al. [72] also reported that at an applied DC potential of 2 V, the inactivation and degradation of virus particles proceeds through direct oxidation by electron transfer.

When the applied voltage was raised to 3 V, the percent removal of ibuprofen by MWNTs under neutral conditions was around 79.9 - 82.8% (Figure 3-5 E), whereas, for MWNTs-COOH under acidic conditions near complete removal of ibuprofen was achieved (Figure 3-5 F). The improved performance of both filter types at 3 V can be attributed to the increased contribution from indirect electrooxidation pathways by the formation of reactive chlorine (hypochlorous acid) with the increased formation of reactive oxygen (superoxide). The significant difference in performance between the acidic (10 mM HCl) and neutral (10 mM NaCl) conditions at 3 V demonstrates a likely favoring of the chlorine-evolution reaction and the formation of reactive chlorine at acidic pH, over the oxygen-evolution reaction, which is delayed by the acidic pH. The results for the hypochlorous acid assay confirm such a conclusion (Figure A-7, Appendix A).

Scialdone et al. [61] also reported that low pH values favor the chlorine-evolution reaction over water-oxidation and the oxygen-evolution reaction as well as the formation of hypochlorous acid, which is a powerful oxidizing agent [61, 96]. However, the predicted products (Table A-3, Appendix A) exhibit a possibility of a higher reactive oxygen species contribution over hypochlorous acid in the degradation of ibuprofen, due to an inability to conclude any chlorinated by-products, as will be discussed in a later section. In the same manner, the effect of the applied potential (2 and 3 V) was also studied at 40 °C. It was observed that by increasing temperature to 40 °C at 2 V of applied potential, electrochemical filtration performance could be negatively impacted, leading to a slight drop in the removal percentage for both conditions of MWNTs and MWNTs-COOH used at neutral and acidic pH. The results at 2 V of applied DC voltage and 40 °C are in agreement with a previously reported effect of increased temperature on the removal of

MO by MWNTs [74]. Therefore, it can be inferred that at an applied potential of 2 V, surface adsorption and filtration are still effective, which can be negatively altered by a lack of efficient surface interactions at high temperatures, due to the higher kinetic energy of the bulk molecules and less chance for the necessary surface interactions to become established and good adsorption of ibuprofen molecules onto the carbon nanotube surface to occur. When the applied voltage was increased to 3 V at 40 °C, as in the case of electrofiltration with MWNTs under neutral conditions, no pronounced effect of temperature was observed in the removal process. This result was unlike what was expected of enhanced indirect oxidation kinetics under the effect of increased temperature. This outcome indicates that the dominant reactions occurring at 3 V and neutral pH are wasting reactions as water oxidation and oxygen evolution. In the case of MWNTs-COOH under acidic conditions, a temperature increase did not affect the process in any way, and the removal of ibuprofen remained at nearly 100%. This indicates that under acidic conditions, and at an applied voltage of 3 V, the removal of ibuprofen primarily depends on indirect bulk oxidation pathways with little contribution from surface adsorption, most probably due to the enhanced indirect oxidation kinetics by increased ibuprofen concentration. Nevertheless, it is hypothesized that by employing MWNTs filters at 3 V and acidic pH, the removal of ibuprofen might be improved due to the enhanced formation of reactive chlorine.

3.3.4. Efficiency of MWNTs and MWNTs-COOH for Ibuprofen Removal at Low Concentration (Breakthrough Experiments)

The performance of both filter types was tested over time for the removal of 1 mg/L ibuprofen in pure electrolytic solutions (10 mM NaCl by MWNTs and 10 mM HCl by MWNTs-COOH) and synthetic secondary wastewater effluent. The composition of the synthetic wastewater effluent was 311 mg/L NaCl, 18 mg/L MgSO₄, 25 mg/L NaHCO₃, 22 mg/L CaCl₂, 2.3 mg/L KH₂PO₄, 8.5 mg/L NH₄Cl, and 33 mg/L Na₃C₆H₅O₇ (as a carbon source) resulting in a pH of 7.3 and a TOC of 34.1 mg/L, modified from previous studies [97, 98]. Figure 3-6 shows the breakthrough trends and flux values ($\mu\text{g}/\text{m}^2\cdot\text{h}$) for the removal of ibuprofen by MWNTs and MWNTs-COOH at 0, 1, 2 and 3 V of applied DC potential. The filtration kinetics at 0 V of the MWNTs was steady at the beginning at around 66%, and significant filter breakthrough began at 60 minutes. For the MWNTs-COOH, in pure electrolytes, a nearly 100% removal rate was achieved in as little as 30 minutes of filtration time (Figure 3-6 A). This behavior shows the

superior performance of MWNTs-COOH in the removal of ibuprofen molecules when a low concentration of ibuprofen (1 mg/L) was present and no DC potential was applied, as compared to the MWNTs performance that showed less removal capacity and therefore later breakthrough.

The slight improvement observed when 1 V was applied confirms that electrostatic attraction is enhancing mass transfer by migration from bulk to surface, but, as compared to the application of both 2 and 3 V, it is evident that no degradation is taking place at 1 V. Also, the similar outcome at both 2 and 3 V of applied potential is an indication that major oxidation pathways are similar, most likely through the interaction of ibuprofen molecules with reactive oxygen species. At 2 and 3 V of applied potential, enhanced removal was observed for both filter types, with slightly better performance seen in the MWNTs-COOH than in the MWNTs (Figure 3-6 A). A relatively smaller increase in C/C_0 values at applied potentials of 2 and 3 V indicates that surface adsorption is still contributing, although oxygen evolution and increased surface hydrophilicity are expected to be dominant. This demonstrates that at applied potentials of 3 V, direct electron transfer might occur at the surface and contribute toward the overall oxidation process. The larger specific surface area of MWNTs-COOH ($133.03 \text{ m}^2/\text{g}$) as compared to MWNTs ($125.04 \text{ m}^2/\text{g}$) may also contribute to slower breakthrough.

When ibuprofen was introduced to both filter types in the same conditions of the synthetic effluent, performance was observed to be almost identical (Figure 3-6 B). The deterioration in MWNTs-COOH performance at 0 V is most likely due to the introduction of NaCl among other salts, leading to hydration formation at the MWNTs-COOH surface and the loss of surface hydrophilic interactions between ibuprofen and MWNTs-COOH at the neutral to alkaline pH. The earlier breakthrough for both filters at 0 V is probably due to the increased TOC of 34.1 mg/L, due to the introduction of $\text{Na}_3\text{C}_6\text{H}_5\text{O}_7$.

Figure 3-6 C and D show the flux values corresponding to 0, 1, 2 and 3 V of applied DC potential of MWNTs and MWNTs-COOH for ibuprofen in 10 mM NaCl and 10 mM HCl, respectively. It can be observed an apparent higher flux for MWNTs over MWNTs-COOH at 1 V. This could be related to poor MWNTs removal over the first 60 minutes, allowing more room for ibuprofen molecules to be adsorbed under the enhanced electrostatic migration, yet a longer time before the breakthrough.

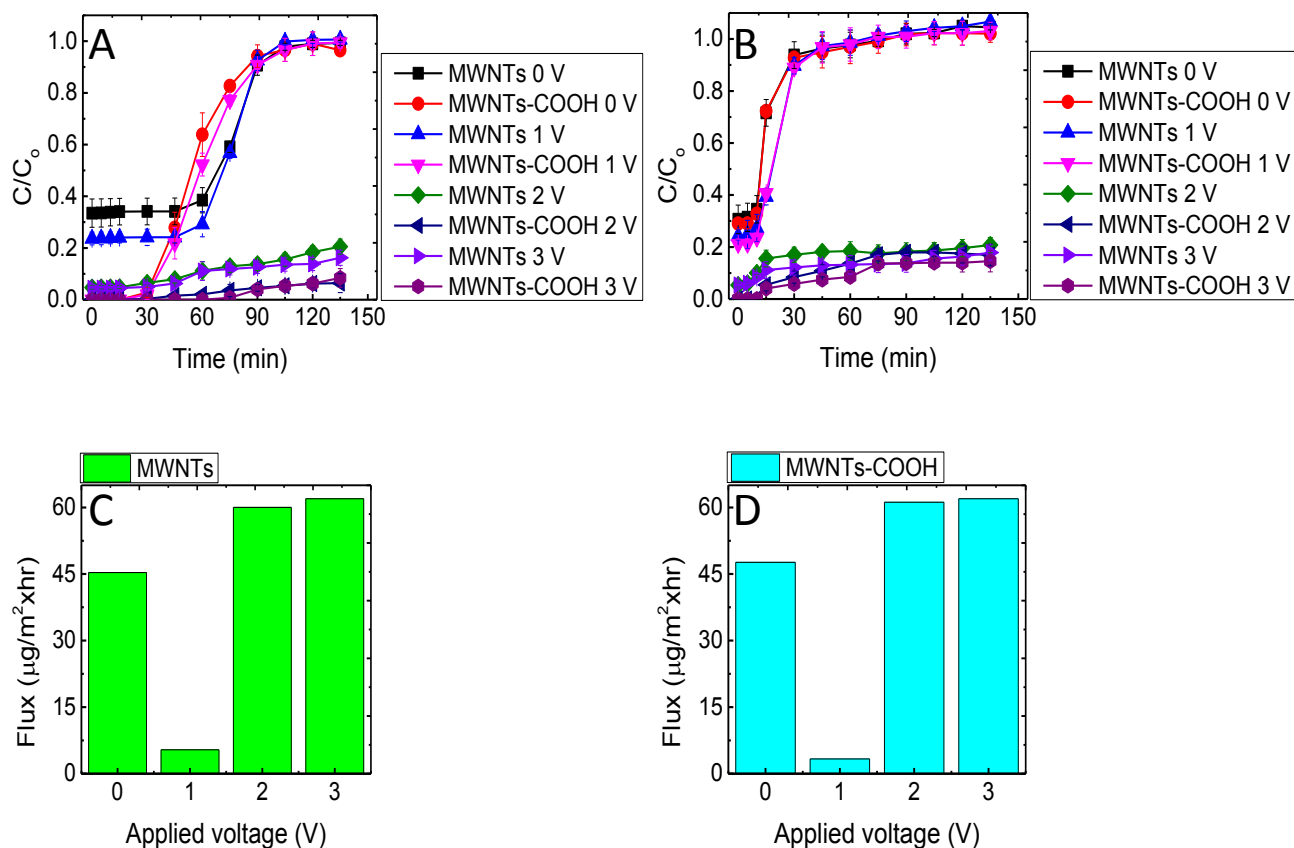


Figure 3-6. Breakthrough trends and flux values for MWNTs and MWNTs-COOH filters over time at 0, 1, 2 and 3 V of applied DC voltage, where (A) is breakthrough plots in pure 10 mM NaCl (pH 6) for MWNTs and 10 mM HCl (pH 2) for MWNTs-COOH, (B) is breakthrough plots in synthetic secondary effluent of the same composition and pH (7.3) for both filter types, (C) are MWNTs flux values corresponding to 0, 1, 2 and 3 V of applied potential for ibuprofen in pure 10 mM NaCl (pH 6) and (D) are MWNTs-COOH flux values corresponding to 0, 1, 2 and 3 V of applied potential for ibuprofen in pure 10 mM HCl (pH 2). The ibuprofen concentration was 1 mg/L (4.8 μM). MWNTs and MWNTs-COOH surface loading was 0.84 mg/cm^2 , and temperature was 23°C.

To further investigate this speculation, flux values were calculated corresponding to the removal of both filter types at the conditions of subsection 3.3.3, Figure 3-5 C and D (Figure 3-7, flux values corresponding to removal of 20 mg/L ibuprofen by MWNTs and MWNTs-COOH at neutral and acidic conditions, respectively). It was observed that when both filter types are supplied with larger concentrations of ibuprofen, flux values are higher for MWNTs-COOH in acidic

conditions over MWNTs at neutral conditions at an applied potential of 1 V. Therefore it can be concluded that even if the MWNTs could adsorb at maximum capacity during the initial period and at lower ibuprofen concentrations, conditions of Figure 3-6, the time to the breakthrough would be less than MWNTs-COOH, due to the lower specific surface area and lower adsorption capacity of MWNTs.

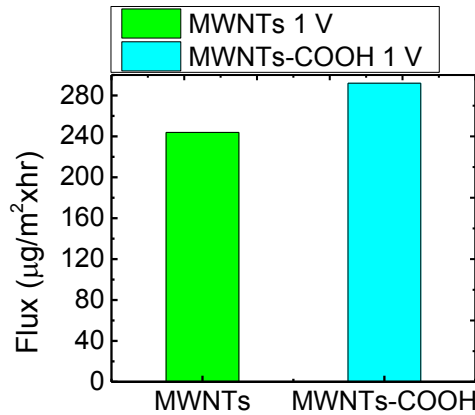


Figure 3-7. Electrostatic filtration flux in $\mu\text{g}/\text{m}^2\cdot\text{h}$ of MWNTs and MWNTs-COOH for 20 mg/L ibuprofen in 10 mM NaCl (pH 6) and 10 mM HCl (pH 2), respectively. MWNTs loadings were $0.32 \text{ mg}/\text{cm}^2$, applied voltage was 1 V and temperature was 23°C (Corresponding to Figure 3-5 C and D).

Integration of the breakthrough curves could provide a quantification of the amount of ibuprofen adsorbed or removed per amount of MWNTs used. The MWNTs adsorption capacities (q) in mg/mg, were first calculated using equation (3-1) [99];

$$q = \frac{F \int (1 - \frac{C}{C_0}) dt}{m} \quad (3 - 1)$$

Where C and C_0 are ibuprofen effluent and influent concentrations in mg/L, F is the flow rate in L/min, and m is the mass of MWNTs and MWNTs-COOH in mg. Table A-1 in Appendix A shows adsorption and removal capacities by MWNTs and MWNTs-COOH, at 0, 1, 2 and 3 volts of applied potential, and the difference between each, represented as the amounts of ibuprofen removed in mg, g, number of moles and number of molecules per mg, g and m^2 of each MWNTs type, for Figure 3-6 A.

Table A-2 in Appendix A shows the adsorption and removal capacities from synthetic secondary wastewater effluent for both MWNTs and MWNTs-COOH. The deterioration of the MWNTs-COOH performance in the removal of ibuprofen from the synthetic secondary effluent at pH 7.3 and 0 V is clear, suggesting that pH adjusting and solution conditions, together with the nature of the target molecule and the type of MWNTs, all are critical factors that must integrate together for an optimal performance at 0 and 1 V application. In the case of 2 and 3 V of applied positive potential, performance was significantly improved for both cases of removal from pure electrolytes and synthetic effluent, confirming the effective contribution from different oxidation pathways toward the overall performance.

3.3.5. Insight into Ibuprofen Degradation and its By-products

Ibuprofen degradation and the characterization of the by-products formed were investigated through liquid chromatography-mass spectrometry (LC-MS), aiming for clear evidence of the stated outcomes, as well as an understanding of degradation pathways. The analyses were performed at various conditions of applied voltage, flow rate, and CNTs loading. Figure 3-8 A and B show the chromatograms of ibuprofen before and after treatment with MWNTs and MWNTs-COOH under neutral and acidic conditions, respectively. The applied voltage was 3 V, the MWNTs and MWNTs-COOH surface loading was 0.32 mg/cm², the flow rate was 2 mL/min, and the electrofiltration was performed at 40 °C. LC-MS results are in agreement with the UV-Vis results, confirming that the removal of ibuprofen can be greatly improved, and approach near complete removal in acidic conditions with an applied potential of 3 V. Two minor product peaks could be observed at retention times (RT) of 2.3 and 4.1 minutes after the electrofiltration of ibuprofen with MWNTs-COOH under acidic conditions (Figure 3-8 B). The fact that product peaks could only be observed in the case of MWNTs-COOH under acidic conditions is not clear, and it was expected that the reaction kinetics for the complete mineralization of ibuprofen would be enhanced by increasing the reaction temperature. This might be attributed to a cleavage or loss of the ionizable groups during the treatment in neutral conditions, or a lower hydraulic residence time for the formed by-products in acidic conditions, due to lower affinity for hydrophilic surface interactions. However, the complete removal of the ibuprofen peak with the appearance of minor product peaks at acidic conditions indicates high electrodegradation efficiency in acidic conditions.

The spectra for the minor product peaks at RT 2.3 and 4.1 minutes are shown in Figure 3-8 E, and 3-8 F. Four spectral peaks occur at 135, 193, 203, and 207 m/z at RT 2.3 minutes (Figure 3-8 E), and a single peak occurs at 193 m/z at RT at 4.1 minutes (Figure 3-8 F). It was possible to predict several, but not all, of the products corresponding to these m/z ratios, due to the vast possibilities of chemical structures corresponding to the m/z values. The minor products at these m/z ratios were identified based on the METLIN metabolites database (<http://metlin.scripps.edu/>). Several of the predicted products were 4-ethylbenzaldehyde, 1-phenyl-1-propanone, 4'-methylacetophenone, 2-phenylpropanal, (4-methylphenyl)acetaldehyde, (Z)-4-(1-propenyl)phenol, 5-methyl-3-hexen-2-one, and 5-methyl-5-hexen-2-one (Table A-3, Appendix A). Other possible by-products could be methyl 4-tert-butylphenylacetate, 2,7-dimethyl-6-nonenoic acid, and 2,7-dimethyl-6-octenoic acid.

4-Ethylbenzaldehyde was observed to be a common by-product of the degradation of ibuprofen by various methods [64, 100-104]. Caviglioli et al. [101] also reported mono- and dimethyl derivatives at m/z values of 135 and 193 using GC-MS.

The formation of these by-products indicates a significant contribution from active oxygen species to the interaction with, and degradation of, ibuprofen. It was previously discussed that the production and reactivity of reactive oxygen species (namely superoxide) greatly depend on the solvent used and that superoxide production and reactivity occur in non-aqueous aprotic solvents [68, 105]. However, it was shown that superoxides could be produced in aqueous solution from a single electron reduction of oxygen at the cathode surface, ultimately resulting in the oxidation of organic molecules [53, 106].

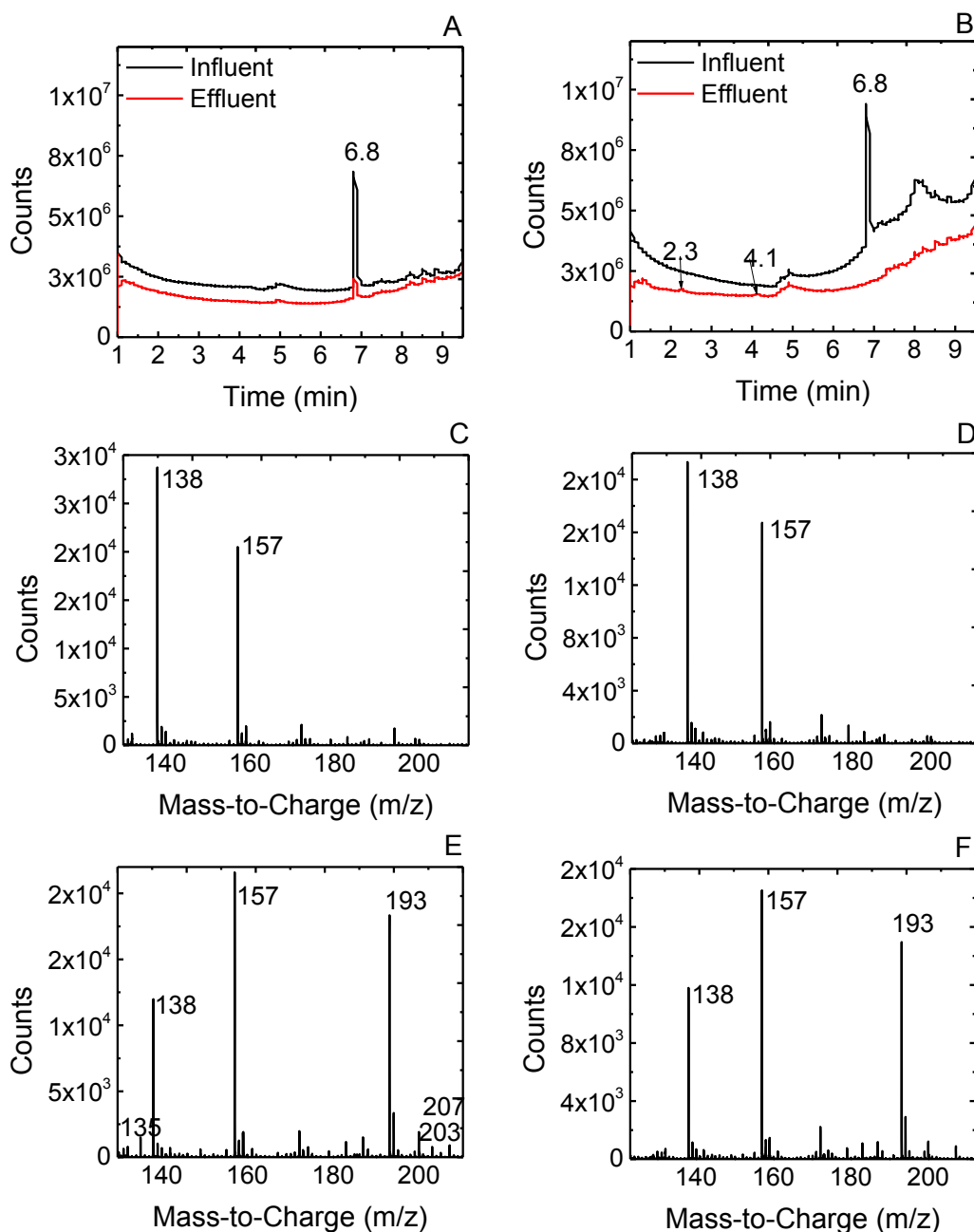


Figure 3-8. (A) Chromatograms of ibuprofen in a 10 mM NaCl background solution at pH 6, where the upper trace is before treatment and the lower is after treatment with MWNTs at a 3 V DC potential. (B) Chromatograms of ibuprofen in a 10 mM HCl background solution at pH 2, where the upper trace is before treatment and the lower is after treatment with MWNTs-COOH at a 3 V DC potential. (C) Mass spectra at RT 2.3 min of ibuprofen in 10 mM HCl (pH2) before treatment. (D) Mass spectra at RT 4.1 min for ibuprofen in 10 mM HCl (pH2) before treatment. (E) Mass

spectra at RT 2.3 min of ibuprofen in 10 mM HCl (pH2) after treatment with MWNTs-COOH at a 3 V DC potential. (F) Mass spectra at RT 4.1 min for ibuprofen in 10 mM HCl (pH2) after treatment with MWNTs-COOH at a 3 V DC potential. The ibuprofen concentration was 20 mg/L, MWNTs and MWNTs-COOH surface loading was 0.32 mg/cm², flow rate was 2 mL/min and temperature was 40°C.

3.3.5.1. Effect of the Flow Rate on MWNTs-COOH Filter Electrochemical Performance

The effect of the flow rate on the MWNTs-COOH filter performance under acidic conditions for the removal of ibuprofen (10 mg/L) and its by-products was studied at a surface loading of 0.84 mg/cm² and an applied DC potential of 2 V. Figure 3-9 A shows the chromatograms for ibuprofen before treatment (black), after treatment with MWNTs-COOH at a flow rate of 1 mL/min (red) and after treatment at a flow rate of 0.2 mL/min (blue).

The effect of the lowest flow rate (0.2 mL/min) was significant for the complete removal of ibuprofen and its by-products, most likely due to sufficient residence time. Providing greater opportunity for the ibuprofen molecules, and formed by-products, to interact and continue degrading with the in situ formed ROS (i.e., superoxide) advances the objective of complete removal of the molecules. At a flow rate of 1 mL/min, ibuprofen was observed to be almost entirely removed at 2 V; however, two by-product peaks were observed at RT 7.3 and 7.7 minutes.

The existence of the treatment products in the filtrate at a flow rate of 1 mL/min may be attributed again to the residence time. With a fivefold lower flow rate (0.2 mL/min), sufficient reaction time was allowed, leading to the total degradation and removal of ibuprofen and its formed by-products.

Therefore, at a higher flow rate (i.e., a low residence time), the by-product molecules were not completely degraded and could infiltrate the CNTs filter and flow into the effluent. The chromatogram products peaks at RT 7.3 and 7.7 minutes were further identified by mass spectrometry. Figure 3-9 B and C shows the mass spectra of ibuprofen (10 mg/L) at 6.8 min before treatment (Figure 3-9 B) and after treatment at 2 V and 0.2 mL/min (Figure 3-9 C). Figure 3-9 D and E show the effluent after treatment at a flow rate of 1 mL/min at RT 7.3 and 7.7 minutes, respectively. At RT 7.3 minutes, three spectral peaks could be observed at 177, 195, and 241 *m/z* values. At RT 7.7 minutes, one spectral peak was observed at 229 *m/z*.

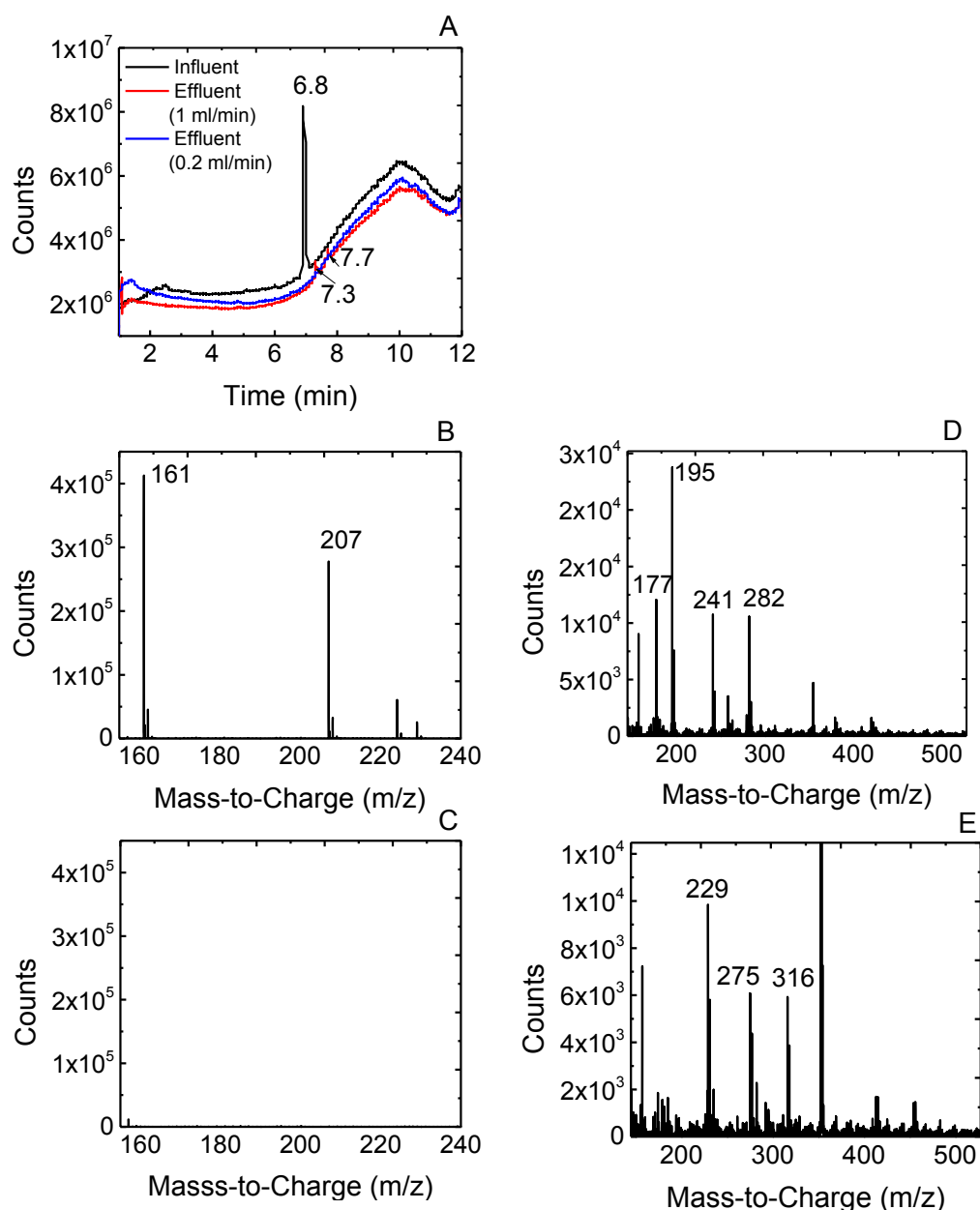


Figure 3-9. (A) Chromatograms of ibuprofen in 10 mM HCl as the background solution at pH 2, where the upper (black) trace is before treatment, the middle (blue) trace is after treatment with MWNTs-COOH at a voltage of 2 DC with a flow rate of 0.2 mL/min, and the lower (red) trace is after treatment with MWNTs-COOH at a voltage of 2 DC with a flow rate of 1 mL/min. (B) Mass spectra for ibuprofen in 10 mM HCl (pH 2) at RT 6.8 min before treatment and (C) after treatment with MWNTs-COOH at a 2V DC potential. (D) Mass spectra for ibuprofen at RT 7.3 min in 10 mM HCl pH 2 after treatment with MWNTs-COOH at a 2V DC potential. (E) Mass spectra for

ibuprofen at RT 7.7 min in 10 mM HCl pH 2 after treatment with MWNTs-COOH at a 2V DC potential. The ibuprofen concentration was 10 mg/L, MWNTs-COOH surface loading was 0.84 mg/cm², and the temperature was 23 °C.

The products obtained from the treatment at a flow rate of 1 mL/min could be identified, and some of the possible structures are [107, 108]: 4-isobutylbenzoic acid, and 1-(4-isobutylphenyl)-1-ethanol, 2-(4-formylphenyl)propanoic acid (Table A-3, Appendix A). Other possible products are 2-chloro-3-oxoadipate and 6-(benzyloxy)-1-chlorohexan-2-one.

Others have reported the formation of methyl derivatives from ibuprofen degradation corresponding to 177 *m/z* [101, 109]. Furthermore, in a study on the electron beam irradiation of ibuprofen, 1-(4-isobutylphenyl)-1-ethanol, 2-(4-formylphenyl)propanoic acid and 4-isobutylbenzoic acid were detected at 177 *m/z* [103]. The authors detected these intermediates attributed to the hydroxyl radical's interaction with the parent molecule. In this current study, it is unlikely that the formation of these by-products at 2 V of applied voltage has the same origin, considering that hydroxyl radical formation requires a higher input voltage and a higher overpotential for oxygen evolution (2.8 V), a characteristic of inactive electrode materials [49, 55], our anode potential corresponding to 2 V of applied DC potential was 0.9 V. Caviglioli et al. [101] also detected the same intermediates from an oxidative and thermal treatment of ibuprofen. Szabó et al. [110] detected 1-(4-isobutylphenyl)-1-ethanol from a photodegradation study of ibuprofen and ketoprofen.

Quintana et al. [111] attributed the formation of the fragment peak at 177 *m/z* to the microbial degradation of the parent molecule in two steps: first, the hydroxylation into 2-hydroxy ibuprofen, and then decarboxylation. Using a liquid chromatography electrospray ionization quadrupole time of flight mass spectrometer, Jacobs et al. [112] observed a chromatographic peak that was related to 4-isobutyl acetophenone at 177 *m/z*, after the photolysis of ibuprofen. The reported retention time of 7.4 min is similar to our retention time of 7.3 min. The formation of this by-product was again related to the possibility of hydroxyl radical interaction with the parent molecule in another study [113]. These observations and their correlation to the findings under this study conditions present an opportunity to further understand electrochemical filtration at different applied voltages and the contribution from oxygen-active species.

3.3.5.2. Possible degradation pathways for ibuprofen during electrochemical filtration

Figure 3-10 shows a possible scheme for ibuprofen degradation based on mass spectrometry data and comparisons to previous studies. It is commonly observed that degradation begins by deformation at the terminal chains and the carboxylic functional group, leading to the formation of large-molecular-weight by-products, such as 4-isobutylbenzoic acid, 1-(4-isobutylphenyl)-1-ethanol and 2-(4-formylphenyl) propanoic acid, with the release of carbon dioxide and aliphatic by-products. In our case, this could be seen only when 2 V was applied. Further chain cleavage followed by opening the benzene ring, leading to the formation of lower-molecular-weight by-products that could be observed in effluents obtained at 3 V of applied DC potential, such as 4-ethylbenzaldehyde, (4-methylphenyl) acetaldehyde, (Z)-4-(1-propenyl) phenol, 2-phenylpropanal, 4'-methylacetophenone, 5-methyl-3-hexen-2-one, and 5-methyl-5-hexen-2-one.

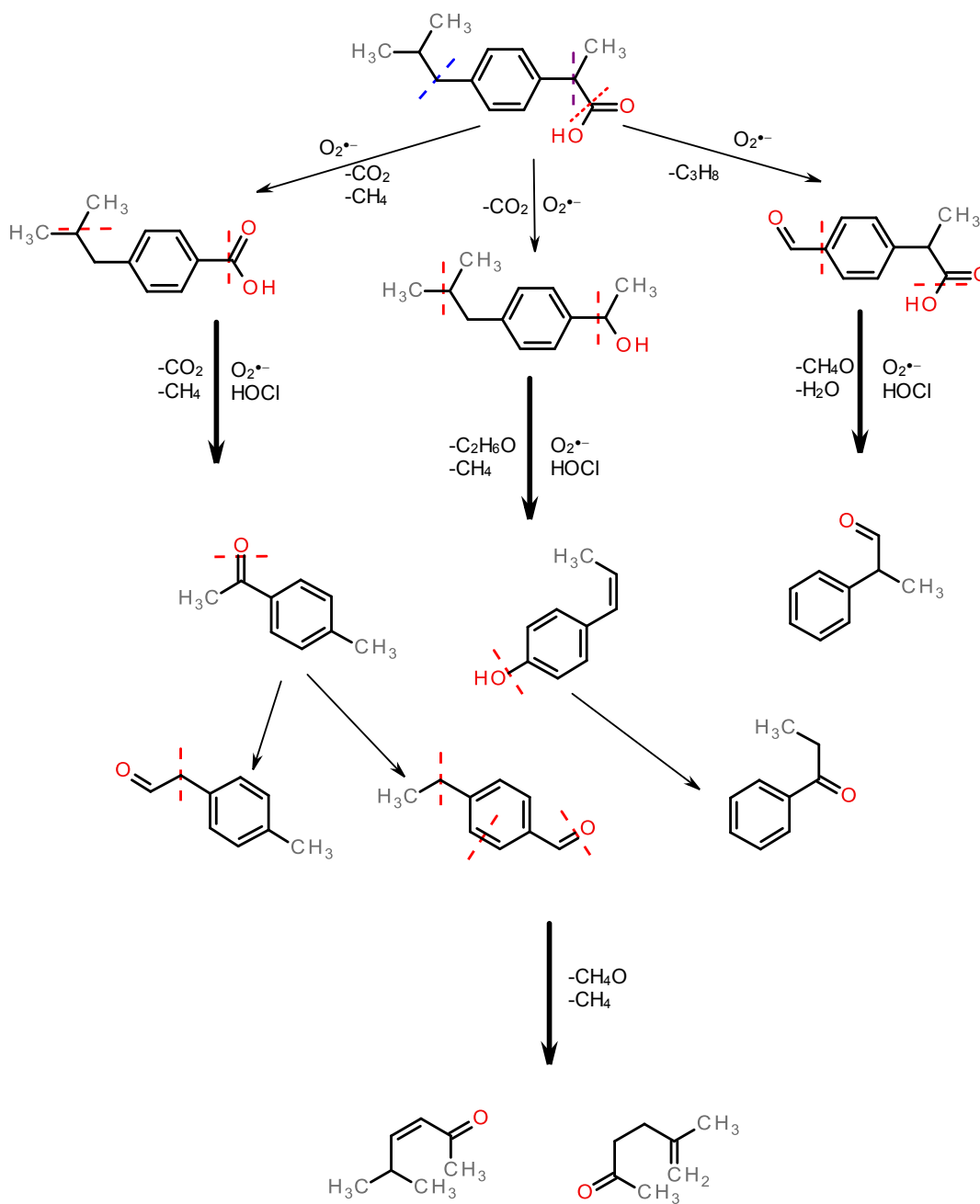


Figure 3-10. Possible degradation pathways for ibuprofen during electrochemical filtration, based on the LC-MS results.

3.4. Conclusion

An evaluation of pristine multiwalled carbon nanotubes (MWNTs) and carboxylated multiwalled carbon nanotubes (MWNTs-COOH) was conducted to determine the removal of an anti-inflammatory drug, ibuprofen, through filtration and electrochemical filtration. The removal of the target molecule from aqueous solutions was successfully achieved at various applied voltages, concentrations, and CNTs surface loadings. It is concluded that the best conditions were employed using electrochemical filtration in acidic conditions, at 2 V of applied DC voltage and a flow rate of 0.2 mL/min. It was evident that the removal of ibuprofen at applied voltages of 2 and 3 V was controlled mainly by bulk indirect oxidation pathways. At an applied voltage of 2 V, complete elimination of the target molecule was achieved when a longer residence time within the filter media was allowed. Three major by-products were detected using electrochemical filtration of the target molecule at 2 V: 4-isobutylbenzoic acid, 1-(4-isobutylphenyl)-1-ethanol, and 2-(4-formylphenyl)propanoic acid, arising from the degradation of ibuprofen, which are known for cytotoxic effects. Subjecting the target molecule to 3 V led to the removal of ibuprofen and its major toxic by-products and the formation of lower-weight products. Lower flow rates and larger CNTs surface loading results in longer residence times within the filter media, leading to a complete removal of ibuprofen and all of its products by electrofiltration at 2 V. A significantly enhanced performance of the MWNTs-COOH filters compared to that of the MWNTs filters was observed at 0 and 1 V, due to the presence of more hydrophilic sites and larger surface area of the former, which allowed for better surface interactions and improved adsorption capacity.

Acknowledgements

This note is to acknowledge the financial contributions of the Natural Sciences and Engineering Research Council (NSERC) of Canada and Concordia University.

Chapter 4: Perceiving Different Factors of Influence during Dead-end Electrochemical Filtration of Bisphenol A using Multiwalled Carbon Nanotubes: Resistance to Surface Passivation, Reactive Oxygen Species and Residence Time

Abstract

Bisphenol A is considered to be one of the most highly produced chemicals in industry. Bisphenol A is widely used in the manufacture of numerous products that are used extensively around the world. One of the major industries that uses bisphenol A is the production of consumer and household goods, which results in pervasive human exposure to the chemical. Both pristine and boron-doped multiwalled carbon nanotubes were employed as filtration and electrochemical filtration materials, resulting in a significant removal of bisphenol A. To understand the optimal conditions for bisphenol A removal and reduction of toxic effects in aqueous solutions, the filters were tested under different conditions and parameters. The electrolytic solutions were tested at various pH in both the presence and absence of salt (NaCl) to better elucidate the role of electrolytic species in the electrodegradation process during electrochemical filtration. It was shown that the presence of salt is not critical for the highest contaminant removal efficiency, likely due to the vital role of other electroactive species (e.g. reactive oxygen species [ROS]). The “salting out” effect was examined by varying salt concentration to observe the fouling nature of bisphenol A and it was concluded that bisphenol A does not passivate the surface of multiwalled carbon nanotubes (MWNTs) during the filtration process. Despite a significant difference in the stability and purity of pristine multiwalled carbon nanotubes (MWNTs) and boron-doped multiwalled carbon nanotubes (BMWNTs), as indicated by thermogravimetric analysis (TGA), the electrochemical performance of both types of MWNT was almost identical. This indicates that a limited number of specific active sites on the MWNT and BMWNT surfaces participate in the electrochemical filtration process. Regardless of the composition and pH of the electrolytic solutions, near complete removal of 1 mg/L bisphenol A at 2 and 3 V of applied DC potentials was achieved, indicating that the electrochemical filtration process is voltage dependent at both 2 and 3 V. A significant reduction in toxicity, with an almost complete removal of 10 mg/L bisphenol A, was achieved after 424 minutes of electrochemical filtration when the electrochemical filter

residence was increased by a multiple of 7.4 fold (from 2.0 to 14.9 seconds) at 3 V of applied potential. The degradation products of bisphenol A were identified using liquid chromatography-mass spectrometry (LC-MS) and it was found that most of the formed products are the short chain aliphatic carboxylic acids with no toxicity concerns, with complete disappearance of aromatic products when a 3 V DC potential was applied. Based on these results, degradation pathways corresponding to different tested conditions were predicted and developed.

Keywords: Bisphenol A, Multiwalled carbon nanotubes, Doping, Electrochemical filtration, Oxidation

4.1. Introduction

Endocrine disrupting chemicals (EDCs) and their existence in nature have been a growing concern due to their dangerous health effects. Bisphenol A (BPA) is among many EDCs used in vital industries and is produced worldwide in large quantities at a reported rate of over six billion pounds daily. BPA is used as a starting chemical in many products such as adhesives, plastics, powder paints, thermal paper and paper coatings, epoxy resins and much more [20, 21]. The presence of BPA in wastewater has been detected in significant amounts ranging from 0.07 to 150 $\mu\text{g/L}$ and 0.013 to 0.24 $\mu\text{g/g}$ in primary and secondary wastewater sludge, respectively [21, 22]. Due to the growing demand for daily household products that contain BPA, it is expected that human and animal exposure to this harmful chemical is a mounting concern.

The electrochemical filtration process is an emerging technology that shows an efficient ability to eliminate pathogens from wastewater and aqueous solutions and remove trace chemicals thus eliminating their harmful and toxic effects from nature [72, 74-76, 82, 83, 86, 114-116]. The electrochemical filtration process has shown a superior time efficiency, and thus energy savings, over batch electrolysis due to the combination of conventional filtration and electrochemical degradation, therefore reducing operation times from hours to minutes. The effective participation of different modes of mass transport was clearly observed during electrochemical filtration in previous studies making this process very efficient and more practical as compared to conventional batch electrolysis [74, 114].

The elimination of BPA from water using various advanced methods was investigated to overcome the limited BPA removal efficiency of conventional wastewater treatment processes [8,

37, 59, 117, 118]. Zhang et al. [8] showed that BPA was successfully degraded through oxidative interactions with permanganate anions and that the formed by-products suggested that the interaction of permanganate with BPA starts at benzoic rings, similar to the degradation of BPA by ozonation. The same group also concluded that occurrence of solutes and humic acids during the treatment process did not show any negative alterations to the removal of BPA via permanganate oxidation at a pH of 7.

Cui et al. [59] studied the electrochemical degradation of BPA in a batch electrolysis system using four different anode materials: boron-doped diamond (BDD), titanium-supported antimony-doped tin dioxide (Ti/Sb–SnO₂), titanium-supported ruthenium oxide (Ti/RuO₂), and platinum (Pt). They found that the different electrode materials have a substantial impact on the overall process effectiveness in eliminating BPA. BDD and Ti/Sb–SnO₂ achieved the highest outcomes in the electrodegradation of BPA, primarily due to their ability to produce reactive hydroxyl radicals during the electrochemical degradation process, with low participation from wasting reactions like heterogeneous water oxidation and oxygen evolution. On the contrary, Pt and Ti/RuO₂ lacked the ability for higher production of hydroxyl radicals, thus culminating in poor outcomes. In the same study, it was concluded that different factors like current density and electrode material are important and should be combined to achieve the best results. They found that at low current densities, Ti/Sb–SnO₂ could perform efficiently but become unstable with increasing current density, and thus BDD was able to perform better at current densities as high as 50 mA/cm².

Rosenfeldt et al. [37] studied UV photolysis and the UV photocatalytic advanced oxidation process (UV/H₂O₂). They concluded that UV/H₂O₂ was a more efficient approach for BPA removal, again due to the production of hydroxyl radicals and their active and unselective ability to interact with and degrade BPA. Fukahori et al. [117] developed TiO₂-zeolite sheets and investigated their ability to surpass the zeolite-free TiO₂ in adsorbing and decomposing BPA. They concluded that the enhanced adsorption on the surface of the zeolites could lead to increased amounts of BPA, thus leading to better degradation by free hydroxyl radicals generated by photolysis on the TiO₂ surface. In their study, Deborde et al. [118] discussed mechanistic insights of the chemical pathways for the ozonation of BPA. They concluded that ozone (O₃) could attack the unsaturation sites in the benzene rings of BPA via 1,3-dipolar cycloaddition, efficiently destabilizing BPA and cause degradation.

In the previous study, an efficient removal of a pharmaceutical (Ibuprofen) was demonstrated through a dead-end electrochemical filtration process using multiwalled carbon nanotubes (MWNTs) as an effective electrochemical filter [114]. In this previous study, we shed light on the importance of assimilating different factors including the surface functionalization of the MWNTs filter, the chemical composition and pH of the background solution, and the flow rate. We concluded that when a low DC potential is applied (0-1 V), surface interactions play a significant role and that adsorption is the dominant mechanism in removing ibuprofen from aqueous solutions. Hydrophilic and hydrophobic interactions were better integrated and provided more efficient adsorption of ibuprofen on the MWNTs surface when carboxylated multiwalled carbon nanotubes (MWNTs-COOH) were used at a low pH. At a higher voltage application (2-3 V), bulk oxidation reactions were observed to dominate. Furthermore, pH of the solution played a significant role throughout the process for both low and high voltage applications regardless of the filtration material. Nevertheless, we concluded that bulk oxidation reactions mainly occurred through ROS formations and that the participation of ROS was greater than reactive chlorine species produced from the background salt electrolyte.

As an extension to our previous observation on the presence and participation of ROS during the electrochemical filtration process by MWNTs, this current study further investigates the involvement of ROS in the process by varying the composition and pH of the background solution in addition to an overview of the effect of doped MWNTs. Moreover, this study is providing a detailed insight into the degradation of BPA during electrochemical MWNTs filtration and the major effect of increased residence time within the filter body for the complete removal of BPA and its phenolic intermediates. The effect of voltage was clearly observed to be an important factor for enhancing the kinetics of overall removal. It was noted that BPA is readily oxidizable and easily removable during electrochemical MWNTs filtration likely due to its relatively low oxidation potential and that BPA has no fouling effects on the MWNT filter.

4.2. Materials and Methods

4.2.1. Materials

Pristine multiwalled carbon nanotubes (MWNTs 20-30 nm OD, average length 10-20 μm and electrical conductivity >100 S/cm) with 95 % purity by weight, as specified by the

manufacturer, was purchased from Cheap Tubes Inc., Cambridge Port, VT, USA. The purity of the pristine MWNTs was measured through TGA analysis and found to be around 99 %. OD was estimated using SEM and ranged between 14-40 nm. Boron-doped multiwalled carbon nanotubes (BMWNTs 20-40 nm OD, average length 50 μm) were purchased from Nanotech Labs, NC, USA with 1-2 % boron lattice doping and 7- 8% residual iron by weight, and were used as received. The measured purity of BMWNTs, as indicated by TGA, was around 80 %. Specific surface area was measured using Brunauer–Emmett–Teller (BET) and determined to be 165.97 m^2/g for pristine MWNTs and 59.52 m^2/g for BMWNTs. Bisphenol A with 99 % purity and molecular weight 228.29 g/mole was purchased from Sigma-Aldrich, Oakville, ON, Canada. Sodium chloride, sodium hydroxide and sulfuric acid with ≥ 98 % purity, were all purchased from Fisher Scientific, Ottawa, ON, Canada and were used in the preparation of background solutions and pH adjustments. Nitro blue tetrazolium chloride (NBT) of assay 98%, N,N-Diethyl-p-phenylenediamine with assay 97%, oxalic acid dehydrate with purity $\geq 99\%$ and peroxidase from horseradish (146 units/mg) were all purchased from Sigma-Aldrich, Oakville, ON, Canada and were used to prepare superoxide and hydrogen peroxide assays. MWNTs and BMWNTs suspensions were prepared in 99% pure dimethyl sulfoxide (DMSO), purchased from Fisher Scientific, Ottawa, ON, Canada. 5- μm polytetrafluoroethylene (PTFE) membranes were purchased from Millipore, Etobicoke, ON, Canada and used as a filter substrate. Magnesium sulfate, sodium bicarbonate, calcium chloride, potassium dihydrogen phosphate, ammonium chloride, and trisodium citrate were purchased from Fisher Scientific, Ottawa, ON, Canada and were used to prepare synthetic secondary wastewater effluent.

4.2.2. Electrochemical MWNTs and BMWNTs Filter Preparation

The preparation method for multiwalled carbon nanotube filters was as introduced in our previous study [72, 114]. Vacuum filtration was used to deposit MWNTs and BMWNTs from suspensions in DMSO on 5- μm PTFE membranes (Millipore) as the substrate material. The filters were prepared using both 20 and 40 mL of MWNTs and BMWNTs suspensions (0.5 mg/mL) each. The 20 mL sample resulted in surface loadings of 1.04 mg/cm^2 and thickness ranges from 39.47 – 43.08 μm , while the 40 mL sample led to a surface loading of 2.08 mg/cm^2 and had a thickness ranging from 78.9 to 82 μm , as indicated by SEM x-sectional view. The preparation process involved depositing the MWNTs or BMWNTs onto the PTFE membrane, then rinsing once with

ethanol (50 mL), rinsing once with a 50:50 ethanol and DI water (50 mL) solution, and finally rinsing six times (50 mL each) with DI water (a total 325 mL of DI water and 75 mL ethanol) to wash off all of the remaining DMSO solvent. The freshly prepared MWNTs and BMWNTs filters were used for each experiment.

4.2.3. Electrolyte Solutions and pH Conditions

The composition and pH of electrolyte (background) solutions were varied to obtain a better understanding of the role of different reactive species in the electrochemical process. Sodium chloride (NaCl) was used as a conductive electrolytic species and as a source of chlorides, which can be oxidized in the process to form reactive chlorine with oxidative abilities [61, 114, 119]. The electrochemical performance was also studied in the absence of NaCl at pH 3 and 9, to track the participation of ROS in the absence of reactive chlorine. Concentrations of NaCl used were varied from 1 to 100 mM, and the pH was around 6. In the presence (pH 6) and absence (pH 3 and 9) of 10 mM NaCl, the conductivity was observed to be in the range of 3×10^{-7} to 4.62×10^{-7} S/cm² for MWNTs and 8.4×10^{-7} to 1.34×10^{-6} S/cm² for BMWNTs, at both 2 and 3 V of applied DC potential. Instantaneous current densities using MWNTs increased significantly when the concentration of NaCl was increased, from 1.8×10^{-4} mA/cm² at 1 mM NaCl to 3.5×10^{-3} mA/cm² at 100 mM NaCl, while steady state currents remained at 6.03×10^{-5} mA/cm². The concentrations of bisphenol A used in this study ranged from 1 to 100 mg/L.

4.2.4. Filtration and Electrochemical Filtration Processes

Conventional and electrochemical dead-end filtration processes were completed using a bench scale electrochemical filtration cell, as described in our previous study [72-74, 83, 114, 116]. An Agilent E364_A power supply, Agilent Technologies, Rockaway, NJ, USA was used for DC voltage application. MWNTs and BMWNTs were used as anode electrochemical filters with a 0.1 mm thick titanium ring as an electrical connector to the surface of the MWNT anode filter and a perforated stainless steel shim of thickness 0.05 mm was used as the cathode. During dead-end electrochemical filtration, 1, 2 and 3 V DC potentials were applied for electrochemical pathways initiation and no voltage was applied during conventional filtration. Flow rates of 0.5 and 2 mL/min were used during electrochemical filtration to investigate the effect of a change in reaction time on the toxicity reduction of bisphenol A during the process. The 2 mL/min flow resulted in a

permeate flux of 0.072 L/m².h on MWNTs and 0.202 L/m².h on BMWNTs at a surface loading of 1.04 mg/cm². All experiments were performed at room temperature (23°C ± 1).

4.2.5. Stability and morphology characterization of the MWNTs and BMWNTs Filters

The content purity and stability of the MWNTs and BMWNTs were examined using thermogravimetric analysis (TGA) TA instruments, Trios V3.3, Waters LLC, New Castle, DE, USA. The protocol used for analysis was the same as described in our previous study [82, 114]. MWNTs and BMWNTs were first exposed to temperature increases of 10°C min⁻¹ up to 150°C maintained for 30 minutes, then the temperature was then further raised at the same rate up to 1000°C and maintained for 30 minutes. The samples were then allowed to cool, then weight % and mass changes were recorded. Brunauer-Emmett-Teller (BET), Quantachrome Autosorb Automated Gas Sorption System, Autosorb 1, Boynton Beach, Florida, USA was used to evaluate the specific surface area (m²/g) and total pore volume (cm³/g). The BET analysis was done using nitrogen gas and outgas temperature was 100°C; bath temperature was 77.3°C and analysis time was 1825.3 minutes. The surface characterization and analysis of the MWNTs and BMWNTs was performed using scanning electron microscopy (SEM) and energy dispersive X-ray (EDS), FEI Inspect F-50 FE-SEM with EDAX Octane Super 60 mm² SDD and TEAM EDS Analysis System, Dawson Creek, Oregon, USA, and the analysis was performed on the MWNT filters before and after use in treatment.

4.2.6. Cyclic Voltammetry

The electrochemical characterization through cyclic voltammetry for bisphenol A and the evaluation of the electrochemical performance of MWNTs and BMWNTs was achieved using a Multi- Potentiostats 8 channels + Frequency Analyzer (MPFA) 1470/1255B, Solartron Instruments, Hampshire, United Kingdom. 1.04 mg/cm² MWNT and BMWT filters were used as working electrodes, perforated stainless steel as a counter electrode, and Ag/AgCl (3 M KCl) as the reference electrode. The scan rate was 50 mV/sec and the scan range was -1 to + 1.5 V vs. Ag/AgCl.

4.2.7. Quantification of Bisphenol A Removal

An Agilent UV/VIS Cary 8454 spectrophotometer, Santa Clara, CA, USA was used to determine concentrations of bisphenol A before and after treatment and to scrutinize bisphenol A changes with time. Furthermore, the UV/VIS spectrophotometer was used to examine the presence and participation of ROS through previously reported photometric assays [120-122]. 2 ml of influent and effluent samples were used for analysis and the quantification was based on the absorbance values at 225 nm. The method detection limit (MDL) for bisphenol A by UV/VIS was determined to be 14 µg/L. Liquid chromatography-mass spectrometry (LC-MS) was used to qualify bisphenol A degradation products and predict its degradation pathways from electrolytic solutions with different compositions, pH and flow rates. The LC-MS analysis was completed using an Agilent 6210 ESI-TOF instrument, Agilent Technologies, Santa Clara, CA, USA in negative ESI mode with a Mass Hunter acquisition software (v B.02.00) using 20 µL of samples for analysis. The ESI source capillary voltage was 4000 V, nitrogen gas temperature was 350°C and flow rate was 12 L/min. The nebulizer pressure was maintained at 35 psi, the fragmenter voltage at 100 V, and skimmer voltage at 60 V. The mass range was 50 - 1000 m/z with internal calibration using the reference masses 119 and 966 m/z in the Agilent reference-mass solution. The injection gradient was: initial conditions of 5 % mobile phase B with a 1 min hold, then raised to 95% at 8 min and held for 1 min. The column was re-equilibrated at 5 % mobile phase B for 5 min before the next injection. The flow rate for mobile phases A (water + 0.1 % formic acid) and B (acetonitrile + 0.1 % formic acid) was 0.4 mL/min.

4.3. Results and Discussion

4.3.1. MWNTs and BMWNTs Stability and Surface Morphology

SEM and EDS were performed on freshly prepared MWNTs and BMWNTs filters as mentioned in the methods section. Figure 4-1 A and 4-1 C, show the SEM images of MWNTs and BMWNTs, respectively. Carbon and oxygen content were examined by EDS (Figure 4-1 B and 4-1 D), for MWNTs and BMWNTs, respectively. The results show a weight percent of 97.55% for carbon and 1.46% for oxygen in MWNTs, and comparatively 93.52% and 2.80% for BMWNTs. The EDS analysis was also done after the use of MWNTs and BMWNTs membranes in treatment and did not show any signs of surface oxidation after treatment (Figure B-3, Appendix B). Figure

4-1 E and 4-1 F represent the TGA results for as-received MWNTs and BMWNTs, respectively. The TGA shows a purity of 99 % for MWNTs and 80% for BMWNTs, indicated by the sharp drop in the weight percent between 600 and 650 °C, the temperature at which all carbon content is degraded. Below this temperature, a gradual and slight drop in weight would be due to the release of hydrogen content as water vapor. For BMWNTs, a plateau like formation at around 22-24 weight % is probably due to the formation of large iron oxide layers at the BMWNTs surface.

Total pore volume for MWNTs is 0.0104 cm^3 ($1.037 \text{ cm}^3/\text{g} \times 0.01 \text{ g}$), the surface area is 16597 cm^2 ($165.97 \text{ m}^2/\text{g} \times 0.01 \text{ g}$) for a loading of $1.04 \text{ mg}/\text{cm}^2$. The total pore volume for BMWNTs is $5.8 \times 10^{-4} \text{ cm}^3$ ($0.058 \text{ cm}^3/\text{g} \times 0.01 \text{ g}$), and the surface area is 5952 cm^2 ($59.52 \text{ m}^2/\text{g} \times 0.01 \text{ g}$) for a loading of $1.04 \text{ mg}/\text{cm}^2$, $6 \times 10^{-4} \text{ cm}^3$, as measured by BET. The thickness is $39.47 - 56.48 \text{ }\mu\text{m}$, as indicated by SEM (for further details, please refer to appendix B).

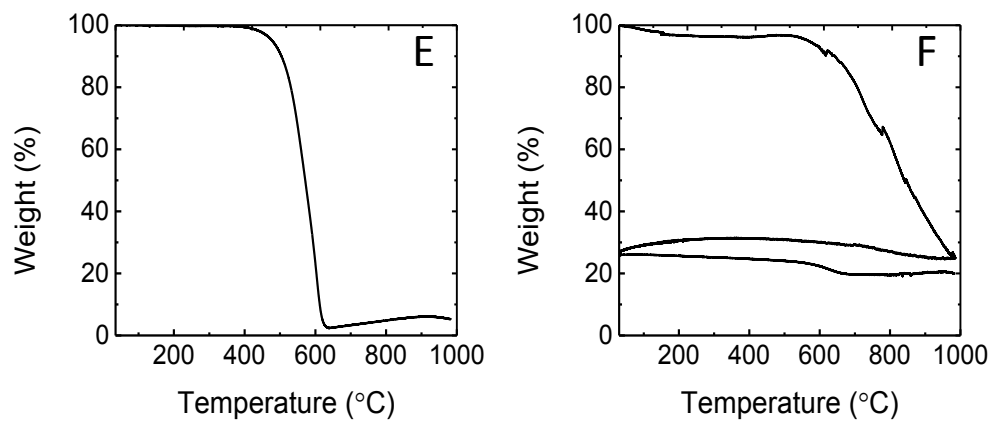
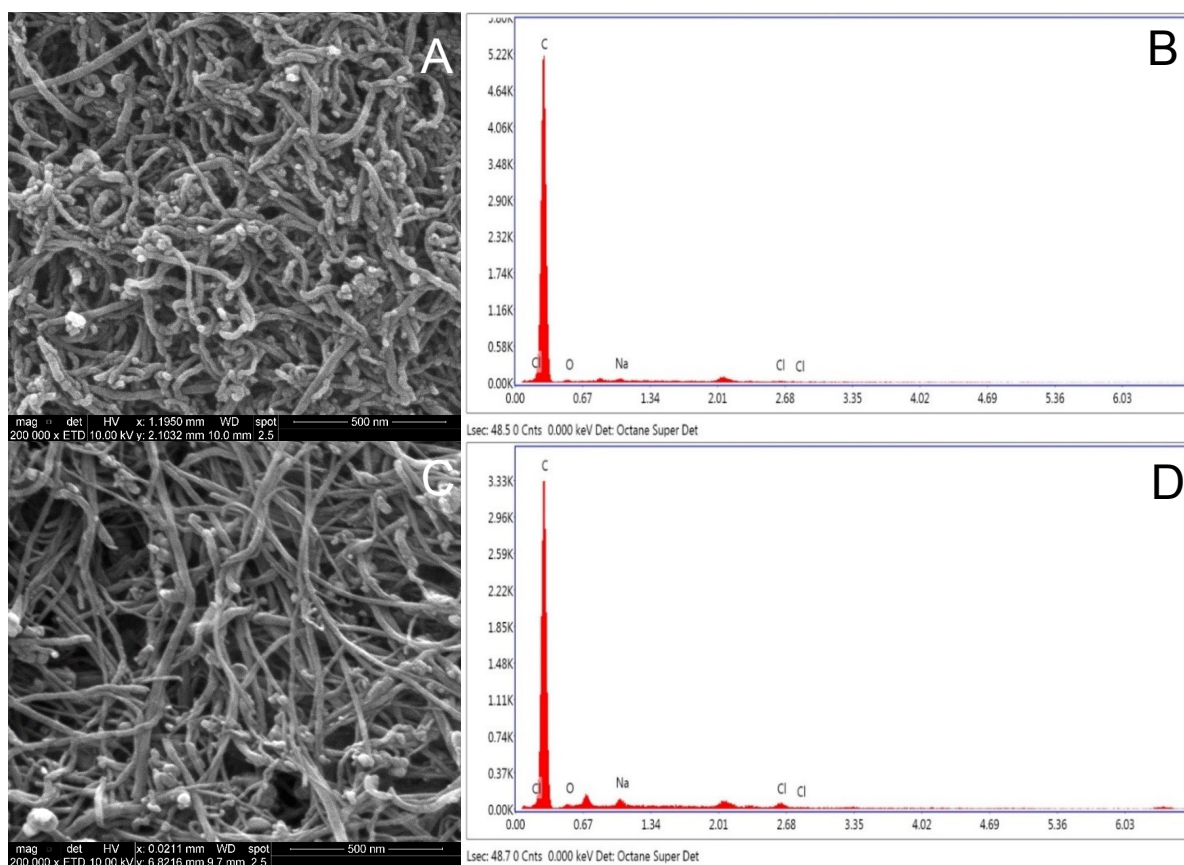


Figure 4-1. SEM and EDX for MWNTs and BMWNTs where (A) is the SEM for the MWNT filter with a surface loading of 1.04 mg/cm^2 , (B) is the EDX analysis for the MWNT filter at a surface loading of 1.04 mg/cm^2 , (C) is the SEM for the BMWNT filter with a surface loading of 1.04 mg/cm^2 , (D) is the EDX analysis for the BMWNT filter with a surface loading of 1.04 mg/cm^2 , (E) is TGA weight percent vs. temperature for MWNTs, (F) is TGA weight percent vs. temperature for BMWNTs. Characterization for the MWNTs and BMWNTs was done before use in treatment.

4.3.2. The Salting Out Effect on Bisphenol A Removal during the Electrochemical Filtration Process

In this portion of the study, we examined the fouling ability of BPA on the MWNTs surface. Thus according to previous studies on enhanced adsorption of neutral organic molecules by increasing salt concentration (Salting out effect), we decided to vary the salt concentration to mainly observe if the increase in salt concentration can enhance the adsorption of BPA on MWNTs surface. The enhanced adsorption of BPA was expected to increase its polymeric fouling ability at the MWNTs surface during the process, and as was previously reported, BPA can induce polymeric passivation during electrochemical degradation [57, 59, 90, 123].

NaCl concentrations were changed from 1 to 100 mM without changing the pH, applied voltage, filter loading nor BPA concentration. In their study on the use of chitosan-based molecularly imprinted polymer adsorbents for the selective removal of perfluorooctane sulfonate (PFOS), Yu et al. [90] reported that increasing the salt (NaCl) concentration from 50 to 500 mM could lead to enhanced adsorption of PFOS from aqueous solutions, and that in salt concentrations below 50 mM the sorption amounts were constant. Therefore, we used low to moderately high salt concentrations (1 to 100 mM), to enable a clear comparison between a wide enough range of salt concentrations and the possible salting out effect of high salt concentrations (50-100 mM) on bisphenol A adsorption or removal by MWNTs as compared to lower concentrations. Higher concentrations of salt would have corrosive effects and were not necessary for this study.

Figure 4-2 A shows the breakthrough plots for the removal of 1 mg/L BPA from 1-100 mM NaCl solutions at 0, 1 and 2 V of applied DC potential by MWNTs, and over 106 minutes of treatment time. The amounts of applied voltages were kept well under 3 V of applied DC potential (1.54 V vs. Ag/AgCl of anode potential) to minimize water oxidation and oxygen evolution (1-1.2 V vs. SCE) [49, 74, 124] which would increase the hydrophilicity of the surface. This would hinder the polymeric passivating effect of BPA on the MWNT surface by altering hydrophobic surface interactions between BPA and MWNTs. Figure 4-2 B shows the instantaneous and steady-state current densities in mA/cm² during the electrochemical filtration treatment of 1 mg/L BPA, corresponding to Figure 4-2 A.

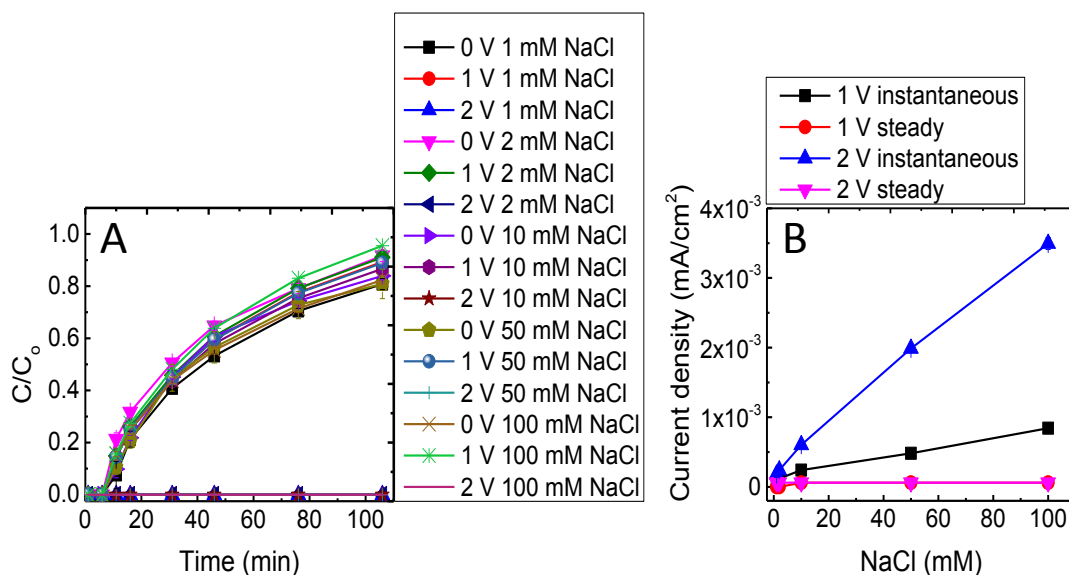


Figure 4-2. (A) Breakthrough plots for filtration and electrochemical filtration of 1 mg/L BPA in 1, 2, 10, 50 and 100 mM NaCl (pH 5.7 – 6) by MWNTs at 0, 1 and 2 V of applied DC potential and (B) is instantaneous and steady-state current densities for electrochemical filtration of 1 mg/L BPA in 1, 2, 10, 50 and 100 mM NaCl by MWNTs at 1 and 2 V of applied DC potential. Flow rate was 2 mL/min., MWNTs surface loading was 1.04 mg/cm² and experiments were performed at room temperature.

From Figure 4-2 A and B, it could be concluded that there were no fouling effects induced during the treatment of 1 mg/L BPA in 1-100 mM NaCl. At 0 and 1 V of applied DC potential, the removal of BPA seemed identical (Figure 4-2 A) indicating that at 1 V (0.35 V vs. Ag/AgCl of anode potential), the removal of BPA is similar to that at 0 V and only occurring due to physical adsorption (at pH 5.7-6). Therefore, the magnitude of the anode potential was not sufficient to initiate any oxidative pathways for BPA. Looking to the breakthrough trends at 0 and 1 V DC potential, an early breakthrough (from 6-10 minutes of filtration and electrofiltration time) can be observed, indicating that BPA excessively consumes the MWNTs active surface sites. Given the enormous surface area of MWNTs (16597cm² at a loading of 1.04 mg/cm²), the reason for such an early breakthrough at 0 and 1 V is not clearly understood. In our previous study, we could shed light on overcoming the limitations of MWNTs adsorption of ibuprofen and we concluded that surface oxy-functionality (-COOH) in MWNTs can lead to enhanced sorption capacity toward

molecules with oxy-functional groups (-COOH) during the electrochemical filtration process at 0 -1 V [114].

Other researchers also reported that oxygen-containing molecules can be readily adsorbed on carbon nanotubes (CNTs) with surface oxy-functionality [88, 89]. In this current study, the previous hypothesis is not our primary interest; rather we wanted to better understand the hydrophobic adsorptive effect of bisphenol A on the surface of pristine MWNTs. When the applied voltage was raised to 2 V, the removal performance was greatly enhanced and achieved a nearly steady, complete removal even after 106 minutes of operation time. This outcome indicated that electrodegradation pathways were initiated at an applied potential of 2 V (0.76 V vs. Ag/AgCl of anode potential) and BPA was promptly and consistently eliminated overtime. The observation that steady-state current densities were not altered over time (stable at 6.03×10^{-5} mA/cm²) at 1 and 2 V (Figure 4-2 B) was another indication that the effect of surface passivation effect was not the case. (For further information on removal flux, permeate flux, removal capacity values, and energy consumption and mineralization current efficiency, please refer to supporting information).

4.3.3. MWNTs and BMWNTs Electrochemical Performance Characterization through Cyclic Voltammetry

Figure 4-3 shows the cyclic voltammograms for the electrochemical filtration of 1, 50 and 100 mg/L BPA in 10 mM NaCl using MWNTs and BMWNTs (Figure 4-3 A and B) and the linear correlation between BPA concentrations and current in mA (Figure 4-3 C and D). BMWNTs were selected for observing their electrochemical performance in the current and a later section. Previous reports have shown that doping increases the conductivity and specific capacitance of CNTs and that among all CNTs, boron-doped CNTs are the least prone to fouling. Furthermore, boron and nitrogen-doped CNTs have a larger work function (the distance from the material Fermi level to the vacuum level) compared to pristine CNTs, with the largest reported for boron-doped CNTs (5.2 eV), making it a more appropriate CNTs type for oxidative processes [82, 125-130]. Thus, in the current study; we wanted to investigate and compare the apparent performance of BMWNTs to that of MWNTs in achieving the best results in BPA elimination by electrochemical filtration.

In agreement with a previous study, the removal of aqueous phenol using pristine, boron-doped and nitrogen-doped CNTs showed the overall performance on total organic carbon removal (TOC) as similar among the doped and pristine CNTs[82]. Our cyclic voltammogram exhibited almost identical electrochemical performance during the treatment of BPA by MWNTs and BMWNTs (Figure 4-3 A and B) and the absence of fouling effects on MWNTs as shown in Figure 4-2.

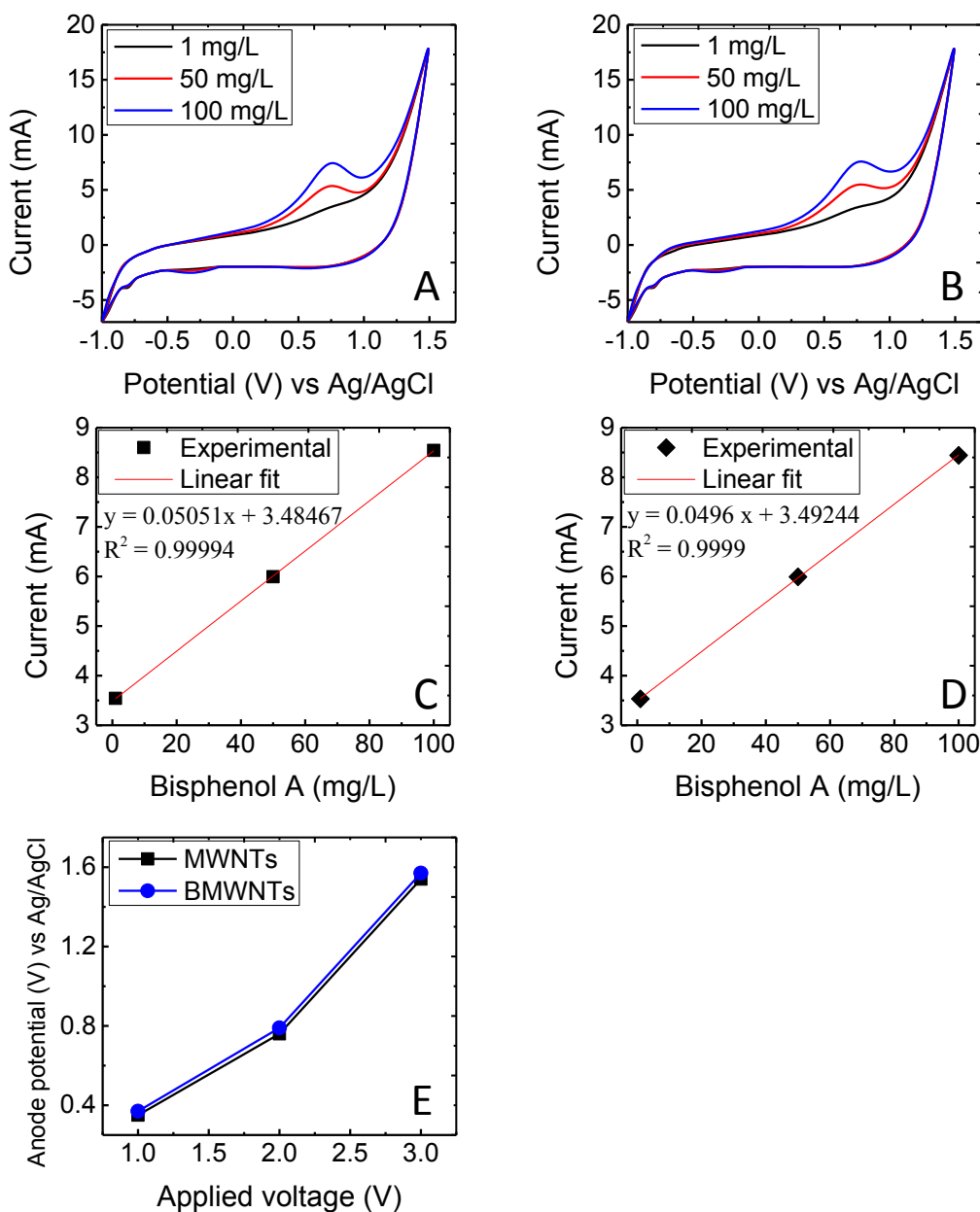


Figure 4-3. Cyclic voltammetry for electrofiltration of 1, 50, and 100 mg/L BPA in 10 mM NaCl. Where (A) is the cyclic voltammogram for electrofiltration by MWNTs, (B) is the cyclic voltammogram for electrofiltration by BMWNTs, (C) is the linear correlation for current vs. BPA concentration on MWNTs (corresponding to (A), current peak at 0.75 V), (D) is the linear correlation for current vs. BPA concentration on BMWNTs (corresponding to (B), current peak at 0.75 V), and (E) is the anode potentials vs. Ag/AgCl corresponding to 1, 2 and 3 V of applied DC potential and. MWNTs and BMWNTs loading was 1.04 mg/cm^2 . Experiments were performed at a flow rate of 2 mL/min and at room temperature.

BPA concentrations were varied on a single electrochemical filter of each MWNT type, and the cyclic voltammograms were overlaid (Figure 4-3 A and B). MWNTs and BMWNTs were used as the working electrode, stainless steel as the counter electrode, and Ag/AgCl (3 M KCl) was used as a reference electrode. The scan rate was 50 mV/sec and the sweep range was -1 to 1.5 V vs. Ag/AgCl. Anode potentials corresponding to 1, 2 and 3 V were 0.35, 0.76 and 1.54 V vs. Ag/AgCl for MWNTs and 0.37, 0.79 and 1.57 V vs. Ag/AgCl for BMWNTs, respectively.

From Figure 4-3 A and B, a consistent increase in oxidation current with increasing BPA concentration from 1 to 100 mg/L was observed corresponding to 0.75 V vs. Ag/AgCl. This behavior suggests that the oxidation potential for BPA is 0.75 V on both types of MWNTs. Previous studies on the electrochemical detection and degradation of BPA using different protocols showed that the oxidation potential of BPA was in the range of 0.5 to 0.9 V [57, 131, 132]. The relatively low oxidation potential of BPA could be the primary reason for BPA being prone to oxidation and hence being readily removed at relatively low to moderate applied voltages (≤ 2 V). Thus, the degradation of BPA takes place through the participation of direct electron transfer from BPA molecules to the MWNTs and BMWNTs surface at 2 and 3 V of applied DC potentials. A sharp rise in oxidation current can be observed at and above 1 V vs. Ag/AgCl, indicating an increased water oxidation with increasing potential (Figure 4-3 A and B). There are also two minor reduction peaks at - 0.45 and - 0.77 V. The peak at - 0.45 V is not in agreement with any previous observations during BPA electroanalysis, thus it could be related to trace iron reduction, while the peak at - 0.77 V is most likely due to oxygen reduction and superoxide formation [86, 114].

BMWNTs have significantly less thermal stability than pristine MWNTs, as observed from the TGA analysis (Figure 4-1 F), likely due to the presence of boron atoms within the sp^2 lattice of the CNTs. Despite this; the electrochemical stability of BMWNTs seems satisfactory, if not high. Furthermore, the cyclic voltammetry showed no clear signs of iron oxidation or release despite the presence of 7-8 % iron by weight on the BMWNTs surface (Figure B-1, Appendix B). Rather, the BPA oxidation took place efficiently, and the TGA analysis suggested the formation of iron oxide layers on the BMWNTs surface, yet not causing active surface sites to be blocked. The linear correlation between increasing BPA concentration and the increase in oxidation current (Figure 4-3 C and D) confirms that diffusion mass transfer is occurring, in agreement with our

previous observation [114]. Therefore, once the molecules approach the surface rapidly under flow, diffusion controlled mass transfer becomes the determining factor for adsorption and oxidation on the MWNTs surface. At pH 6, BPA molecules are expected to be neutral (pKa 9.6 – 11.3) [133, 134], and therefore migration is not considered. The hydrodynamic flow is likely an important factor that could significantly improve the delivery of the neutral BPA molecules from the bulk to MWNTs interface and thus would reduce the time and enhance energy efficiency.

4.3.4. Electrochemical Filtration Performance in the Presence and Absence of NaCl and in Different pH Conditions

The participation of salt (NaCl) in the electrochemical filtration process was examined. Furthermore, the absence of salt enabled the investigation and confirmation of ROS involvement in the oxidation process. Figure 4-4 shows the breakthrough plots for the removal of 1 mg/L BPA by MWNTs at 0 and 3 V of applied DC potential in the presence of 10 mM NaCl at pH 6 (Figure 4-4 A), in the absence of NaCl at pH 3 (Figure 4-4 B), and in the absence of NaCl at pH 9 (Figure 4-4 C). The figure also shows results for BMWNTs filtration in the presence of 10 mM NaCl at pH 6 (Figure 4-4 D), the absence of NaCl at pH 3 (Figure 4-4 E), and the absence of NaCl at pH 9 (Figure 4-4 F).

The breakthrough trends for the absence and presence of salt are very similar indicating that the participation of reactive chlorine species in the electrochemical degradation of BPA is not of critical importance. In our previous study, the presence of NaCl did not result in the formation of chlorinated by-products [114]. Therefore, it can be concluded that the reactive oxygen species are clearly participating in the process, most likely due to a higher reactivity and faster kinetics than reactive chlorine (namely hypochlorous acid, at $\text{pH} \leq 7$) [61, 96, 114]. This observation was further confirmed in the current study through the LC-MS analysis of BPA and its degradation by-products after electrochemical filtration treatment at different conditions (i.e. presence and absence of NaCl, different flow rates, and various MWNTs surface loadings).

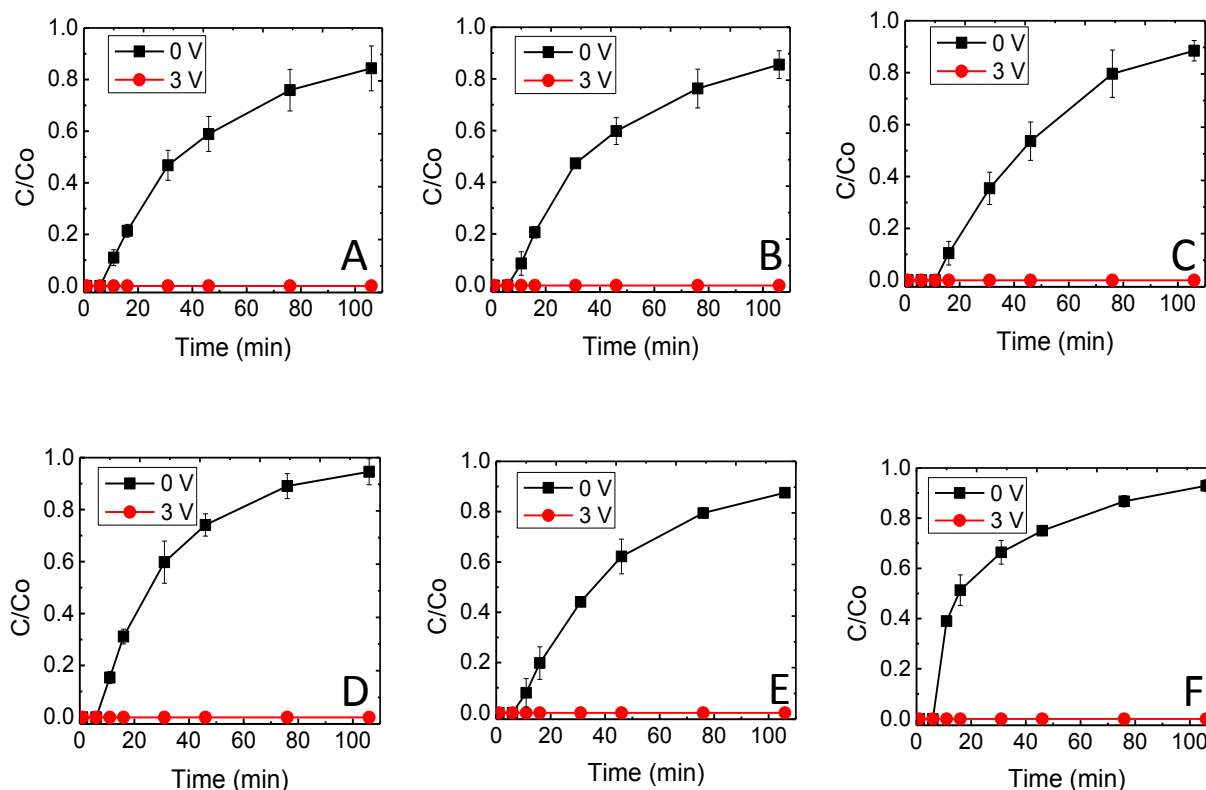
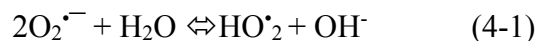


Figure 4-4. Breakthrough plots for filtration and electrochemical filtration of 1 mg/L BPA in the presence and absence of 10 mM NaCl, at different pH values, and at 0 and 3 V of applied DC potential where (A) is electrochemical MWNTs filtration in the presence of 10 mM NaCl (pH 6), (B) is electrochemical MWNTs filtration in the absence of NaCl (pH 3), (C) is electrochemical MWNTs filtration in the absence of NaCl (pH 9), (D) is electrochemical BMWNTs filtration in the presence of 10 mM NaCl (pH 6), (E) is electrochemical BMWNTs filtration absence of NaCl (pH 3) and (D) is electrochemical BMWNTs filtration absence of NaCl (pH 9). Experiments were performed at room temperature with a flow rate of 2 mL/min and the MWNTs and BMWNTs loading was 1.04 mg/cm².

The pH was varied between acidic (pH 3) and alkaline (pH 9) levels in the absence of NaCl to investigate the effect of ROS participation during electrochemical filtration. Equations (4-1) and (4-2) show that superoxide anions ($O_2^{\bullet-}$) would be favorably stable at a neutral to alkaline pH, while at an acidic pH, the formation of hydrogen peroxide (H_2O_2) would be favored [53, 68]:





Thus to differentiate the participation of superoxide and hydrogen peroxide, the pH was varied between acidic and alkaline levels.

However, our current observations comparing the outcome from Figure 4-4 B and E (absence of NaCl at pH 3) to the extent of oxidized diphenyl-p-phenylene diamine (DPD⁺) production in a hydrogen peroxide assay at pH 3 (Figure B-16, Appendix B), suggests that superoxide anions do not completely diminish toward interaction with and degradation of target contaminants during electrochemical filtration in acidic conditions. This was indicated by the seemingly limited production and stability of hydrogen peroxide in the process (as shown by the hydrogen peroxide assay at pH 3).

Moreover, the role of hydrogen peroxide in the electrochemical degradation process is not clear because the oxidative interaction of hydrogen peroxide with organic contaminants has slow kinetics and would require a catalyzed process to generate reactive oxidants (Fenton chemistry) [64, 66, 106, 135]. Therefore, it can be concluded that superoxide participation is the most dominant factor in the electrochemical degradation of BPA at 3 V of applied potential with a more notable contribution and faster reaction kinetics over hypochlorous acid and hydrogen peroxide. Furthermore, a superoxide assay was conducted at 3 V of applied potential in the current study and was found to be positive (Figure B-13 and B-14, Appendix B). (For further information on removal flux, permeate flux, removal capacity values, and energy consumption and mineralization current efficiency, please refer to supporting information).

Figure 4-5 shows the flux values for the treatment of 1 mg/L BPA by MWNTs (Figure 4-5 A) and by BMWNTs (Figure 4-5 B), corresponding to Figure 4-4. From Figure 4-5 it is evident that when a 3 V DC potential is applied, the flux values increase significantly from 21-25 $\mu\text{g}/\text{m}^2\cdot\text{h}$ at 0 V to around 60-64 $\mu\text{g}/\text{m}^2\cdot\text{h}$. The significant increase in flux values is due to the participation of the electrooxidation reactions at the MWNTs and BMWNTs surface and in the bulk of the solution. Figure 4-6 shows the energy consumption (EC) values in kWh/kg (Figure 4-6 A) and the mineralization current efficiency (MCE) in % (Figure 4-6 B), corresponding to Figure 4-4. The sharp increase in EC for the acidic (pH 3) background solution indicates the increased hydrogen evolution and thus the substantial increase in the output current as compared to the cases of neutral and alkaline pH.

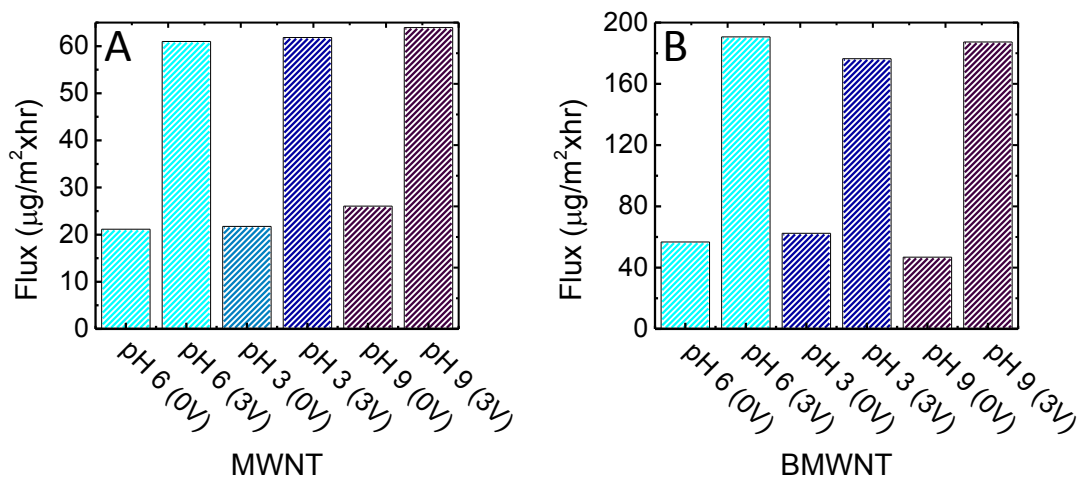


Figure 4-5. Removal flux for filtration and electrochemical filtration of 1 mg/L bisphenol A in the presence of 10 mM NaCl (pH 6), absence of NaCl (pH 3) and absence of NaCl (pH 9) using (A) MWNTs and (B) BMWNTs, corresponding to Figure 4-4.

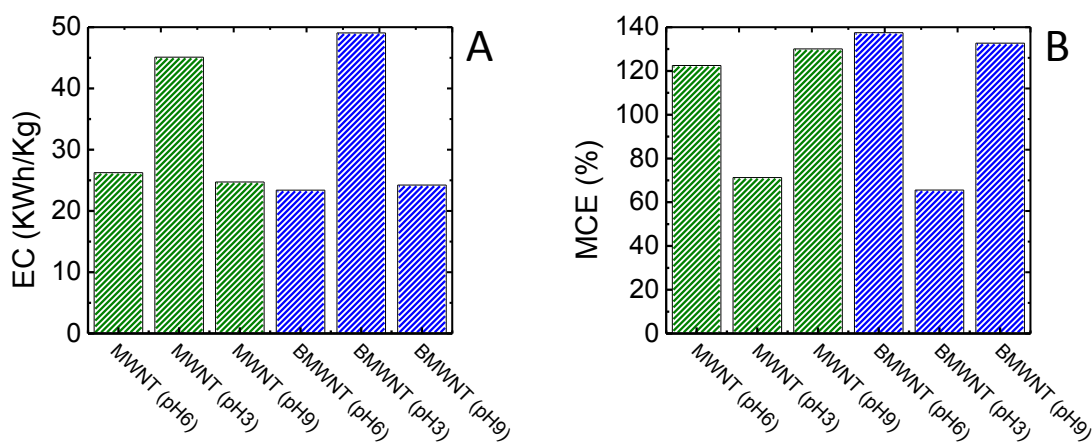


Figure 4-6. Energy consumption and mineralization current efficiency, where (A) is the energy consumption for pH variation in the presence of 10 mM NaCl (pH6) and absence of NaCl (pH 3 and 9) using MWNTs and BMWNTs at 3V of applied DC potential, (B) is the mineralization current efficiency for pH variation in the presence of 10 mM NaCl (pH6) and absence of NaCl (pH 3 and 9) using MWNTs and BMWNTs at 3V of applied DC potential. The loading for MWNTs and BMWNTs was $1.04 \text{ mg}/\text{cm}^2$, the BPA concentration was 1 mg/L and the flow rate was 2 mL/min and at room temperature.

4.3.5. Liquid Chromatography Mass Spectrometry for Monitoring Bisphenol A Degradation and Factors Affecting Degradation Pathways

4.3.5.1. Effect of Applied Voltage

LC-MS was used to monitor the degradation of BPA at different applied voltages (2 and 3 V) and the effect of increasing voltage on the efficiency of BPA electrodegradation. Figure 4-7 shows the mass spectra for 10 mg/L BPA in 10 mM NaCl before electrochemical MWNTs filtration treatment and after treatment at 2 and 3 V of applied DC potential. Samples were taken at 5, 46 and 106 minutes along a total of 106 minutes of operation time. Electrochemical filtration was performed at $23^{\circ}\text{C}\pm 1$ with a flow rate of 2 mL/min and the MWNTs loading was 1.04 mg/cm².

BPA has a major spectral peak at 227 m/z and a fragment at 273 m/z. When 2 V was applied (Figure 4-7), BPA peaks were observed to be eliminated after 5 min of treatment time, spectral traces could be observed after 45 minutes and had increased by 106 minutes. This observation confirms that BPA has an exhaustive effect on MWNTs, similar to our previous observation for the electrochemical filtration of ibuprofen [114]. When 3 V was applied, near complete elimination was achieved after 46 minutes and spectral traces could only be observed after 106 minutes of treatment. These observations led to the conclusion that the adsorption of organic contaminants has yet to take place at 3 V and that there is likely a wide range of reactions (direct and indirect oxidation) occurring at the surface of the MWNTs.

The observation that BPA could consume the active surface sites at 2 and 3 V indicates that surface adsorption takes place and direct electron transfer is likely occurring even at 3 V (1.54 V vs. Ag/AgCl of anode potential). This could indicate that either heterogeneous water oxidation and oxygen evolution are not excessively taking place when the anode potential is 1.54 V, or that it takes place yet not completely hindering the surface π - π interactions or hydrophobic interactions between BPA and the surface of the MWNTs. Furthermore, an applied voltage of 3 V clearly shows an enhanced removal of BPA compared to 2 V for the same operation time. This indicates that both direct electron transfer and indirect oxidation pathways were improved by increasing the applied voltage from 2 to 3 V, thus increasing the overall degradation kinetics for BPA.

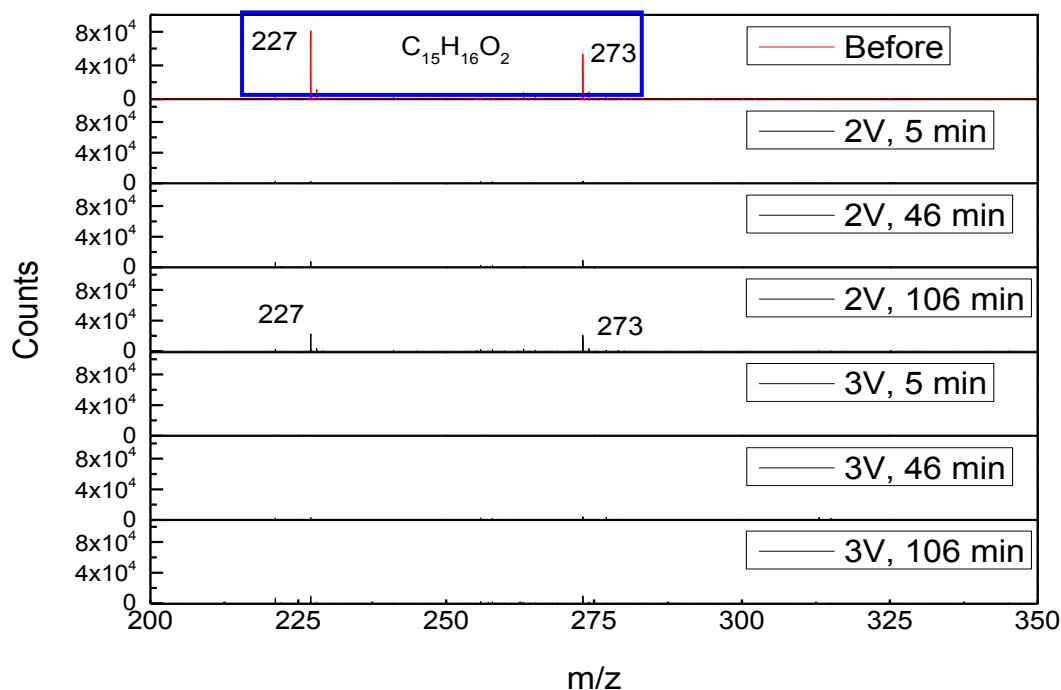


Figure 4-7. Mass spectra of 10 mg/L BPA in 10 mM NaCl (pH6) before treatment (red trace) and after electrochemical MWNT filtration treatment (black traces) at 2 and 3 V of applied DC potential after 5, 46 and 106 minutes of electrochemical filtration time. Experiments were performed at room temperature with a 2 mL/min flow rate and an MWNTs loading of 1.04 mg/cm².

Figure 4-8 A shows the formation of the degradation byproduct at a retention time (RT) of 7.8 min and Figure 4-8 B shows the 243 m/z spectral peak corresponding to RT 7.8 min in the same conditions of treatment for Figure 4-7. The formation of the 243 m/z (RT 7.8 min) indicates the formation of hydroxylated BPA derivatives [59, 65].

Cui et al. [59] reported the formation of BPA hydroxylated derivatives from the electrochemical oxidation of bisphenol A using different electrode materials in a batch electrolysis system. Furthermore, Gözmen et al. [65] stated the formation of the same starting products from an electrochemically generated (in situ) Fenton reagent during electrochemical oxidation of bisphenol A. Klein et al. [136] and Oturan et al. [137] also reported the formation of hydroxylated derivatives from the interaction of hydroxyl radicals with benzoic acid and after formation of cyclohexadienyl intermediates. They also reported that aromatic compounds are susceptible to attacks from hydroxyl radicals [59, 65, 136, 137]. All of the previously reported outcomes

suggested that hydroxyl radicals are primarily responsible for the formation of hydroxylated phenolic intermediates. In our case, we doubt the possibility of the formation of hydroxyl radicals (formation potential 2.8 V) [49, 55] at 2 V (0.76 V vs. Ag/AgCl of anode potential) and 3 V (1.54 V vs. Ag/AgCl of anode potentials). Our current observation for the formation of hydroxylated BPA derivatives in the absence of hydroxyl radicals is in agreement with our previous observation for the formation of oxy-functional by-products from the degradation of ibuprofen by electrochemical filtration [114].

Thus it can be concluded from our current and previous observations that other ROS, likely superoxide anions, are attacking and degrading target organic contaminants during electrochemical filtration, in a very similar manner and close reactivity as that of hydroxyl radicals. Additionally, the relatively rapid flow rate of 2 mL/min results in a residence time of 2.01 seconds for BPA molecules within the MWNT filter, considering MWNTs total volume (at a loading of 1.04 mg/cm²) and cumulative pore volume. Hence it can be understood that a residence time of 2.01 sec is most likely sufficient for superoxide reactions with BPA to take place and form the hydroxylated intermediates, while reactive chlorine (from the NaCl background solution) would probably require longer residence times to interact with and degrade BPA, thus producing chlorinated by-products as proposed in a later section (Figure B-30, Appendix B).

From Figure 4-8 it is clear that the production of the 243 m/z hydroxylated BPA derivatives increased with increasing applied potential from 2 to 3 V at a flow rate of 2 mL/min and a MWNTs loading of 1.04 mg/cm². This suggests an excessive electrodegradation of BPA and a more rapid accumulation of the product with increasing applied potential in the reported conditions in agreement with the declining trend of BPA observed in Figure 4-7.

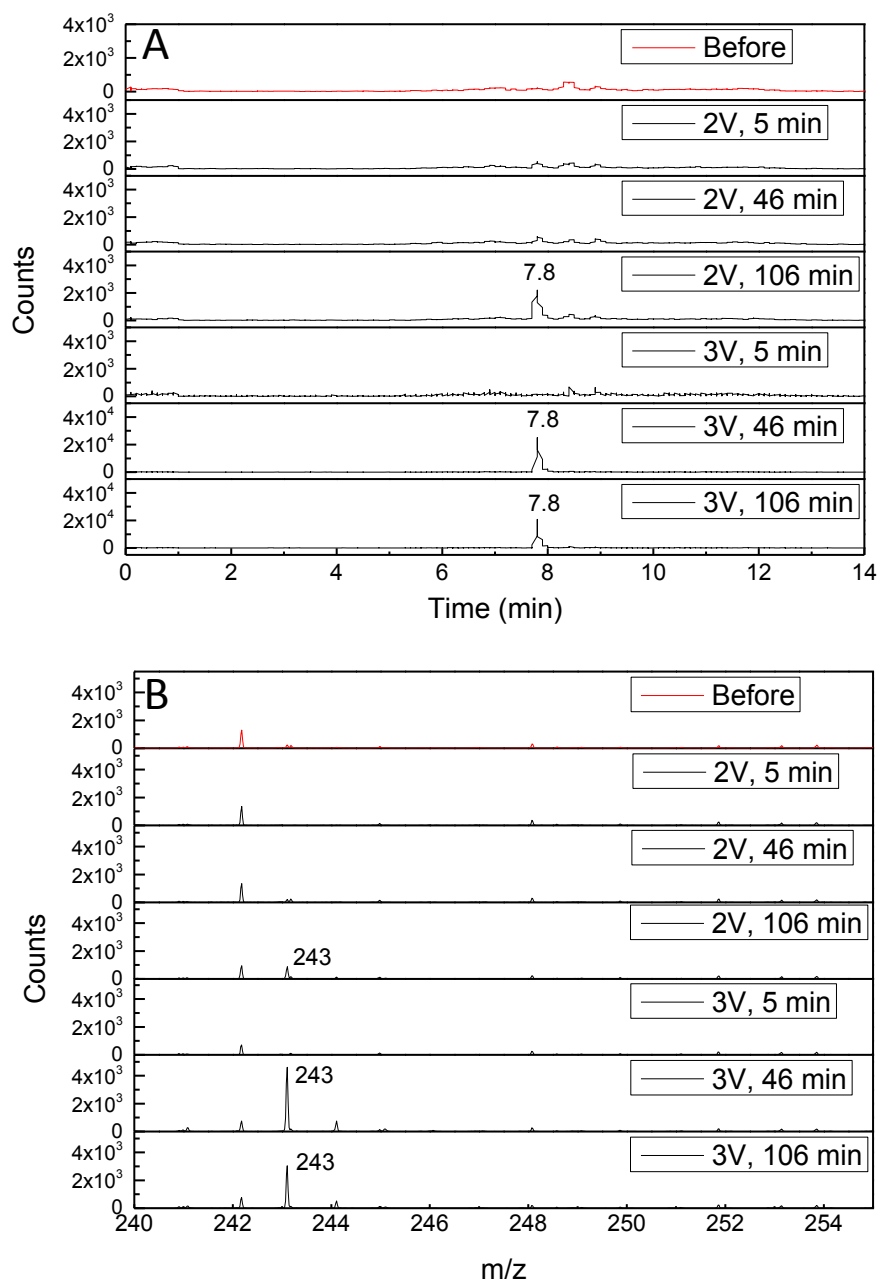


Figure 4-8. LC-MS of 10 mg/L BPA in 10 mM NaCl (pH6) before treatment (red trace) and after electrochemical MWNT filtration treatment at 2 and 3 V of applied DC potential at 5, 46 and 106 minutes of electrochemical filtration time (black traces) showing the formation of a by-product at RT 7.8 min (243 m/z), where (A) is the liquid chromatograms for 7.8 min and (B) is the mass spectra at 243 m/z (corresponding to 7.8 min). Experiments were performed at room temperature with a flow rate of 2 mL/min and the MWNTs loading was 1.04 mg/cm².

4.3.5.2. Major Degradation Pathways of Bisphenol A

The proposed BPA degradation pathways and formed degradation products, Figure 4-9, are in close agreement with previously reported pathways in studies of BPA degradation from different advanced oxidation treatment methods [8, 20, 59, 65, 118, 138]. Figure 4-9 shows the proposed BPA degradation pathways and the degradation products formed during the electrochemical filtration of BPA at a flow rate of 2 mL/min and an MWNT loading of 1.04 mg/cm² (total reaction time of 2.01 sec.).

The BPA degradation products shown in Figure 4-9 are from the set of various conditions of electrochemical filtration at 2 and 3 V of applied DC potential in the presence (pH 6) and absence (pH 3 and 9) of a NaCl salt electrolyte. It was observed that the majority of the BPA degradation products were detected after the electrochemical filtration treatments in the presence of NaCl (pH 6) and absence of NaCl (pH 3), while only the hydroxylated BPA derivatives at RT 7.8 (243 m/z) could be observed in the absence of NaCl (pH 9) (Figure B-19, Appendix B). This likely indicates more enhanced electrochemical activity in the salt and the acidic electrolytes compared to alkaline conditions.

Previous studies have indicated that aromatic compounds and hydroxylated phenol derivatives including hydroquinone, benzoquinone, catechol, hydroxyl-benzoic acid, resorcinol, isopropyl phenol, and isopropenyl phenol can result from the electrochemical oxidation of phenolic compounds [59, 65, 139]. In our analysis, these intermediates were not detected, but hydroquinone and phenol were proposed.

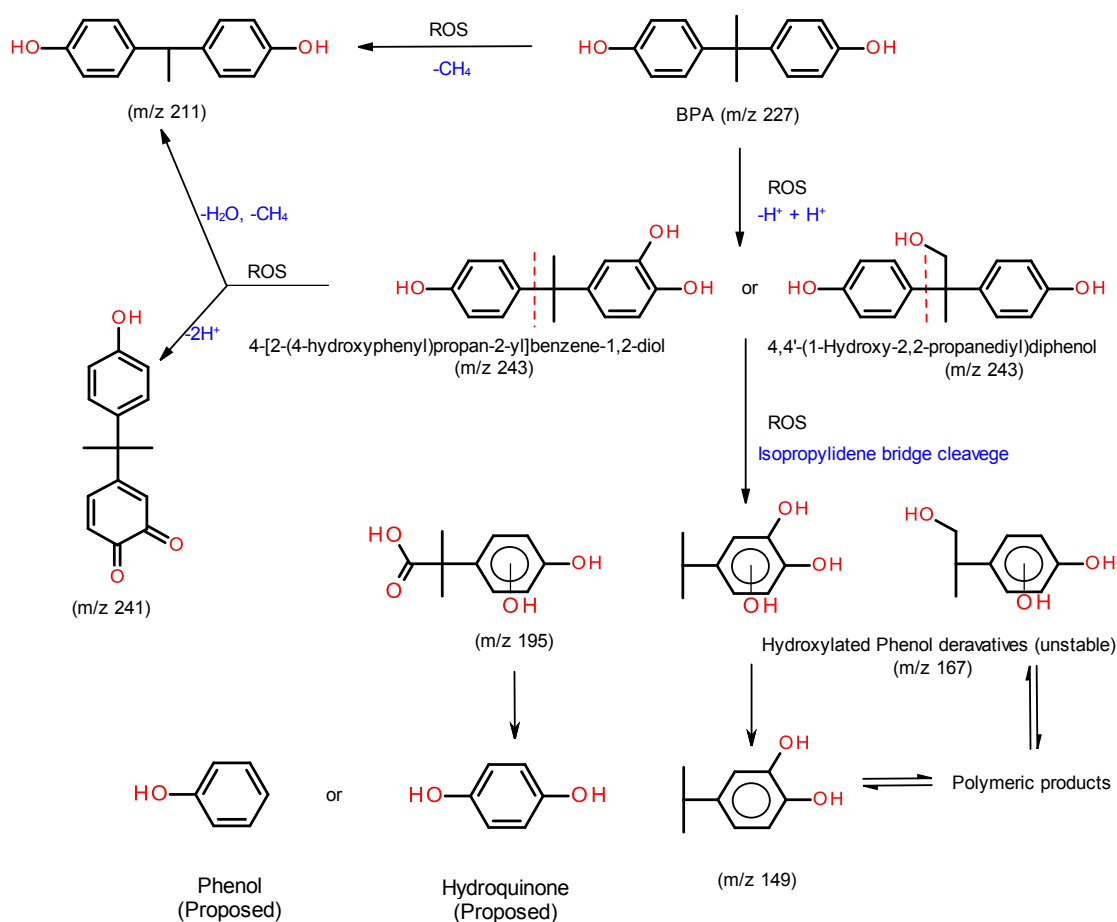


Figure 4-9. Degradation reaction pathways for BPA during the electrochemical filtration process at 2 and 3 V in the presence (pH 6) and absence (pH 3 and 9) of 10 mM NaCl. Experiments were performed at room temperature with a flow rate of 2 mL/min. and an MWNT loading of 1.04 mg/cm².

The degradation of BPA starts by the formation of hydroxylated derivatives due to superoxides' attack on the aromatic rings. Following this step, isopropylidene bridge cleavage takes place, leading to the formation of one-ring hydroxylated phenolic derivatives at 167 and 195 and 149 m/z, Figure 4-9.

The creation of phenolic derivatives is reported to lead to the formation of reversible polymeric products [59]. The lack of any polymeric passivation during the electrochemical filtration process indicates that any polymeric intermediates formed are likely reversible and therefore unstable. Furthermore, phenolic products were detected only during the treatment in

acidic pH (pH 3 with the absence of NaCl) at 211 and 241 m/z. The formation of phenolic derivatives during treatment at the acidic condition and in the absence of NaCl suggests that ROS (Superoxide) are participating in the electrochemical degradation of BPA in acidic conditions.

No aliphatic products could be detected in the conditions above, Figure 4-9. Thus it could be observed that during the electrochemical filtration of BPA at a flow rate of 2 mL/min and an MWNTs loading of 1.04 mg/cm² (2.01 sec. Residence time), only aromatic intermediates can be detected, some of which have toxic properties. To overcome this problem, the residence time was increased by 7.4 times by decreasing the flow rate to 0.5 mL/min and doubling the MWNTs loading (2.08 mg/cm²). This could result in further deformation of the phenolic intermediates (aromatic ring cleavage) and the formation of non-toxic aliphatic products (Figure B-30, Appendix B). It was also observed that chlorination was taking place in these slower conditions with the presence of 10 mM NaCl (pH 6) suggesting that the residence time was sufficient for interaction between the reactive chlorine and the phenolic derivatives.

4.3.5.3. The Effect of Flow Rate and the MWNTs Loading (Residence Time)

Figure 4-10 shows the mass spectra of BPA at RT 8.39 min, showing the disappearance of the BPA spectral peaks at 227, and 273 m/z from effluent samples collected at 20, 184, and 424 min. This suggests that increasing the residence time can significantly improve the participation of different degradation pathways, resulting in a nearly complete elimination of target contaminants.

It is worth noting that direct electron transfer has slower kinetics than indirect oxidation pathways. Thus the participation of electron transfer would be more obvious during longer residence times [114]. Therefore, the constant removal of BPA using 3 V of applied DC potential up to 424 min of operation time demonstrates an effective elimination of BPA by direct electron transfer and other indirect oxidation pathways. (For further details on BPA degradation data, please refer to Appendix B).

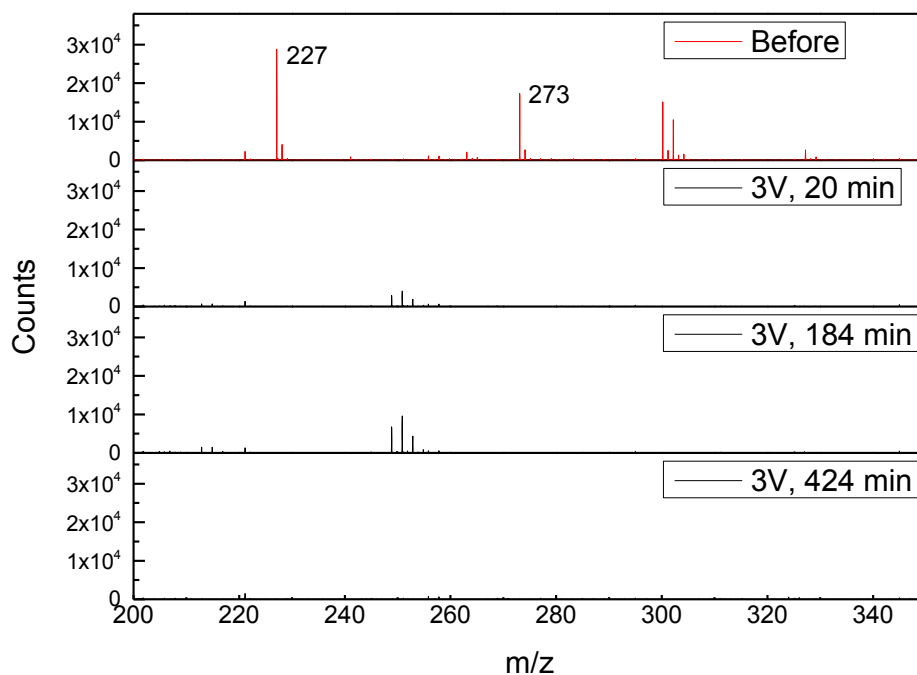


Figure 4-10. Mass spectra for 10 mg/L BPA in 10 mM NaCl before treatment (red trace) and after electrochemical MWNTs filtration treatment at 3 V of applied DC potential after 20, 184, and 424 minutes of electrochemical filtration time (black traces). Experiments were performed at room temperature with a flow rate of 0.5 mL/min and an MWNTs loading of 2.08 mg/cm².

4.3.6. The Effect of the Initial Concentration of Bisphenol A on Electrochemical Oxidation Reaction Kinetics during the Electrochemical Filtration Process

The rates of electrochemical removal were calculated to obtain a mechanistic insight into the effect of increasing the BPA influent concentration at different applied potentials assuming first order kinetics for the degradation of BPA. Figure 4-11 shows the electrochemical removal rates of BPA in $\mu\text{M}/\text{min}$ versus influent BPA concentration changes from 4.4 to 439.6 μM (1 to 100 mg/L) at 1, 2 and 3V of applied DC potentials with a flow rate of 2 mL/min and an MWNT loading of 1.04 mg/cm².

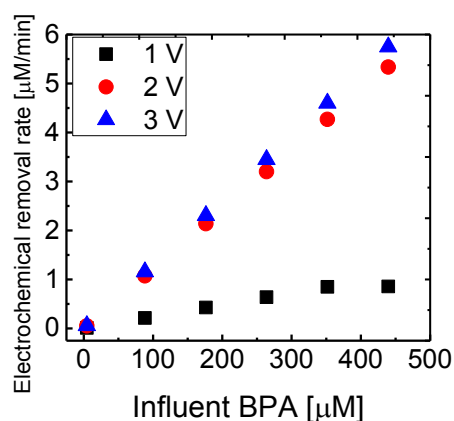


Figure 4-11. Electrochemical removal rates vs. initial concentration for the electrochemical MWNT filtration of 4.4 to 439.6 μM BPA in 10 mM NaCl (pH 6) at 1, 2 and 3 V of DC potential. Experiments were performed at room temperature using a flow rate of 2 mL/min and an MWNT loading of 1.04 mg/cm².

The trend at 1 V of applied potential in Figure 4-11 shows a mild increase in rate up to 0.85 $\mu\text{M}/\text{min}$, with increasing influent BPA concentration up to 351.7 μM followed by a plateau at BPA concentrations of 351.7 and 439.6 μM . This behavior shows an enhanced surface interaction (adsorption) with increasing initial concentration followed by saturation where no growth in the rate is observed. As previously mentioned, this indicates the absence of BPA degradation on the surface of the MWNTs when 1 V is applied. When the applied potential is increased to 2 and 3 V, a steep increase in the rate vs. BPA concentration can be seen with a linear dependence ($R^2 = 1$). This indicates that the degradation kinetics are rapid at 2 and 3 V and continue to increase with increasing initial BPA concentration, as observed with cyclic voltammetry, Figure 4-3. Contrary to the behavior at 1 V, this indicates that at 2 and 3 V, electrochemical reactions are taking place and that the process is diffusion-controlled.

The close resemblance for the rate values at 2 and 3 V indicates similar degradation pathways through the combination of both direct and indirect oxidation. There is also a significantly higher participation from indirect oxidation pathways given the significant difference between the anode potentials of 0.76 and 1.54 V corresponding to 2 and 3 V of applied DC potentials, respectively. The anode potential (0.76 V) corresponding to 2 V is almost half that (1.54

V) corresponding to 3 V of applied potential resulting in a massive positive shift in direct electron transfer participation from 2 to 3 V; however, this is expected to be the case if the adsorbed molecule is negatively charged. Liu et al. [74] noted that methylene blue (MB) was less oxidized than methyl orange (MO) at an applied voltage of 3 V. They attributed this to increased charge repulsion between the positively charged surface of the CNTs and the positive charges in the MB molecules and an enhanced surface interaction between the CNTs and the negatively charged MO (electromigration enhanced mass transfer). This leads to greater direct electron transfer rate for MO at 3 V due to charge accumulation at the CNT surface. In this case, we expect the neutrality of BPA at pH 6 to be a sort of barrier against such an effect. Therefore, it is anticipated that at pH values of 11-12, the effect of electrostatic attraction for BPA electrofiltration can be more pronounced and direct electron transfer participation will then be more obvious.

Based on these findings, it can be assumed that at 2 and 3 V of applied DC potential, the electrochemical removal of BPA is mainly controlled by the production and reactivity of bulk reactive species and that the rate of indirect oxidation pathways is significantly higher than the rate of direct electron transfer.

4.4. Conclusion

BPA removal was evaluated using pristine and boron doped MWNTs. It was found that BPA can be eliminated by both types of MWNTs under 2 and 3 V of applied DC potential, which indicates the efficient and sufficient performance of pristine MWNTs and the absence of the polymeric passivation effect of BPA on MWNTs during the electrochemical filtration process. The lack of the polymeric passivation effect of BPA on MWNTs was further evaluated by increasing the salt electrolyte concentration above 50 mM, and it was found that BPA does not induce a fouling effect, most likely due to the fast overall electrochemical degradation kinetics during the process. By varying the background solution pH in presence and absence of salt electrolyte, it was concluded that ROS (namely “superoxide”) are the predominant species during electrochemical filtration at and below 3 V of applied DC potential. Increasing the residence time by 7.4 fold lead to aromatic ring cleavage and the formation of non-toxic aliphatic products.

Acknowledgements

This note is to acknowledge the financial contributions of the Natural Sciences and Engineering Research Council (NSERC) of Canada and Concordia University.

Chapter 5: Crossflow Electrochemical Filtration for Eliminating Ibuprofen and Bisphenol A from Electrolytic Solutions in Pure and Fouling Conditions

Abstract

Crossflow electrochemical filtration was employed for the removal of two contaminants of emerging concern, Ibuprofen and Bisphenol A. A flat sheet crossflow setup was studied for the first time for the removal of the two contaminants, and multiwalled carbon nanotubes (MWNTs) blend buckypaper was used as a flat sheet dual membrane electrode. The crossflow mode was studied to observe the contribution of the shear flow and the enormous surface area of the buckypaper membrane in an electrochemical filtration process. Ibuprofen and bisphenol A quantification was achieved using a UV/Vis spectrophotometer and the degradation pathways of the two contaminants were followed using liquid chromatography-mass spectrometry (LC-MS). Breakthrough experiments revealed that crossflow configuration could contribute to a significantly increased efficiency in the elimination of the two contaminants when 2 and 3 V DC potentials were applied, and over an operation time of 300 minutes. The shear flow mechanism provided a consistent surface coverage that resulted in better sorption performance. The long residence time of the two contaminants within the membrane (18.3 seconds) was sufficient to allow for complete degradation of the phenolic aromatic products and quinoid rings into the formation of aliphatic carboxylic acids, which was significant at the highest applied voltage (3 V). The formation of the non-toxic aliphatic carboxylic acids is a clear indication of the superior electrochemical performance of the crossflow mode.

Keywords: Crossflow electrochemical filtration, Buckypaper, Ibuprofen, Bisphenol A

5.1. Introduction

Electrochemical filtration is an emerging technology that aims to advance both electrochemical degradation and adsorptive filtration. Electrochemical filtration combines the favorable outcomes of both processes, while at the same time, reducing the limitations of both processes, aiming for effective elimination of trace organic contaminants of a persistent and hazardous nature. The incorporation of electrochemistry with the sorption mechanism can reduce the membrane fouling rate and increase sorption efficiency through the destruction of adsorbed organic foulants. This property results in a reduced requirement for membrane regeneration through chemical or physical cleaning processes, to maintain optimal permeability [140, 141].

Mass transfer limitations are a common problem in batch electrolysis, which results in long operation times and thus increased energy consumption. Also, electrode fouling problems lead to the requirement for a high voltage input to decrease fouling propensity during batch electrolysis. The high voltage input results in increased surface hydrophilicity, hence poor hydrophobic adsorption of target contaminants, and requires high power consumption [51, 52, 56, 57, 59, 61, 142-144]. Electrochemical filtration provides a multi-fold enhancement of electrochemical degradation reaction kinetics due to the convection motivated mass transfer of contaminants under flow. This offers the advantageous results of faster and more efficient removal of target contaminants by the contribution of both direct electron transfer and indirect oxidation pathways [73-76, 116, 140]. Moreover, electrochemical filtration has proven to be a very successful process in viral and bacterial inactivation through the electrodisinfection mechanism [72, 83].

The incorporation of the crossflow mechanism in electrochemical water treatment has not been profoundly studied. However, there exists vast research on crossflow filtration for wastewater treatment and the enhancement of antifouling capacity during crossflow filtration [145-157]. The inclusion of electrical fields towards an increased antifouling capacity during crossflow micro- and ultra-filtration was also extensively examined in previous studies [158-171]. In these studies, an original approach to the role of electric fields in capacitive antifouling was provided, aiming to decrease micro and ultra-membrane fouling propensity and thus improve membrane expectancy and maintain permeate efficiency.

Zhang et al. [168] studied the use of highly conductive carbon nanotubes-polyvinylidene fluoride (CNT-PVDF) as a capacitive organic fouling reduction electrode, with the aim of lessening the natural organic matter (NOM) fouling of polyethersulfone (PES) membranes. They studied the effect of constructing different electrode-membrane configurations to achieve the best antifouling performance by motivating electrokinetic improvement, and thus improving the rejection rate of negatively charged organic matter and maintain a time efficient permeability. In their study, attention was drawn to the nature of the fouling molecules toward the capacitive rejection performance. They concluded that higher charge density, together with the limited molecular weight distribution of the fouling molecule, can lead to greater foulant rejection. It was also found that capacitive filtration increased energy efficiency by maintaining effective ultra-filtration membrane performance, thus improving permeate flux over time, as compared to traditional crossflow filtration.

Huotari et al. [158] studied the effect of applying an external electric field to enhance the flux for the crossflow membrane filtration of a model oily wastewater using a carbon fiber-carbon composite membrane as the cathode. They found that limiting flux was improved significantly by the application of electrical field and was increased from 75 L/m².h to 350 L/m².h. The same authors reported that permeate quality was improved when an electric field was applied during crossflow filtration and when testing a membrane with a relatively large pore size. They concluded that the most important factors for enhancing the limiting flux were the electrophoretic mobility of the oily droplets and the strength of the applied electric field. Thus, it was concluded that to obtain a good flux in oily wastewater, all other depositing foulants must be affected by surface charge and must have the negative electrophoretic mobility. The authors also concluded that further increases in the electric field strength above a specific “critical value” did not lead to flux improvements and would only result in increased energy consumption. The same authors stated that increasing crossflow velocity for particles larger than 100 nm in size results in a drop of flux values. The authors also indicated that the capacitive antifouling model resulted in increased foam formation at the cathode surface, which led to a significant decrease in flux, a feature that would only be considered to be a problem in significantly oily wastewater applications.

Therefore, applying the capacitive antifouling mechanism in order to decrease fouling propensity in membrane filtration has some disadvantages including: increased fouling of cathode

surface when using oily wastewater, a requirement for all depositing foulants to have a negative electrophoretic mobility hence only working with negatively charged particles, the possibility that they lead to increased fouling of the oppositely charged electrode which may result in deterioration of the electric field and a drop in process efficiency, and a requirement for adjustments of electric field strength and crossflow velocity in order to maintain both energy and economic efficacies.

Therefore, these approaches can be useful for lessening the deposition of negatively charged species like natural organic matter (NOM) on micro and ultra-filtration membranes. However, they do not discuss the effect of the capacitive anti-fouling on the electrochemical degradation of hazardous and toxic contaminants in water and wastewater. In other words, they do not mention the contribution of the crossflow mechanism in the electrochemical degradation of these pollutants.

The application of crossflow filtration in electrochemical degradation of contaminants of a hazardous and persistent nature (i.e. emerging contaminants (ECs)), has not been covered in the literature. However, Zaky et al. [172] studied the electrochemical removal of p-methoxyphenol using a reactive electrochemical membrane (REM) consisting of a porous substoichiometric titanium dioxide (Ti_4O_7) tubular ceramic electrode operated in cross-flow filtration mode. In their study, they reported that the major oxidation pathway took place through the reaction of the contaminant with the in-situ generated reactive hydroxyl radicals at the anode surface. Adsorption of the target contaminant and its by-products was reported to be neglected in the absence of applied current. At potentials lower than the formation potential of hydroxyl radicals electro-assisted adsorption took place and direct oxidation was observable. From this study, it can be concluded that crossflow mechanism can perform efficiently in the electrodegradation of target contaminants.

The advantage of using carbon-based electrodes is the high adsorption affinity to organics at low or no voltage, which results in a higher filtration efficiency. In previous studies, it was shown that carbon nanotubes (CNTs) demonstrate excellent efficiency in dead-end electrochemical filtration processes for the removal of emerging contaminants and for viral and bacterial inactivation [72, 114]. In our previous studies, the removal of ibuprofen, which is an anti-inflammatory drug reported to exist in natural water and wastewater in different concentrations with reported health concerns, was investigated. In this study, we employed a conductive carboxylated multi-walled carbon nanotube (MWNTs-COOH) membrane electrode in a dead-end electrochemical filtration process [114]. Employing the same dead-end electrochemical filtration

system, the removal of bisphenol A, an endocrine disrupting chemical reported to be released into natural water and wastewater from different industries, was also successful under different applied conditions.

In the current study, superconductive MWNTs blend buckypaper electrode membranes were used in a crossflow electrochemical filtration setup to study the removal of both chemicals: ibuprofen and bisphenol A. The purpose of the study is, for the first time, to observe the electrochemical removal performance of both contaminants separately from pure electrolytic solutions in a crossflow filtration mode. Moreover, it aims to observe the removal of both contaminants in a mixture of organics, free electrolytes, and from fouling conditions using synthetic secondary wastewater of a total organic carbon (TOC) of 34 mg/L, aiming to mimic a real application challenge. Finally, the goal is to perceive and highlight the difference in outcome between crossflow electrochemical filtration in removing these two contaminants, and previously stated outcomes from dead-end electrochemical filtration using CNTs based membrane electrodes.

5.2. Materials and Methods

5.2.1. Materials

Highly conductive 20 gsm MWNTs blend buckypaper was purchased from Nanotech Labs, NC, USA, and was used as received. The measured purity of the MWNTs buckypaper, as analyzed by Thermogravimetric analysis (TGA) was 92 %. Specific surface area was measured by Brunauer–Emmett–Teller (BET) and determined to be 106.79 m²/g and have a total porosity of 0.4 cm³/g. Ibuprofen (C₁₃H₁₈O₂) with 98% purity and a molecular weight of 206.29 g/mole and Bisphenol A (C₁₅H₁₆O₂) with 99 % purity and a molecular weight 228.29 g/mole were purchased from Sigma-Aldrich, Oakville, ON, Canada. Sodium chloride with ≥ 99 % purity, was purchased from Sigma-Aldrich, Oakville, ON, Canada, and was used as a supporting electrolyte in background solutions. Magnesium sulfate, sodium bicarbonate, calcium chloride, potassium dihydrogen phosphate, ammonium chloride, and trisodium citrate were purchased from Fisher Scientific, Ottawa, ON, Canada, and were used to prepare synthetic secondary wastewater effluent.

5.2.2. Electrolyte solution

10 mM NaCl electrolytic solutions (pH 5.7 – 6) were used for the electrochemical crossflow filtration of ibuprofen and bisphenol A by an MWNTs blend buckypaper sheet of a geometric area of 50 cm² and 109459.75 cm² of total surface area (106.79 m²/g x 0.1025 g). NaCl was used as a background electrolytic species, as chlorides are a constituent of natural water and wastewater and are known to provide reactive chlorine for indirect oxidation processes under applied voltage, and for conductivity improvement during electrochemical applications. The conductivity was measured at 2.17×10^{-7} , 2.16×10^{-7} and 2.14×10^{-6} S/cm² and the current densities were measured at 2.17×10^{-3} , 4.33×10^{-3} and 6.42×10^{-3} mA/cm², corresponding to 1, 2 and 3 V of applied DC potential during the study, respectively. The concentrations of ibuprofen and bisphenol A used in the study were 0.5, 1 and 10 mg/L for each chemical.

5.2.3. Crossflow electrochemical filtration setup

Crossflow electrochemical filtration experiments were done using a constructed bench-scale flat-sheet crossflow filtration holder, similar to as described previously [168]. Anode and cathode membrane electrodes were both a flat MWNTs buckypaper sheet of the same geometrical area of 50 cm² and thickness of 52.7 μm. The electrode sheets were connected to external terminals of an Agilent E364_A power supply, Agilent Technologies, Rockaway, NJ, USA using titanium sheets of 1 x 5 cm in dimension, for 1, 2 and 3 V of DC voltage application. A porous Teflon rubber separator of 2 mm thickness was used to separate the anode from cathode and was the same geometrical area as buckypaper sheets, to prevent short-circuiting. The influent solution was driven from a feed reservoir into the cell holder using a 75211-10 model, 115 VAC Gear pump drive purchased from the Cole-Parmer Instrument Company, Vernon Hill, USA. The pressure was adjusted to 20-25 psi, resulting in a permeate flow rate of 1 ± 0.5 mL/min during electrochemical filtration experiments, giving a permeate flux of $2.7 \times 10^{-3} - 8.2 \times 10^{-3}$ L/m².h. The flow rate was calibrated using a graduated measuring cylinder of 10 mL ± 0.1 total volume at permeate (effluent) outlet. 1 mL of effluent (permeate) samples were collected for analysis. The concentrate was not recirculated to the feed reservoir in order to keep the feed concentration at a constant value during experiments. Flow rate at the concentrate outlet was measured at 3-4 mL/min.

5.2.4. Buckypaper surface characterization and purity

Scanning electron microscopy (SEM) and energy dispersive X-ray (EDX) were performed using FEI Inspect F-50 FE-SEM with EDAX Octane Super 60 mm² SDD and TEAM EDS Analysis System (Dawson Creek, Oregon, USA) for buckypaper surface inspection and thickness determination. The stability and purity were qualified by thermogravimetric analysis using TA instruments, Trios V3.3 (Waters LLC, New Castle, DE, USA) and the analysis protocol was performed as previously described [114]. Brunauer-Emmett-Teller (BET) was done to quantify membrane surface area and total pore volume using a Quantachrome Autosorb Automated Gas Sorption System (Autosorb 1, Boynton Beach, Florida, USA), and the analysis conditions were as described previously in Chapter 4.

5.2.5. Analysis and quantification

Individual concentrations of ibuprofen and bisphenol A were calculated from the absorbance values of samples before and after treatment, at 222 and 225 nm, respectively, using a UV/VIS Agilent Cary 8454 spectrophotometer, Santa Clara, CA, USA. In mixed samples of ibuprofen and bisphenol A (1:1), a major (220-226 nm) and a minor (273-285 nm), broad spectral peak was observed in one spectrum. The average wavelength of the major spectral peak (223 nm) was used for determination of mixture concentrations. Liquid chromatography-mass spectrometry was done using maXis impact MALDI Autoflex III- TOF-(BRUKER), Bruker Daltonics Inc. Massachusetts, USA, in negative ESI mode, using 20 μ L of samples for analysis. The ESI source capillary voltage was 4500 V, nitrogen gas temperature was 350°C, and the flow rate was 8 L/min. The nebulizer pressure was maintained at 1 bar. The mass range was 50 - 1000 m/z with internal calibration using the reference masses 119 and 966 m/z in the Agilent reference-mass solution. The injection gradient was: initial conditions of 5 % acetonitrile with a 1 min hold, then increased to 100 % at 8 min and held for 1 min. The column was re-equilibrated at 30 % acetonitrile for 5 min before the next injection. The flow rate for was 0.3 mL/min.

5.3. Results and discussion

5.3.1. Buckypaper surface characterization, purity and stability

SEM and EDS were performed on buckypaper membrane filter before use in treatment. Figure 5-1 A shows the SEM images of the MWNTs blend buckypaper membrane, found to be a rich collection of MWNTs of different diameters ranging from below 20 nm to above 250 nm. Carbon content and impurity content were examined by EDS (Figure 5-1 B). The results show a weight percent of 89 % for carbon and 8 % for iron. EDS was also performed after subjecting the filter to solutions of 1 mg/L of ibuprofen and bisphenol A (1:1) at a neutral condition (10 mM NaCl, pH 6) under 3 volts of applied potential and a flow rate of 1 mL/min, and room temperature. The EDS analysis did not show any signs of surface corrosion after this treatment. Figure 5-1 C represents the TGA results for MWNTs blend buckypaper. The TGA shows a purity of around 92 %, indicated by the sharp drop in the weight percent between 600 and 650 °C, the temperature at which all carbon content is degraded. The plateau formation at around 8 % by weight would be related to residual iron.

Total pore volume for a 50 cm² buckypaper membrane is 0.041 cm³ (0.4 cm³/g x 0.1025 g), the surface area is 109459.75 cm² (106.79 m²/g x 0.1025 g) for a loading of 102.5 mg/cm², as measured by BET. The thickness is 52.7 μm, as indicated by SEM (for further details, please refer to Appendix C).

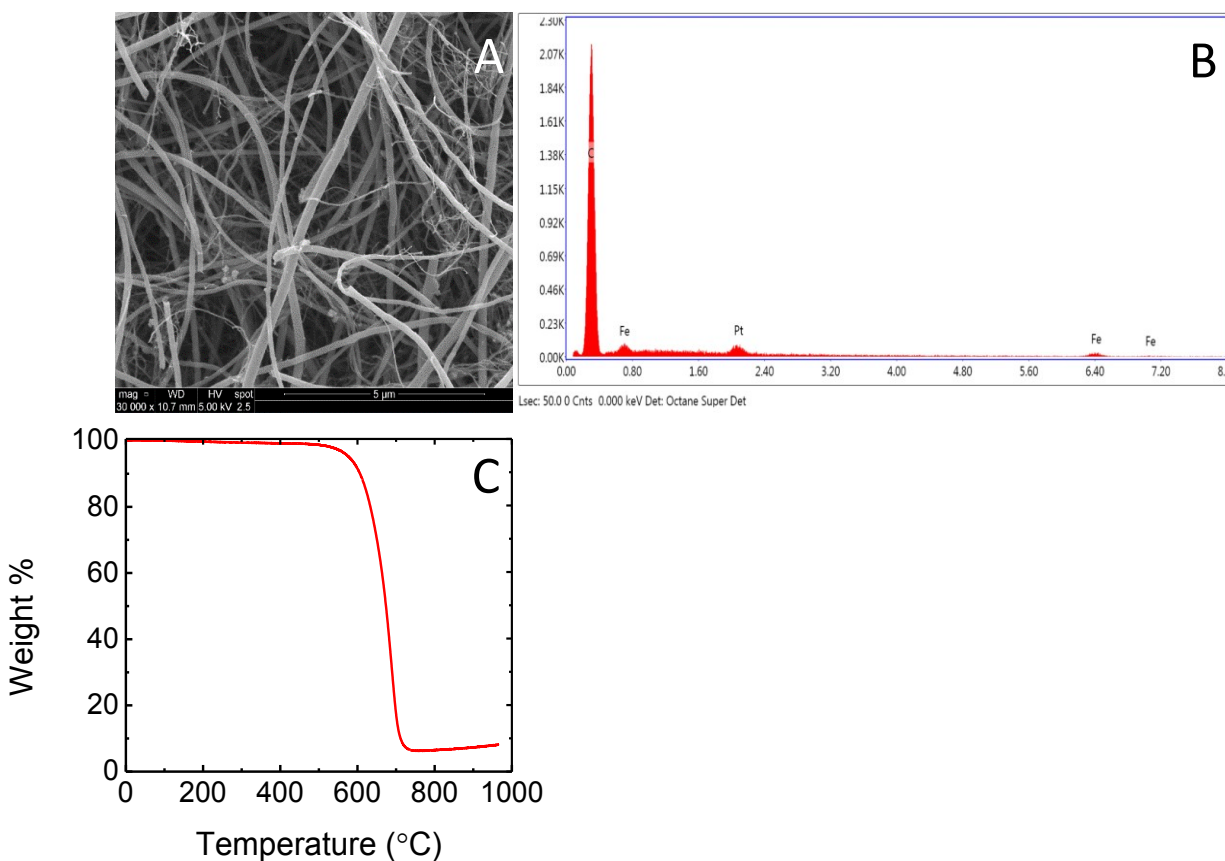


Figure 5-1. SEM images, EDS and TGA analysis for MWNT blend buckypaper where (A) is SEM for buckypaper membrane at a surface loading of 102.5 mg/cm^2 , (B) EDS analysis for buckypaper membrane filter at a surface loading of 102.5 mg/cm^2 , (C) is TGA analysis for MWNTs blend buckypaper.

5.3.2. Crossflow filtration and electrochemical filtration performance over time

Crossflow filtration and electrochemical filtration performance were evaluated over time for the removal of individual ibuprofen and bisphenol A from pure 10 mM NaCl solutions (breakthrough experiments). Breakthrough plots were developed to observe the best sorption and electrochemical degradation outcomes of the two contaminants by MWNTs buckypaper membranes in a crossflow mode. Furthermore, this allows us to relate the findings to those previously reported from the dead-end process. Figure 5-2 shows the breakthrough plots for individual 1 mg/L ibuprofen and 1 mg/L bisphenol A, in pure 10 mM NaCl solution. From Figure 5-2 A, ibuprofen sorption kinetics at 0 V were steady starting at a C/C_0 value of 0.12 up to 20

minutes of operation time. This behavior is consistent with previous observations from dead-end filtration of ibuprofen on MWNTs membrane and indicates a poor adsorption of ibuprofen on MWNTs membranes due to lack of efficient hydrophilic surface interactions between the molecule and MWNTs and the presence of the hydration shell effect at the polar groups [114].

However in the current study, sorption seems improved, and the C/C_0 started at lower values (0.12 at 0 V for Figure 5-2 A), compared to the previous observation for dead-end filtration of ibuprofen (0.33 at 0 V). This could be attributed to the shear flow, which is most likely providing a better and more consistent coverage of the molecules at the buckypaper surface, compared to the flow through in dead-end filtration. Additionally, the large surface area of 109459.75 cm² of the buckypaper membrane is providing more sorption sites. However, and despite this enormous surface area, the breakthrough starts at around 25-30 minutes, indicating that sorption active sites are limited and therefore, breakthrough starts earlier than expected. When 1 V of DC potential was applied (Figure 5-2 A), a slight increase in adsorption capacity was observed, which can be attributed to electrostatic interactions taking place between the positively charged surface and the negatively charged deprotonated ibuprofen molecules (pKa, 4.9) at pH 5.7-6. For bisphenol A sorption kinetics at 0 and 1 V (Figure 5-2 B), a near complete removal of the molecule could be observed within 10 minutes of sampling time.

The filtration kinetics were almost identical for bisphenol A at applications of 0 and 1 V indicating that adsorption is likely through hydrophobic surface interactions, due to the neutrality of the molecule. The sharper plateauing for ibuprofen adsorption (Figure 5-2 A) compared to the case of bisphenol A (Figure 5-2 B) at 0 and 1 V, indicates faster adsorption kinetics for the former. Although the reason for the faster ibuprofen adsorption at 0 V is not clear, it can be better explained in the case of 1 V application to the electrostatic surface interactions. The overall behavior in the case of both 0 and 1 V application is in agreement with our previous observations using dead-end filtration, indicating the absence of electrochemical activity when 1 V is applied.

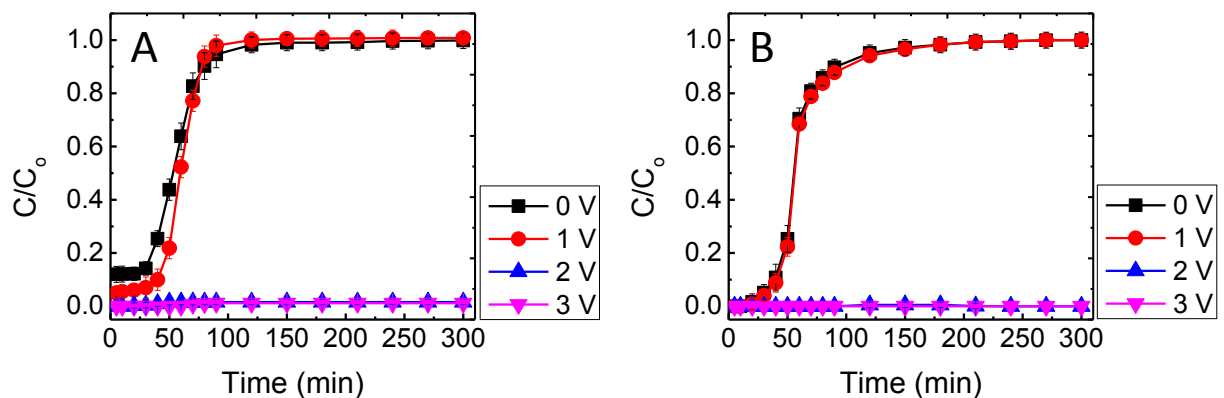


Figure 5-2. (A) Breakthrough plots for the removal of 1 mg/L Ibuprofen from 10 mM NaCl and (B) for the removal of 1 mg/L bisphenol A from 10 mM NaCl, under 0, 1, 2 and 3 V of applied DC potential, applied pressure is 20 psi (137.9 kPa), permeate flow rate is 1 mL/min and experiments performed at room temperature.

Due to the inability to perform cyclic voltammetry and electrode potential measurements using the current crossflow setup, we rely on previously reported values obtained from our dead-end studies for ibuprofen and bisphenol A in order to interpret the existing behavior (0.33 – 0.35 V vs. Ag/AgCl of anode potential corresponding to 1 V of applied potential, oxidation potentials for ibuprofen and bisphenol A were determined to be 1.13 and 0.75 V, respectively).

The filtration kinetics at 2 and 3 V of applied potential for both contaminants show nearly complete removal up to 300 minutes of sampling time. This outcome shows an outstanding electrochemical performance of the blend MWNTs buckypaper in a crossflow configuration. Previous superoxide assays from dead-end electrochemical filtration showed the formation of the reactive anion radical on MWNTs at 2 and 3 V of applied DC potential. Also, it was reported that carbon based electrodes can provide electrocatalytic reductive sites for the efficient production of reactive oxygen species (ROS) from diatomic oxygen with high oxidative power [68, 114]. The enormous surface area (109459.75 cm²) and the great conductivity (274 – 703 mA corresponding to 1 – 3 V) of MWNTs buckypaper, are important factors in providing superior electrochemical performance at the membrane surface at an affordable rate. Electrochemical degradation takes place through direct electrolysis by electron transfer and indirect oxidation pathways.

Figure 5-3 A and B shows the breakthrough plots for the treatment of the 1 mg/L (1:1) ibuprofen /bisphenol A mixture from 10 mM NaCl solution (Figure 5-3 A), and from synthetic

secondary wastewater of the same composition as previously reported (Figure 5-3 B) [114]. The breakthrough trends are similar to those of individual molecules, shown in Figure 5-3 A, with a breakthrough starting at 10-20 minutes at 0 V and 25-30 minutes at 1 V. For Figure 5-3 B, a breakthrough starts at 10-20 minutes at 0 and 1 V. Remarkably, and despite the high TOC concentration of the synthetic secondary wastewater (TOC 34 mg/L), the overall breakthrough behavior is very similar to the case of electrofiltration from 10 mM NaCl. While in our previous studies on dead-end mode, the performance clearly deteriorated for breakthrough with the same composition synthetic wastewater, due to the incorporation of such high TOC content and the filtration kinetics started at higher C/C_0 values. This again can be explained in terms of better surface coverage through the use of the crossflow shearing mechanism, and to the larger membrane surface area of the buckypaper membrane employed in the current study compared to the constructed MWNTs membranes used in dead-end studies. At 1 V of applied DC potential, and comparing the performance from pure 10 mM NaCl (Figure 5-3 A) to that from synthetic secondary wastewater (Figure 5-3 B), there is a slight shift to higher C/C_0 and an earlier breakthrough for figure 5-3 B. The citrate molecules (33 mg/L) which constitute the major content of the synthetic secondary wastewater, and which contain three carboxylate groups per each molecule, might be responsible for such an outcome. The presence of citrate results in a slightly rapid blocking and consumption of surface sorption sites, motivated by electrostatic interactions, as compared to the case of organics free electrolytes (Figure 5-3 A).

When 2 and 3 V of DC potential were applied, near complete removal of the contaminants was observed for the mixture from 10 mM NaCl up to 300 minutes of operation time (Figure 5-3 A). In the case of electrofiltration from synthetic wastewater at 2 V (Figure 5-3 B), a slight deterioration can be observed starting at 120 minutes and increasing at 270 minutes of operation time.

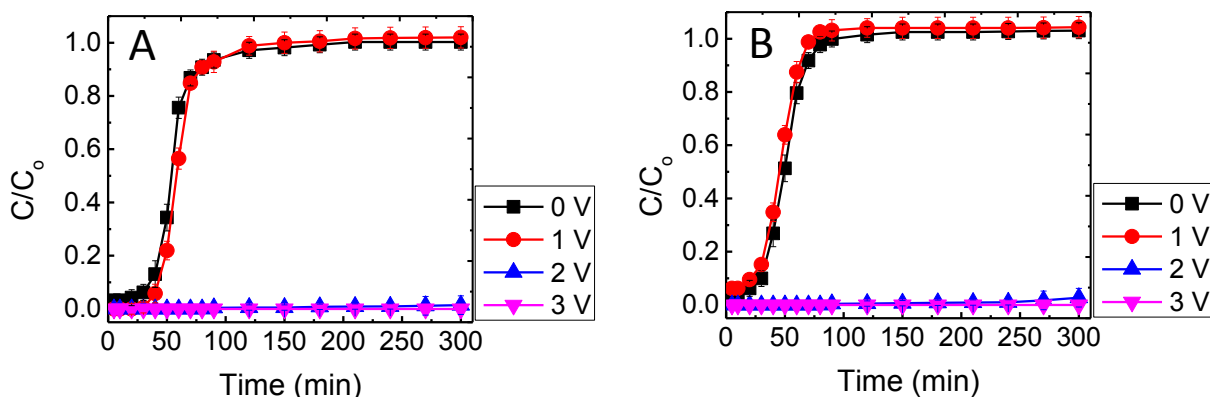


Figure 5-3. (A) Breakthrough plots for the removal of 1 mg/L Ibuprofen and bisphenol A (1:1) mixture from 10 mM NaCl and (B) from synthetic secondary wastewater (TOC 34 mg/L, pH 7.4), under 0, 1, 2 and 3 V of applied DC potential, applied pressure is 20 psi (137.9 kPa), permeate flow rate is 1 mL/min and at room temperature.

The fact that the deterioration is very slight ($C/C_0 = 0.01- 0.035$) is again due to the combination of good surface coverage by the shear flow, the great conductivity, and the enormous surface area, which all contribute toward great electrochemical performance, compared to the flow-through mechanism in dead-end studies. On the other hand, it was previously reported that using conductive carbon-based CNTs as cathode materials results in an excellent contribution toward improving anode performance. This is mainly due to the enormously larger specific surface area of CNTs compared to conventional metallic electrodes, which in turn leads to a significant reduction of the cathodic charge transfer resistance and reflects in increased anode potential. Therefore, the magnitude of electrooxidation at the anode surface would be of a greater extent [140].

5.3.3. Crossflow filtration and electrochemical filtration flux

The insightful numerical quantification of filtration and electrochemical filtration kinetics with being obtained from the integration of the breakthrough plots. Figure 5-4 and Figure 5-5 show the filtration and electrochemical filtration flux values for the removal of individual 1 mg/L ibuprofen and bisphenol A from 10 mM NaCl (Figure 5-4), and the removal of 1 mg/L (1:1)

ibuprofen and bisphenol A mixture from 10 mM NaCl and synthetic secondary wastewater (Figure 5-5), corresponding to Figure 5-2 and 5-3.

Despite the previously reported effect of the large specific surface area of CNTs on increasing anode potential and hence increasing the magnitude of electrooxidation [140, 173, 174], the contribution of a 1 V of applied DC potential is yet to be limited to insignificant in the current study. In Figure 5-4 A, the difference between flux values for 0 V and the application of 1 V for ibuprofen removal is $0.12 \mu\text{g m}^{-2} \text{h}^{-1}$, and in Figure 5-4 B, the difference value for bisphenol A removal is $0.04 \mu\text{g m}^{-2} \text{h}^{-1}$. The higher flux value for ibuprofen (pKa, 4.9) compared to bisphenol A (pKa 9.6 -11.3) can only, and as reported previously here, be attributed to the incorporation of electrostatic surface interactions toward the adsorption of the former. In our previous dead-end studies, we could not conclude any electrochemical activity when a 1 V DC potential was applied, which was mainly due to the higher oxidation potential of ibuprofen and bisphenol A as compared to anode potentials corresponding to 1 V of applied potential.

Additionally, the increased MWNTs buckypaper membrane surface area used in the current study, compared to the MWNTs membrane surface area used in dead-end research (10 -11 folds larger for MWNTs buckypaper crossflow membrane) didn't show any dramatic improvement. The significantly greater flux values when 2 and 3 V DC potentials were applied show an agreement with our previous dead-end study observations, in which electrochemical oxidation pathways of ibuprofen and bisphenol A are generated at ≥ 2 V. Moreover, the nearly similar outcomes at 2 and 3 V DC potential application confirms that electrooxidation pathways are analogous at these voltages, which are due to the contribution from direct electrolysis and indirect oxidation by oxidative intermediates (i.e. superoxide and reactive chlorine).

In Figure 5-5 A, a similar outcome of a slight increase in flux value at 1 V above 0 V by $0.14 \mu\text{g m}^{-2} \text{h}^{-1}$, likewise the case of individual molecules could be observed. In Figure 5-5 B, the opposite trend of a drop in flux value at the application of 1 V below that at 0 V by $-0.09 \mu\text{g m}^{-2} \text{h}^{-1}$ confirms the competition on surface sorption sites between the target contaminants and, most likely, citrate molecules in the synthetic wastewater background solution.

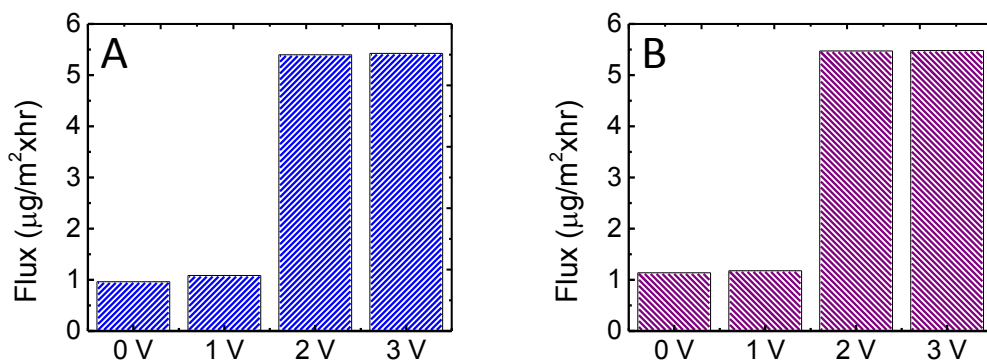


Figure 5-4. (A) Electrochemical filtration flux for the removal of 1 mg/L Ibuprofen from 10 mM NaCl and (B) for the removal of 1 mg/L bisphenol a from 10 mM NaCl, under 0, 1, 2 and 3 V of applied DC potential, applied pressure is 20 psi (137.9 kPa), permeate flow rate is 1 mL/min and at room temperature.

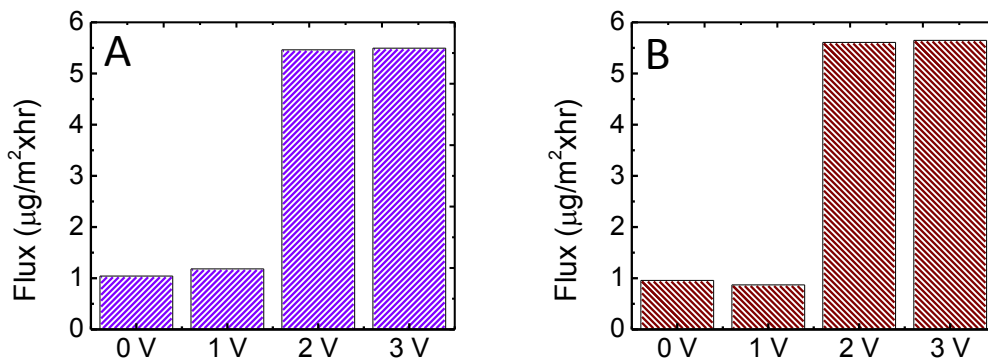


Figure 5-5. (A) Electrochemical filtration flux for the removal of 1 mg/L Ibuprofen and bisphenol A (1:1) mixture from 10 mM NaCl and (B) from synthetic secondary wastewater (TOC 34 mg/L, pH 7.4), under 0, 1, 2 and 3 V of applied DC potential, applied pressure is 20 psi (137.9 kPa), permeate flow rate is 1 mL/min and at room temperature.

The small drop of $-0.09 \mu\text{g m}^{-2} \text{h}^{-1}$ also shows that despite the presence of 33 mg/L citrate in the solution, the surface sorption sites within the large membrane surface area were not largely depleted by the effect of the competing citrate molecules.

At 2 and 3 V, similar observations of significantly greater increases in flux values can be observed (Figure 5-5 A and B), for the removal of the contaminant mixture from 10 mM NaCl and synthetic wastewater, as seen in Figure 5-4. The closely similar flux values at applications of 2 and 3 V and in both cases removal of 10 mM NaCl and synthetic wastewater ($5.5 - 5.6 \mu\text{g m}^{-2} \text{h}^{-1}$) confirms that major degradation pathways are through indirect oxidation by the interaction of ibuprofen and bisphenol A with oxidative intermediates (i.e. superoxide and reactive chlorine) at bulk. This observation is in agreement with our previous observations during dead-end studies. In our previous dead-end studies, it was shown that bisphenol A is more readily oxidizable at 2 and 3 V as compared to ibuprofen, mainly due to the lower oxidation potential of the former. Similar outcomes for the removal from pure NaCl solution and synthetic wastewater also show that production of reactive species is greatly efficient in both solution conditions.

5.3.4. Qualification of Ibuprofen and bisphenol A (1:1) mixture removal, and by-products characterization by liquid chromatography mass spectrometry

Ibuprofen and bisphenol A mixture samples were analyzed by LC-MS before and after crossflow electrochemical filtration treatment to obtain an insight into the effectiveness of the process in eliminating the two target molecules and reducing their toxicity. A large initial concentration of 20 mg/L of (1:1) ibuprofen and bisphenol A mixture in 10 mM NaCl was used to enhance electrochemical reaction kinetics, obtain a significant by-product spectra, and to avoid spectral noise interference from any background species. Figure 5-6 shows the LC-MS analysis for ibuprofen and bisphenol A mixture before and after treatment under 2 and 3 V of applied DC potentials, at 5, 150, and 300 minutes of operation time.

Figure 5-6 A shows the overlaid LC chromatograms in which two significant peaks were detected in the sample before treatment (blue trace) at retention times (RT) of 7.1 and 8.7 minutes, that were assigned to ibuprofen and bisphenol A, respectively. After treatment under 2 V, the two peaks were not detected in the samples obtained at 5 and 150 minutes of operation time, while traces of ibuprofen and bisphenol A could be detected only in the samples obtained at 300 minutes.

Under 3 V, similar observations were found with fewer traces observed only after 300 minutes. Figure 5-6 B shows the mass spectra corresponding to Figure 5-6 A, confirming the complete removal of ibuprofen (m/z 205) and bisphenol A (m/z 227) within 150 minutes of electrochemical filtration. Nine other MS peaks were detected in samples after treatment at m/z 59, 73, 89, 103, 107, 109, 115, 157 and 171 (Figure C-6 to C-9, Appendix C). The peaks at m/z 107 and 109 were only detected after treatment under 2 V and were predicted to correspond to the formation of p-benzoquinone (m/z 107), hydroquinone, and catechol (m/z 109). Several authors previously detected and reported the formation of hydroquinone and p-benzoquinone from the degradation of ibuprofen and bisphenol A [8, 57, 59, 139, 175].

Ambuludi et al. [175] detected the formation of p-benzoquinone from the oxidation of ibuprofen through the hydroxyl radical attack on the parent molecule and a consecutive hydroxylation, in an electro-Fenton process. Cui et al. [59] detected the formation of hydroquinone and benzoquinone during the electrochemical degradation of bisphenol A using different electrode materials in a batch electrolysis process. The authors attributed the formation of such single-ring aromatic products from bisphenol A, to the first step of Isopropylidene bond cleavage resulting in the splitting of the molecule, followed by further hydroxylation to phenolic intermediates and the deprotonation of hydroquinone to benzoquinone. Moreover, the formation of hydroquinone and benzoquinone is an indication of a formation of phenolic derivatives, and that could herald the formation of unstable polymeric compounds during bisphenol A electrolysis [60, 65, 176-178]. Murugananthan et al. [57], Zhang et al. [8], Cui et al. [59], Gözmen et al. [65] and Katsumata et al. [179] all reported the formation of hydroquinone and benzoquinone from the degradation of bisphenol A, which is reported to be followed by the formation of simple aliphatic carboxylic acids.

Watanabe et al. [138] attributed the formation of a catechol group from bisphenol A, firstly to the creation of phenolic derivatives at an m/z of 149, which upon further oxidation yield a 1,2-quinone group. Such phenolic derivatives at m/z 149 were detected in our previous study on dead-end electrochemical filtration of bisphenol A. Thus the formation of the m/z 109 (catechol) suggests the same oxidative sequence in the current study. Figure 5-7 shows a suggested common degradation pathway for both ibuprofen and bisphenol A, based on our detected products.

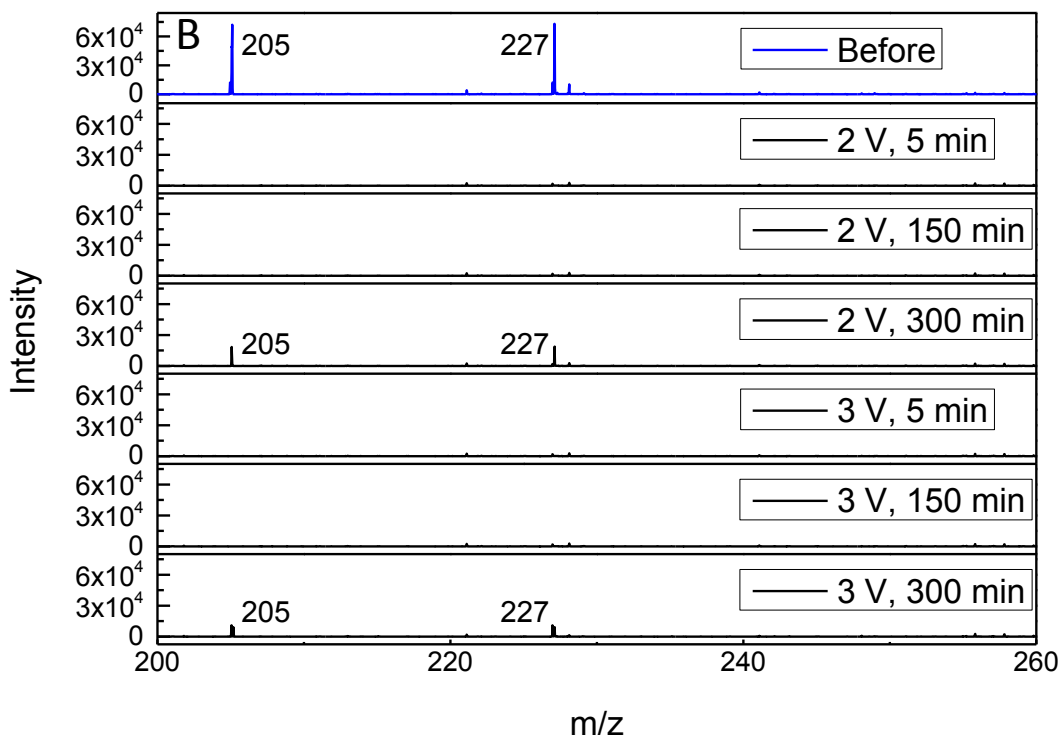
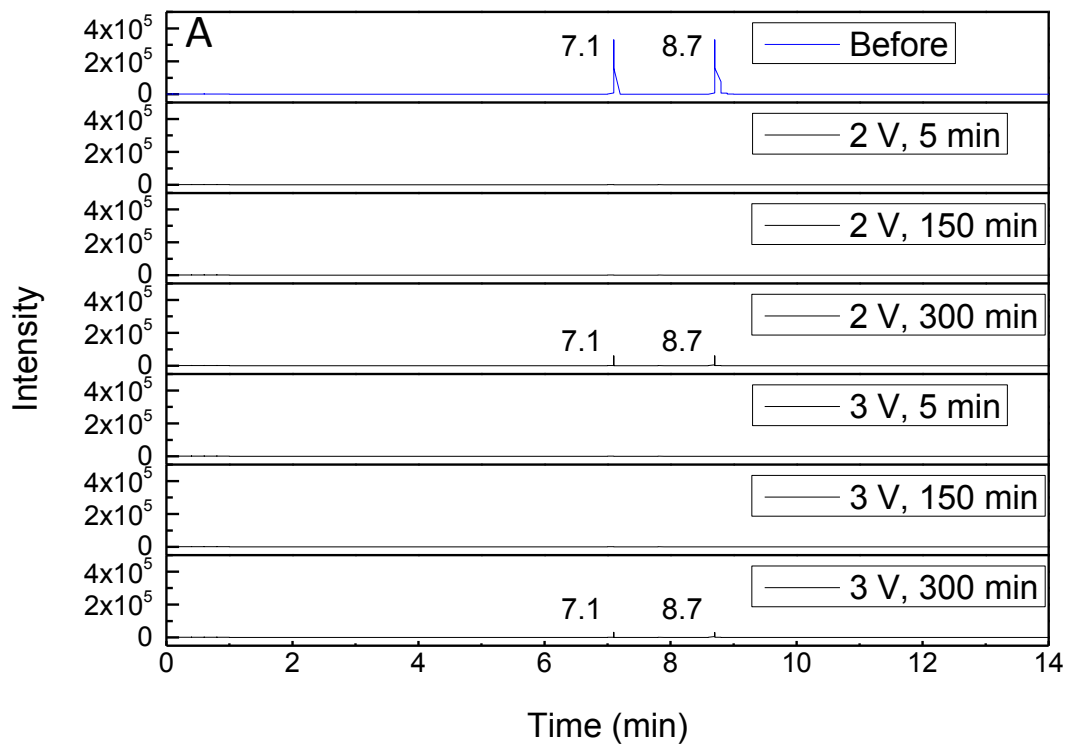


Figure 5-6. LCMS for the treatment of 20 mg/L Ibuprofen and bisphenol A (1:1) mixture from 10 mM NaCl, where (A) are the overlaid LC chromatograms for mixture before treatment (Blue

trace) and after treatment (Black traces) and (B) is MS spectra for mixture before treatment (Blue trace) and after treatment (Black traces). Applied voltages were 2 and 3 V of applied DC potential, applied pressure is 20 psi (137.9 kPa), permeate flow rate is 1 mL/min and at room temperature.

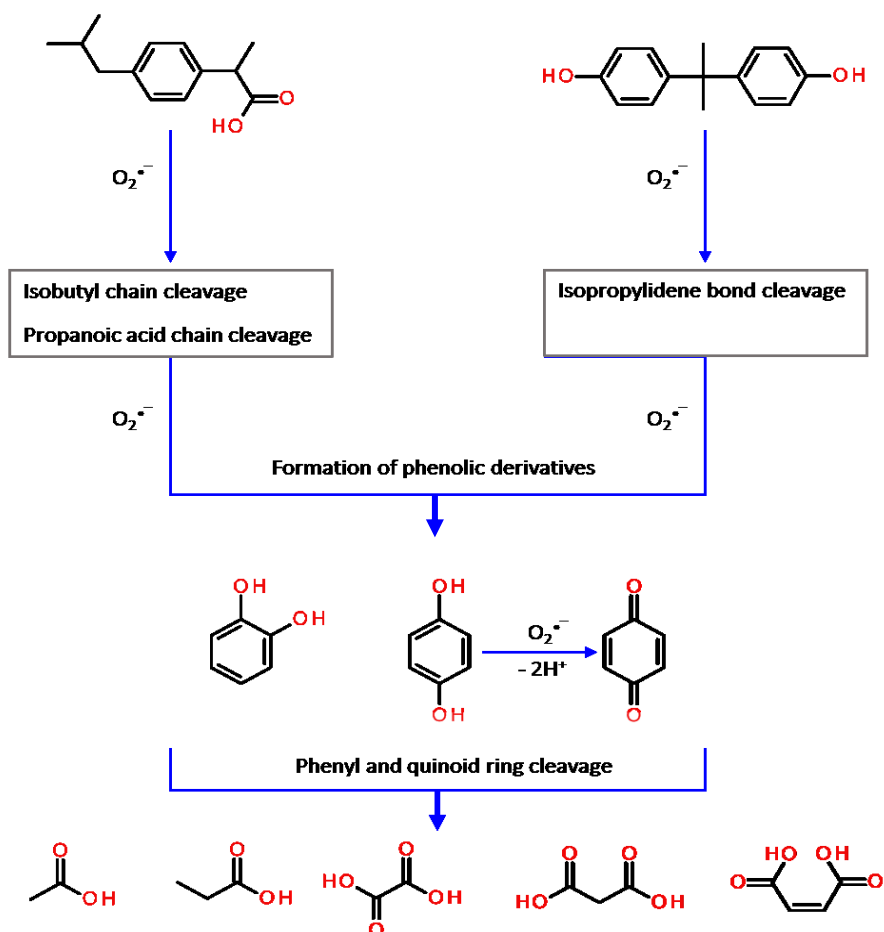


Figure 5-7. Possible degradation pathway for ibuprofen and bisphenol A during crossflow electrochemical filtration

As reported, the formation of single-ring phenolic products could be a common outcome from the oxidative degradation of both ibuprofen and bisphenol A. The fact that these phenolic products could only be detected in the samples obtained from the treatment under 2 V, while at 3 V they were not detected (Figure C-8, Appendix C) is a clear indication to the effect of increased voltage toward faster degradation kinetics. This result also indicates a more efficient transformation of the parent molecules and their phenolic products during treatment using the

current crossflow configuration and applied conditions. Moreover, the longer residence time of 18.3 seconds (corresponding to an average flow rate of 1 mL/min), compared to the lower residence times in our previous dead-end study on bisphenol A degradation, is another critical factor in further degradation to the point of first formation of aliphatic by-products in the current study.

The degradation pathway starts with cleavage of aliphatic chains in ibuprofen (isobutyl and propanoic acid chains) and bisphenol A (Isopropylidene group) by the effect of superoxides or other possible ROS. Further hydroxylation would take place at the phenyl and quinoid rings, resulting in ring cleavage and subsequent formation of simple aliphatic carboxylic acids. The aliphatic carboxylic acids detected in the current study were acetic acid (m/z 59), propanoic acid (m/z 73), oxalic acid (m/z 89), malonic acid (m/z 103), and maleic acid (m/z 115). The formation of these aliphatic acids also suggests a possibility of further complete mineralization of ibuprofen and bisphenol A into the final products of carbon dioxide and water. The observed spectral trend of increased intensity of these acids at 3 V as compared to 2 V also indicates their faster and more intense production when the voltage was raised from 2 to 3 V.

Other possible chlorinated products could be formed, as indicated by the formation of m/z 157 and m/z 171 only in the samples treated under 3 V. These m/z values were also detected from our previous dead-end electrochemical filtration treatment of bisphenol A under 3 V and low flow rate. The m/z values of 157 and 171 suggest that reactive chlorine interaction with bisphenol A is of significantly slow kinetics and requires high input voltage as compared to ROS (superoxide) interactions.

5.4. Conclusion

A superconductive blend MWNTs buckypaper membrane was successfully employed in an electrochemical filtration treatment for two emerging contaminants, ibuprofen and bisphenol A, using a flat sheet crossflow configuration. The removal of the two target molecules was evaluated individually and in a mixture of 1:1 equimolar composition. It was shown that the crossflow configuration shows great potential in eliminating the two contaminants in individual and mixture solutions. The superior electrochemical efficiency of the crossflow mode in the elimination of the two contaminants was mainly attributed to the shear flow, which likely leads to a consistent surface

coverage and the excellent conductivity of the MWNTs blend buckypaper membrane when 2 and 3 V DC potentials were applied. The long residence time of 18.3 seconds led to a degradation outcome of the two contaminants and their toxic aromatic products, at both 2 and 3 V of applied DC potential. The LCMS analysis showed a complete removal of the two target contaminants, and the total degradation of their phenolic products into aliphatic carboxylic acids at 3 V. This outcome has a major indication that there is a possibility of complete degradation into the final products of carbon dioxide and water during the process.

Acknowledgements

This note is to acknowledge the financial contributions of the Natural Sciences and Engineering Research Council (NSERC) of Canada and Concordia University.

Chapter 6: Contribution, Conclusion and Future Recommendations

In this chapter, major contributions of this thesis are outlined. A summary of the findings is also provided, and future recommendations for making the processes noted more efficient and implementable are made.

6.1. Contribution

In this study, electrochemical filtration, an emerging technology for water and wastewater treatment, was employed for the first time for the removal of two chemicals of emerging concern, ibuprofen and bisphenol A. Ibuprofen is a non-steroidal anti-inflammatory over-the-counter drug (NSAID OTC), which is a drug of significant production and consumption worldwide. Continued exposure to Ibuprofen has been reported to cause adverse health effects, with serious negative consequences on various human and animal organs. Bisphenol A is an endocrine disrupting chemical of heavy use and production in numerous industries, primarily in plastics. Therefore, due to the large quantities of bisphenol A produced, its accumulation in water and soil is a serious concern. Both chemicals have shown resilience against conventional methods of wastewater treatment. Thus, efforts and advancements in the field of wastewater treatment toward the efficient removal of these chemicals are a necessity.

Through this study of electrochemical filtration for the removal of ibuprofen and bisphenol A, different factors were investigated to varying degrees and various parameters were implemented. This systematic investigation was for the purpose of better understanding of the process as a step forward toward real world applications. The qualities of the electrochemical filtration materials were reasonably varied as an important factor in this process, aiming to show the importance of membrane electrode material's bulk crystalline structure and its ability for surface interactions with the target contaminant. MWNTs were selected as the basic electrochemical filtration material, and attention was drawn to their application capacity and limitations in conventional filtration and electrochemical filtration at low applied voltages. Improving the selectivity and increasing the functional surface area of MWNTs was shown to be a feasible endeavor, and which may be controlled for better performance.

Background solution pH and composition were studied as two different factors aimed at providing a deeper insight into the role of electroactive species in the process. Different

electroactive species were assayed and characterized, and in addition, a detailed investigation into the importance of the nature of background solution during conventional filtration was conducted. The important role of applied voltage in initiating different electrochemical routes was comprehensively discussed, and the understanding of these various routes was clearly and concisely provided. The study also considered the relation between the magnitude of applied voltage, the degradation potential of the target contaminants, and the formation potential of electroactive species participating in the process.

However, the major contributions of this work are: Firstly, exploring and mapping the different degradation pathways of the two chemicals, ibuprofen and bisphenol A, during electrochemical filtration, and shedding light on the major factors that greatly contribute to the elimination of the two chemicals and their toxic products during the process. Secondly, applying two different modes of electrochemical filtration (dead-end and crossflow), and pointing out the strength and weakness of each mode compared to the other technologies in removing the two emerging chemicals. This way of comparing dead-end and crossflow modes provided a clear understanding of the mechanistic role and contribution of the flow through the mechanism of dead-end mode and the horizontal shear flow mechanism of crossflow mode.

Journal Papers

1. Bakr, A.R. and M.S. Rahaman, *Electrochemical efficacy of a carboxylated multiwalled carbon nanotube filter for the removal of ibuprofen from aqueous solutions under acidic conditions*. Chemosphere, 2016. **153**: p. 508-520.
2. Bakr, A.R. and M.S. Rahaman, *Perceiving Different Factors of Influence during Dead-end Electrochemical Filtration of Bisphenol A using Multiwalled Carbon Nanotubes: Resistance to Surface Passivation, Reactive Oxygen Species and Residence Time*. (In Preparation).
3. Bakr, A.R. and M.S. Rahaman, *Crossflow Electrochemical Filtration for Eliminating Ibuprofen and Bisphenol A from Electrolytic Solutions in Pure and Fouling Conditions*. (In Preparation).

6.2. Conclusion

This work provides a systematic investigation of different aspects and characteristics of electrochemical filtration as an emerging technology for water and wastewater treatment for two model emerging contaminants of concern. In this study, parameters of the process of varying importance were deeply explored and discussed with the aim of understanding the true importance of these parameters for the process, and in ways that were not delivered previously. The competence of the electrochemical filtration process in removing two contaminants of growing concern, ibuprofen and bisphenol A, was investigated under different conditions. These conditions were proposed and tested for the purpose of revealing the adequate chemistry for removal of the two contaminants and elimination of their hazardous effects during electrochemical filtration. The study provides a comprehensive investigation into the performance dead-end and crossflow electrochemical filtration, with an in-depth discussion of the similarities and differences between the two processes.

Dead-end electrochemical filtration was used for the first time, in this study, to remove ibuprofen. Ibuprofen is a molecule of a weak acidic nature, which carries a polar carboxylic group. Therefore, a carboxylated multiwalled carbon nanotube (MWNTs-COOH) membrane was used and tested under acidic conditions for the removal of ibuprofen in a dead-end electrochemical filtration process. A comparison was also made between MWNTs-COOH and pristine MWNTs to underline the enhanced performance of MWNTs-COOH for the removal of ibuprofen using electrochemical filtration process under acidic conditions. Using MWNTs-COOH under acidic conditions (pH 2) provided suitable conditions for the creation of hydrophilic surface interactions between MWNTs-COOH and the polar carboxylated ibuprofen molecules. This hydrophilic surface interaction could be clearly observed from the standard filtration performance during application of 0-1 V DC potential. Moreover, hydrophobic surface interactions between ibuprofen and MWNTs-COOH were better accommodated due to the absence of hydration effects at the MWNTs-COOH surface in the acidic condition. It was also shown that complete removal of ibuprofen could be achieved at a 2 V of applied DC potential when a low flow rate was applied in the same solution conditions. This outcome was attributed to the in-situ generation of reactive oxygen species (Superoxide) and their rapid interactions with ibuprofen, and simultaneous degradation of its by-products, under these conditions.

Observing the removal behavior of ibuprofen over time (breakthrough), when a 3 V DC potential was applied, the contributions of direct (Direct electron transfer) and indirect (bulk oxidative interactions) electrooxidation pathways could be confidently proposed. The application of 3 V DC potential under acidic conditions resulted in an excellent removal outcome, which was attributed to the improved formation of electroactive species (Reactive chlorine) and its contribution in the bulk oxidative reactions. Furthermore, the application of 3 V under acidic conditions resulted in less wasting reactions, which consume the electrode surface active sites, during the process. Therefore, this increased the chances for the contribution of ibuprofen degradation by direct electron transfer at the electrode surface.

Ibuprofen degradation by-products were successfully identified, and it was found that major toxic by-products were 4-isobutylbenzoic acid, 1-(4-isobutylphenyl)-1-ethanol, and 2-(4-formylphenyl) propanoic acid, both known for their cytotoxic effects. When the applied voltage was raised from 2 to 3 V DC potential, it was possible to eliminate ibuprofen and its cytotoxic by-products completely. When lower flow rates and larger MWNTs-COOH surface loading were applied, longer residence times were achieved within the filter media, leading to a complete removal of ibuprofen and all of its products by electrochemical filtration at 2 V.

Dead-end electrochemical filtration was also employed for the first time for the treatment of bisphenol A. To have a clear understanding of the best conditions for bisphenol A removal; treatment conditions were varied. Bisphenol A is a phenolic molecule with previous reports into its ability to create a polymeric passivation to electrode's surfaces during batch electrochemical and sorption treatments. Therefore, to observe bisphenol A deformation behavior and whether or not bisphenol A might exert surface polymeric fouling during electrochemical filtration, the salting out effect during bisphenol A removal was studied, and boron doped MWNTs were tested. It was concluded that bisphenol A does not exert surface polymeric fouling to MWNTs, which could be attributed to the accelerated degradation kinetics of bisphenol A during dead-end electrochemical filtration. The electrolytic solutions were tested at various pH in both the presence and absence of salt (NaCl) to better elucidate the role of electrolytic species and greatly observe the extent of their role in the electrodegradation process during electrochemical filtration. It was shown that the presence of salt is not critical for the highest contaminant removal efficiency likely due to the vital role of other electroactive species (e.g. reactive oxygen species [ROS]).

It was observed that regardless of the composition and pH of the electrolytic solutions, complete removal of bisphenol A at 2 and 3 V of applied DC potentials was achievable, indicating that electrochemical filtration of bisphenol A is voltage dependent at both 2 and 3 V. It was concluded that bisphenol A is readily oxidizable under sufficient voltage applications, likely due to its low oxidation potential. The influence of allowing sufficient residence (Reaction) time was carefully examined by observing the degradation outcomes and pathways of bisphenol A in two residence times within the MWNTs membranes, 2.0 and 14.9 seconds, and under 3 V of applied DC potential. It was concluded that during a residence time of 14.9 seconds, further degradation to the point of formation of non-toxic aliphatic products could be reached.

ROS was concluded to be the predominant species responsible for the indirect oxidative degradation of contaminants during electrochemical filtration by MWNTs. Different assays were repeatedly performed and it was found that superoxide ($O_2^{\bullet-}$) is greatly contributing to the electrochemical filtration process. It was also found that other electroactive species are produced during the process (i.e. hydrogen peroxide and hypochlorous acid), with limited to insignificant contributions during the process. The minor contribution from hydrogen peroxide and hypochlorous acid can mainly be attributed to their slow interaction kinetics as compared to that of superoxides. Different parameters were systematically studied for in-depth evaluation of dead-end electrochemical filtration processes for ibuprofen and bisphenol A removal, including electrochemical performance (Voltammetry), adsorption capacities, removal, and permeate flux. Moreover, the performance of dead-end electrochemical filtration was evaluated for the removal of the two contaminants from synthetic secondary wastewater to mimic real conditions. It was found that under 2-3 V of applied DC potential, the removal outcomes of the two contaminants from synthetic secondary wastewater was similar to the removal from pure electrolytic solutions.

Crossflow electrochemical filtration was employed using a flat sheet setup for the removal of ibuprofen and bisphenol A, in individual and equimolar solutions. The novelty in using crossflow electrochemical filtration was introduced in differing aspects of the study including the use of MWNTs based material (Buckypaper) for the removal of ibuprofen and bisphenol A. The study provides an in-depth mechanistic overview of the removal of the two contaminants and their degradation fates in the crossflow mode. Overall, this study provides an integrated communication on the electrochemical filtration process with its commonly employed modes (Dead-end and

crossflow) and a comparison of their outcomes. The importance of studying the crossflow mode is due to its challenging integration, yet imminent capacity for real application due to its provision of an antifouling mechanism and thus increased membrane expectancy. Thus, the incorporation of the crossflow mode in electrochemical filtration is considered to be of great importance in making the process more applicable.

MWNTs blend buckypaper was used as a dual (anode and cathode) membrane electrode. The MWNTs blend buckypaper was found to provide a larger specific surface area and high conductivity for electrochemical applications, due to its rich MWNT content per unit area. From the filtration and electrochemical filtration over time (breakthrough), it was observed that the crossflow configuration could offer great performance results. The high-performance relative to operation time was significant in treating individual and mixture forms of both contaminants in pure and fouling electrolytic conditions, which was significant at 2-3 V DC potential. It was concluded that the shear flow mechanism in crossflow mode could result in better and more consistent surface coverage, and provide longer residence times for the contaminants within the membrane at a given flow rate, compared to the dead-end mode. It was observed that the substantial residence time of 18.3 seconds during the crossflow electrochemical filtration is sufficient to allow for complete degradation of the phenolic aromatic products and quinoid rings into the formation of final non-toxic aliphatic carboxylic acids, which was significant at the highest applied voltage (3 V).

6.3. Future Recommendations

Through this work, some challenges were observed with electrochemical filtration, requiring further work to improve the process. These challenges can be summarized under three axes. The first axis is the sorption capacity of MWNTs and MWNTs based materials. Through the course of the study, it was found that conventional filtration resulted in limited outcomes. Given the enormous surface area of MWNTs, as measured by BET, the reason behind the limited adsorption of the two contaminants by MWNTs was not completely understood. In this study, limitation in adsorption capacity was attributed to the probable low number of surface adsorptive sites on MWNTs. Therefore, increasing the sorption capacity of MWNTs could be a key solution to such a limitation. During conventional dead-end filtration of ibuprofen in this study, it was clearly observed that the use of carboxylated MWNTs could significantly improve the adsorption

of carboxylated ibuprofen under adequate solution conditions. Therefore, it was proposed that selectivity between adsorbing substrate (adsorbent) and the adsorbate be a parameter that must be considered during conventional filtration. Future work on increasing functional area or adsorptive sites of MWNTs is important, and which can be explored through increasing the oxy-functional groups at MWNTs surface, and the creation of networks of these functional groups. Such surface modification can culminate in improved filtration performance of contaminants with oxy-functional groups.

The second axis is the electrocatalytic activity. When sufficient DC potentials were applied in this study, the electrochemical performance of MWNTs and MWNTs blend buckypaper was found to be very efficient. However, in a scaled-up process, a higher magnitude applied potential might be required, which could result in larger energy consumption and hence lower economic efficiency. Therefore, increasing the electrocatalytic activity of MWNTs by incorporating surface catalytic materials could be essential. Innovations in carbon composite synthesis may be a step forward in providing faster toxicity reduction of treated contaminants. Of the chemical structures that can be explored and that can be blended with MWNTs in suitable proportions, are oxides of perovskite structure (e.g. strontium cerium oxide (SrCeO_3), barium cerium oxide (BaCeO_3), strontium zirconium oxide (SrZrO_3), and barium zirconium oxide (BaZrO_3)). These oxides have been shown to be super stable in electrochemical applications, superconductive, and have a great catalytic capacity for hydrogen fuel generation.

The third axis is the chemical activity in the bulk of the solution. Bulk electrochemical activity was concluded to be effective in the removal of ibuprofen and bisphenol A in this study and shown to be due to the in-situ generation of electroactive species. Therefore, enhancing the properties of bulk chemical activity was not concluded to be of critical necessity in this study. However, other emerging contaminants could be more stubborn and may require further inputs to an efficient process. Therefore, advancements in chemical catalysis may need to be tackled and assimilated with the electrochemical filtration process. The incorporation of catalytic processes such as Fenton's chemistry with electrochemical filtration needs to be further explored as a proactive step for future challenges.

References

1. Liu H. CNT-based Electrochemical Filter for Water Treatment: Mechanisms and Applications. Graduate School of Arts & Sciences: Harvard University; 2015.
2. Pendergast M. M., Hoek E. M. V. A review of water treatment membrane nanotechnologies. Energy & Environmental Science. 2011;4(6):1946-71.
3. Coping with Water Scarcity. Challenge of the Twenty-first Century. United Nations (UN) Water. Food and Agricultural Association: (FAO); 2007.
4. Cooley H. A. N., Ha M., Srinivasan V., Morrison J., Donnelly K., and Christian-Smith J. Global Water Governance in the Twenty-First Century. Chapter 1: Pacific Institute 2013.
5. Spellman F. R. Handbook of water & wastewater treatment plant operations. 2000 N.W. Corporate Blvd., Boca Raton, Florida 33431: CRC Press LLC; 2003.
6. Michael R. Templeton D. B. An Introduction to Wastewater Treatment: bookboon.com; 2011.
7. Cheremisinoff N. P. Chapter 1 - An Overview of Water and Waste- Water Treatment. Handbook of Water and Wastewater Treatment Technologies. Woburn: Butterworth-Heinemann; 2002. p. 1-61.
8. Zhang J., Sun B., Guan X. Oxidative removal of bisphenol A by permanganate: Kinetics, pathways and influences of co-existing chemicals. Separation and Purification Technology. 2013;107:48-53.
9. Treating water: American Water. Available from: <http://www.amwater.com/>.
10. Sperling M. v. Basic Principles of Wastewater Treatment. Biological Wastewater Treatment Series: IWA Publishing; 2007.
11. Conventional Wastewater Treatment Process: <http://www.sheffy6marketing.com/>. Available from: <http://www.sheffy6marketing.com/>.
12. Contaminants of Emerging Concern in the Environment: U.S Geological Survey "USGS". Available from: <http://toxics.usgs.gov/>.
13. Raghav M. E. S., Mitchell K., Witte B. Contaminants of Emerging Concern in Water. "Arroyo". Water Resources Research Center College of Agriculture and Life Sciences • The University of Arizona, 2013.

14. Contaminants of Emerging Concern: Water Quality Association. Available from: <https://www.wqa.org>.
15. Petrie B., Barden R., Kasprzyk-Hordern B. A review on emerging contaminants in wastewaters and the environment: current knowledge, understudied areas and recommendations for future monitoring. *Water Res.* 2015;72:3-27.
16. Richardson S. D. Water Analysis: Emerging Contaminants and Current Issues. *Analytical Chemistry.* 2009;81(12):4645-77.
17. Petrie B., Barden R., Kasprzyk-Hordern B. A review on emerging contaminants in wastewaters and the environment: Current knowledge, understudied areas and recommendations for future monitoring. *Water Research.* 2015;72:3-27.
18. USGS. Emerging Contaminants In the Environment. Available from: <http://toxics.usgs.gov/>.
19. Rivera-Utrilla J., Sánchez-Polo M., Ferro-García M. Á., Prados-Joya G., Ocampo-Pérez R. Pharmaceuticals as emerging contaminants and their removal from water. A review. *Chemosphere.* 2013;93(7):1268-87.
20. Ye X., Zhou X., Needham L. L., Calafat A. M. In-vitro oxidation of bisphenol A: Is bisphenol A catechol a suitable biomarker for human exposure to bisphenol A? *Analytical and bioanalytical chemistry.* 2011;399(3):1071-9.
21. Mohapatra D. P., Brar S. K., Tyagi R. D., Surampalli R. Y. Occurrence of bisphenol A in wastewater and wastewater sludge of CUQ treatment plant. *Journal of Xenobiotics.* 2011;1(1):3.
22. Mohapatra D. P., Brar S. K., Tyagi R. D., Surampalli R. Y. Physico-chemical pre-treatment and biotransformation of wastewater and wastewater sludge--fate of bisphenol A. *Chemosphere.* 2010;78(8):923-41.
23. Thompson K. C., Rennie A. R., King M. D., Hardman S. J. O., Lucas C. O. M., Pfrang C., Hughes B. R., Hughes A. V. Reaction of a Phospholipid Monolayer with Gas-Phase Ozone at the Air–Water Interface: Measurement of Surface Excess and Surface Pressure in Real Time. *Langmuir.* 2010;26(22):17295-303.
24. von Gunten U. Ozonation of drinking water: Part I. Oxidation kinetics and product formation. *Water Research.* 2003;37(7):1443-67.
25. Salgado P., Melin V., Contreras D., Moreno Y., Mansilla H. D. FENTON REACTION DRIVEN BY IRON LIGANDS. *Journal of the Chilean Chemical Society.* 2013;58:2096-101.

26. Facile N., Barbeau B., Prévost M., Koudjonou B. Evaluating bacterial aerobic spores as a surrogate for Giardia and Cryptosporidium inactivation by ozone. *Water Research*. 2000;34(12):3238-46.
27. von Gunten U. Ozonation of drinking water: Part II. Disinfection and by-product formation in presence of bromide, iodide or chlorine. *Water Research*. 2003;37(7):1469-87.
28. Hoigne J. Chemistry of aqueous ozone, and transformation of pollutants by ozonation and advanced oxidation processes. Berlin: Springer; 1998.
29. Lin A. Y.-C., Lin C.-F., Chiou J.-M., Hong P. K. A. O₃ and O₃/H₂O₂ treatment of sulfonamide and macrolide antibiotics in wastewater. *Journal of Hazardous Materials*. 2009;171(1-3):452-8.
30. Ozone Generator in Waste Water Treatment: <http://www.digitalmarketing.com.ph/>. Available from: <http://www.digitalmarketing.com.ph/>.
31. Water Resources Management and Water Quality Protection: <http://www.tankonyvtar.hu/>. Available from: <http://www.tankonyvtar.hu/>.
32. Hollender J., Zimmermann S. G., Koepke S., Krauss M., McArdell C. S., Ort C., Singer H., von Gunten U., Siegrist H. Elimination of Organic Micropollutants in a Municipal Wastewater Treatment Plant Upgraded with a Full-Scale Post-Ozonation Followed by Sand Filtration. *Environmental Science & Technology*. 2009;43(20):7862-9.
33. Canonica S. Oxidation of Aquatic Organic Contaminants Induced by Excited Triplet States. *CHIMIA International Journal for Chemistry*. 2007;61(10):641-4.
34. De la Cruz N., Gimenez J., Esplugas S., Grandjean D., de Alencastro L. F., Pulgarin C. Degradation of 32 emergent contaminants by UV and neutral photo-fenton in domestic wastewater effluent previously treated by activated sludge. *Water Res*. 2012;46(6):1947-57.
35. Kim I., Yamashita N., Tanaka H. Photodegradation of pharmaceuticals and personal care products during UV and UV/H₂O₂ treatments. *Chemosphere*. 2009;77(4):518-25.
36. Giri R. R., Ozaki H., Takayanagi Y., Taniguchi S., Takanami R. Efficacy of ultraviolet radiation and hydrogen peroxide oxidation to eliminate large number of pharmaceutical compounds in mixed solution. *International Journal of Environmental Science & Technology*. 2011;8(1):19-30.

37. Rosenfeldt E. J., Linden K. G. Degradation of Endocrine Disrupting Chemicals Bisphenol A, Ethinyl Estradiol, and Estradiol during UV Photolysis and Advanced Oxidation Processes. *Environmental Science & Technology*. 2004;38(20):5476-83.
38. Sanches S., Barreto Crespo M. T., Pereira V. J. Drinking water treatment of priority pesticides using low pressure UV photolysis and advanced oxidation processes. *Water Research*. 2010;44(6):1809-18.
39. Kim I., Tanaka H. Photodegradation characteristics of PPCPs in water with UV treatment. *Environment International*. 2009;35(5):793-802.
40. Canonica S., Meunier L., von Gunten U. Phototransformation of selected pharmaceuticals during UV treatment of drinking water. *Water Research*. 2008;42(1-2):121-8.
41. Lopez A., Bozzi A., Mascolo G., Kiwi J. Kinetic investigation on UV and UV/H₂O₂ degradations of pharmaceutical intermediates in aqueous solution. *Journal of Photochemistry and Photobiology A: Chemistry*. 2003;156(1-3):121-6.
42. De la Cruz N., Esquius L., Grandjean D., Magnet A., Tungler A., de Alencastro L. F., Pulgarin C. Degradation of emergent contaminants by UV, UV/H₂O₂ and neutral photo-Fenton at pilot scale in a domestic wastewater treatment plant. *Water Res*. 2013;47(15):5836-45.
43. Kim I., Yamashita N., Tanaka H. Performance of UV and UV/H₂O₂ processes for the removal of pharmaceuticals detected in secondary effluent of a sewage treatment plant in Japan. *J Hazard Mater*. 2009;166(2-3):1134-40.
44. Zheng T., Zhang T., Wang Q., Tian Y., Shi Z., Smale N., Xu B. Advanced treatment of acrylic fiber manufacturing wastewater with a combined microbubble-ozonation/ultraviolet irradiation process. *RSC Adv*. 2015;5(95):77601-9.
45. Rivas F. J., Beltran F. J., Encinas A. Removal of emergent contaminants: integration of ozone and photocatalysis. *Journal of environmental management*. 2012;100:10-5.
46. Esplugas S., Giménez J., Contreras S., Pascual E., Rodríguez M. Comparison of different advanced oxidation processes for phenol degradation. *Water Research*. 2002;36(4):1034-42.
47. Comninellis C. Electrocatalysis in the electrochemical conversion/combustion of organic pollutants for waste water treatment. *Electrochimica Acta*. 1994;39(11):1857-62.
48. Cięciwa A. F. G., and Comninellis C. *Electrochemistry for the Environment*: Springer; 2010.

49. Martinez-Huitle C. A., Ferro S. Electrochemical oxidation of organic pollutants for the wastewater treatment: direct and indirect processes. *Chemical Society reviews*. 2006;35(12):1324-40.
50. V. Shanthi K. R., C. Ahmed Basha. Domestic Sewage treatment using Batch Stirred Tank Electrochemical Reactor. *International Journal of ChemTech Research*. 2011;3(3):1711-21.
51. Panizza M., Cerisola G. Direct And Mediated Anodic Oxidation of Organic Pollutants. *Chemical Reviews*. 2009;109(12):6541-69.
52. Panizza M., Cerisola G. Removal of colour and COD from wastewater containing acid blue 22 by electrochemical oxidation. *Journal of Hazardous Materials*. 2008;153(1-2):83-8.
53. Fabiańska A., Ossowski T., Stepnowski P., Stolte S., Thöming J., Siedlecka E. M. Electrochemical oxidation of imidazolium-based ionic liquids: The influence of anions. *Chemical Engineering Journal*. 2012;198-199(0):338-45.
54. Chen Y., Li H., Liu W., Tu Y., Zhang Y., Han W., Wang L. Electrochemical degradation of nitrobenzene by anodic oxidation on the constructed TiO₂-NTs/SnO₂-Sb/PbO₂ electrode. *Chemosphere*. 2014;113(0):48-55.
55. Yun-Hai W. Q.-Y. C., Guo L., and Xiang-Lin L. . Anodic Materials with High Energy Efficiency for Electrochemical Oxidation of Toxic Organics in Waste Water. In: Show PK-Y, editor. *Industrial Waste*2012.
56. Flox C., Arias C., Brillas E., Savall A., Groenen-Serrano K. Electrochemical incineration of cresols: A comparative study between PbO₂ and boron-doped diamond anodes. *Chemosphere*. 2009;74(10):1340-7.
57. Murugananthan M., Yoshihara S., Rakuma T., Shirakashi T. Mineralization of bisphenol A (BPA) by anodic oxidation with boron-doped diamond (BDD) electrode. *J Hazard Mater*. 2008;154(1-3):213-20.
58. Rabaaoui N., Moussaoui Y., Allagui M. S., Ahmed B., Elaloui E. Anodic oxidation of nitrobenzene on BDD electrode: Variable effects and mechanisms of degradation. *Separation and Purification Technology*. 2013;107:318-23.
59. Cui Y.-h., Li X.-y., Chen G. Electrochemical degradation of bisphenol A on different anodes. *Water Research*. 2009;43(7):1968-76.

60. Li X.-y., Cui Y.-h., Feng Y.-j., Xie Z.-m., Gu J.-D. Reaction pathways and mechanisms of the electrochemical degradation of phenol on different electrodes. *Water Research*. 2005;39(10):1972-81.
61. Scialdone O., Randazzo S., Galia A., Silvestri G. Electrochemical oxidation of organics in water: Role of operative parameters in the absence and in the presence of NaCl. *Water Research*. 2009;43(8):2260-72.
62. Ciriaco L., Anjo C., Correia J., Pacheco M. J., Lopes A. Electrochemical degradation of Ibuprofen on Ti/Pt/PbO₂ and Si/BDD electrodes. *Electrochimica Acta*. 2009;54(5):1464-72.
63. Dirany A., Sirés I., Oturan N., Özcan A., Oturan M. A. Electrochemical Treatment of the Antibiotic Sulfachloropyridazine: Kinetics, Reaction Pathways, and Toxicity Evolution. *Environmental Science & Technology*. 2012;46(7):4074-82.
64. Skoumal M., Rodríguez R. M., Cabot P. L., Centellas F., Garrido J. A., Arias C., Brillas E. Electro-Fenton, UVA photoelectro-Fenton and solar photoelectro-Fenton degradation of the drug ibuprofen in acid aqueous medium using platinum and boron-doped diamond anodes. *Electrochimica Acta*. 2009;54(7):2077-85.
65. Gözmen B., Oturan M. A., Oturan N., Erbatır O. Indirect Electrochemical Treatment of Bisphenol A in Water via Electrochemically Generated Fenton's Reagent. *Environmental Science & Technology*. 2003;37(16):3716-23.
66. Loaiza-Ambuludi S., Panizza M., Oturan N., Özcan A., Oturan M. A. Electro-Fenton degradation of anti-inflammatory drug ibuprofen in hydroorganic medium. *Journal of Electroanalytical Chemistry*. 2013;702(0):31-6.
67. Feng Y., Yang L., Liu J., Logan B. E. Electrochemical technologies for wastewater treatment and resource reclamation. *Environmental Science: Water Research & Technology*. 2016.
68. Song C., Zhang J. Electrocatalytic Oxygen Reduction Reaction. In: Zhang J, editor. *PEM Fuel Cell Electrocatalysts and Catalyst Layers*: Springer London; 2008. p. 89-134.
69. Decontamination and Bioremediation: <http://decontaminationandbioremediation.blogspot.ca/>. Available from: <http://decontaminationandbioremediation.blogspot.ca/>.
70. Fleszar B. w., Poszyńska J. An attempt to define benzene and phenol electrochemical oxidation mechanism. *Electrochimica Acta*. 1985;30(1):31-42.

71. Zhu X., Tong M., Shi S., Zhao H., Ni J. Essential Explanation of the Strong Mineralization Performance of Boron-Doped Diamond Electrodes. *Environmental Science & Technology*. 2008;42(13):4914-20.
72. Rahaman M. S., Vecitis C. D., Elimelech M. Electrochemical Carbon-Nanotube Filter Performance toward Virus Removal and Inactivation in the Presence of Natural Organic Matter. *Environmental Science & Technology*. 2012;46(3):1556-64.
73. Vecitis C. D., Gao G., Liu H. Electrochemical Carbon Nanotube Filter for Adsorption, Desorption, and Oxidation of Aqueous Dyes and Anions. *The Journal of Physical Chemistry C*. 2011;115(9):3621-9.
74. Liu H., Vecitis C. D. Reactive Transport Mechanism for Organic Oxidation during Electrochemical Filtration: Mass-Transfer, Physical Adsorption, and Electron-Transfer. *The Journal of Physical Chemistry C*. 2011;116(1):374-83.
75. Gao G., Vecitis C. D. Electrochemical Carbon Nanotube Filter Oxidative Performance as a Function of Surface Chemistry. *Environmental Science & Technology*. 2011;45(22):9726-34.
76. Gao G., Zhang Q., Vecitis C. D. CNT-PVDF composite flow-through electrode for single-pass sequential reduction-oxidation. *Journal of Materials Chemistry A*. 2014;2(17):6185-90.
77. Shao D., Hu J., Jiang Z., Wang X. Removal of 4,4'-dichlorinated biphenyl from aqueous solution using methyl methacrylate grafted multiwalled carbon nanotubes. *Chemosphere*. 2011;82(5):751-8.
78. Li Y., Niu J., Shen Z., Feng C. Size effect of single-walled carbon nanotube on adsorption of perfluorooctanesulfonate. *Chemosphere*. 2013;91(6):784-90.
79. Hébert C., Mazellier J. P., Scorsone E., Mermoux M., Bergonzo P. Boosting the electrochemical properties of diamond electrodes using carbon nanotube scaffolds. *Carbon*. 2014;71(0):27-33.
80. Li H., Zhang D., Han X., Xing B. Adsorption of antibiotic ciprofloxacin on carbon nanotubes: pH dependence and thermodynamics. *Chemosphere*. 2014;95(0):150-5.
81. Motoc S., Remes A., Pop A., Manea F., Schoonman J. Electrochemical detection and degradation of ibuprofen from water on multi-walled carbon nanotubes-epoxy composite electrode. *Journal of Environmental Sciences*. 2013;25(4):838-47.

82. Gao G., Vecitis C. D. Doped Carbon Nanotube Networks for Electrochemical Filtration of Aqueous Phenol: Electrolyte Precipitation and Phenol Polymerization. *ACS Applied Materials & Interfaces*. 2012;4(3):1478-89.
83. Vecitis C. D., Schnoor M. H., Rahaman M. S., Schiffman J. D., Elimelech M. Electrochemical Multiwalled Carbon Nanotube Filter for Viral and Bacterial Removal and Inactivation. *Environmental Science & Technology*. 2011;45(8):3672-9.
84. Soomro M. T., Ismail I., Hameed A., Aslam M. A Simple Electrochemical Approach for Determination and Direct Monitoring of Drug Degradation in Water. *Current World Environment Journal*. 2013;8(3):375-80.
85. Manea F., Motoc S., Pop A., Remes A., Schoonman J. Silver-functionalized carbon nanofiber composite electrodes for ibuprofen detection. *Nanoscale research letters*. 2012;7(1):331.
86. Liu Y., Xie J., Ong C. N., Vecitis C. D., Zhou Z. Electrochemical wastewater treatment with carbon nanotube filters coupled with in situ generated H₂O₂. *Environ Sci: Water Res Technol*. 2015;1(6):769-78.
87. Chen Z., Pierre D., He H., Tan S., Pham-Huy C., Hong H., Huang J. Adsorption behavior of epirubicin hydrochloride on carboxylated carbon nanotubes. *International Journal of Pharmaceutics*. 2011;405(1-2):153-61.
88. Lin D., Xing B. Adsorption of Phenolic Compounds by Carbon Nanotubes: Role of Aromaticity and Substitution of Hydroxyl Groups. *Environmental Science & Technology*. 2008;42(19):7254-9.
89. Chen W., Duan L., Zhu D. Adsorption of Polar and Nonpolar Organic Chemicals to Carbon Nanotubes. *Environmental Science & Technology*. 2007;41(24):8295-300.
90. Yu Q., Deng S., Yu G. Selective removal of perfluorooctane sulfonate from aqueous solution using chitosan-based molecularly imprinted polymer adsorbents. *Water Research*. 2008;42(12):3089-97.
91. Tang C. Y., Allen H. C. Ionic Binding of Na⁺ versus K⁺ to the Carboxylic Acid Headgroup of Palmitic Acid Monolayers Studied by Vibrational Sum Frequency Generation Spectroscopy†. *The Journal of Physical Chemistry A*. 2009;113(26):7383-93.
92. Bian H. T., Feng R. R., Guo Y., Wang H. F. Specific Na⁺ and K⁺ cation effects on the interfacial water molecules at the air/aqueous salt solution interfaces probed with nonresonant second harmonic generation. *The Journal of chemical physics*. 2009;130(13):134709.

93. Feng R.-r., Bian H.-t., Guo Y., Wang H.-f. Spectroscopic evidence for the specific Na⁺ and K⁺ interactions with the hydrogen-bonded water molecules at the electrolyte aqueous solution surfaces. *The Journal of chemical physics*. 2009;130(13):134710.
94. Zhang D., Pan B., Wu M., Wang B., Zhang H., Peng H., Wu D., Ning P. Adsorption of sulfamethoxazole on functionalized carbon nanotubes as affected by cations and anions. *Environmental Pollution*. 2011;159(10):2616-21.
95. Wang J., Musameh M. Carbon Nanotube/Teflon Composite Electrochemical Sensors and Biosensors. *Analytical Chemistry*. 2003;75(9):2075-9.
96. Ghernaout D., Naceur M. W., Aouabed A. On the dependence of chlorine by-products generated species formation of the electrode material and applied charge during electrochemical water treatment. *Desalination*. 2011;270(1-3):9-22.
97. Glueckstern P., Priel M., Gelman E., Perlov N. Wastewater desalination in Israel. *Desalination*. 2008;222(1-3):151-64.
98. Kwan S. E., Bar-Zeev E., Elimelech M. Biofouling in forward osmosis and reverse osmosis: Measurements and mechanisms. *Journal of Membrane Science*. 2015;493:703-8.
99. Wang H., Tang M., Han L., Cao J., Zhang Z., Huang W., Chen R., Yu C. Synthesis of hollow organosiliceous spheres for volatile organic compound removal. *J Mater Chem A*. 2014;2(45):19298-307.
100. Madhavan J., Grieser F., Ashokkumar M. Combined advanced oxidation processes for the synergistic degradation of ibuprofen in aqueous environments. *Journal of Hazardous Materials*. 2010;178(1-3):202-8.
101. Caviglioli G., Valeria P., Brunella P., Sergio C., Attilia A., Gaetano B. Identification of degradation products of Ibuprofen arising from oxidative and thermal treatments. *Journal of Pharmaceutical and Biomedical Analysis*. 2002;30(3):499-509.
102. Méndez-Arriaga F., Esplugas S., Giménez J. Photocatalytic degradation of non-steroidal anti-inflammatory drugs with TiO₂ and simulated solar irradiation. *Water Research*. 2008;42(3):585-94.
103. Illés E., Takács E., Dombi A., Gajda-Schrantz K., Rác G., Gonter K., Wojnárovits L. Hydroxyl radical induced degradation of ibuprofen. *Science of The Total Environment*. 2013;447(0):286-92.

104. Zheng B. G., Zheng Z., Zhang J. B., Luo X. Z., Wang J. Q., Liu Q., Wang L. H. Degradation of the emerging contaminant ibuprofen in aqueous solution by gamma irradiation. *Desalination*. 2011;276(1-3):379-85.
105. Afanas'ev I. B. *Superoxide Ion: Chemistry and Biological Implications*. Boca Raton, FL: CRC Press 1989.
106. Smith B. A., Teel A. L., Watts R. J. Identification of the Reactive Oxygen Species Responsible for Carbon Tetrachloride Degradation in Modified Fenton's Systems. *Environmental Science & Technology*. 2004;38(20):5465-9.
107. Scripps Center for Metabolomics "METLIN". Available from: <https://metlin.scripps.edu/index.php>.
108. Chemspider. Available from: <http://www.chemspider.com/>.
109. Winkler M., Lawrence J. R., Neu T. R. Selective degradation of ibuprofen and clofibrac acid in two model river biofilm systems. *Water Research*. 2001;35(13):3197-205.
110. Szabó R. K., Megyeri C., Illés E., Gajda-Schranz K., Mazellier P., Dombi A. Phototransformation of ibuprofen and ketoprofen in aqueous solutions. *Chemosphere*. 2011;84(11):1658-63.
111. Quintana J. B., Weiss S., Reemtsma T. Pathways and metabolites of microbial degradation of selected acidic pharmaceutical and their occurrence in municipal wastewater treated by a membrane bioreactor. *Water Research*. 2005;39(12):2654-64.
112. Jacobs L. E., Fimmen R. L., Chin Y.-P., Mash H. E., Weavers L. K. Fulvic acid mediated photolysis of ibuprofen in water. *Water Research*. 2011;45(15):4449-58.
113. Ruggeri G., Ghigo G., Maurino V., Minero C., Vione D. Photochemical transformation of ibuprofen into harmful 4-isobutylacetophenone: Pathways, kinetics, and significance for surface waters. *Water Research*. 2013;47(16):6109-21.
114. Bakr A. R., Rahaman M. S. Electrochemical efficacy of a carboxylated multiwalled carbon nanotube filter for the removal of ibuprofen from aqueous solutions under acidic conditions. *Chemosphere*. 2016;153:508-20.
115. Gao G., Pan M., Vecitis C. D. Effect of the oxidation approach on carbon nanotube surface functional groups and electrooxidative filtration performance. *Journal of Materials Chemistry A*. 2015;3(14):7575-82.

116. Gao G., Vecitis C. D. Electrocatalysis aqueous phenol with carbon nanotubes networks as anodes: Electrodes passivation and regeneration and prevention. *Electrochimica Acta*. 2013;98:131-8.
117. Fukahori S., Ichiura H., Kitaoka T., Tanaka H. Photocatalytic Decomposition of Bisphenol A in Water Using Composite TiO₂-Zeolite Sheets Prepared by a Papermaking Technique. *Environmental Science & Technology*. 2003;37(5):1048-51.
118. Deborde M., Rabouan S., Mazellier P., Duguet J.-P., Legube B. Oxidation of bisphenol A by ozone in aqueous solution. *Water Research*. 2008;42(16):4299-308.
119. Bonfatti F., Ferro S., Lavezzo F., Malacarne M., Lodi G., De Battisti A. Electrochemical Incineration of Glucose as a Model Organic Substrate. II. Role of Active Chlorine Mediation. *Journal of The Electrochemical Society*. 2000;147(2):592-6.
120. Hsieh H.-S., Jafvert C. T. Reactive oxygen species generation and dispersant-dependent electron transfer through single-walled carbon nanotubes in water. *Carbon*. 2015;89:361-71.
121. Hsieh H. S., Wu R., Jafvert C. T. Light-independent reactive oxygen species (ROS) formation through electron transfer from carboxylated single-walled carbon nanotubes in water. *Environ Sci Technol*. 2014;48(19):11330-6.
122. Bader H., Sturzenegger V., Hoigné J. Photometric method for the determination of low concentrations of hydrogen peroxide by the peroxidase catalyzed oxidation of N,N-diethyl-p-phenylenediamine (DPD). *Water Research*. 1988;22(9):1109-15.
123. Endo S., Pfennigsdorff A., Goss K.-U. Salting-Out Effect in Aqueous NaCl Solutions: Trends with Size and Polarity of Solute Molecules. *Environmental Science & Technology*. 2012;46(3):1496-503.
124. Lide D. R. *CRC handbook of chemistry and physics*. 85th ed. Press C, editor. Boca Raton, FL2004.
125. Bandow S., Numao S., Iijima S. Variable-Range Hopping Conduction in the Assembly of Boron-Doped Multiwalled Carbon Nanotubes. *The Journal of Physical Chemistry C*. 2007;111(32):11763-6.
126. Czerw R., Terrones M., Charlier J. C., Blase X., Foley B., Kamalakaran R., Grobert N., Terrones H., Tekleab D., Ajayan P. M., Blau W., Rühle M., Carroll D. L. Identification of Electron Donor States in N-Doped Carbon Nanotubes. *Nano Letters*. 2001;1(9):457-60.

127. Mukhopadhyay I., Hoshino N., Kawasaki S., Okino F., Hsu W. K., Touhara H. Electrochemical Li Insertion in B-Doped Multiwall Carbon Nanotubes. *Journal of The Electrochemical Society*. 2002;149(1):A39-A44.
128. Wiggins-Camacho J. D., Stevenson K. J. Effect of Nitrogen Concentration on Capacitance, Density of States, Electronic Conductivity, and Morphology of N-Doped Carbon Nanotube Electrodes. *The Journal of Physical Chemistry C*. 2009;113(44):19082-90.
129. Barone V., Peralta J. E., Uddin J., Scuseria G. E. Screened exchange hybrid density-functional study of the work function of pristine and doped single-walled carbon nanotubes. *The Journal of chemical physics*. 2006;124(2):024709.
130. Lee J. M., Park J. S., Lee S. H., Kim H., Yoo S., Kim S. O. Selective Electron- or Hole-Transport Enhancement in Bulk-Heterojunction Organic Solar Cells with N- or B-Doped Carbon Nanotubes. *Advanced Materials*. 2011;23(5):629-33.
131. Ntsendwana¹ B., Mamba¹ B. B., Sampath² S., Arotiba O. A. Electrochemical Detection of Bisphenol A Using Graphene-Modified Glassy Carbon Electrode. *Int J Electrochem Sci*. 2012;7:3501-12.
132. Tu X., Yan L., Luo X., Luo S., Xie Q. Electroanalysis of Bisphenol A at a Multiwalled Carbon Nanotubes-gold Nanoparticles Modified Glassy Carbon Electrode. *Electroanalysis*. 2009:NA-NA.
133. Clara M., Strenn B., Saracevic E., Kreuzinger N. Adsorption of bisphenol-A, 17 beta-estradiol and 17 alpha-ethinylestradiol to sewage sludge. *Chemosphere*. 2004;56(9):843-51.
134. Rykowska I., Wasiak W. PROPERTIES, THREATS, AND METHODS OF ANALYSIS OF BISPHENOL A AND ITS DERIVATIVES. *ACTA CHROMATOGRAPHICA*. 2006;16.
135. Gao G., Zhang Q., Hao Z., Vecitis C. D. Carbon Nanotube Membrane Stack for Flow-through Sequential Regenerative Electro-Fenton. *Environmental Science & Technology*. 2015.
136. Klein G. W., Bhatla K., Madhavan V., Schuler R. H. Reaction of $^{\bullet}\text{OH}$ with benzoic acid. Isomer distribution in the radical intermediates. *Journal of Physical Chemistry*. 1975;79(17):1767–74.
137. Oturan M. A., Pinson J. Hydroxylation by electrochemically generated OH radicals. Mono- and polyhydroxylation of benzoic acid: products and isomers' distribution. *Journal of Physical Chemistry*. 1995;99(38):13948–54.

138. Watanabe I., Harada K., Matsui T., Miyasaka H., Okuhata H., Tanaka S., Nakayama H., Kato K., Bamba T., Hirata K. Characterization of bisphenol A metabolites produced by *Portulaca oleracea* cv. by liquid chromatography coupled with tandem mass spectrometry. *Bioscience, biotechnology, and biochemistry*. 2012;76(5):1015-7.
139. Boscolo Boscoletto A., Gottardi F., Milan L., Pannocchia P., Tartari V., Tavan M., Amadelli R., Battisti A., Barbieri A., Patracchini D., Battaglin G. Electrochemical treatment of bisphenol-A containing wastewaters. *Journal of Applied Electrochemistry*.24(10):1052-8.
140. Liu Y., Liu H., Zhou Z., Wang T., Ong C. N., Vecitis C. D. Degradation of the Common Aqueous Antibiotic Tetracycline using a Carbon Nanotube Electrochemical Filter. *Environmental Science & Technology*. 2015;49(13):7974-80.
141. Boo C., Elimelech M., Hong S. Fouling control in a forward osmosis process integrating seawater desalination and wastewater reclamation. *Journal of Membrane Science*. 2013;444:148-56.
142. Gattrell M., Kirk D. W. A Fourier Transform Infrared Spectroscopy Study of the Passive Film Produced during Aqueous Acidic Phenol Electro-oxidation. *Journal of The Electrochemical Society*. 1992;139(10):2736-44.
143. Gattrell M., MacDougall B. The Anodic Electrochemistry of Pentachlorophenol. *Journal of The Electrochemical Society*. 1999;146(9):3335-48.
144. Debiemme-Chouvy C., Hua Y., Hui F., Duval J. L., Cachet H. Electrochemical treatments using tin oxide anode to prevent biofouling. *Electrochimica Acta*. 2011;56(28):10364-70.
145. Al-Malack M. H., Anderson G. K. Use of crossflow microfiltration in wastewater treatment. *Water Research*. 1997;31(12):3064-72.
146. Al-Malack M. H. Technical and economic aspects of crossflow microfiltration. *Desalination*. 2003;155(1):89-94.
147. Zhang J., Sun Y., Chang Q., Liu X., Meng G. Improvement of crossflow microfiltration performances for treatment of phosphorus-containing wastewater. *Desalination*. 2006;194(1-3):182-91.
148. Ripperger S., Altmann J. Crossflow microfiltration ? state of the art. *Separation and Purification Technology*. 2002;26(1):19-31.
149. Gekas V., Hallstrom B. Microfiltration membranes, cross-flow transport mechanisms and fouling studies. *Desalination*. 1990;77:195-218.

150. Gan Q. Evaluation of solids reduction and backflush technique in crossflow microfiltration of a primary sewage effluent. *Resources, Conservation and Recycling*. 1999;27:9-14.
151. Thomassen J. K., Faraday D. B. F., Underwood B. O., Cleaver J. A. S. The effect of varying transmembrane pressure and crossflow velocity on the microfiltration fouling of a model beer. *Separation and Purification Technology*. 2005;41(1):91-100.
152. Vera L., Villarroel-Lopez R., Delgado S., Elmaleh S. Cross-flow microfiltration of biologically treated wastewater. *Desalination*. 1997;114(1):65-75.
153. Al-Malack M. H., Anderson G. K. Crossflow microfiltration with dynamic membranes. *Water Research*. 1997;31(8):1969-79.
154. Al-Malack M. H., Anderson G. K., Almasi A. Treatment of anoxic pond effluent using crossflow microfiltration. *Water Research*. 1998;32(12):3738-46.
155. Kazemi M. A., Soltanieh M., Yazdanshenas M. Mathematical modeling of crossflow microfiltration of diluted malt extract suspension by tubular ceramic membranes. *Journal of Food Engineering*. 2013;116(4):926-33.
156. Bailey S. M., Meagher M. M. The effect of denaturants on the crossflow membrane filtration of *Escherichia coli* lysates containing inclusion bodies. *Journal of Membrane Science*. 1997;131(1-2):29-38.
157. El Rayess Y., Albasi C., Bacchin P., Taillandier P., Raynal J., Mietton-Peuchot M., Devatine A. Cross-flow microfiltration applied to oenology: A review. *Journal of Membrane Science*. 2011;382(1-2):1-19.
158. Huotari H. M., Huisman I. H., Tragardh G. Electrically enhanced crossflow membrane filtration of oily waste water using the membrane as a cathode. *Journal of Membrane Science*. 1999;156(1):49-60.
159. Huotari H. M., Trägårdh G., Huisman I. H. Crossflow Membrane Filtration Enhanced by an External DC Electric Field: A Review. *Chemical Engineering Research and Design*. 1999;77(5):461-8.
160. Akay G., Wakeman R. J. Electric field enhanced crossflow microfiltration of hydrophobically modified water soluble polymers. *Journal of Membrane Science*. 1997;131(1-2):229-36.
161. Wakeman R. J., Tarleton E. S. Membrane fouling prevention in crossflow microfiltration by the use of electric fields. *Chemical Engineering Science*. 1987;42(4):829-42.

162. Chuang C.-J., Wu C.-Y., Wu C.-C. Combination of crossflow and electric field for microfiltration of protein/microbial cell suspensions. *Desalination*. 2008;233(1-3):295-302.
163. Enevoldsen A. D., Hansen E. B., Jonsson G. Electro-ultrafiltration of industrial enzyme solutions. *Journal of Membrane Science*. 2007;299(1-2):28-37.
164. Molla S. H., Bhattacharjee S. Prevention of colloidal membrane fouling employing dielectrophoretic forces on a parallel electrode array. *Journal of Membrane Science*. 2005;255(1-2):187-99.
165. Weigert T., Altmann J., Ripperger S. Crossflow electrofiltration in pilot scale. *Journal of Membrane Science*. 1999;159(1-2):253-62.
166. Yang G. C. C., Yang T.-Y. Reclamation of high quality water from treating CMP wastewater by a novel crossflow electrofiltration/electrodialysis process. *Journal of Membrane Science*. 2004;233(1-2):151-9.
167. Yang G. C. C., Yang T.-Y., Tsai S.-H. Crossflow electro-microfiltration of oxide-CMP wastewater. *Water Research*. 2003;37(4):785-92.
168. Zhang Q., Vecitis C. D. Conductive CNT-PVDF membrane for capacitive organic fouling reduction. *Journal of Membrane Science*. 2014;459(0):143-56.
169. Chiu T. Y., Garcia Garcia F. J. Critical flux enhancement in electrically assisted microfiltration. *Separation and Purification Technology*. 2011;78(1):62-8.
170. Lin Y.-T., Sung M., Sanders P. F., Marinucci A., Huang C. P. Separation of nano-sized colloidal particles using cross-flow electro-filtration. *Separation and Purification Technology*. 2007;58(1):138-47.
171. Weng Y.-H., Li K.-C., Chung-Hsieh L. H., Huang C. P. Removal of humic substances (HS) from water by electro-microfiltration (EMF). *Water Research*. 2006;40(9):1783-94.
172. Zaky A. M., Chaplin B. P. Porous Substoichiometric TiO₂ Anodes as Reactive Electrochemical Membranes for Water Treatment. *Environmental Science & Technology*. 2013;47(12):6554-63.
173. A.J. Bard L. R. F. *Electrochemical Methods, Fundamentals and Applications*. second ed: John Wiley & Sons, Inc.: New York, 2001.; 2001.
174. Schnoor M. H., Vecitis C. D. Quantitative Examination of Aqueous Ferrocyanide Oxidation in a Carbon Nanotube Electrochemical Filter: Effects of Flow Rate, Ionic Strength, and Cathode Material. *The Journal of Physical Chemistry C*. 2013;117(6):2855-67.

175. Ambuludi S. L., Panizza M., Oturan N., Özcan A., Oturan M. A. Kinetic behavior of anti-inflammatory drug ibuprofen in aqueous medium during its degradation by electrochemical advanced oxidation. *Environmental Science and Pollution Research*. 2013;20(4):2381-9.
176. Tanaka S., Nakata Y., Kimura T., Yustiawati, Kawasaki M., Kuramitz H. Electrochemical decomposition of bisphenol A using Pt/Ti and SnO₂/Ti anodes. *Journal of Applied Electrochemistry*. 2002;32(2):197-201.
177. Mengoli G., Musiani M. M. Protective coatings on iron by anodic oxidation of phenols in oxalic acid medium. *Electrochimica Acta*. 1986;31(2):201-10.
178. Rodgers J. D., Jedral W., Bunce N. J. Electrochemical Oxidation of Chlorinated Phenols. *Environmental Science & Technology*. 1999;33(9):1453-7.
179. Katsumata H., Kawabe S., Kaneco S., Suzuki T., Ohta K. Degradation of bisphenol A in water by the photo-Fenton reaction. *Journal of Photochemistry and Photobiology A: Chemistry*. 2004;162(2-3):297-305.
180. Ye L., Deng K., Xu F., Tian L., Peng T., Zan L. Increasing visible-light absorption for photocatalysis with black BiOCl. *Physical chemistry chemical physics : PCCP*. 2012;14(1):82-5.
181. Zhong D. K., Gamelin D. R. Photoelectrochemical Water Oxidation by Cobalt Catalyst ("Co-Pi")/ α -Fe₂O₃ Composite Photoanodes: Oxygen Evolution and Resolution of a Kinetic Bottleneck. *Journal of the American Chemical Society*. 2010;132(12):4202-7.
182. Feng Y., Smith D. W., Bolton J. R. Photolysis of aqueous free chlorine species (HOCl and OCl⁻) with 254 nm ultraviolet light. *Journal of Environmental Engineering and Science*. 2007;6(3):277-84.
183. Connick R. E. The Interaction of Hydrogen Peroxide and Hypochlorous Acid in Acidic Solutions Containing Chloride Ion. 1947.
184. Miyamoto S., Martinez G. R., Rettori D., Augusto O., Medeiros M. H., Di Mascio P. Linoleic acid hydroperoxide reacts with hypochlorous acid, generating peroxy radical intermediates and singlet molecular oxygen. *Proceedings of the National Academy of Sciences of the United States of America*. 2006;103(2):293-8.
185. Weiss S. J., Klein R., Slivka A., Wei M. Chlorination of Taurine by Human Neutrophils: EVIDENCE FOR HYPOCHLOROUS ACID GENERATION. *The Journal of Clinical Investigation*. 1982;70(3):598-607.

Appendices

Appendices include supporting data, information and setups images for chapters 3, 4 and 5. Each of the aforementioned chapters has a separate appendix section titled as Appendix A, B or C corresponding to Chapter 3, 4 or 5, respectively. Appendix D shows different images for dead-end electrochemical filtration, crossflow electrochemical filtration, and multiwalled carbon nanotubes different crystalline structure and membrane types.

Appendix A

Appendix A contains supporting information and additional data that further elucidates and confirms the information provided for the electrochemical treatment of Ibuprofen using MWNTs and MWNTs-COOH in neutral and acidic conditions.

In appendix A, additional data are provided around: the surface characterization, stability and purity of MWNTs and MWNTs-COOH including SEM images for MWNTs and MWNTs-COOH after use in treatment (Figure A-1), TGA mass loss plots (Figure A-2), BET plots, cumulative surface area, and pore volume relative to pore width and their differential distribution for both MWNTs types (Figures A-3 and A-4). Superoxide and hypochlorous acid assays with their procedures and explanation (Figures A-5 to A-8). Breakthrough for the treatment of Ibuprofen using MWNTs-COOH containing 7% COOH by weight and the permeate flux for MWNTs and MWNTs-COOH (Figure A-9). Mass spectra for the treatment of Ibuprofen by MWNTs and MWNTs-COOH (Figure A-10). Removal flux values for the treatment of Ibuprofen by MWNTs and MWNTs-COOH from pure electrolytic solutions and synthetic secondary wastewater (Tables A-1 and A-2). Furthermore, the degradation products for electrochemical filtration treatment are listed (Table A-3).

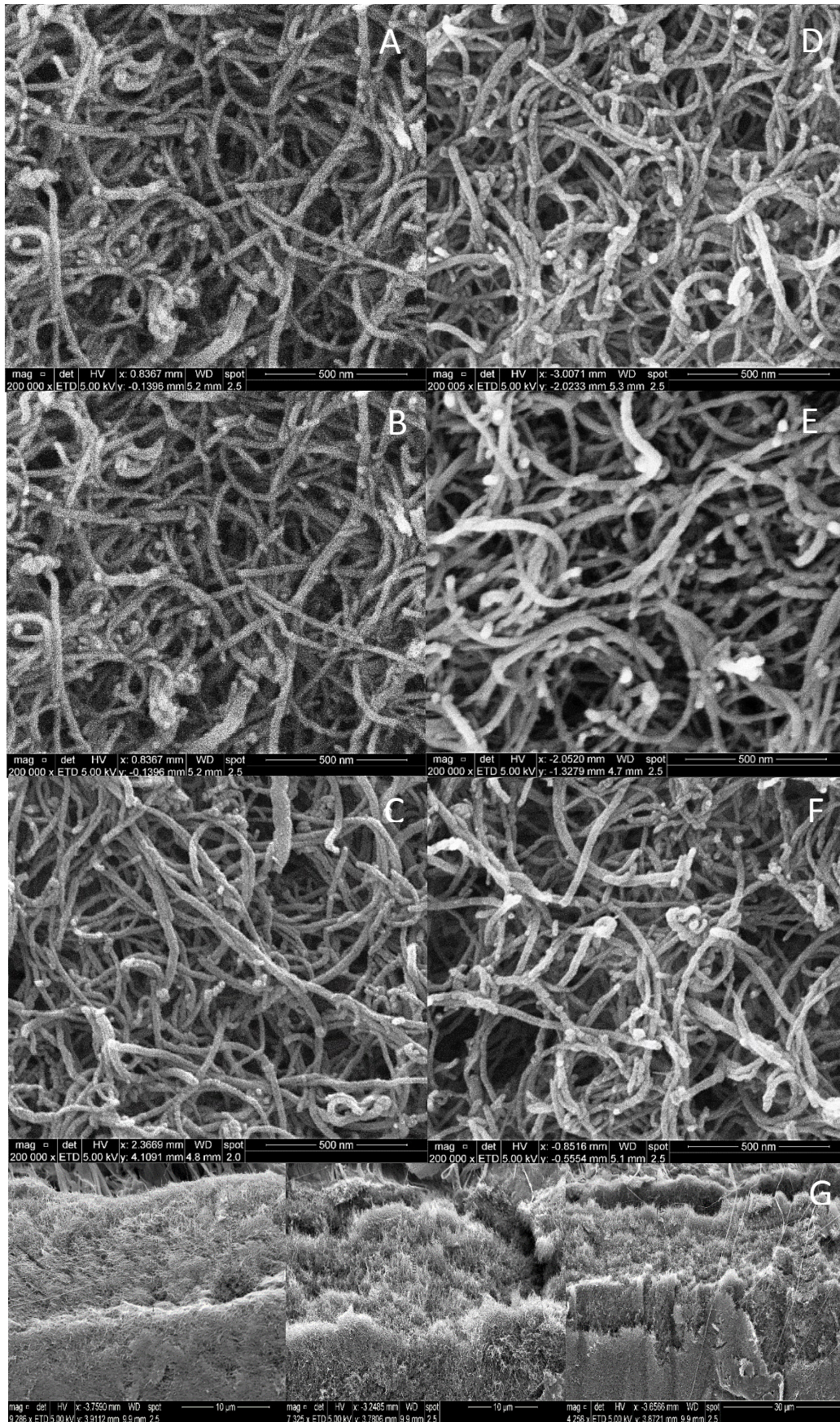


Figure A-1. SEM after subjecting of MWNTs and MWNTs-COOH to 270 mL of 1 mg/L ibuprofen for 135 minutes where (A) is MWNTs under conditions of ibuprofen in 10 mM NaCl, pH 6 and under 0 V of applied potential, (B) is MWNTs under conditions of ibuprofen in 10 mM NaCl, pH 6 and under 2 V of applied potential, (C) is MWNTs under conditions of ibuprofen in 10 mM NaCl, pH 6 and under 3 V of applied potential, (D) is MWNTs-COOH under conditions of ibuprofen in 10 mM HCl, pH 2 and under 0 V of applied potential, (E) is MWNTs-COOH under conditions of ibuprofen in 10 mM HCl, pH 2 and under 2 V of applied potential, (F) is MWNTs-COOH under conditions of ibuprofen in 10 mM HCl, pH 2 and under 03V of applied potential and (G) is lateral thickness (14.2-24 μm taken on different sides of 1 membrane). Surface loading for both MWNTs types was 0.84 mg/cm^2 . Experiments were performed at 23 $^{\circ}\text{C}$.

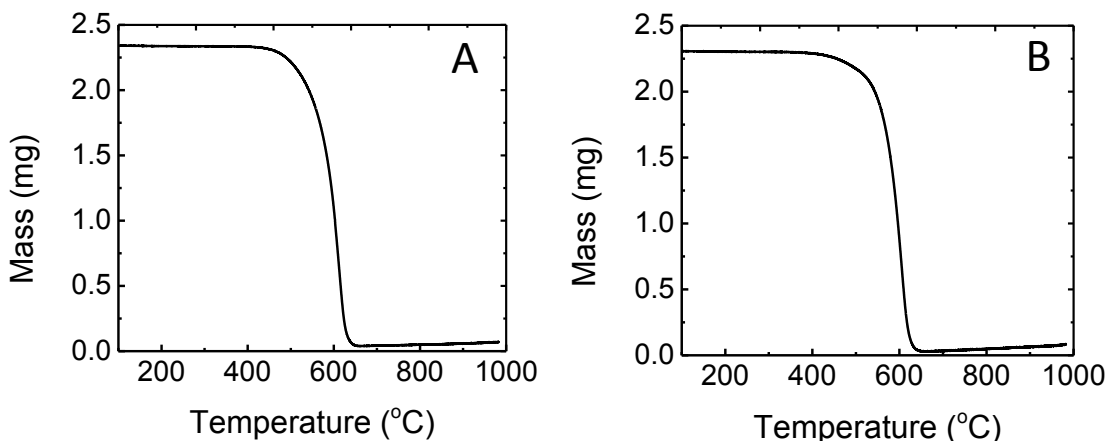


Figure A-2. TGA mass loss plots, (A) MWNTs, (B) MWNTs-COOH

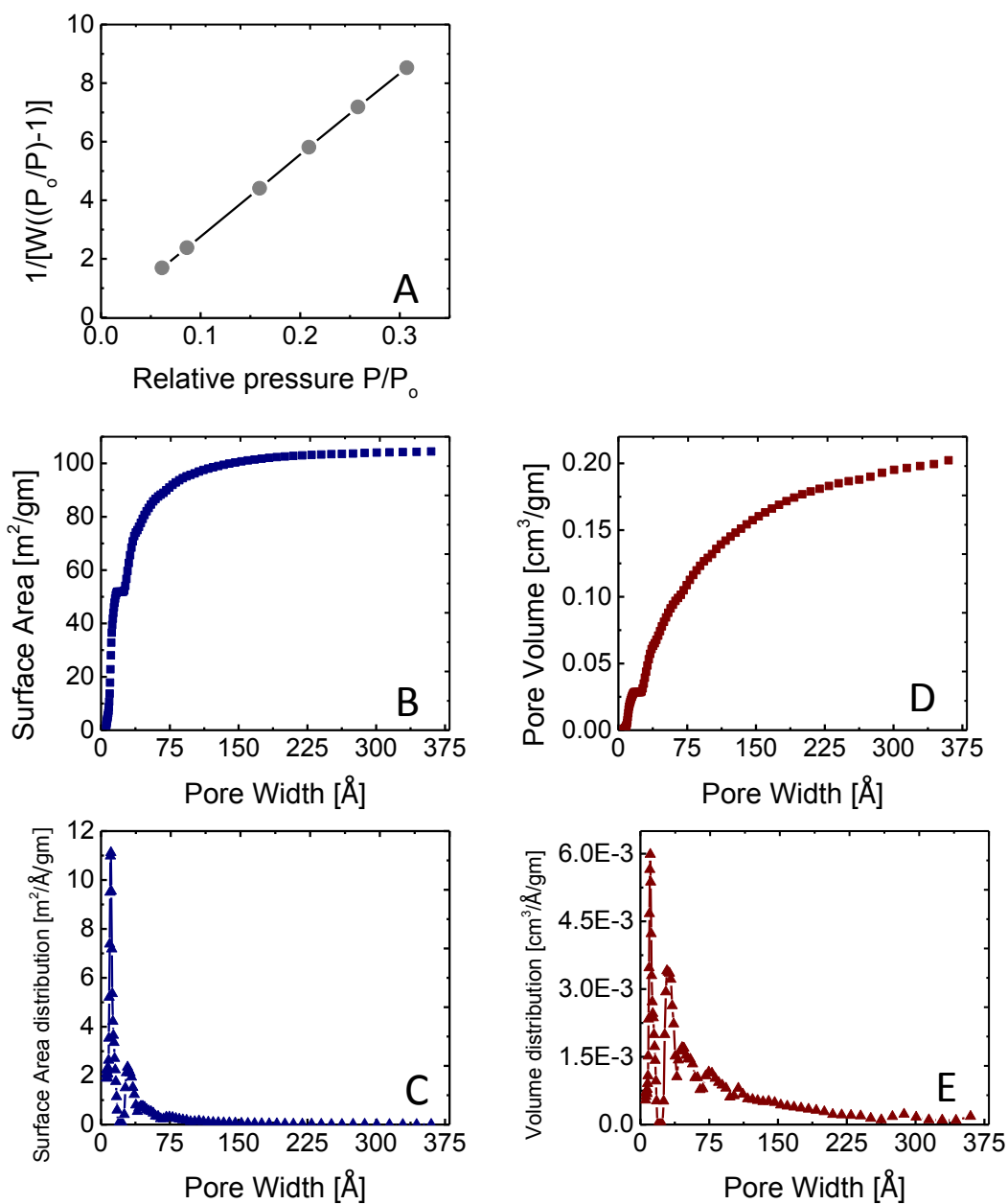


Figure A-3. (A) BET plot for MWNTs, (B) cumulative surface area relative to pore width for MWNTs, (C) differential surface area distribution relative to pore width for MWNTs, (D) cumulative pore volume relative to pore width for MWNTs and (E) differential pore volume distribution relative to pore width for MWNTs.

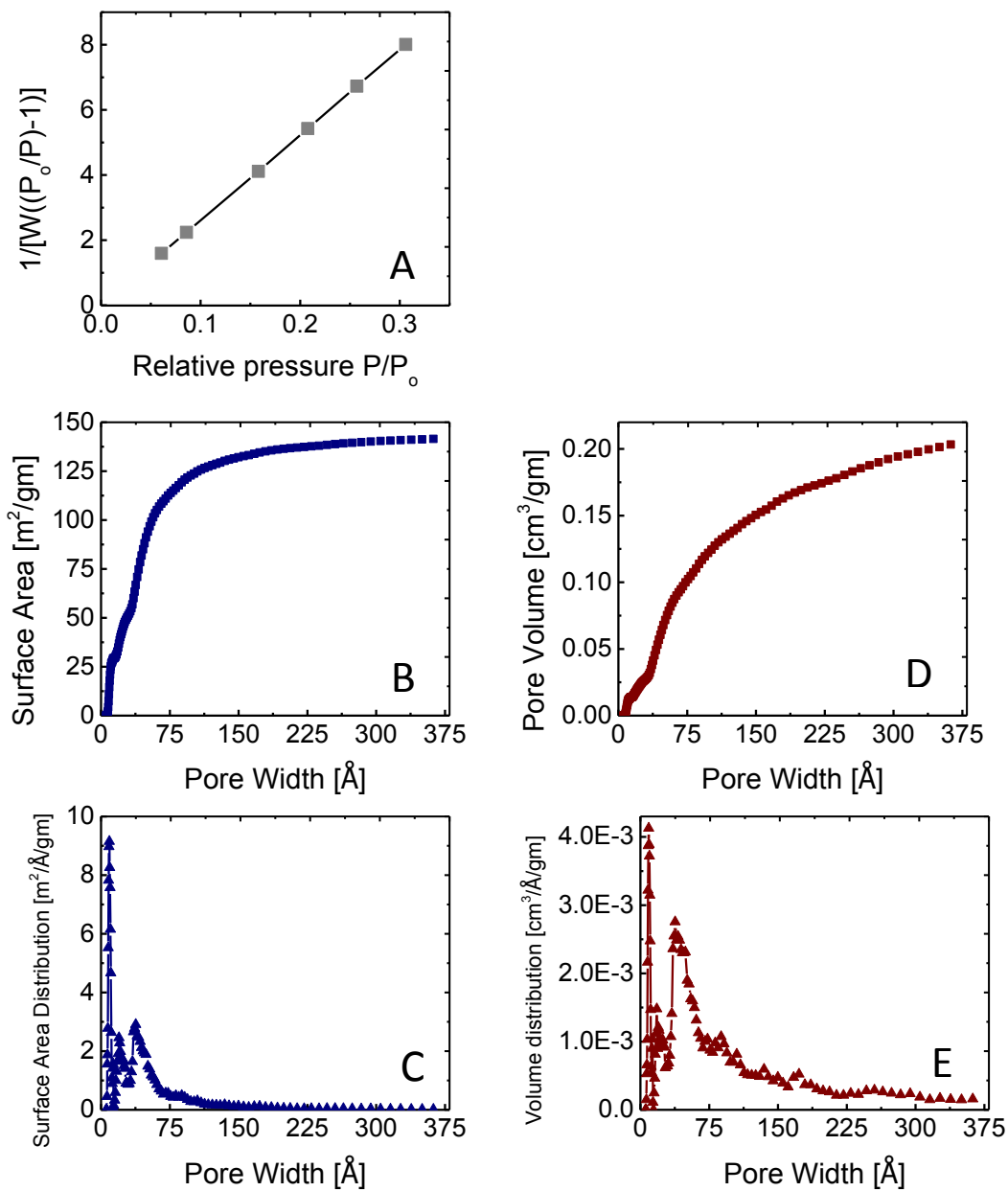


Figure A-4. (A) BET plot for MWNTs-COOH, (B) cumulative surface area relative to pore width for MWNTs-COOH, (C) differential surface area distribution relative to pore width for MWNTs-COOH, (D) cumulative pore volume relative to pore width for MWNTs-COOH and (E) differential pore volume distribution relative to pore width for MWNTs-COOH.

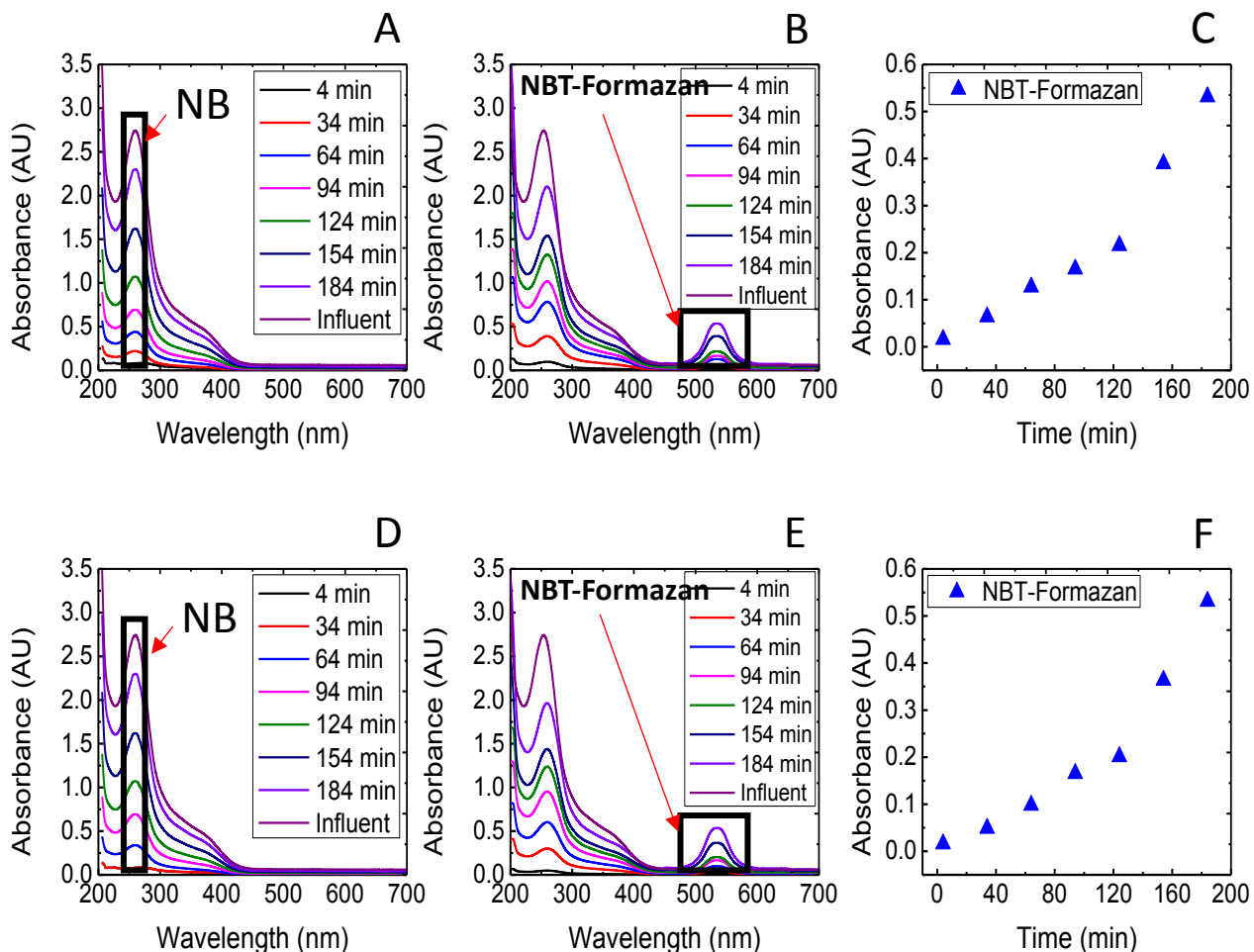


Figure A-5. Superoxide assay, where (A) is absorbance spectra for filtration of NBT at 0 V by MWNTs, (B) is absorbance spectra for electrofiltration of NBT at 2 V by MWNTs, (C) is absorbance with time for the NBT-Formazan (Product of reaction of NBT with superoxide) for electrofiltration of NBT at 2 V by MWNTs, (D) is absorbance spectra for filtration of NBT at 0 V by MWNTs-COOH, (E) is absorbance spectra for electrofiltration of NBT at 2 V by MWNTs-COOH and (F) is absorbance with time for the NBT-Formazan (Product of reaction of NBT with superoxide) for electrofiltration of NBT at 2 V by MWNTs-COOH. When a concentration of 0.05 mM (41 mg/L) NBT in 10 mM NaCl (pH 6) was filtered and electrofiltered by 0.84 mg/cm² MWNTs at 2 V and when a concentration of 0.05 mM (41 mg/L) NBT in 10 mM HCl (pH 2) was filtered and electrofiltered by 0.84 mg/cm² MWNTs-COOH a flow rate of 2 mL/min and temperature of 23°C.

The mechanism of reaction of NBT with superoxide anion is electron saturation of the 2 tetrazolium rings by 4 mole ratio of superoxides, followed by the N-N bond cleavage of the tetrazolium rings. Acceptance of 1 proton by each nitrogen bonded to the nitro-benzene groups then follows (Figure A-6).

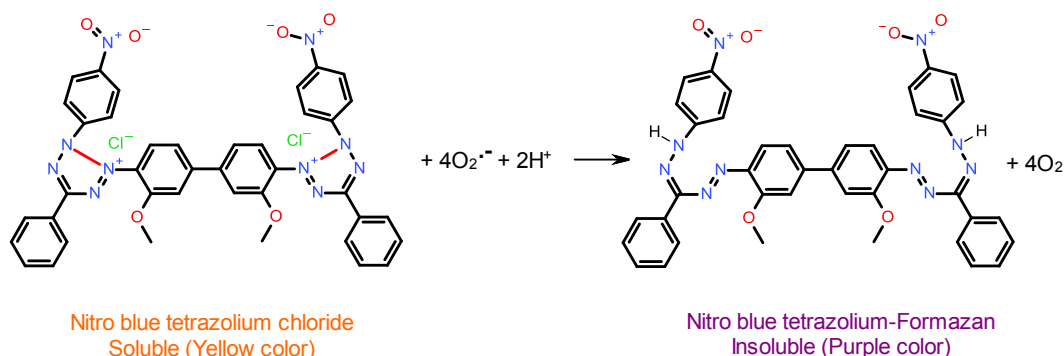


Figure A-6. Reaction mechanism of NBT with superoxide to form NBT-Formazan and diatomic oxygen

Superoxide Assay

This assay was employed for the specific detection of the presence and performance of the Superoxide anion or (Superoxide radical) [120, 121, 180]. In our case, electrofiltration is employed as the experimental technique for removal of emerging contaminants. Our LC-MS results always indicated the presence of ROS (reactive oxygen species) as well as CV results, and which was suspected to participate in the electrodegradation of target molecules. Therefore, it was essential to perform such assay to help observe and understand if superoxide is among the suspected ROS and to obtain experimental confirmation on their contribution. By undertaking this assay, it is now obvious that superoxide anion plays a role in the elimination of organic molecules under applied voltages.

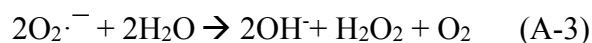
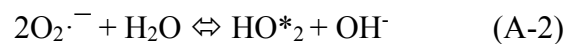
The experimental procedure was simply introducing an “Indicator” to the electrochemical filtration process. This indicator (Nitro blue tetrazolium salt or NBT) has a specific behavior if interacts with superoxide. NBT has a characteristic very pale yellow color with a specific absorbance at the invisible UV wavelength of 259 nm [180], (*) Sigma-Aldrich.

If NBT reacts with superoxide, it will get reduced in an explicit manner, leading to the formation of NBT-Formazan, which has a purple color and a specific visible absorbance at 530 nm (Reaction above). The experiment was performed at the following conditions:

- 0.84 mg/cm² pristine MWNTs and MWNTs-COOH
- 2 ml/min of flow
- 0.05 (~ 41 mg/L) mM NBT in 10 mM NaCl or HCl
- 0 and 2 V of applied DC potential

Results showed that filtration of 0.05 mM NBT at 0 V had an excessive breakthrough effect on the MWNTs filter, the same thing was also observed when the same concentration was introduced at 2V. As well, at 2V another peak showed a breakthrough trend at 486-590 nm and peak at 530 nm, indicating the formation of NBT-Formazan.

The observation of NBT-Formazan in 10 mM HCl (pH2) electrolyte, and despite the fact that stability of superoxide anions decrease in acidic pH, is an indication that formation of superoxide in the first place is independent of the pH conditions and its interaction with the introduced target organic molecule is as fast if not faster than its interaction with water molecules, (Reactions A-1, A-2 and A-3) [53, 106].



In conclusion, the formation of the 530 nm peak that corresponds to the formation of NBT-Formazan, is a strong confirmation of the contribution of superoxide in the removal of organic molecules by electrochemical filtration process.

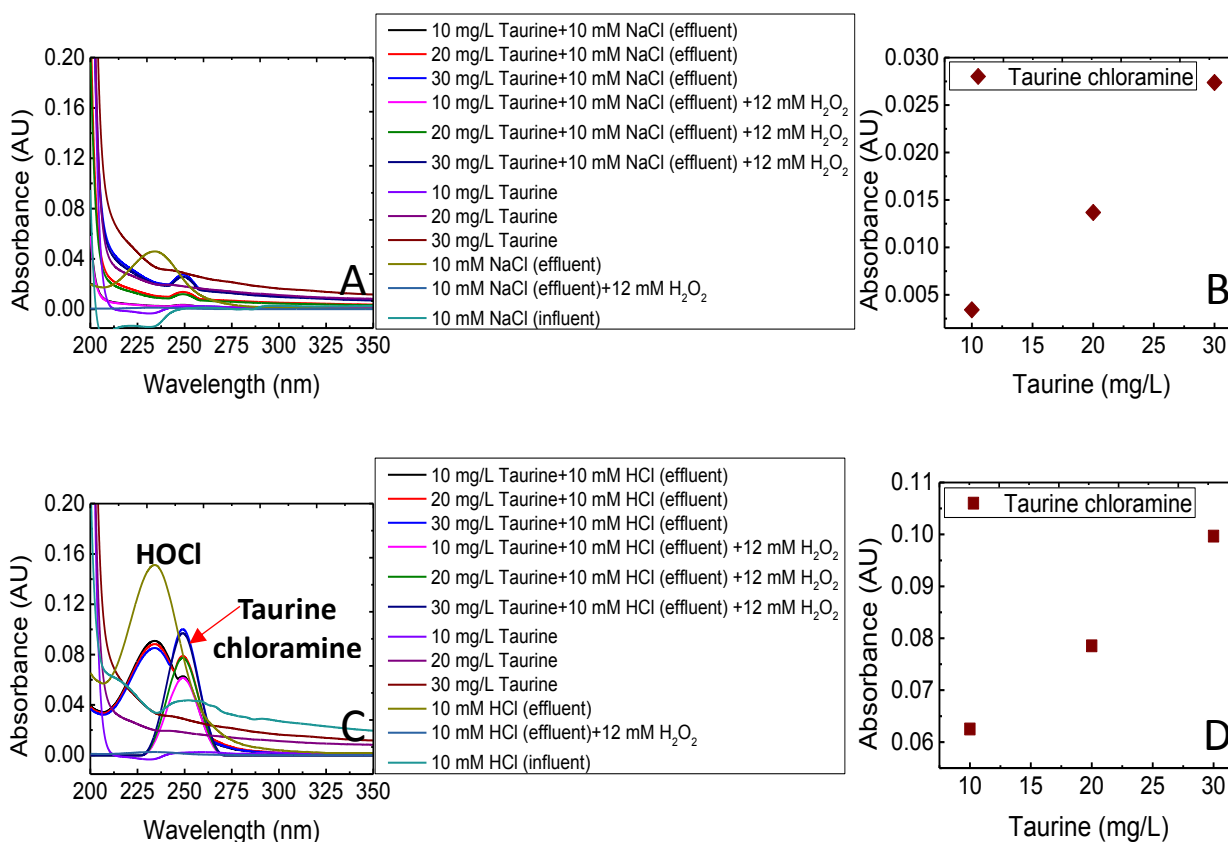


Figure A-7. Hypochlorous acid assay where (A) is UV absorbance spectra for taurine, taurine plus effluent of 10 Mm NaCl with and without addition of 12 mM H₂O₂, influent 10 mM NaCl (pH 6) and effluent of 10 mM NaCl with and without addition of 12 mM H₂O₂, (B) is taurine chloramine absorbance corresponding to 250 nm vs. taurine concentration for 10 mM NaCl (pH 6) assay, where MWNTs was used as electrofiltration membrane. (C) is UV absorbance spectra for taurine, taurine plus effluent of 10 mM HCl with and without addition of 12 mM H₂O₂, influent 10 mM HCl (pH 2) and effluent of 10 mM HCl with and without addition of 12 mM H₂O₂ and (D) is taurine chloramine absorbance corresponding to 250 nm vs. taurine concentration for 10 mM HCl (pH 2) assay, where MWNTs-COOH was used as electrofiltration membrane. MWNTs and MWNTs-COOH filters loading was 0.84 mg/cm², applied voltage was 3 V of DC potential, taurine concentrations were 10, 20 and 30 mg/L, flow rate was 2 mL/min, temperature was 23°C and measurement blank was pure DI water.

Hypochlorous acid Assay

Hypochlorous acid (HOCl) formation comes as a spontaneous step following chloride oxidation to chlorine under an applied positive potential. If HOCl is formed, it can interact with taurine forming taurine chloramine that has a specific UV absorbance at 250 nm (Figure A-8).

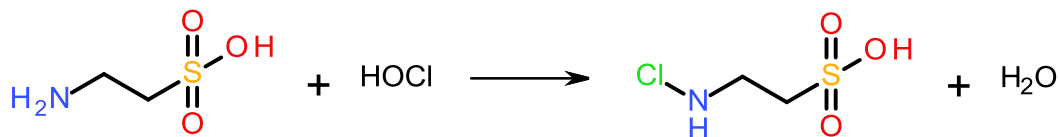
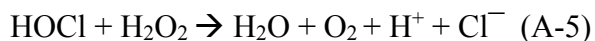


Figure A-8. Reaction of taurine with hypochlorous acid to form taurine monochloramine and water

This assay was done to have a clear vision of whether or not hypochlorous acid formation takes place under our experimental conditions. Figure A-7 is showing a positive assay in both our neutral and acidic conditions as mentioned, with a much lower outcome for the neutral conditions (pH 6) (Figure A-7 A and B). It was obvious to us from the cyclic voltammetry results that chlorine evolution was much more significant for electrofiltration of ibuprofen by MWNTs-COOH in acidic conditions. This observation is built on the knowledge that water oxidation and oxygen evolution is delayed at acidic conditions by delaying the forward reaction (A-4) [181].



The HOCl was observed to have a broad absorbance peak at 235-236 nm [182]. To further qualify that peak, addition of 12 mM H_2O_2 was done which is known to be capable of decomposing of HOCl, reaction (A-5) [183, 184].



The same step was done for taurine added aliquots, and the broad peaks also disappeared. Therefore, it can be deduced that chlorine evolution takes place with better efficiency in acidic conditions and its transformation to HOCl is taking place efficiently as well, the pH in acidic effluents rose from 2 to around 3.2 after electrofiltration at 3 V, most probably due to hydrogen evolution and loss of

protons from the solution, by that allowing a fast kinetics for the transformation of chlorine to hypochlorous acid.

The assay procedure was modified from Weiss et al. [185]. And our procedure was as follow;

- Taurine was used as an oxidation substrate (MW 125.15 g/mole)
- Taurine was first measured by UV taking a spectral scan range from 200-700 nm, no significant spectral peaks could be observed
- A solution of 10, 20 and 30 mg/L taurine was prepared in pure DI
- 10 mM NaCl and 10 mM HCl were electrofiltered at 3V through MWNTs and MWNTs-COOH at a flow of 2 mL/min using the same procedure for electrofiltration of emerging contaminants. 5 min passage of background solution at no voltage, 1 min of passage at applied voltage (Influent background solutions were measured within the same scan range) then aliquot collection
- 1 mL was collected, which was added to 9 mL taurine solutions, mixed, incubated for 5 minutes then 2 mL of the mixed solution was measured at 200-700 nm scan
- After aliquots were measured, 10 μ L of 12 mM H₂O₂ was added, kept for 5 minutes then re- measured.

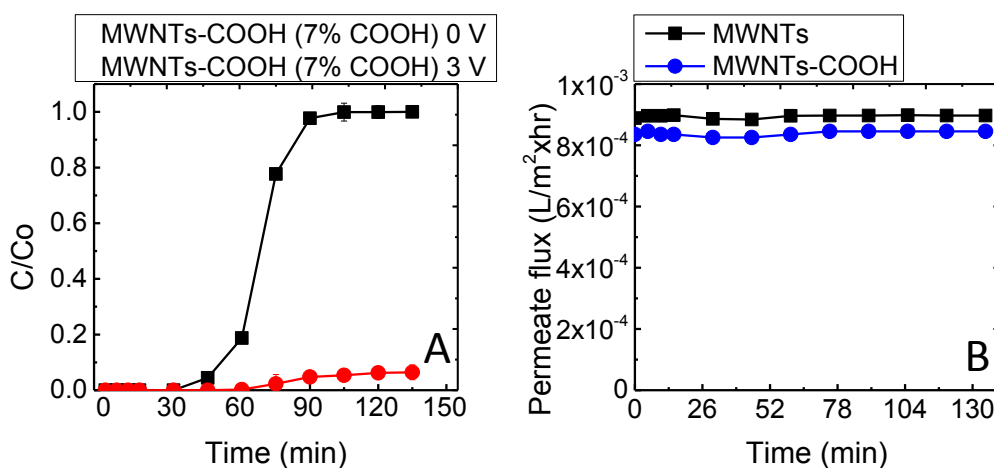


Figure A-9. (A) Breakthrough plot for filtration at 0 V and electrochemical filtration at 3 V of 1 mg/L ibuprofen in 10 mM HCl (pH 2) by 0.84 mg/cm² MWNTs-COOH (7% COOH by weight), at 23°C. (B) Average permeate flux in (L/m².h) for MWNTs and MWNTs-COOH of several runs

at 0 V, flow rate of 2 mL/min and using output aliquots of 2 mL measured using a graduated cylinder of total volume 10 mL \pm 0.1.

| Unit | Removal capacity (q) by MWNTs | Removal capacity (q) by MWNTs-COOH | Δq | |
|-------------------------|-------------------------------|------------------------------------|-----------------------|------------------------------------|
| | | | | Δq $\mu\text{g}/\text{mg}$ |
| 0 V | | | | |
| | | | | Δq $\mu\text{g}/\text{mg}$ |
| mg/mg | 0.013 | 0.014 | 1.00×10^{-3} | 2 |
| g/m^2 | 1.02×10^{-4} | 1.07×10^{-4} | 5.00×10^{-6} | |
| moles/g | 6.18×10^{-5} | 6.91×10^{-5} | 7.30×10^{-6} | |
| molecules/g | 3.72×10^{19} | 4.16×10^{19} | 4.40×10^{18} | |
| molecules/ m^2 | 2.98×10^{17} | 3.13×10^{17} | 1.50×10^{16} | |
| 1 V | | | | |
| | | | | Δq $\mu\text{g}/\text{mg}$ |
| mg/mg | 0.014 | 0.015 | 1.00×10^{-3} | 1 |
| g/m^2 | 1.14×10^{-4} | 1.15×10^{-4} | 1.00×10^{-6} | |
| moles/g | 6.92×10^{-5} | 7.40×10^{-5} | 4.80×10^{-6} | |
| molecules/g | 4.17×10^{19} | 4.45×10^{19} | 2.80×10^{18} | |
| molecules/ m^2 | 3.33×10^{17} | 3.35×10^{17} | 2.00×10^{15} | |
| 2 V | | | | |
| | | | | Δq $\mu\text{g}/\text{mg}$ |
| mg/mg | 0.030 | 0.033 | 3.00×10^{-3} | 3 |
| g/m^2 | 2.37×10^{-4} | 2.45×10^{-4} | 8.00×10^{-6} | |
| moles/g | 1.44×10^{-4} | 1.58×10^{-4} | 1.40×10^{-5} | |
| molecules/g | 8.65×10^{19} | 9.51×10^{19} | 8.60×10^{18} | |
| molecules/ m^2 | 6.92×10^{17} | 7.15×10^{17} | 2.30×10^{16} | |

| | 3 V | | | Δq $\mu\text{g}/\text{mg}$ |
|-------------------------|-----------------------|-----------------------|-----------------------|------------------------------------|
| | | | | |
| mg/mg | 0.030 | 0.033 | 3.00×10^{-3} | 3 |
| g/m^2 | 2.41×10^{-4} | 2.47×10^{-4} | 6.00×10^{-6} | |
| moles/g | 1.46×10^{-4} | 1.60×10^{-4} | 1.40×10^{-5} | |
| molecules/g | 8.81×10^{19} | 9.58×10^{19} | 7.70×10^{18} | |
| molecules/ m^2 | 7.05×10^{17} | 7.20×10^{17} | 1.50×10^{16} | |

Table A-1. Adsorption and removal capacities of ibuprofen from 10 mM NaCl (pH 6) by MWNTs and 10 mM HCl (pH 2) by MWNTs-COOH, corresponding to Figure 3-6 A. The removal capacity values were calculated cumulatively corresponding to the total amount removed at an applied voltage.

| Unit | Removal capacity (q) by MWNTs | Removal capacity (q) by MWNTs-COOH |
|-------------------------|-------------------------------------|--|
| | 0 V | |
| mg/mg | 4.4×10^{-3} | 4.0×10^{-3} |
| g/m^2 | 3.51×10^{-5} | 2.98×10^{-5} |
| moles/g | 2.13×10^{-5} | 1.92×10^{-5} |
| molecules/g | 1.28×10^{19} | 1.16×10^{19} |
| molecules/ m^2 | 1.02×10^{17} | 9.25×10^{16} |
| 1 V | | |
| mg/mg | 5.6×10^{-3} | 5.0×10^{-3} |
| g/m^2 | 4.21×10^{-5} | 3.76×10^{-5} |
| moles/g | 2.55×10^{-5} | 2.42×10^{-5} |
| molecules/g | 1.54×10^{19} | 1.46×10^{19} |
| molecules/ m^2 | 1.23×10^{17} | 1.10×10^{17} |
| 2 V | | |
| mg/mg | 0.0295 | 0.0302 |
| g/m^2 | 2.4×10^{-4} | 2.3×10^{-4} |
| moles/g | 1.43×10^{-4} | 1.46×10^{-4} |
| molecules/g | 8.60×10^{19} | 8.81×10^{19} |
| molecules/ m^2 | 6.88×10^{17} | 6.62×10^{17} |
| 3 V | | |
| mg/mg | 0.0308 | 0.0313 |
| g/m^2 | 2.5×10^{-4} | 2.4×10^{-4} |
| moles/g | 1.5×10^{-4} | 1.5×10^{-4} |
| molecules/g | 8.99×10^{19} | 9.12×10^{19} |

| | | |
|--------------------------|------------------------|------------------------|
| molecules/m ² | 7.19 x10 ¹⁷ | 6.86 x10 ¹⁷ |
|--------------------------|------------------------|------------------------|

Table A-2. Adsorption and removal capacities of ibuprofen from synthetic secondary wastewater effluent (pH 7.3) by MWNTs and MWNTs-COOH corresponding to Figure 3-6 B. The removal capacity values were calculated cumulatively corresponding to the total amount removed at an applied voltage.

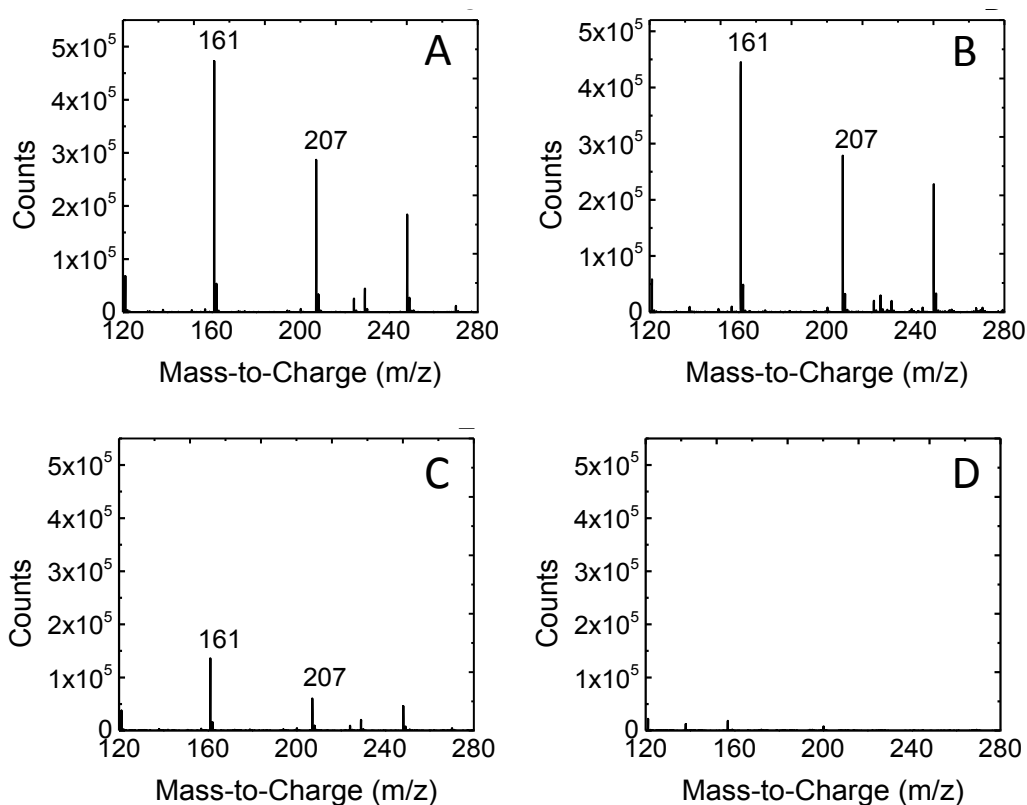
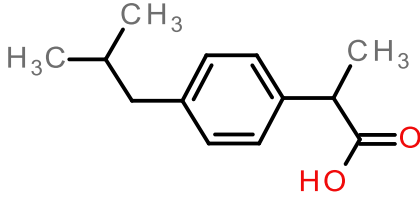
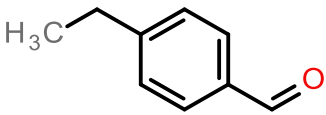
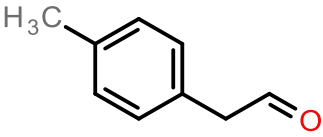
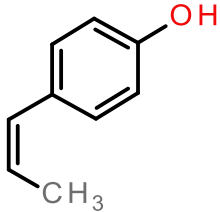
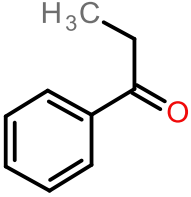
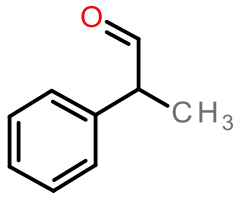
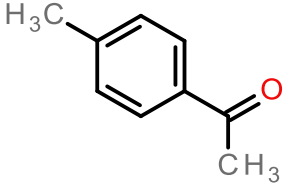
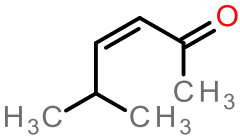
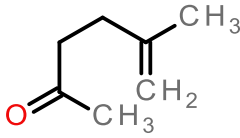
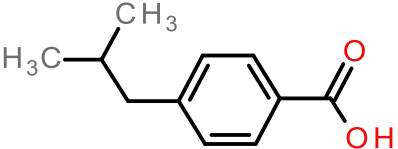
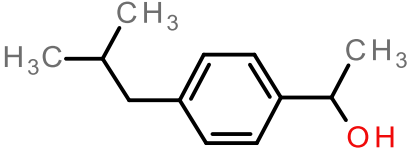


Figure A-10. (A) Mass spectra of ibuprofen in 10 mM NaCl (pH 6) at RT 6.8 min before treatment and (B) Mass spectra for ibuprofen in 10 mM HCl (pH 2) at RT 6.8 min before treatment. (C) After treatment with MWNTs at a 3 V DC potential and (D) after treatment with MWNTs-COOH at a 3 V DC potential. The ibuprofen concentration was 20 mg/L, MWNTs and MWNTs-COOH surface loading was 0.32 mg/cm², and the temperature was 40 °C.

Figure A-10 shows the MS spectra of ibuprofen at RT 6.8 minutes before and after treatment at 3 V and 40 °C with MWNTs and MWNTs-COOH under neutral and acidic conditions. It is obvious that the total removal of the ibuprofen spectral peak and its fragments at 207 and 161 *m/z* could be achieved only after treatment under acidic conditions with MWNTs-COOH (B and D). In contrast, ibuprofen and its fragments can still be observed in the case of treatment under neutral conditions with MWNTs (A and C).

| m/z | Molecular name | Molecular formula | Structural formula |
|-----|---|--|---|
| 207 | (2-[4-(2-Methylpropyl)phenyl]propanoic acid) “ibuprofen” | C ₁₃ H ₁₈ O ₂ |  |
| 135 | 4-Ethylbenzaldehyde | C ₉ H ₁₀ O |  |
| 135 | (4-Methylphenyl) acetaldehyde | C ₉ H ₁₀ O |  |
| 135 | (Z)-4-(1-Propenyl) phenol | C ₉ H ₁₀ O |  |
| 135 | 1-Phenyl-1-propanone | C ₉ H ₁₀ O |  |

| | | | |
|-----|--------------------------------|-------------------|--|
| 135 | 2-Phenylpropanal | $C_9H_{10}O$ |  |
| 135 | 4'-Methylacetophenone | $C_9H_{10}O$ |  |
| 135 | 5-Methyl-3-hexen-2-one | $C_7H_{12}O$ |  |
| 135 | 5-Methyl-5-hexen-2-one | $C_7H_{12}O$ |  |
| 177 | 4-Isobutylbenzoic acid | $C_{11}H_{14}O_2$ |  |
| 177 | 1-(4-Isobutylphenyl)-1-ethanol | $C_{12}H_{18}O$ |  |

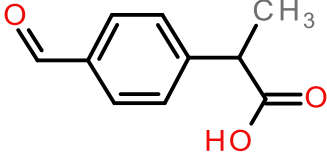
| | | | |
|-----|----------------------------------|-------------------|--|
| 177 | 2-(4-Formylphenyl)propanoic acid | $C_{10}H_{10}O_3$ |  |
|-----|----------------------------------|-------------------|--|

Table A-3. Possible degradation by-products of ibuprofen from electrochemical filtration.

Appendix B

Appendix B contains supporting information and additional data that further elucidate and confirm the information provided for the electrochemical treatment of Bisphenol A using MWNTs and BMWNTs in various conditions.

In appendix B, additional data are provided around the surface characterization of MWNTs and BMWNTs including SEM x-sectional images for MWNTs and BMWNTs, EDX after use in treatment (Figure B-1 to B-3), TGA mass loss plots (Figure B-4). BET plots, cumulative surface area and pore volume relative to pore width and their differential distribution for both MWNTs types (Figures B-5 and B-6). Breakthrough plots for the removal of Bisphenol A from synthetic secondary wastewater using MWNTs and BMWNTs (Figure B-7). Removal capacity values from in all stated conditions (Table B-1 to B-3). Removal flux values corresponding to breakthrough for the salting out effect section (Figure B-8) and removal flux values from synthetic secondary wastewater (Figure B-9). Permeate flux values for both MWNTs types (Figure B-10). Energy consumption values in KWh/Kg for the salting out effect section (Figure B-11). Superoxide and hydrogen peroxide assays with their procedures and explanation (Figures B-13, B-14 and B-16). LC-MS chromatograms and mass spectra for different detected products corresponding to various applied conditions (Figure B-17 to B-29). And Bisphenol A degradation pathways at applied slow residence time (Figure B-30).

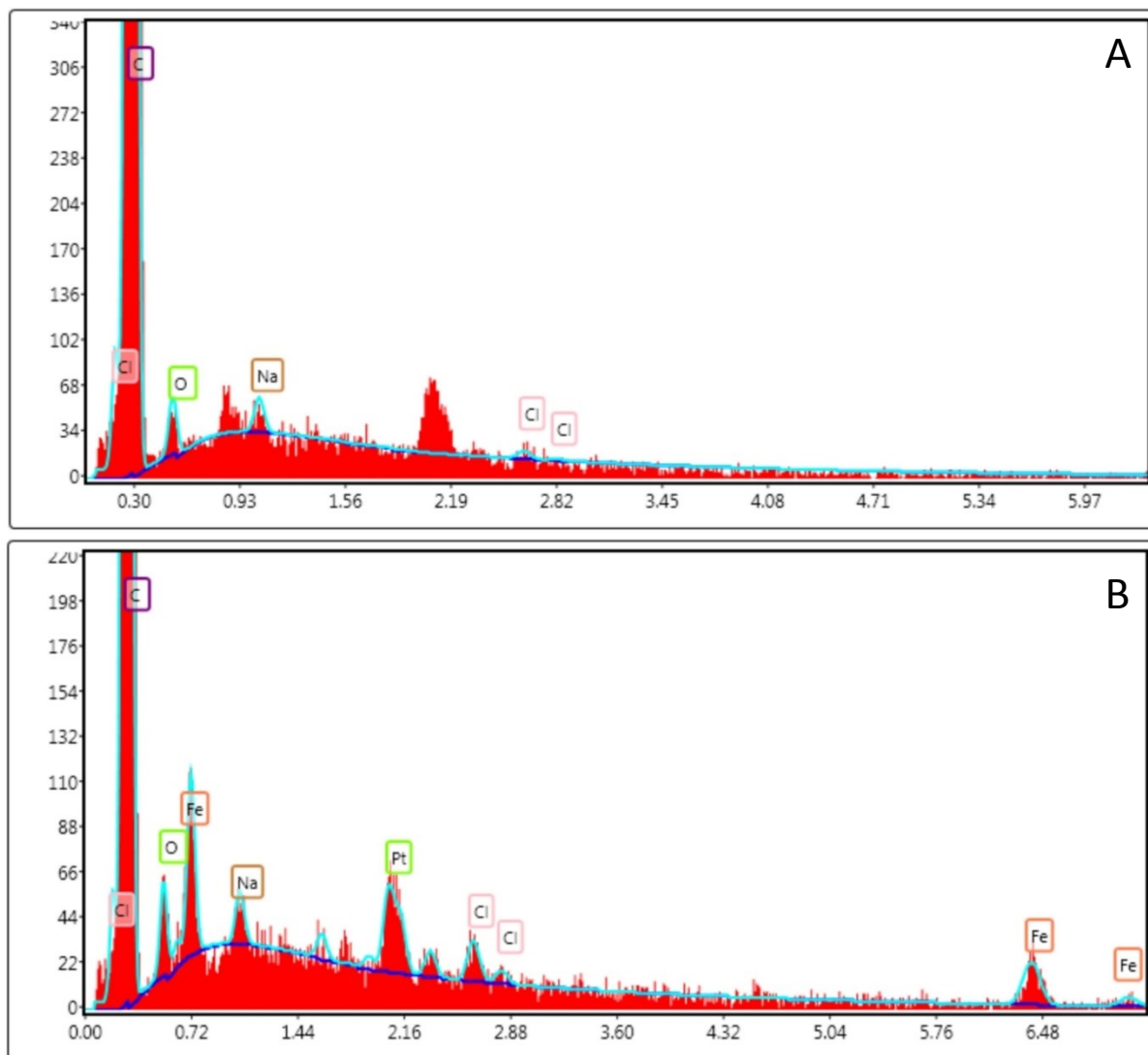


Figure B-1. (A) EDX (Zoom view) for MWNTs, (B) EDX (Zoom view) for BMWNTs. Showing the presence of iron (Fe) in BMWNTs (7%) at the surface which can be responsible for the formation of oxide layers when subjected to TGA analysis. The loading for both MWNTs and BMWNTs was 1.04 mg/cm^2 and the surface of the filters were analyzed before use in treatment. No boron could be detected at the surface of the BMWNT filter indicating that boron atoms are embedded within the sp^2 carbon lattice.

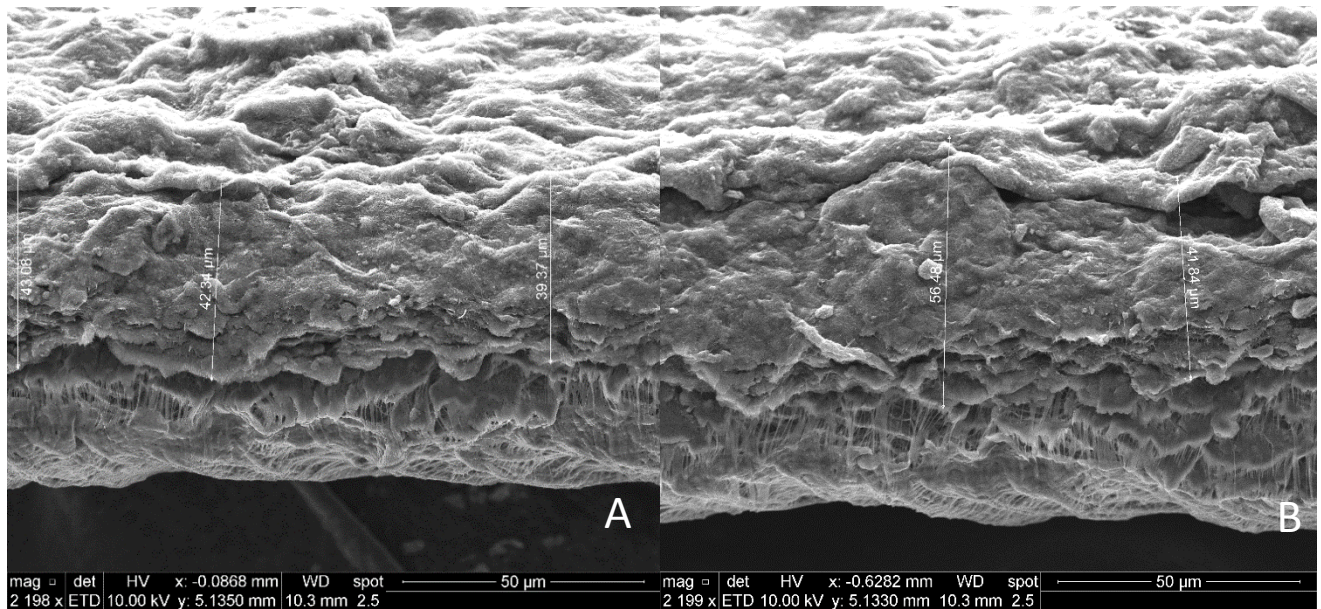


Figure B-2. (A) Thickness (lateral view) for 1.04 mg/cm² MWNT filter ranging from 39.47 – 43.08 μm and (B) Thickness (lateral view) for 1.04 mg/cm² BMWNT filter ranging from 41.84 – 56.48 μm. The loading for both the MWNT and BMWNT filters was 1.04 mg/cm². The filters were prepared at room temperature using the same procedure as previously reported and the surface of each filter was analyzed before use in treatment [114].

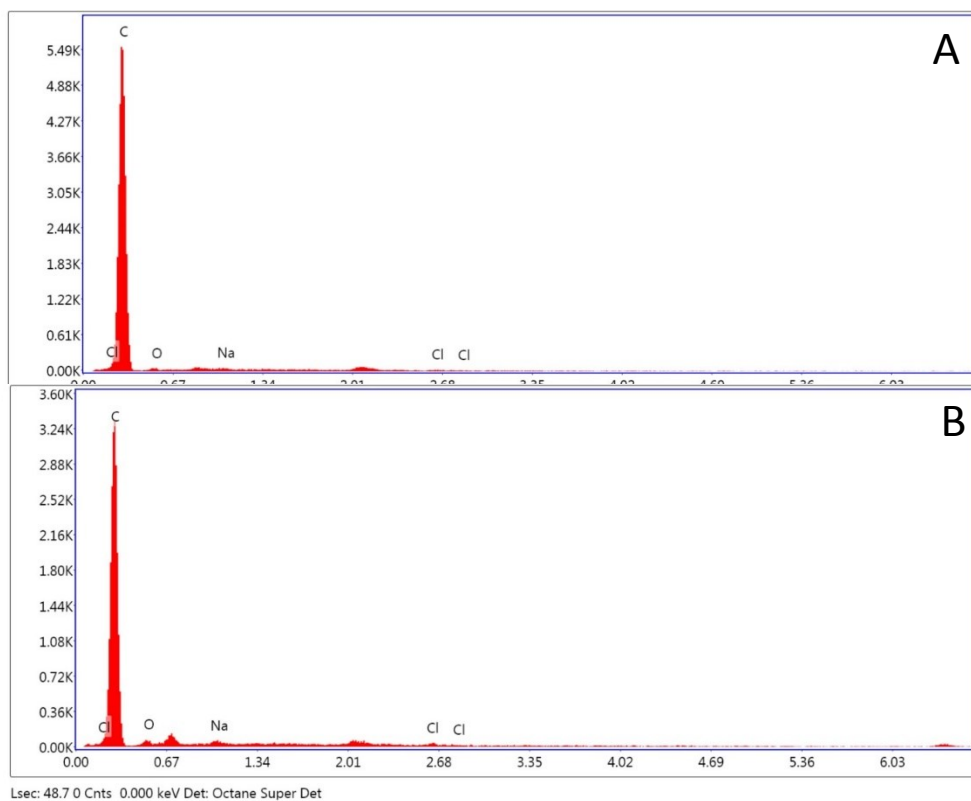


Figure B-3. (A) EDX for MWNTs and (B) EDX for BMWNTs after the filtration of 1 mg/L BPA in 10 mM NaCl (pH 6) using 3 V of applied DC potential and a flow rate of 2 mL/min for 106 minutes. The filters were prepared at room temperature using the same procedure as previously reported and the surface loading for both the MWNTs and BMWNTs was 1.04 mg/cm² [114].

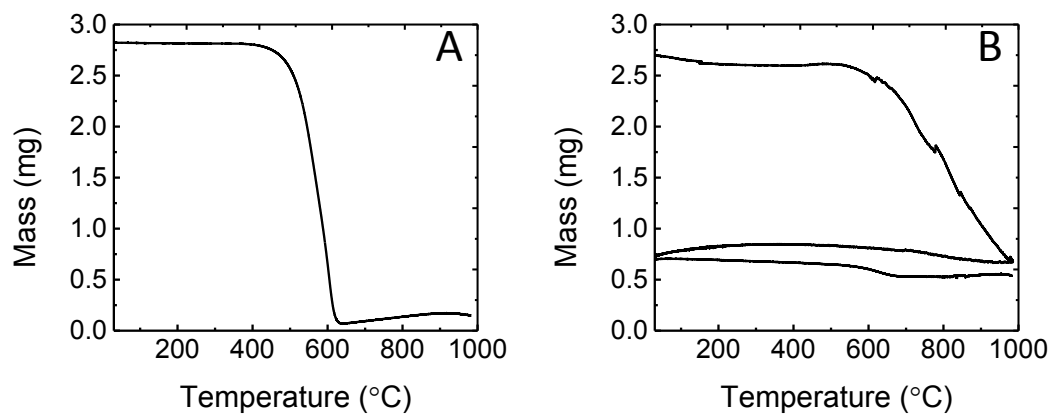


Figure B-4. TGA analysis for MWNTs and BMWNTs where (A) is TGA mass change vs. temperature for MWNTs and (B) is TGA mass change vs. temperature for BMWNTs. The surface loading for both the MWNTs and BMWNTs was 1.04 mg/cm².

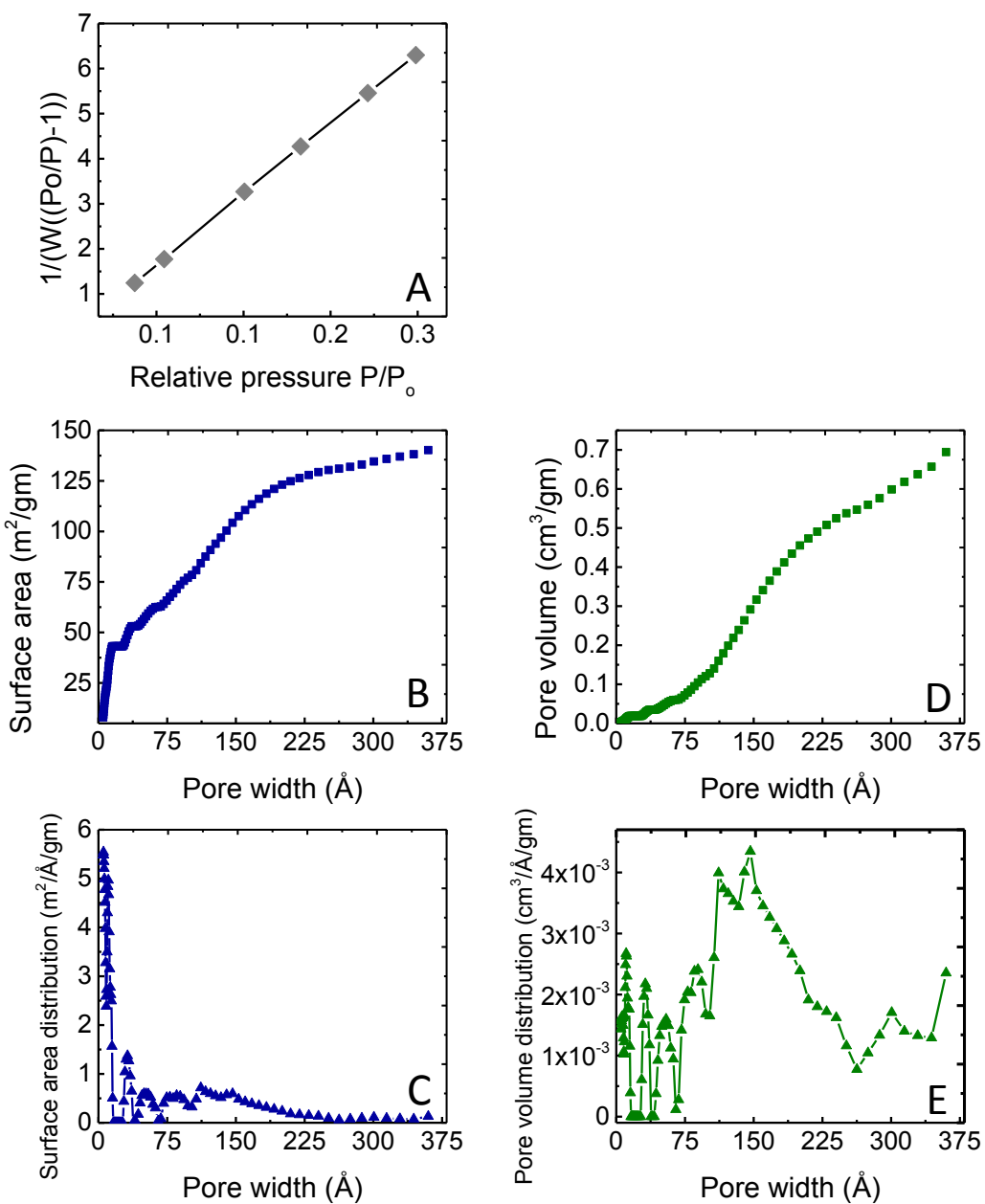


Figure B-5. (A) BET plot, (B) cumulative surface area relative to pore width (C) differential surface area distribution relative to pore width, (D) cumulative pore volume relative to pore width and (E) differential pore volume distribution relative to pore width, for MWNTs.

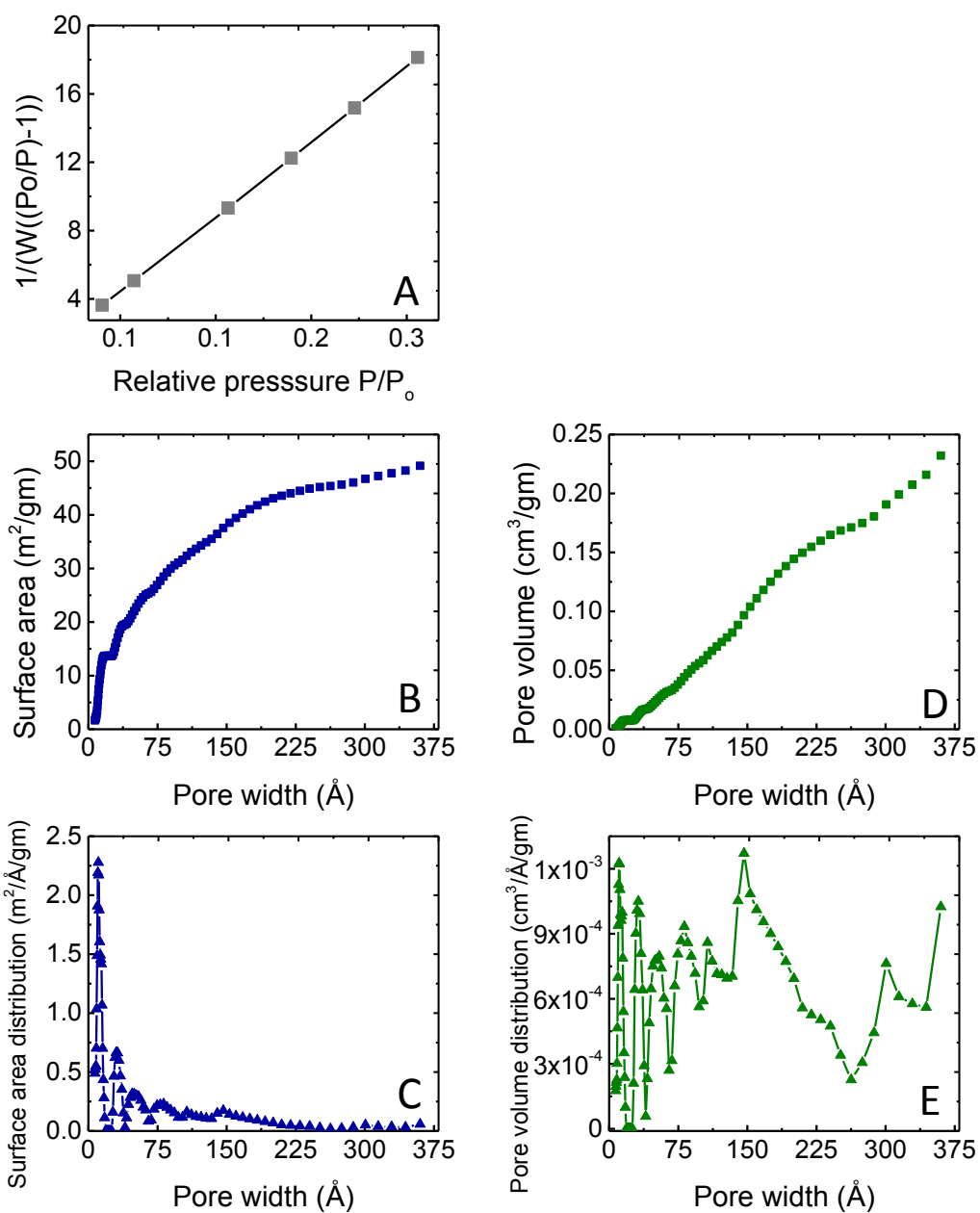


Figure B-6. (A) BET plot, (B) cumulative surface area relative to pore width and (C) differential surface area distribution relative to pore width, (D) cumulative pore volume relative to pore width and (E) differential pore volume distribution relative to pore width, for BMWNTs.

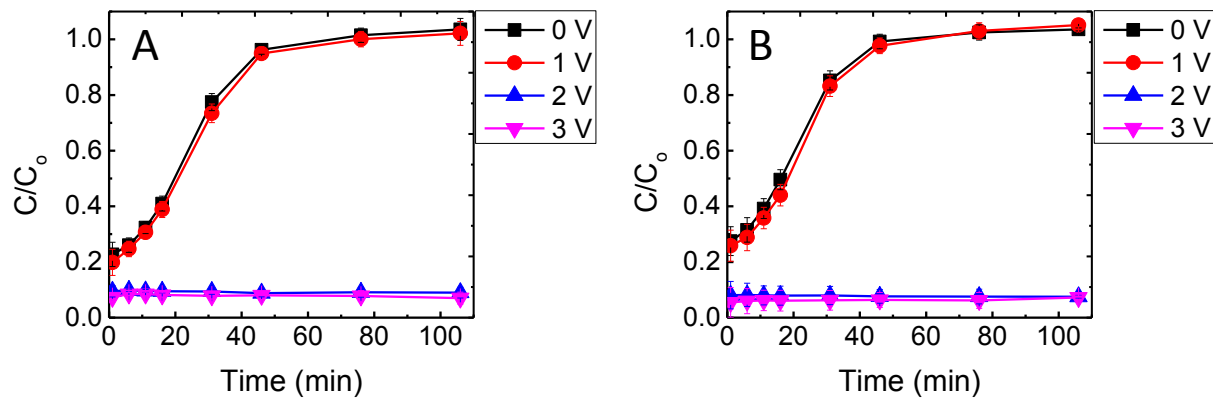


Figure B-7. Breakthrough plots for 1 mg/L bisphenol A in synthetic secondary effluent of the same composition as previously reported [114] and at pH (7.3-7.4) for both filter types overtime, at 0, 1, 2 and 3 V of applied DC voltage, where (A) is breakthrough plots by MWNTs and (B) by BMWNTs. Experiments performed at room temperature using a flow rate of 2 mL/min and the loading for both MWNTs and BWMNTs was 1.04 mg/cm².

| NaCl (mM) | Applied voltage (V) | q Units | By MWNT |
|-----------|---------------------|-----------------------|-----------------------|
| 1 | 0 | mg/mg | 0.006358 |
| | | g/m ² | 3.83x10 ⁻⁵ |
| | | moles/g | 2.79x10 ⁻⁵ |
| | | Molec./g | 1.68x10 ¹⁹ |
| | | Molec./m ² | 1.01x10 ¹⁷ |
| 1 | 1 | q Units | MWNT |
| | | mg/mg | 0.006901 |
| | | g/m ² | 4.16x10 ⁻⁵ |
| | | moles/g | 3.02x10 ⁻⁵ |
| | | Molec./g | 1.82x10 ¹⁹ |
| 1 | 2 | q Units | MWNT |
| | | mg/mg | 0.01713 |
| | | g/m ² | 0.000103 |
| | | moles/g | 7.5x10 ⁻⁵ |
| | | Molec./g | 4.52x10 ¹⁹ |
| 2 | 0 | q Units | MWNT |
| | | mg/mg | 0.006657 |
| | | g/m ² | 4.01x10 ⁻⁵ |
| | | moles/g | 2.92x10 ⁻⁵ |
| | | Molec./g | 1.76x10 ¹⁹ |
| 2 | 0 | Molec./m ² | 1.06x10 ¹⁷ |

| | | | |
|----|---|-----------------------|-----------------------|
| 2 | 1 | q Units | MWNT |
| | | mg/mg | 0.007039 |
| | | g/m ² | 4.24x10 ⁻⁵ |
| | | moles/g | 3.08x10 ⁻⁵ |
| | | Molec./g | 1.86x10 ¹⁹ |
| | | Molec./m ² | 1.12x10 ¹⁷ |
| 2 | 2 | q Units | MWNT |
| | | mg/mg | 0.019435 |
| | | g/m ² | 0.000117 |
| | | moles/g | 8.51x10 ⁻⁵ |
| | | Molec./g | 5.13x10 ¹⁹ |
| | | Molec./m ² | 3.09x10 ¹⁷ |
| 10 | 0 | q Units | MWNT |
| | | mg/mg | 0.006197 |
| | | g/m ² | 3.73x10 ⁻⁵ |
| | | moles/g | 2.71x10 ⁻⁵ |
| | | Molec./g | 1.63x10 ¹⁹ |
| | | Molec./m ² | 9.85x10 ¹⁶ |
| 10 | 1 | q Units | MWNT |
| | | mg/mg | 0.0067 |
| | | g/m ² | 4.04x10 ⁻⁵ |
| | | moles/g | 2.93x10 ⁻⁵ |
| | | Molec./g | 1.77x10 ¹⁹ |
| | | Molec./m ² | 1.06x10 ¹⁷ |
| 10 | 2 | q Units | MWNT |
| | | mg/mg | 0.017793 |
| | | g/m ² | 0.000107 |
| | | moles/g | 7.79x10 ⁻⁵ |
| | | Molec./g | 4.69x10 ¹⁹ |
| | | Molec./m ² | 2.83x10 ¹⁷ |

| | | | |
|-----|---|-----------------------|-----------------------|
| 50 | 0 | q Units | MWNT |
| | | mg/mg | 0.00595 |
| | | g/m ² | 3.58x10 ⁻⁵ |
| | | moles/g | 2.61x10 ⁻⁵ |
| | | Molec./g | 1.57x10 ¹⁹ |
| | | Molec./m ² | 9.46x10 ¹⁶ |
| 50 | 1 | q Units | MWNT |
| | | mg/mg | 0.006874 |
| | | g/m ² | 4.14x10 ⁻⁵ |
| | | moles/g | 3.01x10 ⁻⁵ |
| | | Molec./g | 1.81x10 ¹⁹ |
| | | Molec./m ² | 1.09x10 ¹⁷ |
| 50 | 2 | q Units | MWNT |
| | | mg/mg | 0.017146 |
| | | g/m ² | 0.000103 |
| | | moles/g | 7.51x10 ⁻⁵ |
| | | Molec./g | 4.52x10 ¹⁹ |
| | | Molec./m ² | 2.73x10 ¹⁷ |
| 100 | 0 | q Units | MWNT |
| | | mg/mg | 0.006243 |
| | | g/m ² | 3.76x10 ⁻⁵ |
| | | moles/g | 2.73x10 ⁻⁵ |
| | | Molec./g | 1.65x10 ¹⁹ |
| | | Molec./m ² | 9.92x10 ¹⁶ |
| 100 | 1 | q Units | MWNT |
| | | mg/mg | 0.007383 |
| | | g/m ² | 4.45x10 ⁻⁵ |
| | | moles/g | 3.23x10 ⁻⁵ |
| | | Molec./g | 1.95x10 ¹⁹ |
| | | Molec./m ² | 1.17x10 ¹⁷ |

| | | | |
|-----|---|-----------------------|-----------------------|
| 100 | 2 | q Units | MWNT |
| | | mg/mg | 0.017465 |
| | | g/m ² | 0.000105 |
| | | moles/g | 7.65x10 ⁻⁵ |
| | | Molec./g | 4.61x10 ¹⁹ |
| | | Molec./m ² | 2.78x10 ¹⁷ |

Table B-1. Adsorption and removal capacities of 1 mg/L bisphenol A from 1, 2, 10, 50 and 100 mM NaCl (pH 6) by MWNT filtration, corresponding to Figure 4-2 A. The removal capacity values were calculated cumulatively corresponding to the total amount removed at the given voltage.

| | | | | |
|---|------------------------|-----------------------|-----------------------|-----------------------|
| pH | Applied voltage (V) | q Units | MWNT | BMWNT |
| NaCl (pH6) | 0 | mg/mg | 0.006202 | 0.005966 |
| | | g/m ² | 3.74x10 ⁻⁵ | 0.0001 |
| | | moles/g | 2.72x10 ⁻⁵ | 2.61x10 ⁻⁵ |
| | | Molec./g | 1.64x10 ¹⁹ | 1.57x10 ¹⁹ |
| | | Molec./m ² | 9.86x10 ¹⁶ | 2.64x10 ¹⁷ |
| pH | Applied voltage (V) | q Units | MWNT | BMWNT |
| NaCl (pH6) | 3 | mg/mg | 0.017882 | 0.020048 |
| | | g/m ² | 0.000108 | 0.000337 |
| | | moles/g | 7.83x10 ⁻⁵ | 8.78x10 ⁻⁵ |
| | | Molec./g | 4.72x10 ¹⁹ | 5.29x10 ¹⁹ |
| | | Molec./m ² | 2.84x10 ¹⁷ | 8.89x10 ¹⁷ |
| pH | Applied voltage (V) | q Units | MWNT | BMWNT |
| H ₂ SO ₄ (pH3) | 0 | mg/mg | 0.00638 | 0.006565 |
| | | g/m ² | 3.84x10 ⁻⁵ | 0.00011 |
| | | moles/g | 2.79x10 ⁻⁵ | 2.88x10 ⁻⁵ |
| | | Molec./g | 1.68x10 ¹⁹ | 1.73x10 ¹⁹ |
| | | Molec./m ² | 1.01x10 ¹⁷ | 2.91x10 ¹⁷ |
| pH | Applied voltage (V) | q Units | MWNT | BMWNT |
| H ₂ SO ₄ (pH3) | 3 | mg/mg | 0.01813 | 0.018553 |
| | | g/m ² | 0.000109 | 0.000312 |
| | | moles/g | 7.94x10 ⁻⁵ | 8.13x10 ⁻⁵ |
| | | Molec./g | 4.78x10 ¹⁹ | 4.89x10 ¹⁹ |
| | | Molec./m ² | 2.88x10 ¹⁷ | 8.22x10 ¹⁷ |
| pH | Applied voltage (V) | q Units | MWNT | BMWNT |

| | | | | |
|---------------|------------------------|-----------------------|-----------------------|-----------------------|
| NaOH (pH9) | 0 | mg/mg | 0.007638 | 0.004927 |
| | | g/m ² | 4.6x10 ⁻⁵ | 8.28x10 ⁻⁵ |
| | | moles/g | 3.35x10 ⁻⁵ | 2.16x10 ⁻⁵ |
| | | Molec./g | 2.01x10 ¹⁹ | 1.3x10 ¹⁹ |
| | | Molec./m ² | 1.21x10 ¹⁷ | 2.18x10 ¹⁷ |
| pH | Applied voltage (V) | q Units | MWNT | BMWNT |
| NaOH (pH9) | 3 | mg/mg | 0.018752 | 0.019701 |
| | | g/m ² | 0.000113 | 0.000331 |
| | | moles/g | 8.21x10 ⁻⁵ | 8.63x10 ⁻⁵ |
| | | Molec./g | 4.95x10 ¹⁹ | 5.2x10 ¹⁹ |
| | | Molec./m ² | 2.98x10 ¹⁷ | 8.73x10 ¹⁷ |

Table B-2. Adsorption and removal capacities of 1 mg/L bisphenol A in the presence of 10 mM NaCl (pH 6), absence of NaCl (pH 3) and absence of NaCl (pH 9) by both MWNT and BMWNT filters, corresponding to Figure 4-4. The removal capacity values were calculated cumulatively corresponding to the total amount removed at the given voltage.

| Applied voltage (V) | q Units | MWNT | BMWNT |
|---------------------|-----------------------|-----------------------|-----------------------|
| 0 | mg/mg | 0.004593 | 0.003845 |
| | g/m ² | 2.77x10 ⁻⁵ | 6.46x10 ⁻⁵ |
| | moles/g | 2.01x10 ⁻⁵ | 1.68x10 ⁻⁵ |
| | Molec./g | 1.21x10 ¹⁹ | 1.01x10 ¹⁹ |
| | Molec./m ² | 7.3x10 ¹⁶ | 1.7x10 ¹⁷ |
| 1 | mg/mg | 0.004685 | 0.004412 |
| | g/m ² | 2.82x10 ⁻⁵ | 7.41x10 ⁻⁵ |
| | moles/g | 2.05x10 ⁻⁵ | 1.93x10 ⁻⁵ |
| | Molec./g | 1.24x10 ¹⁹ | 1.16x10 ¹⁹ |
| | Molec./m ² | 7.45x10 ¹⁶ | 1.96x10 ¹⁷ |
| 2 | mg/mg | 0.020033 | 0.020335 |
| | g/m ² | 0.000121 | 0.000342 |
| | moles/g | 8.78x10 ⁻⁵ | 8.91x10 ⁻⁵ |
| | Molec./g | 5.28x10 ¹⁹ | 5.36x10 ¹⁹ |
| | Molec./m ² | 3.18x10 ¹⁷ | 9.01x10 ¹⁷ |
| 3 | mg/mg | 0.020317 | 0.020627 |
| | g/m ² | 0.000122 | 0.000347 |
| | moles/g | 8.9x10 ⁻⁵ | 9.04x10 ⁻⁵ |
| | Molec./g | 5.36x10 ¹⁹ | 5.44x10 ¹⁹ |
| | Molec./m ² | 3.23x10 ¹⁷ | 9.14x10 ¹⁷ |

Table B-3. Adsorption and removal capacities of 1 mg/L bisphenol A from synthetic wastewater effluent (pH 7.3-7.4) by both the MWNT and BMWNT filters, corresponding to Figure B-7. The removal capacity values were calculated cumulatively corresponding to the total amount removed the given voltage.

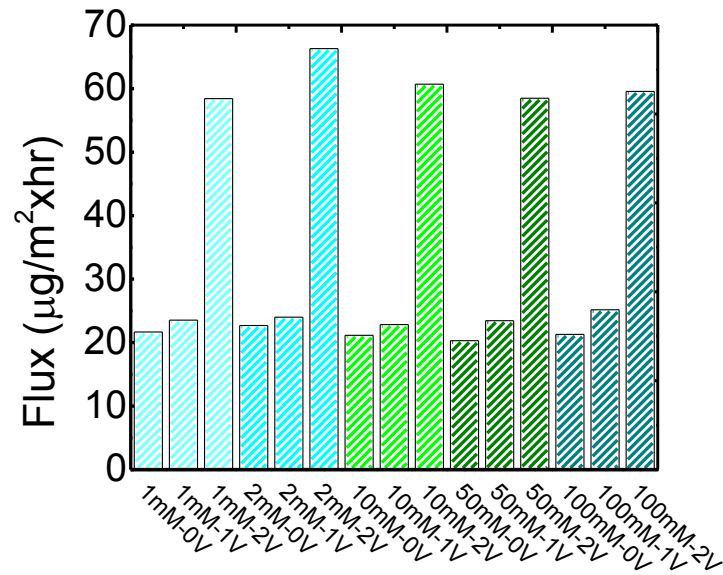


Figure B-8. Removal flux for filtration and electrochemical MWNT filtration of 1 mg/L bisphenol A in 1, 2, 10, 50 and 100 mM NaCl, at 0, 1 and 2 V of applied DC potential, corresponding to Figure 4-2 A.

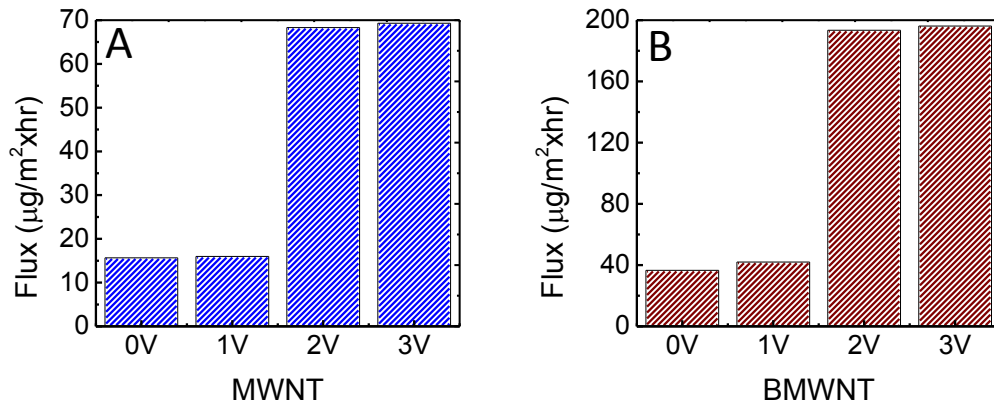


Figure B-9. Removal flux for filtration and electrochemical filtration of 1 mg/L bisphenol A from synthetic wastewater effluent (pH 7.3-7.4) using (A) MWNTs and (B) BMWNTs. Corresponding to Figure B-7.

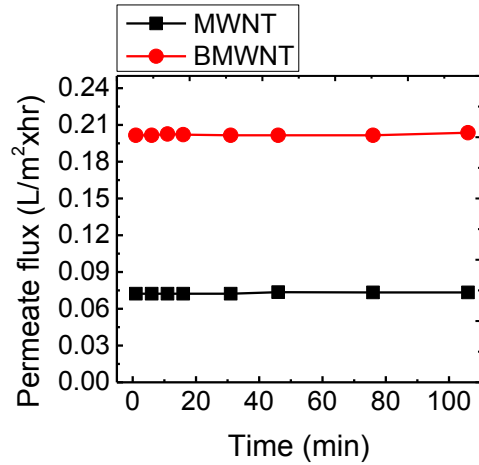


Figure B-10. Average permeate flux for 2 runs at 0 V using 1mg/L BPA in 10 mM NaCl filtered by MWNTs and BMWNTs for 106 minutes of total filtration time. The loading for both the MWNTs and BMWNTs was 1.04 mg/cm² and the flow rate was 2 mL/min and at room temperature.

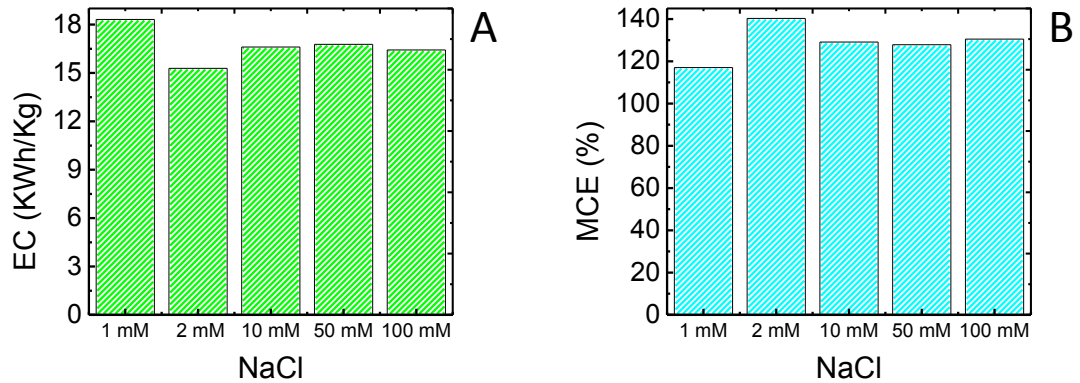


Figure B-11. Energy consumption and mineralization current efficiency, where (A) is the energy consumption for salting out using MWNTs at 2V of applied DC potential and (B) is the mineralization current efficiency for salting out using MWNTs at 2V of applied DC potential. The loading for MWNTs was 1.04 mg/cm², the BPA concentration was 1 mg/L and the flow rate was 2 mL/min and at room temperature.

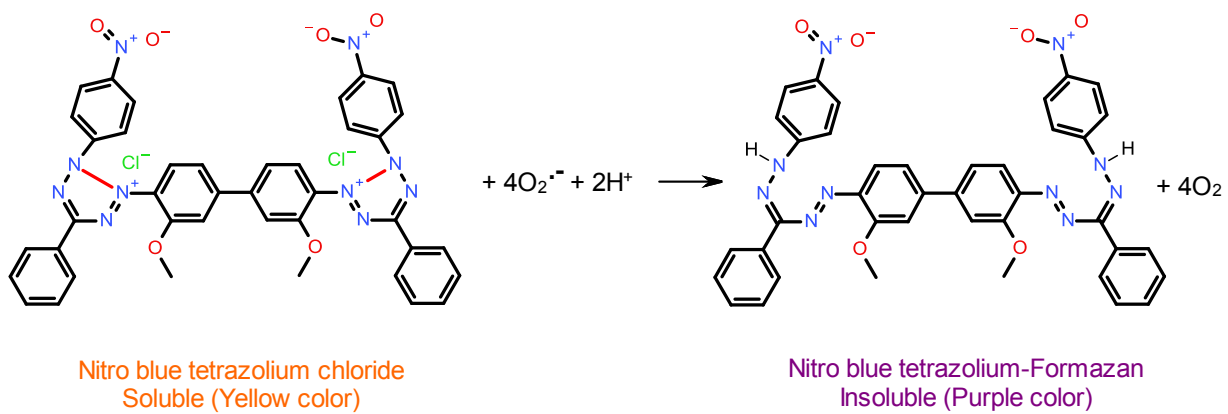


Figure B-12. Reaction mechanism of NBT with superoxide to form NBT-Formazan and diatomic oxygen.

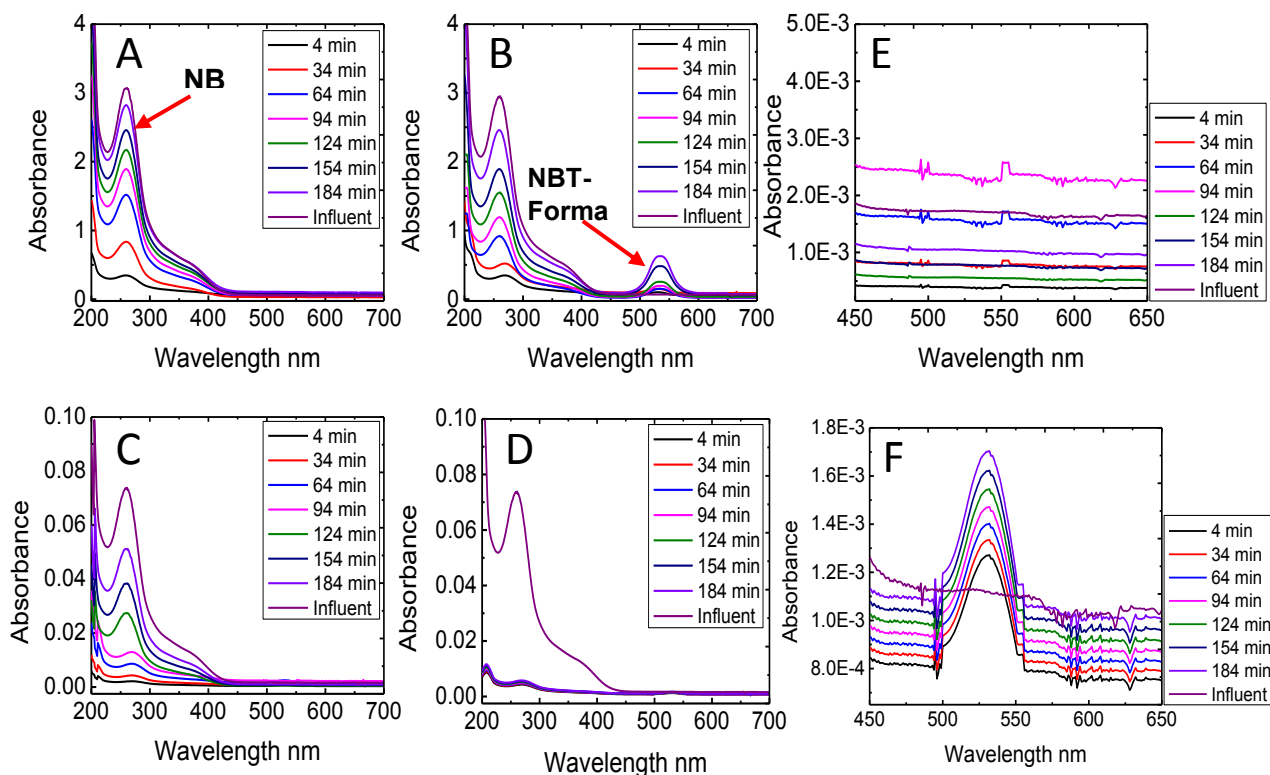


Figure B-13. Superoxide assay, where (A) is the absorbance spectra for MWNT filtration of 0.05 mM NBT at 0 V, (B) is the absorbance spectra for MWNT filtration of 1.25 μ M NBT at 0 V, (C) is the absorbance spectra for electrochemical MWNT filtration of 0.05 mM NBT at 3 V, (D) is the absorbance spectra for electrochemical MWNT filtration of 1.25 μ M NBT at 3 V, (E) is the zoomed view (450 nm-650 nm) of the absorbance spectra for MWNT filtration of 1.25 μ M NBT at 0 V and (F) is the zoomed view (450 nm-650 nm) of the absorbance spectra for electrochemical MWNT filtration of 1.25 μ M NBT at 3 V. All experiments for the indicated NBT concentrations were performed at room temperature in 10 mM NaCl (pH 6) was filtered by 1.04 mg/cm² MWNTs at 0 and 3 V using a flow rate of 0.5 mL/min.

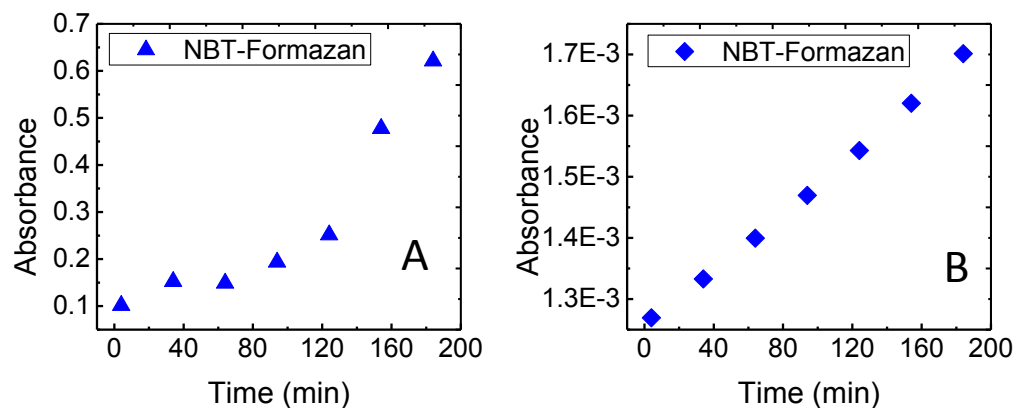


Figure B-14. Absorbance with time for the NBT-Formazan (product of the reaction of NBT with superoxide) for electrofiltration of (A) 0.05 mM NBT in 10 mM NaCl and (B) 1.25 μ M NBT in 10 mM NaCl at 3 V using 1.04 mg/cm² MWNTs and a flow rate of 0.5 mL/min at room temperature (Corresponding to Figure B-13 C and D).

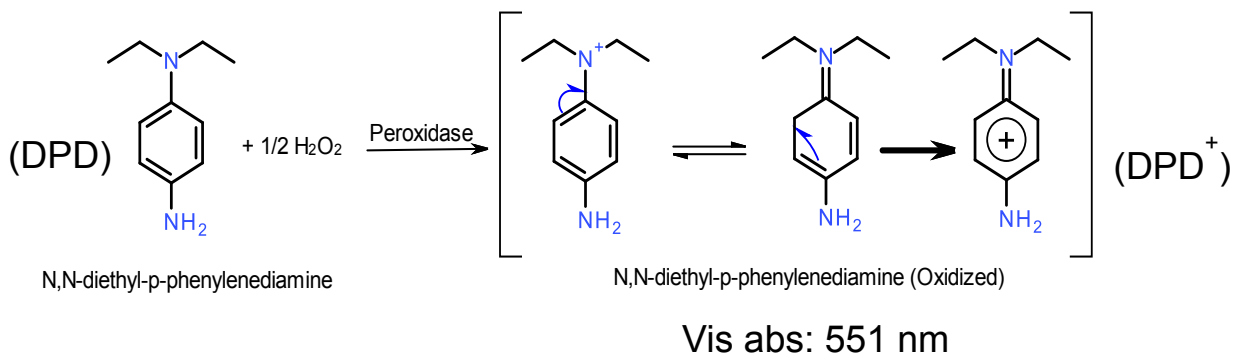


Figure B-15. Reaction mechanism of DPD with hydrogen peroxide to form DPD⁺, catalyzed by horseradish peroxidase.

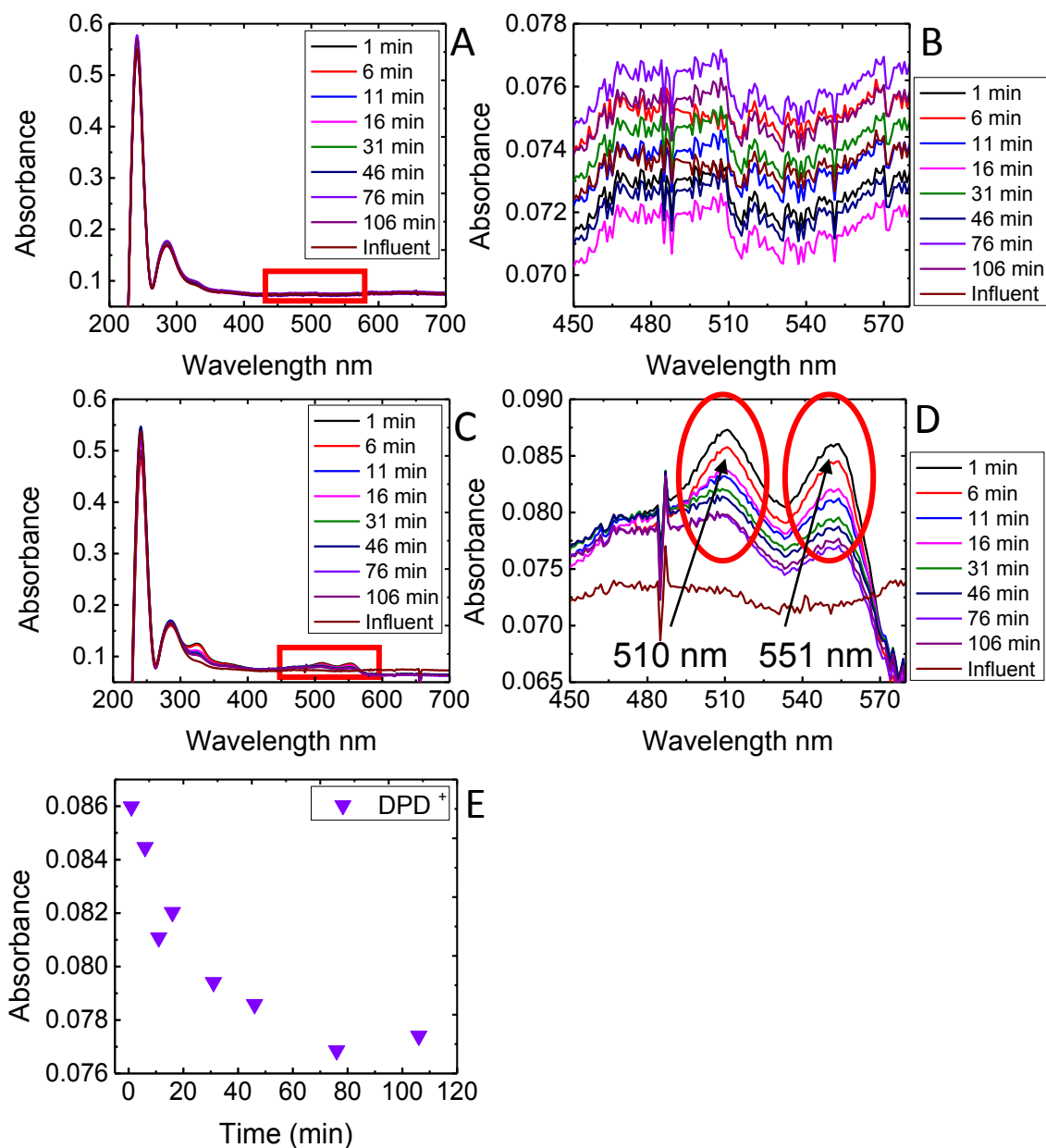


Figure B-16. Hydrogen peroxide assay, where (A) is the absorbance spectra for MWNT filtration of 0.25 mM DPD at 0 V, (B) is the zoomed view (450 nm-570 nm) of the absorbance spectra for MWNT filtration of 0.25 mM DPD at 0 V, (C) is the absorbance spectra for electrochemical MWNT filtration of 0.25 mM DPD at 3 V, (D) is the zoomed view (450 nm-570 nm) of the absorbance spectra for electrochemical MWNT filtration of 0.25 mM DPD at 3 V and (E) is the absorbance over time for the DPD^+ (product of the reaction of DPD with hydrogen peroxide). After DI (pH 3) effluents were treated by DPD reagent, the MWNT loading was 1.04 mg/cm^2 , the applied voltages were 0 and 3 V and the flow rate was 2 mL/min at room temperature.

Hydrogen peroxide Assay

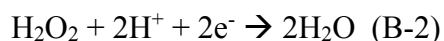
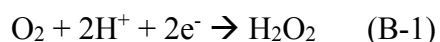
To be compatible with electrochemical filtration conditions, the hydrogen peroxide assay was undertaken using the following modified method adopted from Bader et al. [122] and Hsieh et al. [120]:

- A DPD reagent was prepared by dissolving the indicator (DPD) in 1:1 molar ratio with oxalic acid to enable 100 % miscibility resulting in a concentration of 10 mM which was then added to a 0.1 % sulfuric acid solution.
- DI was adjusted to a pH of 3 using a few drops of 1 M sulfuric acid and was used as the electrofiltration influent. Sources of chlorides were entirely avoided to prevent any interference from reactive chlorine on the oxidation of DPD in the collected effluent subsamples. Furthermore, no organic molecules were dissolved in the influent to avoid the consumption of the generated hydrogen peroxide under voltage.
- The influent was electrofiltered at 3 V of applied DC potential and 1 ml effluent subsamples were collected at various time intervals using a flow rate of 2 ml/min.
- Effluents were then treated with the addition of:
 1. 1 ml of concentrated phosphate buffered saline pH 6 to raise and maintain the pH to 6, the optimal pH for the reaction of DPD with hydrogen peroxide. The pH after the addition of the buffer in a 1:1 volume ratio was measured to be 5.9.
 2. 50 μ L of the 10 mM DPD reagent (resulting in a concentration of 0.25 mM in the effluent subsample)
 3. 100 μ L of horseradish peroxidase enzyme at a concentration of 10 units/ml
 4. After 15 seconds, the subsample mixture was analyzed by UV/Vis at a wavelength of 551 nm (scan from 200-700 nm).
 5. The blank solution was prepared from all of the species mentioned except DPD.

As can be seen from Figure B-16 A and B, DPD absorbs in the UV range and has a very minor peak around 510 nm. When DPD is oxidized to DPD^+ , it forms another peak at 551 nm (Figure B-16 D), which could only be detected in effluent subsamples collected from electrofiltration at 3 volts. The formation of DPD^+ is in agreement with previous reports [122]: [120].

In the absence of any interfering oxidizing species (e.g. chlorides), it is speculated that DPD oxidation takes place in a reaction with electro-generated hydrogen peroxide ($E^{\circ}_{\text{red}} = 0.7\text{V}$) catalyzed by peroxidase enzyme forming the oxidized DPD^+ radical cation, Figure B-15.

Adjusting the influent pH to 3 enhances the formation of hydrogen peroxide, as can be seen from the formation reaction (B-1) below:



This is due to an increased amount of protons available to produce hydrogen peroxide from the reduction of diatomic oxygen at the cathode surface. However, Figure B-16 E shows a decline in the amount of produced DPD^+ produced over time indicating that the hydrogen peroxide formed at acidic pH has a low stability and reacts with the excess protons to form water as shown in reaction (B-2).

Overall, this assay could provide an indication of the generation and presence of hydrogen peroxide during the electrochemical filtration process. Although, the exact chemical role or contribution of hydrogen peroxide in this particular process is not clear, its presence could open the possibility for the formation of different oxidative radicals such as hydroperoxiradicals and hydroxyl radicals. Furthermore, its formation gives another indication of the abundance of superoxide radicals, reaction (B-3), as mentioned earlier in this study (refer to superoxide assay, Fig. S15 and S16) and in previous studies [86, 114].



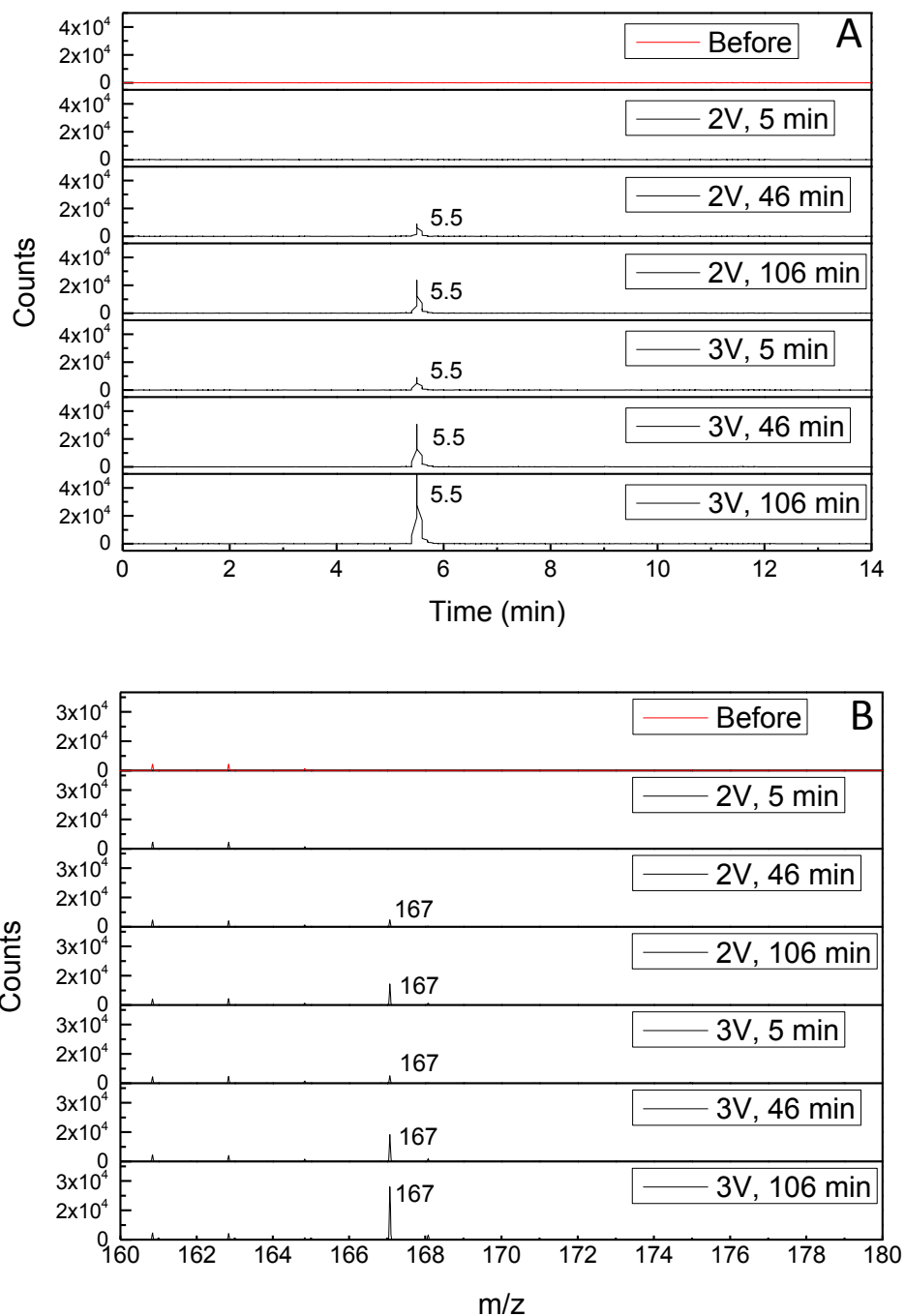


Figure B-17. LC-MS of 10 mg/L BPA in 10 mM NaCl (pH 6) before (red traces) and after 5, 46 and 106 minutes of electrochemical MWNT filtration (black traces) at 2 and 3 V of applied DC potential, where (A) is the liquid chromatograms showing the formation of a by-product at RT 5.5 min ($167 m/z$) and (B) is the mass spectra at $167 m/z$ (corresponding to 5.5 min) after treatment at 2 and 3 V. Experiments were performed at room temperature using a flow rate of 2 mL/min and an MWNT loading of 1.04 mg/cm^2 .

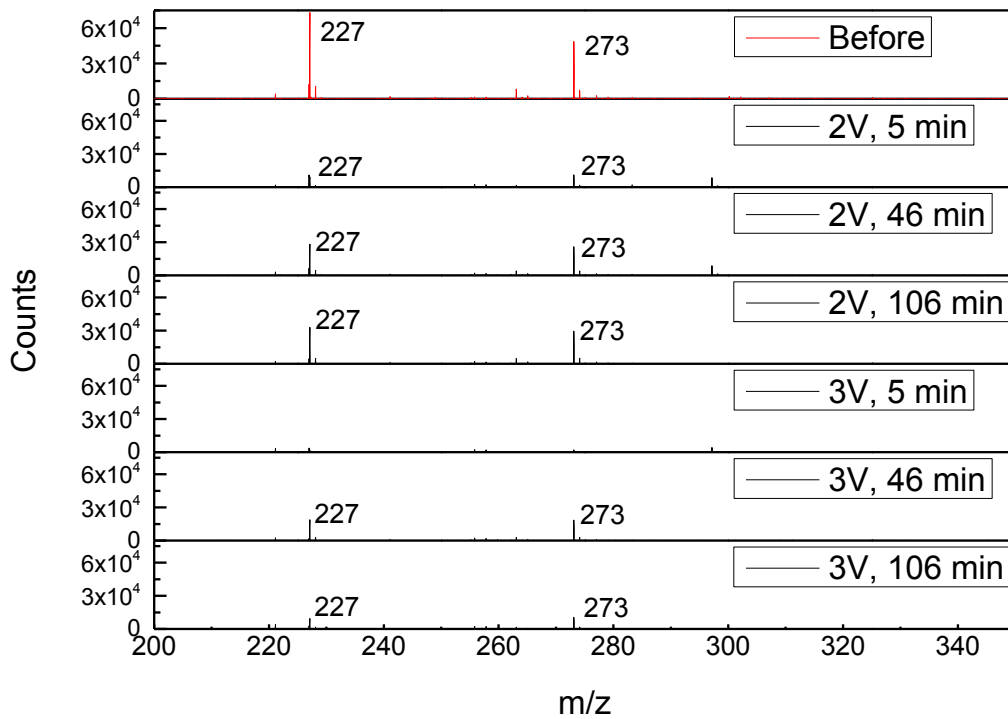


Figure B-18. Mass spectra of 10 mg/L BPA (227 m/z) in the absence of NaCl (pH 9) before (red trace) and after 5, 46 and 106 minutes of electrochemical MWNT filtration (black traces) treatment at 2 and 3 V of applied DC potential. Experiments were performed at room temperature using a flow rate of 2 mL/min and an MWNT loading of 1.04 mg/cm².

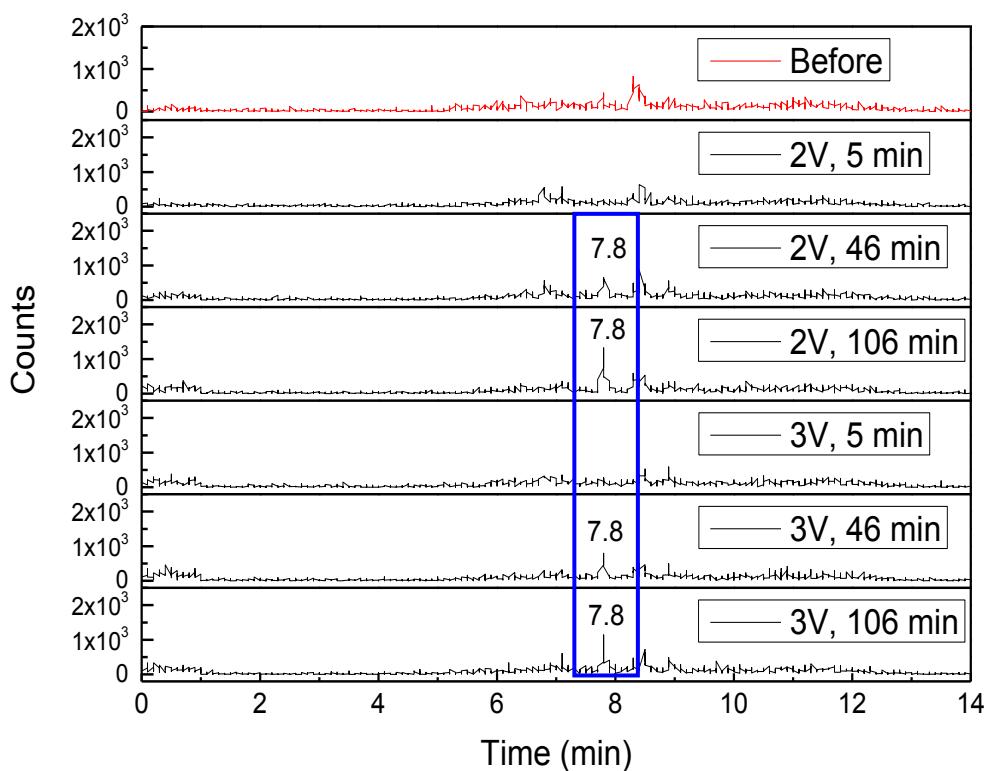


Figure B-19. Liquid chromatograms of 10 mg/L BPA in the absence of NaCl (pH 9) before (red trace) and after 5, 46 and 106 minutes of electrochemical MWNT filtration treatment (black traces) at 2 and 3 V of applied DC potential showing the formation of a by-product at RT 7.8 min. The flow rate was 2 mL/min the MWNT loading was 1.04 mg/cm^2 .

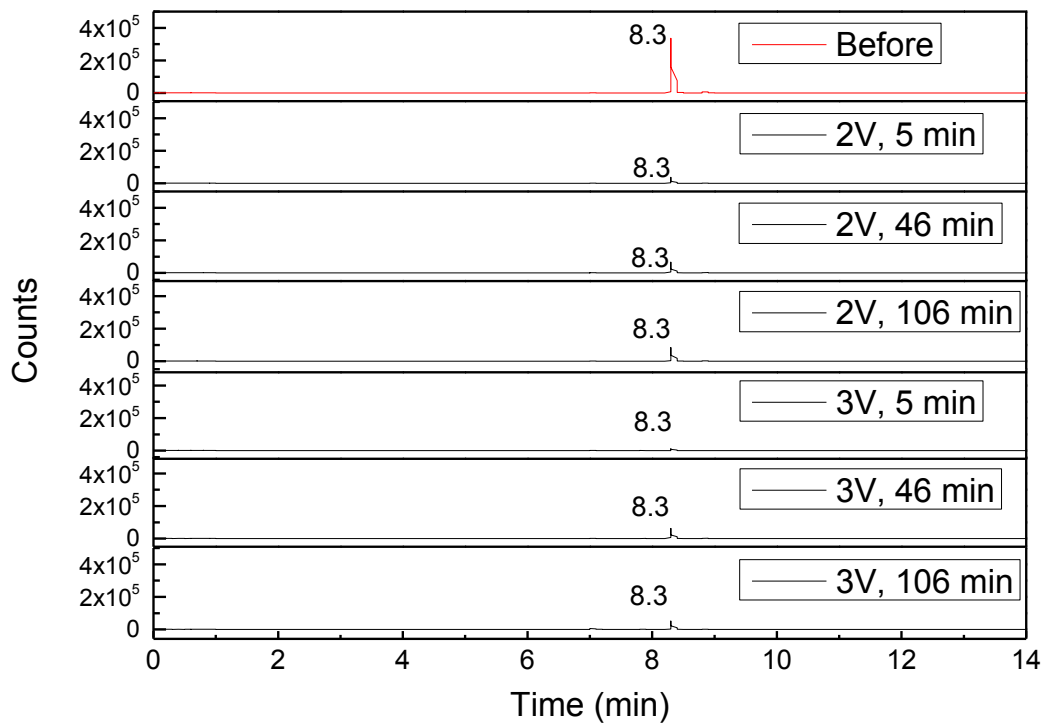


Figure B-20. Liquid chromatograms of 10 mg/L BPA in the absence of NaCl (pH 3) before (red trace) and after 5, 46 and 106 minutes of electrochemical MWNT filtration treatment (black traces) at 2 and 3 V of applied DC potential. The flow rate was 2 mL/min and the MWNT loading was 1.04 mg/cm².

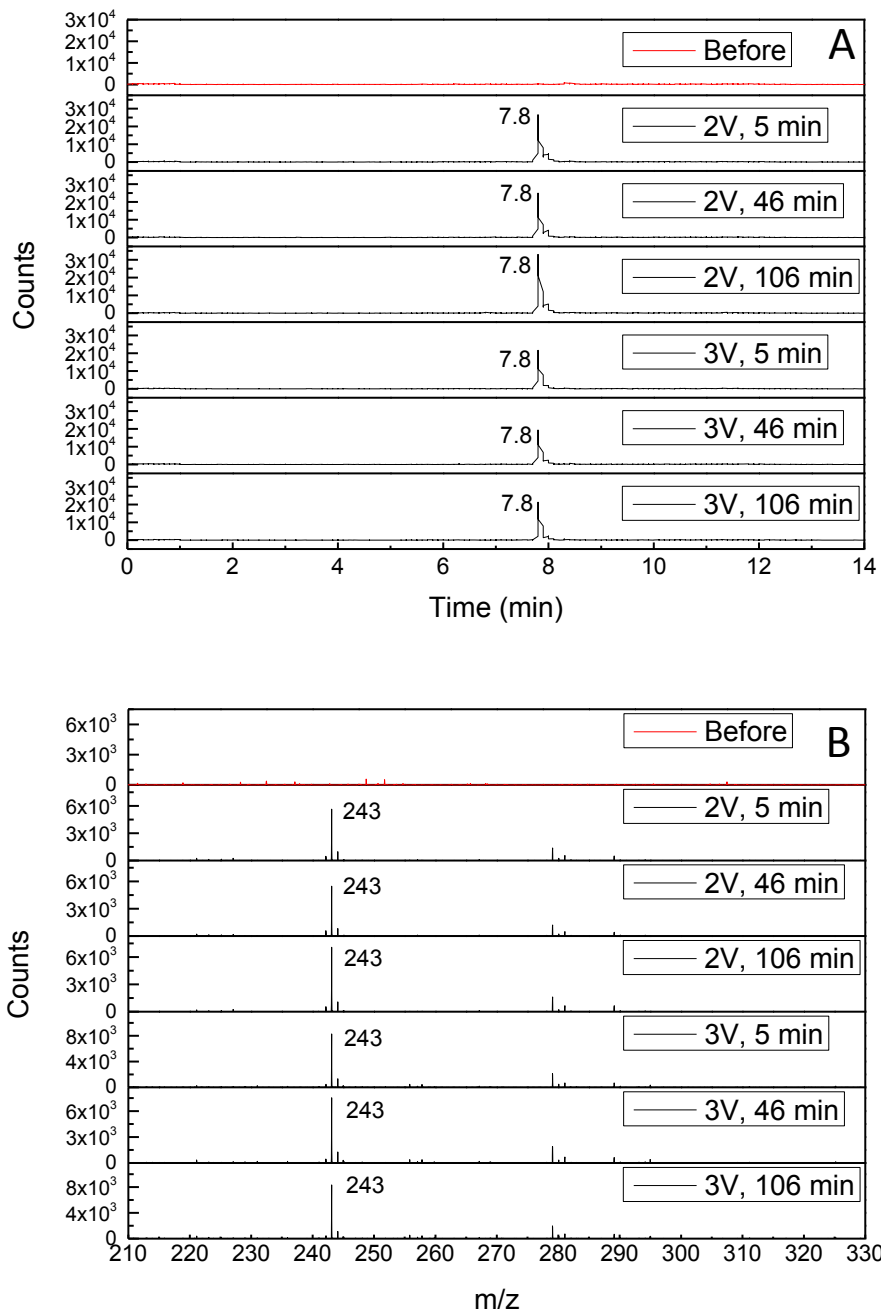


Figure B-21. LC-MS of 10 mg/L BPA in the absence of NaCl (pH 3) before (red trace) and after 5, 46 and 106 minutes of electrochemical MWNT filtration treatment (black traces) at 2 and 3 V of applied DC potential showing the formation of a by-product at RT 7.8 min (243 m/z), where (A) is the liquid chromatograms for RT 7.8 min and (B) is the mass spectra at 243 m/z (corresponding to 7.8 min). Experiments were performed at room temperature using a flow rate of 2 mL/min and an MWNT loading of 1.04 mg/cm².

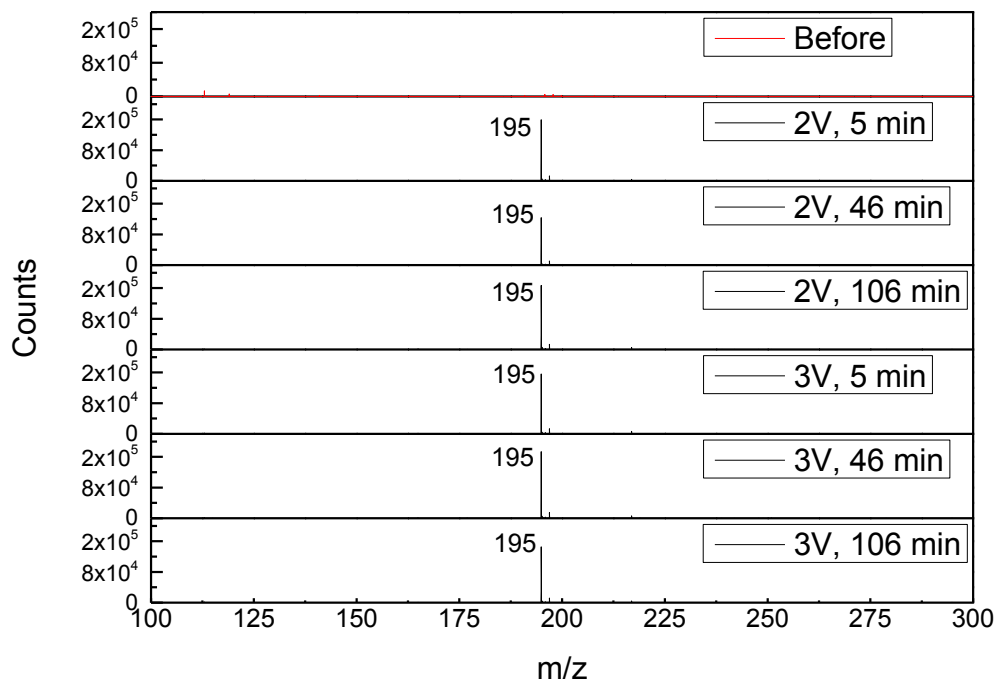


Figure B-22. Mass spectra of 10 mg/L BPA in absence of NaCl (pH 3) before (red trace) and after 5, 46 and 106 minutes of electrochemical MWNT filtration treatment (black traces) at 2 and 3 V of applied DC potential, showing the formation of a by-product at 195 m/z (RT 1.1 min). Experiments were performed at room temperature using a flow rate of 2 mL/min and an MWNT loading of 1.04 mg/cm².

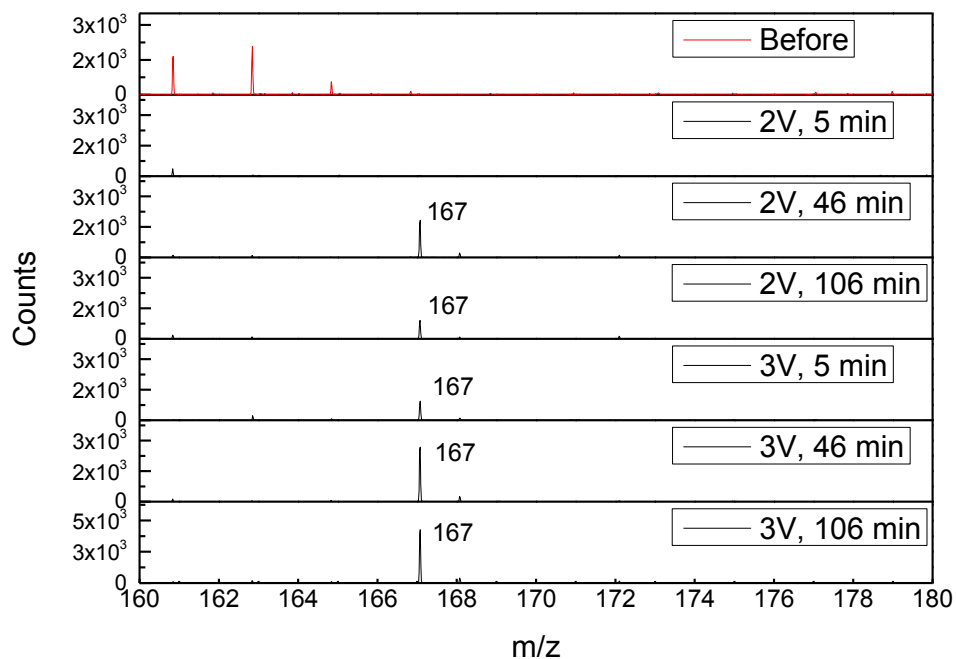


Figure B-23. Mass spectra of 10 mg/L BPA in the absence of NaCl (pH 3) before (red trace) and after 5, 46 and 106 minutes of electrochemical MWNT filtration treatment (black traces) at 2 and 3 V of applied DC potential, showing the formation of a by-product at 167 m/z (RT 5.5 min). Experiments were performed at room temperature using a flow rate of 2 mL/min and an MWNT loading of 1.04 mg/cm².

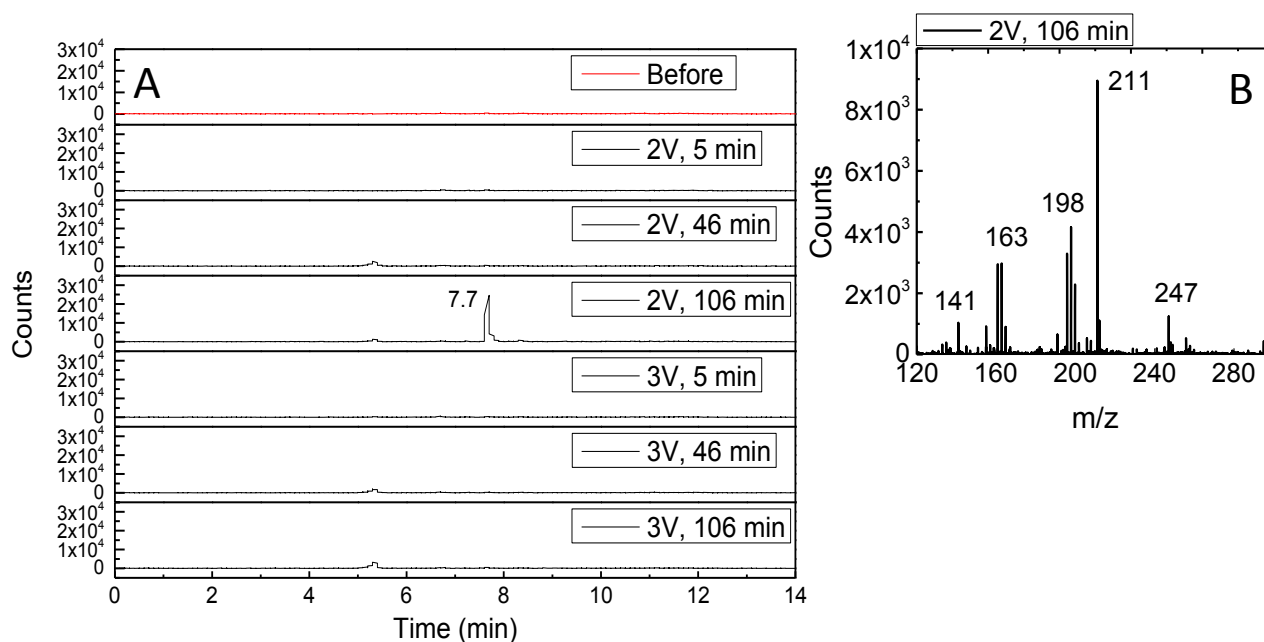


Figure B-24. LC-MS of 10 mg/L BPA in the absence of NaCl (pH 3) before (red trace) and after 5, 46 and 106 minutes of electrochemical MWNT filtration treatment (black traces) at 2 and 3 V of applied DC potential, where (A) is liquid chromatograms showing the formation of a by-product at RT 7.7 min (211 m/z) at 2V after 106 minutes and (B) is the mass spectrum for 211 m/z (corresponding to RT 7.7 min). Experiments were performed at room temperature using a flow rate of 2 mL/min and an MWNT loading of 1.04 mg/cm².

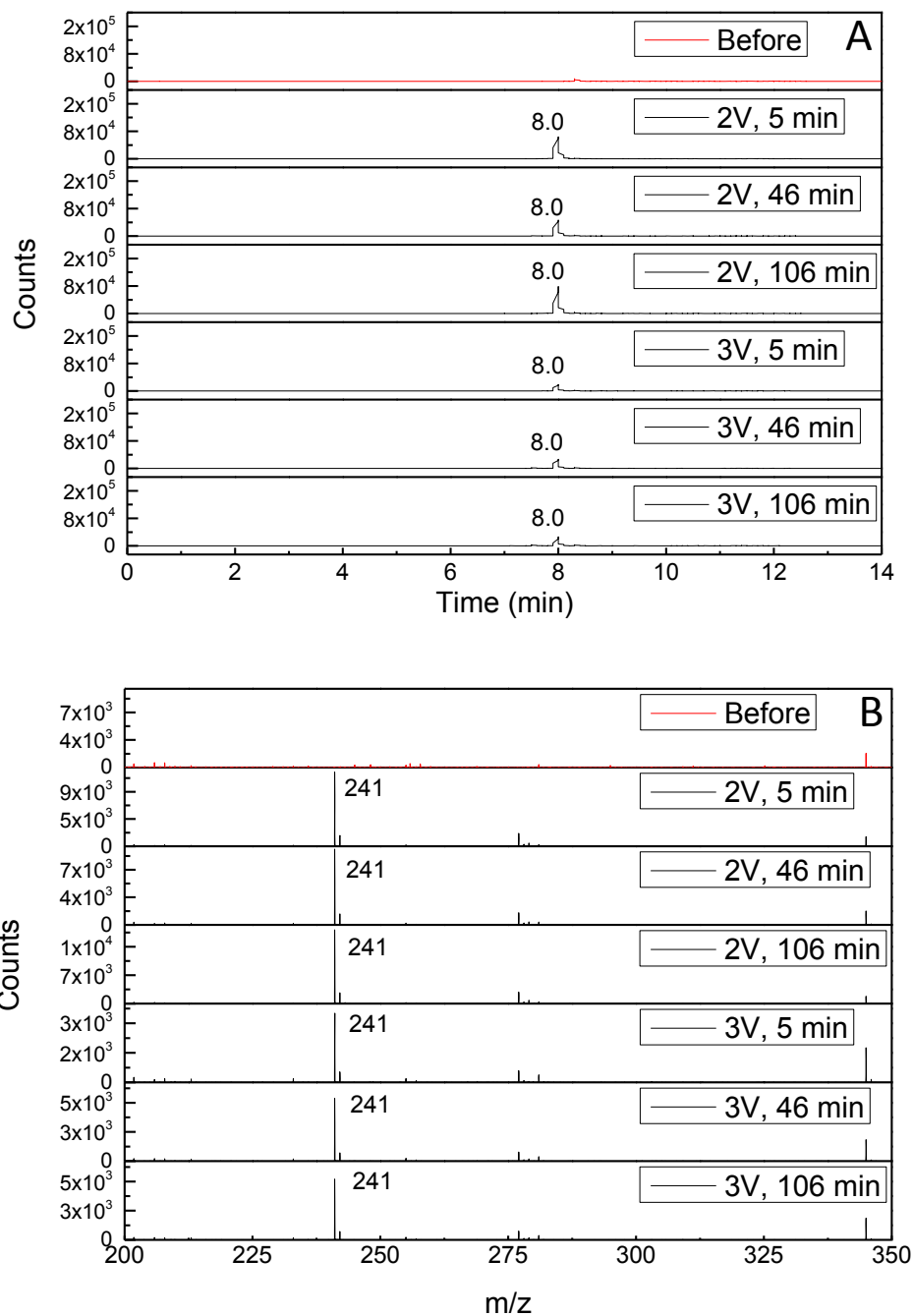


Figure B-25. LC-MS of 10 mg/L BPA in the absence of NaCl (pH 3) before (red trace) and after 5, 46 and 106 minutes of electrochemical MWNT filtration treatment (black traces) at 2 and 3 V of applied DC potential, where (A) is liquid chromatograms showing the formation of a by-product at RT 8 min (241 m/z) and (B) is the mass spectra for the 241 m/z (corresponding to 8 min). Experiments were performed at room temperature using a flow rate of 2 mL/min and an MWNT loading of 1.04 mg/cm².

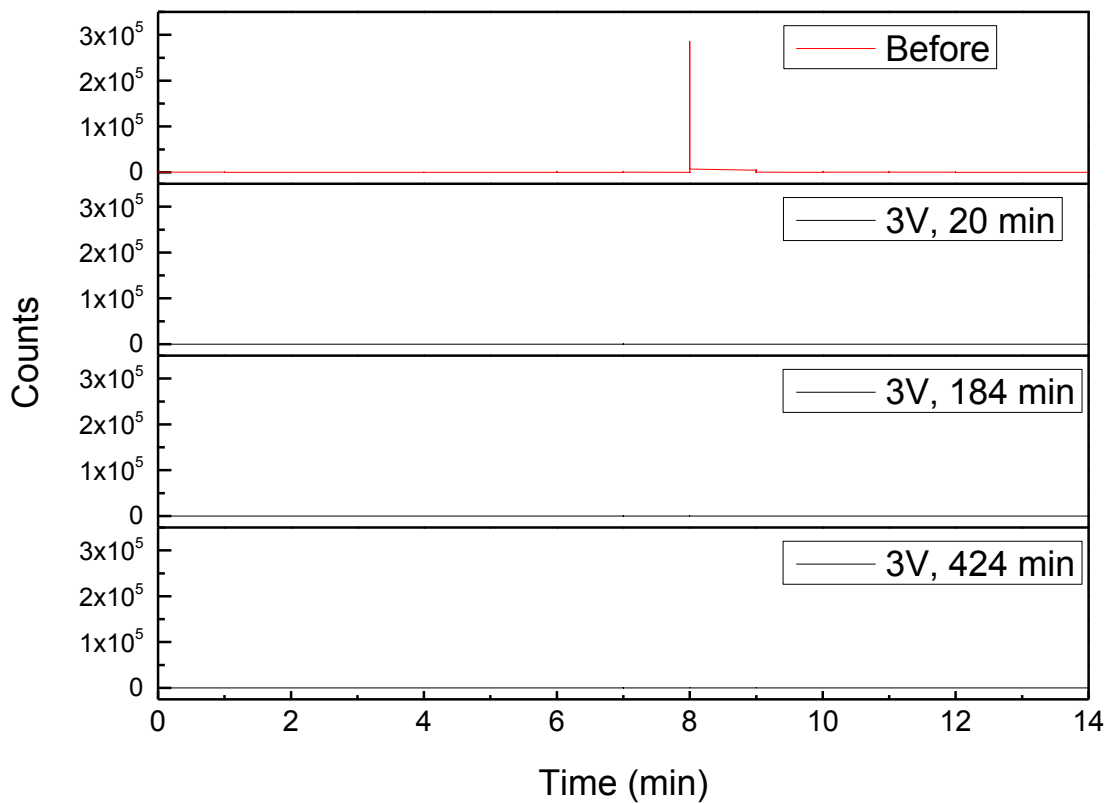


Figure B-26. Liquid chromatograms of 10 mg/L BPA (8.39 min) in 10 mM NaCl (pH 6) before (red trace) and after 20, 184 and 424 minutes of electrochemical MWNT filtration treatment (black traces) at 3 V of applied DC potential. The flow rate was 0.5 mL/min the MWNT loading was 1.04 mg/cm².

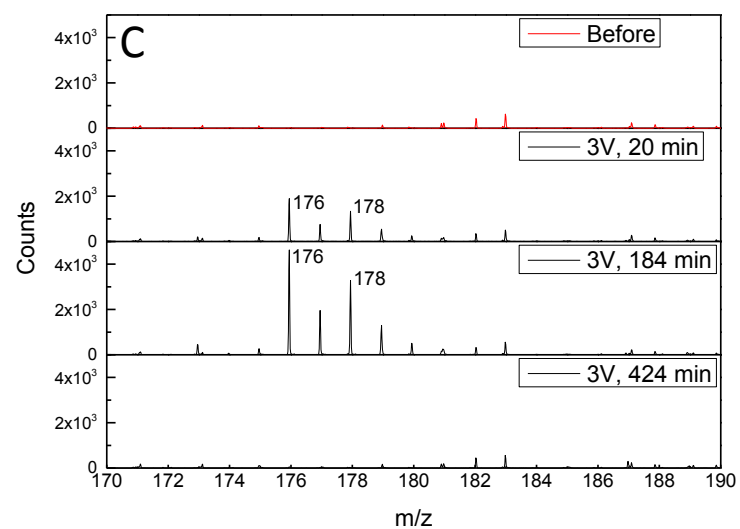
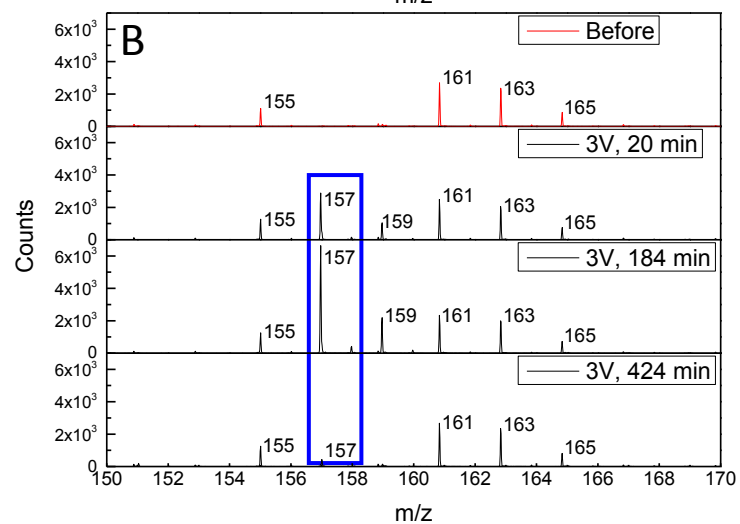
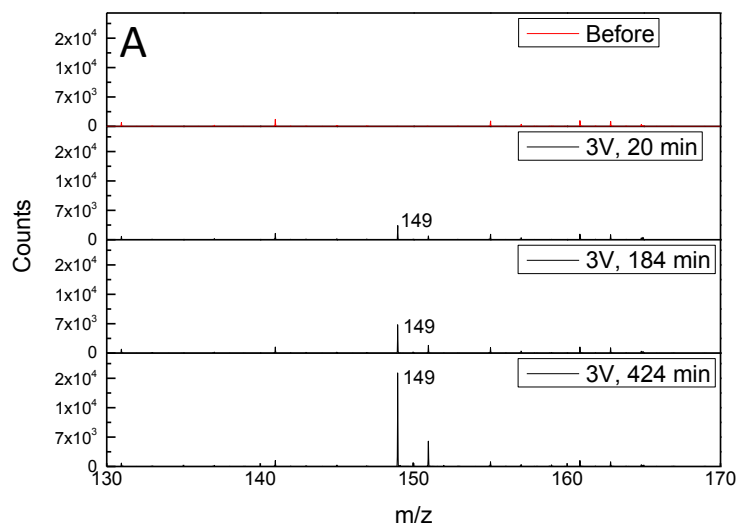


Figure B-27. Mass spectra of 10 mg/L BPA in 10 mM NaCl (pH6) before (red trace) and after 20, 184 and 424 minutes of electrochemical MWNT filtration treatment (black traces) at 3 V of applied DC potential, where (A) shows the formation of a by-product at RT 1.8 min (149 m/z), (B) shows the formation of a by-product at RT 7.1 min (157 m/z) and (C) shows the formation of a by-product at RT 7.3 min (176 m/z). Experiments were performed at room temperature using a flow rate of 0.5 mL/min and an MWNT loading of 2.08 mg/cm².

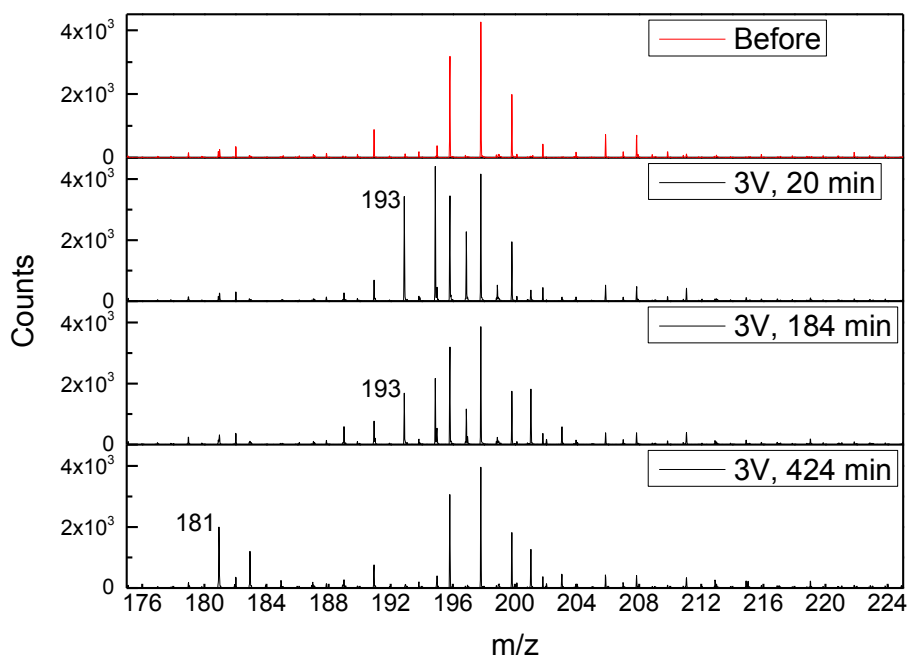


Figure B-28. Mass spectra of 10 mg/L BPA in 10 mM NaCl (pH 6) before (red trace) and after 20, 184 and 424 minutes of electrochemical MWNT filtration treatment (black traces) at 3 V of applied DC potential showing the formation of by-products at 193 and 181 m/z. Experiments were performed at room temperature using a flow rate of 0.5 mL/min and an MWNT loading of 1.04 mg/cm².

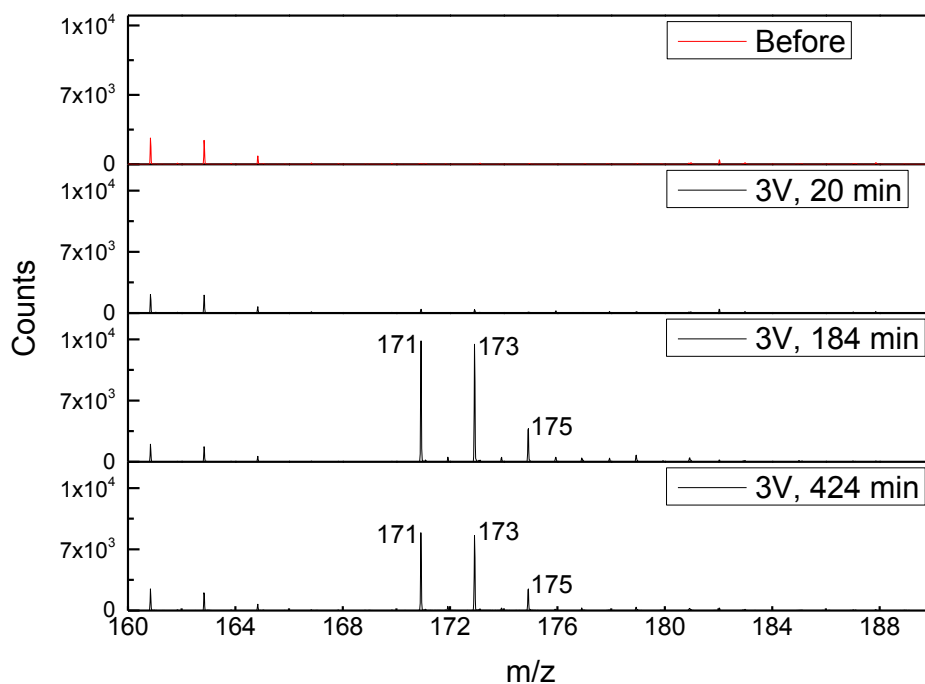


Figure B-29. Mass spectra of 10 mg/L BPA in 10 mM NaCl (pH 6) before (red trace) and after 20, 184 and 424 minutes of electrochemical MWNT filtration treatment (black traces) at 3 V of applied DC potential, showing the formation of by-products at 171 m/z. Experiments were performed at room temperature using a flow rate of 0.5 mL/min and an MWNT loading of 1.04 mg/cm².

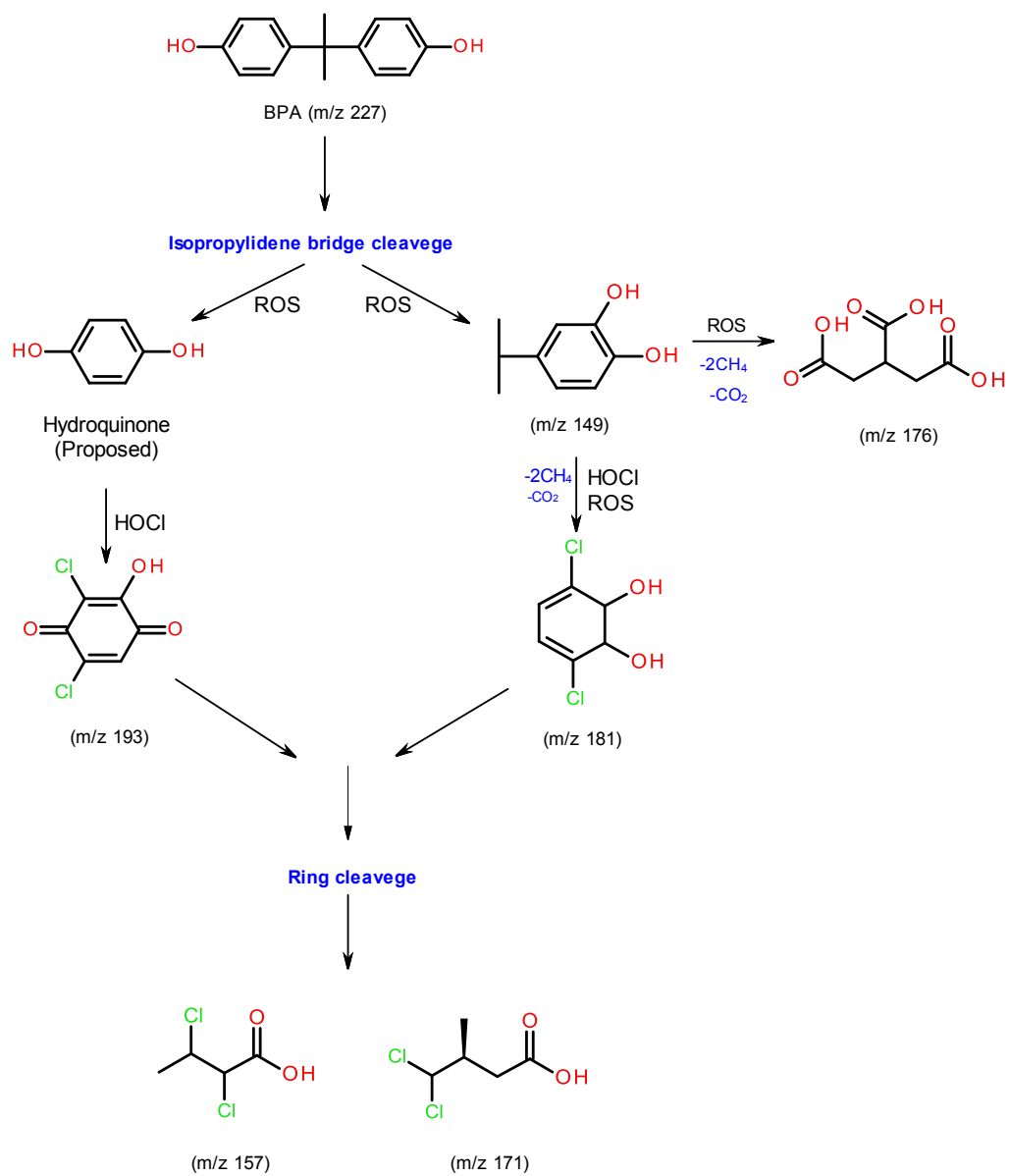


Figure B-30. Degradation reaction pathways for BPA during the electrochemical filtration process in the presence of 10 mM NaCl. Experiments were performed at room temperature using a flow rate of 0.5 mL/min and an MWNT loading of 2.08 mg/cm².

Appendix C

Appendix C contains supporting information and additional data that further elucidate and confirm the information provided for the crossflow electrochemical treatment of Ibuprofen and Bisphenol A using MWNT blend buckypaper as a super-conductive electrochemical filtration membrane.

In appendix C, additional data around the surface characterization of MWNTs and BMWNTs including EDX after use in treatment and SEM x-sectional images for MWNT buckypaper membrane (Figures C-1 and C-2), TGA mass loss plots (Figure C-3), BET plots, cumulative surface area and pore volume relative to pore width, and their differential distribution for MWNT buckypaper (Figure C-4). Removal capacity values in all stated conditions (Table C-1) and membrane recovery (Mass balance) percentages (Table C-2). Permeate flux values for MWNT buckypaper membrane filter (Figure C-5). Mass spectra for different detected products corresponding from crossflow electrochemical filtration (Figures C-6 to C-9). Energy consumption values in KWh/Kg for the treatment of individual and mixture ibuprofen and bisphenol A (Figure C-10). Energy consumption price rates in Canadian dollars corresponding to figure C-10 (Figure C-11).

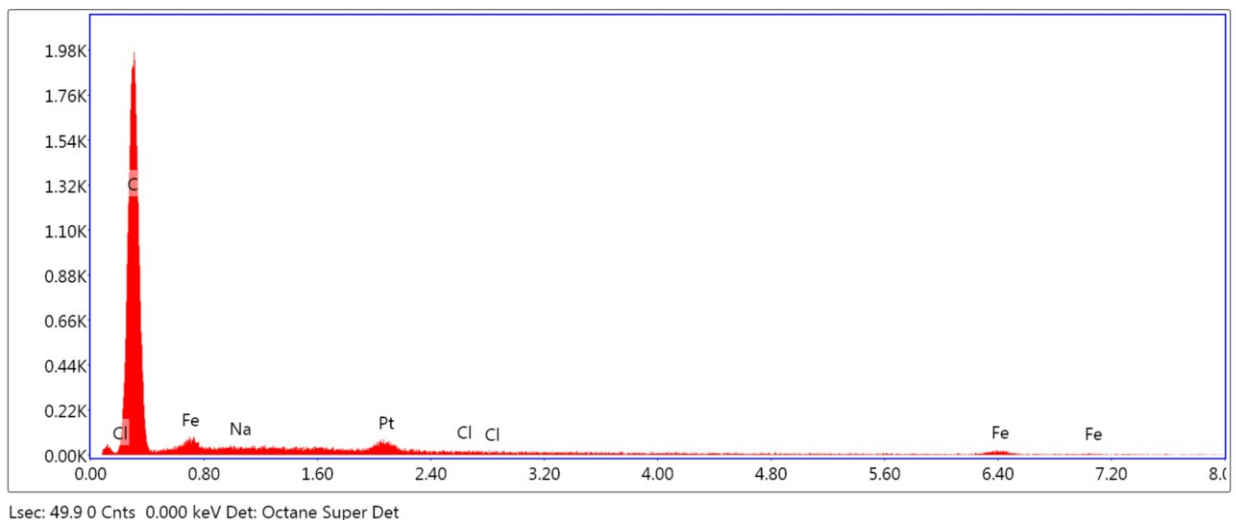


Figure C-1. EDS analysis for buckypaper membrane filter at a surface loading of 102.5 mg/cm^2 after use in electrochemical filtration of a 1 mg/L ibuprofen and bisphenol A (1:1) mixture under 3 V of applied DC potential and at room temperature.

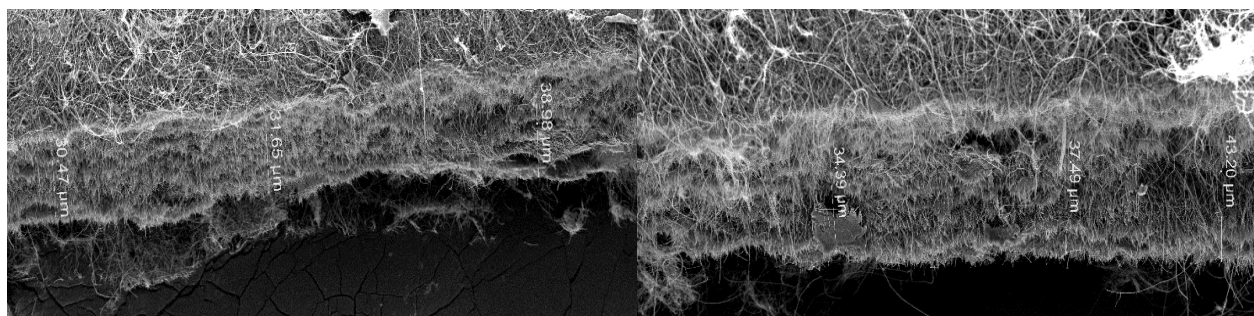


Figure C-2. SEM lateral (x-sectional) view images for buckypaper membrane filter at a surface loading of 102.5 mg/cm^2 .

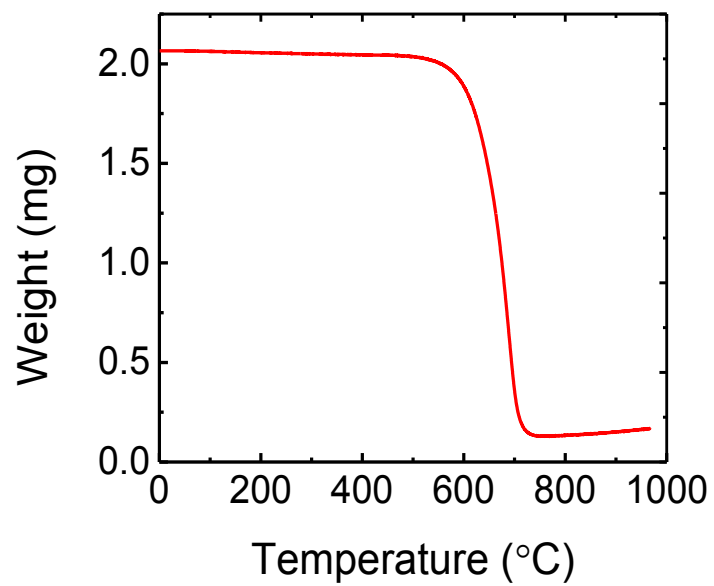


Figure C-3. TGA mass plot analysis for MWNT blend buckypaper

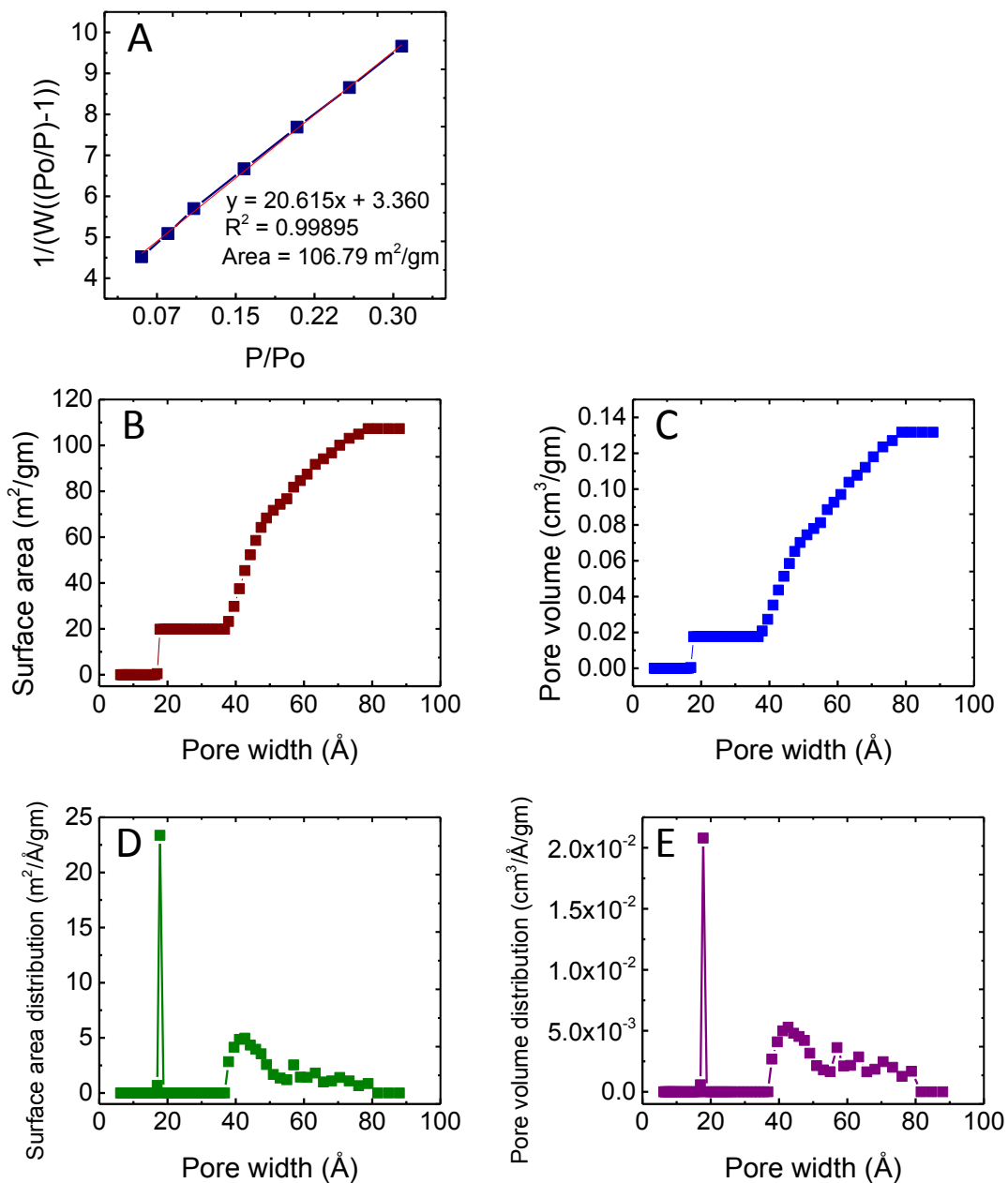


Figure C-4. (A) BET plot, (B) cumulative surface area relative to pore width (C) cumulative pore volume relative to pore width, (D) differential surface area distribution relative to pore width and (E) differential pore volume distribution relative to pore width, for MWNT blend buckypaper.

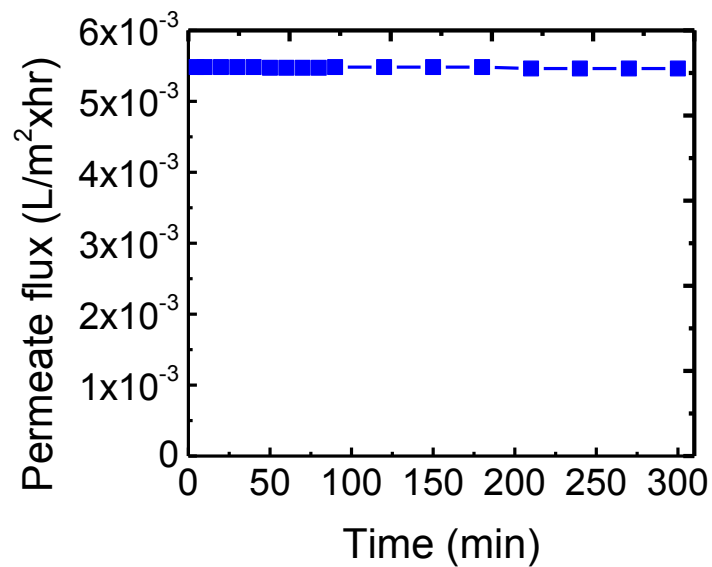


Figure C-5. Average Permeate flux (L/m².h) for the removal of 1 mg/L ibuprofen bisphenol A mix (1:1) at 0 V using MWNT blend buckypaper membrane of 50 cm² geometrical surface area, 109459.75 cm² of total surface area. Flow rate was 1 mL/min (20 psi) and at room temperature.

| | | | | |
|---------------------------------|-------|-------------------------|-------------------------|-------------------------|
| Ibuprofen | Volts | q (mg/mg) | q (g/m ²) | q (moles/g) |
| | 0 V | 5.14 x 10 ⁻⁴ | 4.8 x 10 ⁻⁶ | 2.49 x 10 ⁻⁶ |
| | 1 V | 5.79 x 10 ⁻⁴ | 5.4 x 10 ⁻⁶ | 2.81 x 10 ⁻⁶ |
| | 2 V | 2.88 x 10 ⁻³ | 2.7 x 10 ⁻⁵ | 1.4 x 10 ⁻⁵ |
| | 3 V | 2.90 x 10 ⁻³ | 2.71 x 10 ⁻⁵ | 1.4 x 10 ⁻⁵ |
| Bisphenol A | Volts | q (mg/mg) | q (g/m ²) | q (moles/g) |
| | 0 V | 6.07 x 10 ⁻⁴ | 5.7 x 10 ⁻⁶ | 2.66 x 10 ⁻⁶ |
| | 1 V | 6.28 x 10 ⁻⁴ | 5.9 x 10 ⁻⁶ | 2.75 x 10 ⁻⁶ |
| | 2 V | 2.92 x 10 ⁻³ | 2.74 x 10 ⁻⁵ | 1.28 x 10 ⁻⁵ |
| | 3 V | 2.93 x 10 ⁻³ | 2.74 x 10 ⁻⁵ | 1.28 x 10 ⁻⁵ |
| Mix (1:1) 10 mM NaCl pH 6 | Volts | q (mg/mg) | q (g/m ²) | q (moles/g) |
| | 0 V | 5.56 x 10 ⁻⁴ | 5.2 x 10 ⁻⁶ | 2.56 x 10 ⁻⁶ |
| | 1 V | 6.31 x 10 ⁻⁴ | 5.9 x 10 ⁻⁶ | 2.91 x 10 ⁻⁶ |
| | 2 V | 2.92 x 10 ⁻³ | 2.73 x 10 ⁻⁵ | 1.34 x 10 ⁻⁵ |
| | 3 V | 2.93 x 10 ⁻³ | 2.75 x 10 ⁻⁵ | 1.35 x 10 ⁻⁵ |
| Mix (1:1) SSWW pH 7.3 | Volts | q (mg/mg) | q (g/m ²) | q (moles/g) |
| | 0 V | 5.11 x 10 ⁻⁴ | 4.8 x 10 ⁻⁶ | 2.35 x 10 ⁻⁶ |
| | 1 V | 4.64 x 10 ⁻⁴ | 4.3 x 10 ⁻⁶ | 2.14 x 10 ⁻⁶ |
| | 2 v | 3.00 x 10 ⁻³ | 2.8 x 10 ⁻⁵ | 1.38 x 10 ⁻⁵ |
| | 3 V | 3.02 x 10 ⁻³ | 2.82 x 10 ⁻⁵ | 1.39 x 10 ⁻⁵ |

Table C-1. Removal capacity (q) values for the treatment of 1 mg/L ibuprofen, bisphenol A and mixed ibuprofen/bisphenol A (1:1) in 10 mM NaCl at pH 5.8-6 and mixed ibuprofen/bisphenol A (1:1) in synthetic secondary wastewater of 34mg TOC/L and pH 7.3, at 0, 1, 2 and 3 V applied DC potential and using MWNT blend buckypaper membrane of MWNT blend buckypaper membrane of 50 cm² geometrical surface area, 109459.75 cm² of total surface area. Flow rate was 1 mL/min (20 psi) and at room temperature.

| Voltage | Mass balance | |
|---------|--------------|------------------|
| | Background | Memb. Recovery % |
| 0 | Pure | 98.80 |
| | Synth | 98.71 |
| 1 | Pure | 98.85 |
| | Synth | 98.65 |
| 2 | Pure | 99.90 |
| | Synth | 99.90 |
| 3 | Pure | 99.92 |
| | Synth | 99.91 |

Table C-2. Membrane recovery (Mass balance, %) percentages for the removal of 1 mg/L ibuprofen, bisphenol A, and mixed ibuprofen/bisphenol A (1:1) in 10 mM NaCl at pH 5.8-6 (Pure) and mixed ibuprofen/bisphenol A (1:1) in synthetic secondary wastewater of 34mg TOC/L and pH 7.3 (Synth), at 0, 1, 2 and 3 V applied DC potential and using MWNT blend buckypaper membrane of MWNT blend buckypaper membrane of 50 cm² geometrical surface area, 109459.75 cm² of total surface area. Flow rate was 1 mL/min (20 psi) and at room temperature.

Membrane recovery percentages were calculated using eqn. (C-1)

$$\text{Membrane Recovery (\%)} = \frac{(C_F V_F - C_C V_C - [\sum_1^n C_P V_P])}{C_F V_F} \times 100 \quad (\text{C-1})$$

Where,

$C_F V_F$ = Feed concentration x Feed volume

$C_C V_C$ = Concentrate concentration x Concentrate volume

$C_P V_P$ = Permeate concentration x Permeate volume

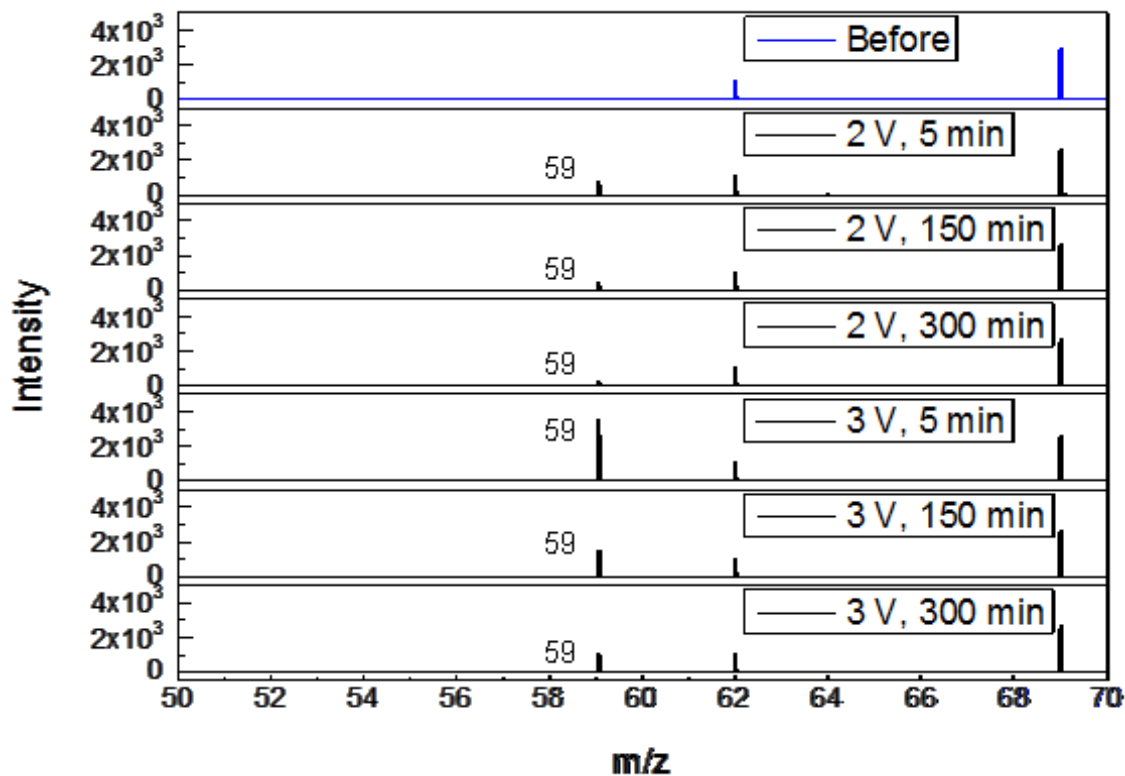


Figure C-6. Mass spectra of 10 mg/L ibuprofen and bisphenol A (1:1) mixture in 10 mM NaCl (pH 6) before (blue trace) and after 5, 150 and 300 minutes of crossflow electrochemical filtration treatment using MWNT blend buckypaper membrane (black traces) at 2 and 3 V of applied DC potential, showing the formation of a by-product at 59 m/z. Experiments were performed at room temperature using a flow rate of 1 mL/min and a buckypaper membrane of loading of 1.04 mg/cm².

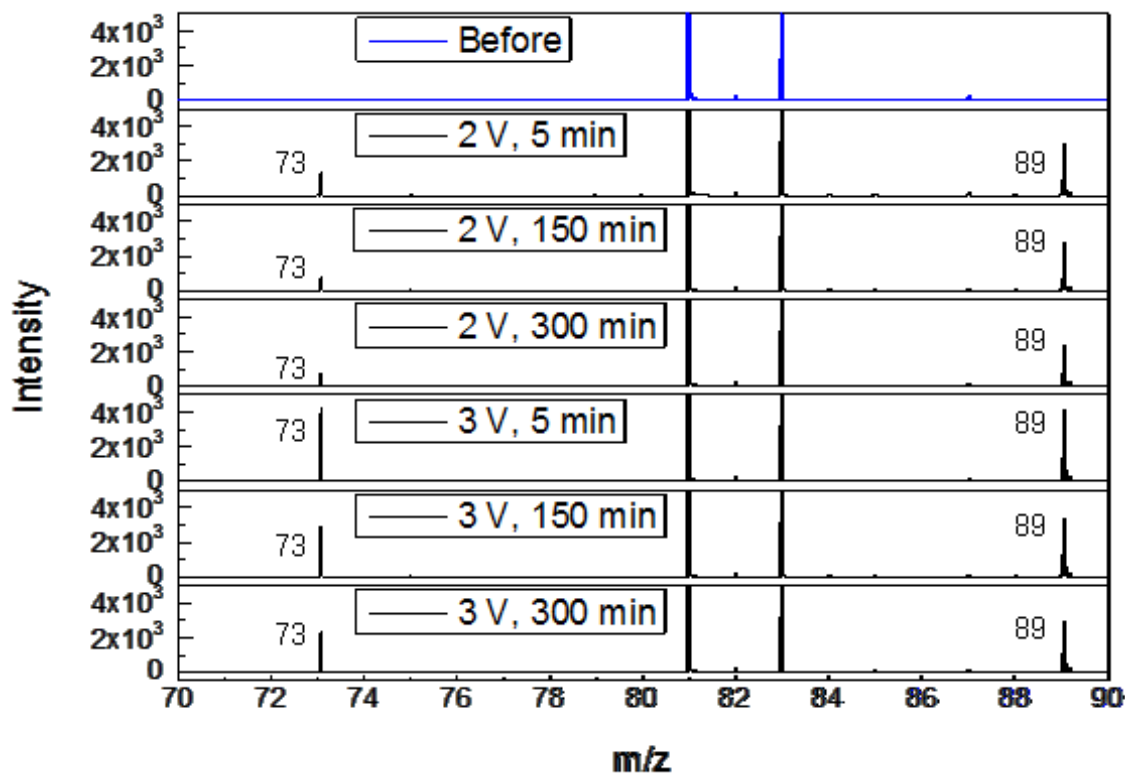


Figure C-7. Mass spectra of 10 mg/L ibuprofen and bisphenol A (1:1) mixture in 10 mM NaCl (pH 6) before (blue trace) and after 5, 150 and 300 minutes of crossflow electrochemical filtration treatment using MWNT blend buckypaper membrane (black traces) at 2 and 3 V of applied DC potential, showing the formation of the by-products at 73 and 89 m/z. Experiments were performed at room temperature using a flow rate of 1 mL/min and a buckypaper membrane of loading of 1.04 mg/cm².

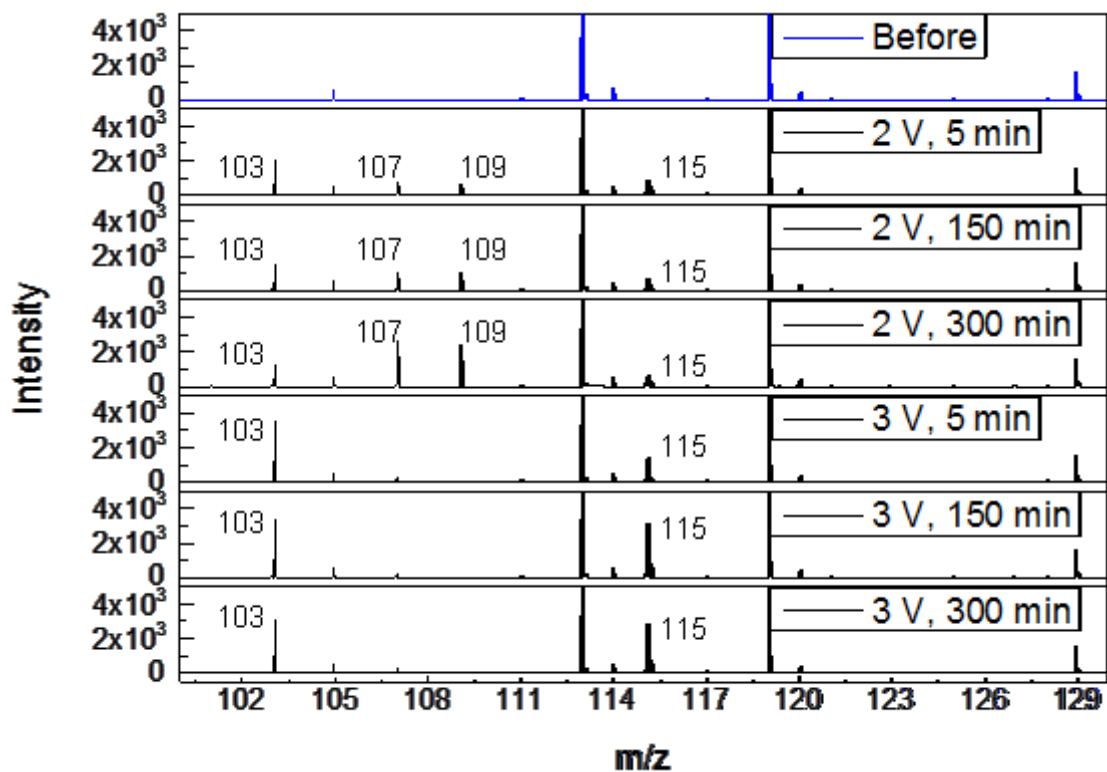


Figure C-8. Mass spectra of 10 mg/L ibuprofen and bisphenol A (1:1) mixture in 10 mM NaCl (pH 6) before (blue trace) and after 5, 150 and 300 minutes of crossflow electrochemical filtration treatment using MWNT blend buckypaper membrane (black traces) at 2 and 3 V of applied DC potential, showing the formation of the by-products at 103, 107, 109 and 115 m/z. Experiments were performed at room temperature using a flow rate of 1 mL/min and a buckypaper membrane of loading of 1.04 mg/cm².

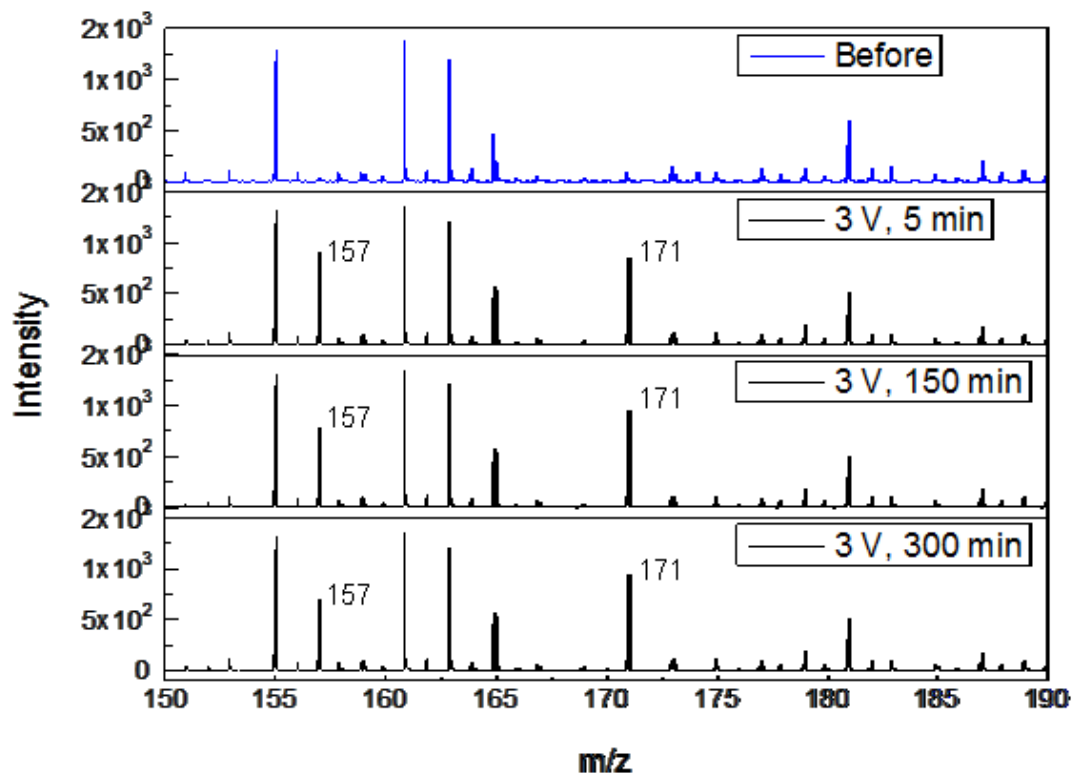


Figure C-9. Mass spectra of 10 mg/L ibuprofen and bisphenol A (1:1) mixture in 10 mM NaCl (pH 6) before (blue trace) and after 5, 150 and 300 minutes of crossflow electrochemical filtration treatment using MWNT blend buckypaper membrane (black traces) at 3 V of applied DC potential, showing the formation of the by-products at 157 and 171 m/z . Experiments were performed at room temperature using a flow rate of 1 mL/min and a buckypaper membrane of loading of 1.04 mg/cm^2 .

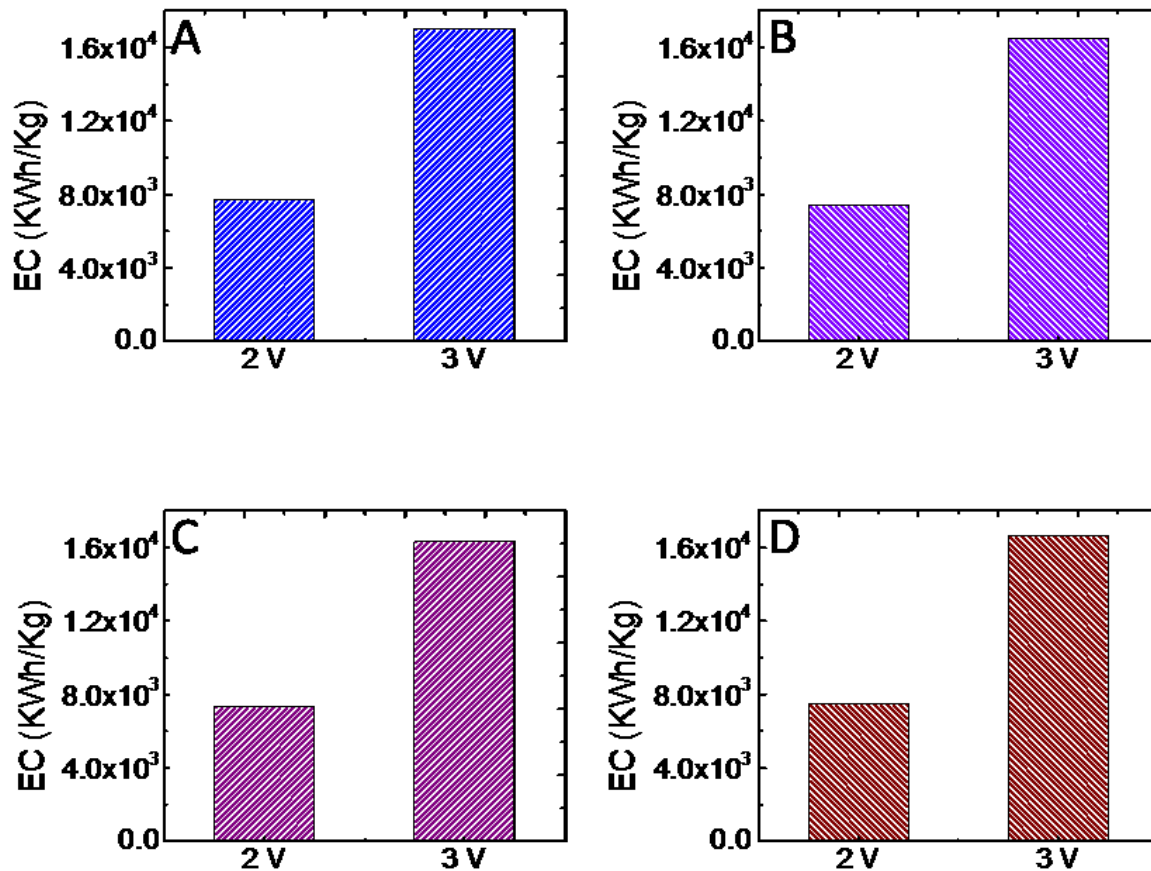


Figure C-10. Energy consumption for crossflow electrochemical filtration using MWNT blend buckypaper, where (A) is the energy consumption for the treatment of 1 mg/L ibuprofen from 10 mM NaCl at 2 and 3 V of applied DC potential and (B) is the energy consumption for the treatment of 1 mg/L bisphenol A from 10 mM NaCl at 2 and 3 V of applied DC potential, (C) is the energy consumption for the treatment of 1 mg/L ibuprofen and bisphenol A (1:1) mixture from 10 mM NaCl at 2 and 3 V of applied DC potential and (D) is the energy consumption for the treatment of 1 mg/L ibuprofen and bisphenol A (1:1) mixture from synthetic secondary wastewater (34 mg TOC/L, pH 7.4) at 2 and 3 V of applied DC potential. At MWNT buckypaper membrane surface loading of 102.5 mg/cm², flow rate was 1 mL/min and at room temperature.

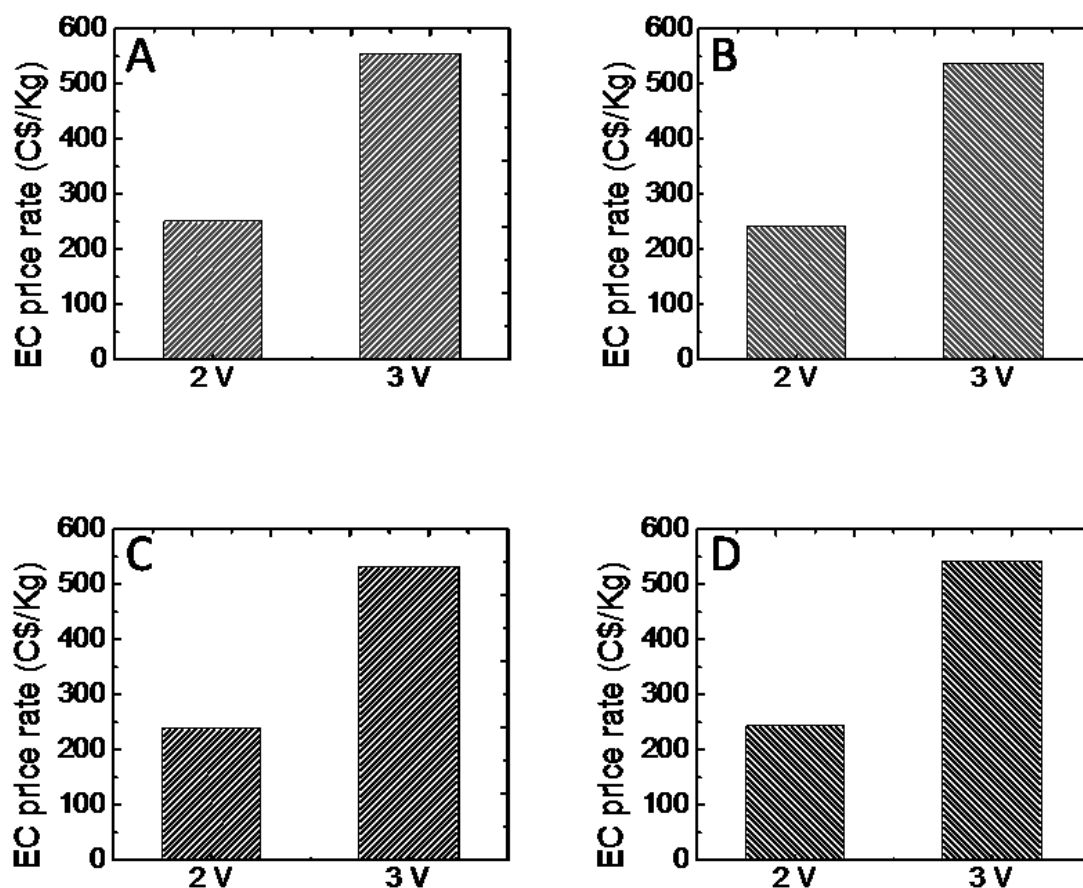


Figure C-11. Energy consumption price rates for crossflow electrochemical filtration using MWNT blend buckypaper, where (A) is the energy consumption price rates for the treatment of 1 mg/L ibuprofen from 10 mM NaCl at 2 and 3 V of applied DC potential, (B) is the energy consumption price rates for the treatment of 1 mg/L bisphenol A from 10 mM NaCl at 2 and 3 V of applied DC potential, (C) is the energy consumption price rates for the treatment of 1 mg/L ibuprofen and bisphenol A (1:1) mixture from 10 mM NaCl at 2 and 3 V of applied DC potential and (D) is the energy consumption price rates for the treatment of 1 mg/L ibuprofen and bisphenol A (1:1) mixture from synthetic secondary wastewater (34 mg TOC/L, pH 7.4) at 2 and 3 V of applied DC potential. Corresponding to figure C-8 (Price rates considering Hydro-Quebec's energy rates in effect April 1st 2016, Industrial rate for large-power customers: 3.62 ¢/kWh).

Appendix D

Appendix D contains images and schematics for dead-end electrochemical filtration and crossflow electrochemical filtration setups with their different components. Appendix D also contains images of multiwalled carbon nanotubes (Crystalline structures) and different membrane types.

In appendix D, the dead-end electrochemical filtration setup and operation schematic is shown with its parts (Figure D-1), crossflow electrochemical filtration setup is shown with different its parts, and a schematic of the crossflow mode operation is demonstrated (Figures D-2 and D-3). As well, appendix D contains images and crystalline structures of pristine MWNTs, carboxylated MWNTs and boron doped MWNTs and MWNTs blend buckypaper (Figure D-4).

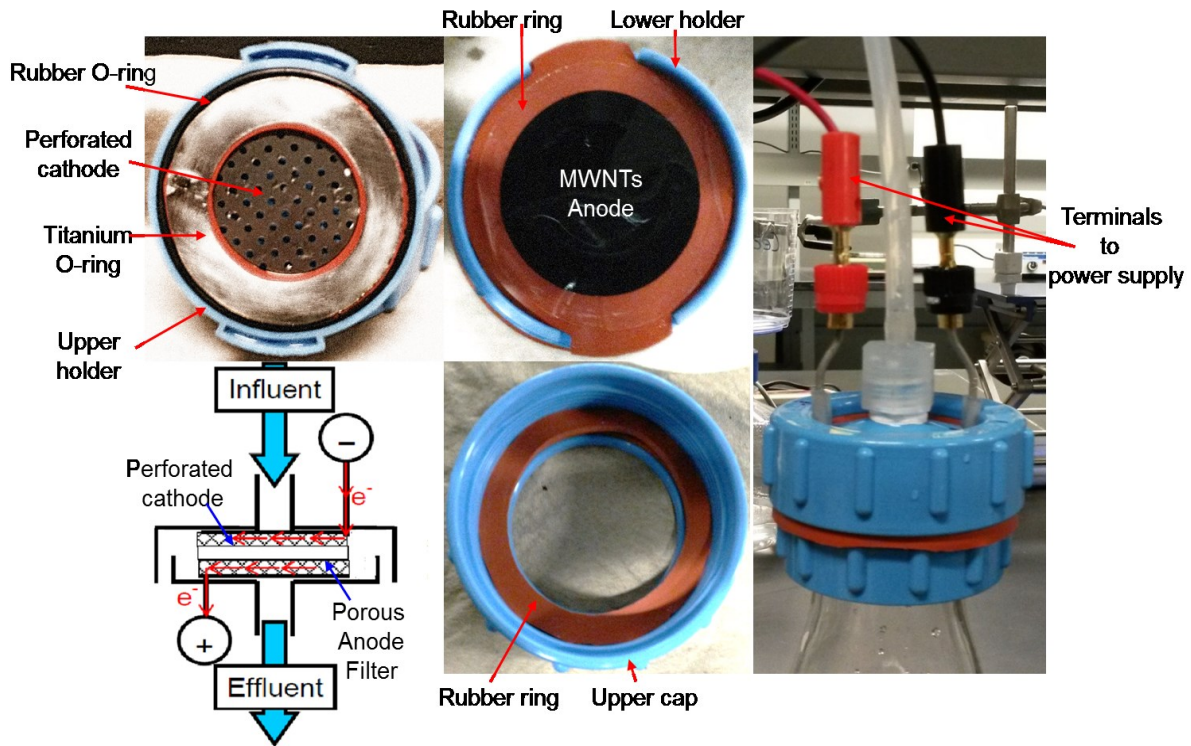


Figure D-1. Bench-scale dead-end electrochemical filtration setup and schematic
(Figure shows different parts)

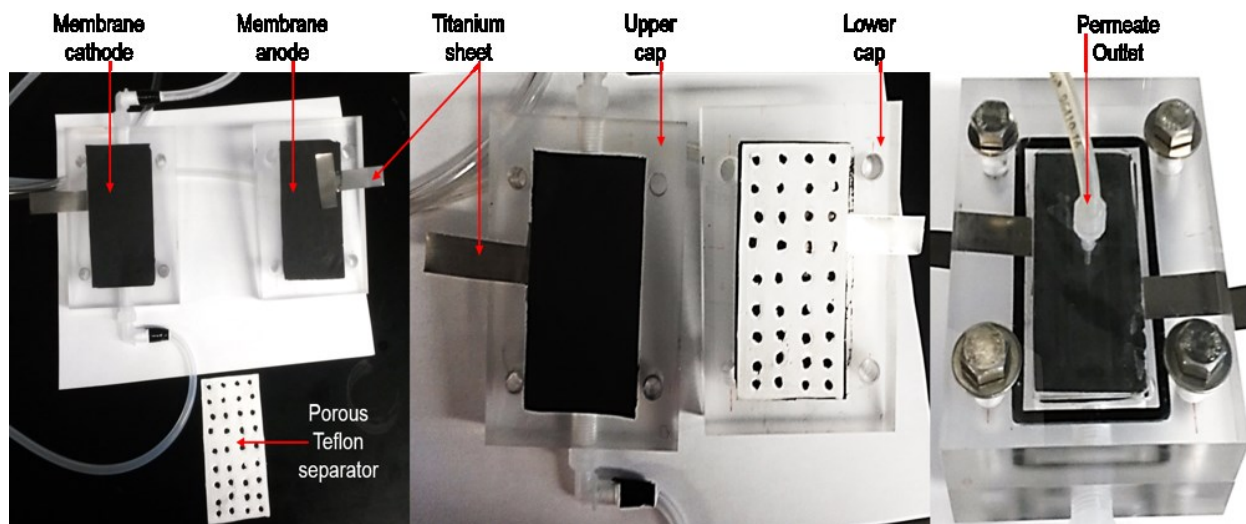


Figure D-2. Bench-scale crossflow electrochemical filtration setup (Figure shows different parts)

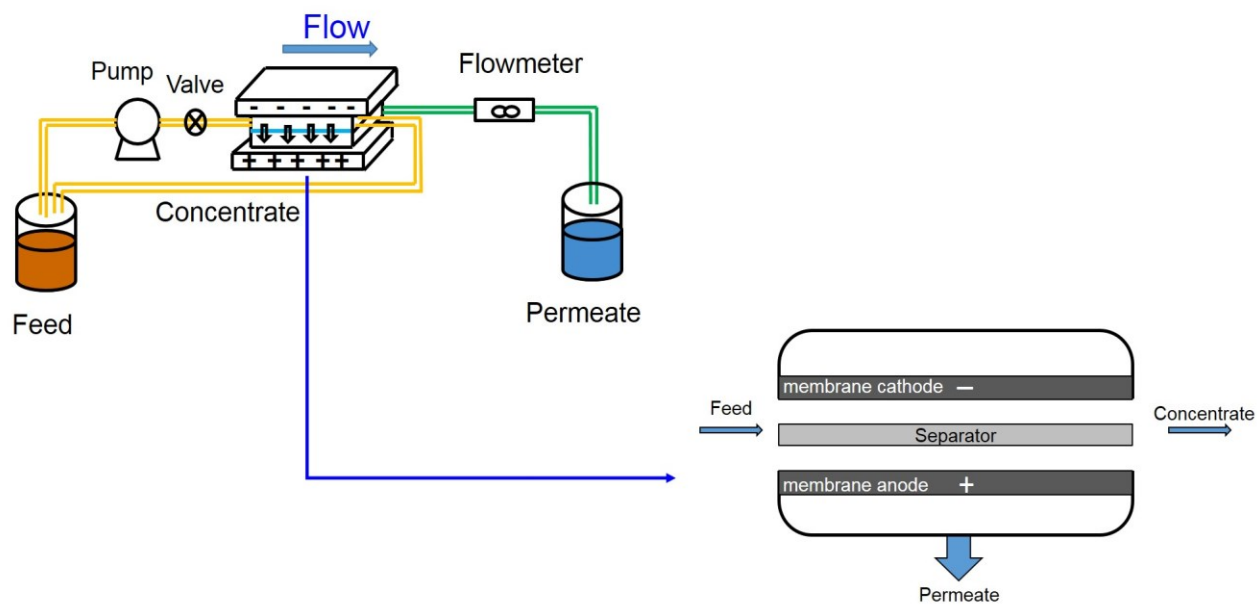
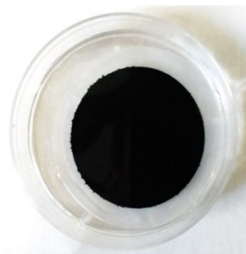
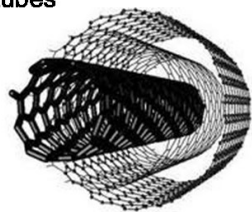


Figure D-3. Schematics for crossflow electrochemical filtration and the shear flow mechanism

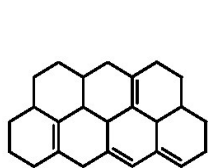
Multi-Walled Carbon nanotubes
(MWNTs)



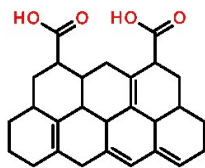
MWNTs filter



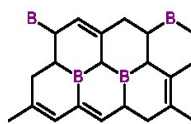
MWNTs Buckypapers



Prist. MWNTs



MWNTs-COOH



BMWNTs

Figure D-4. Diagrams/images and crystalline structures of pristine multiwalled carbon nanotubes, dead-end electrochemical filtration MWNTs membrane, and crossflow MWNTs buckypaper